Molecular and functional characterization of genes involved in setting up and reading histone methylation in Arabidopsis thaliana

Wei Zhao

UNIVERSITÉ DE STRASBOURG

***ÉCOLE DOCTORALE*- Sciences de la Vie et de la Santé - ED 414**

Institut de biologie moléculaire des plantes (IBMP) - UPR2357 CNRS

THÈSE présentée par :

Wei ZHAO

soutenue: le 30 juin 2017

pour obtenir le grade de: **Docteur de l'université de Strasbourg**
Discipline/ Spécialité: **Aspects moléculaires et cellulaires de la biologie**

Caractérisation moléculaire et fonctionnelle des gènes impliqués dans la mise en place et la lecture de la méthylation d'histones chez l'*Arabidopsis thaliana*

THÈSE dirigée par :
M. Wen-Hui SHEN — Directeur de Recherche, CNRS

RAPPORTEURS :
M. Fredy BARNECHE — Directeur de Recherche, CNRS
Mme. Célia JAGER-BAROUX — Group leader, HDR, Université de Zürich

AUTRES MEMBRES DU JURY :
Mme. Anne-Catherine SCHMIT — Professor, Université de Strasbourg
Mme. Franziska TURCK — Group leader, PI, Max Planck Institute
M. Alexandre BERR — Chargé de Recherche, CNRS

CONTENT

Acknowledgements

I wish to first thank Dr. Wen-hui Shen and Dr. Alexandre Berr for accepting me in the laboratory and for kindly supervising my work along these almost four year of my PhD study. I greatly appreciate their support, guidance and suggestions provided throughout my studies. I am also grateful to their high level of expertise as scientists they exhibited that will undoubtedly benefit me for my future career. I owe sincere and earnest thankfulness to Dr. Alexandre Berr, for his valuable advice on my experiments and data analyzing. As a non-French speaker, I also benefit a lot from him in my daily life.

I am grateful to the European Commission - Research: The Seventh Framework Programme for financial support. I thank the selection committee of the Chromatin in Plants–European Training and Mobility (CHIP-ET) program for giving me the opportunity. In particular, I would like to thank Dr. Mieke Van Lijsebettens, the coordinator of CHIP-ET, for helpful scientific discussions and for hosting me for a month in her laboratory at VIB in Belgium. I also thank Pia Neyt from her laboratory for helping me to carry out the root and leaf analysis experiments. I thank all the PIs and students from the CHIP-ET network for all the great training meetings and fruitful discussions we shared together.

I am particularly grateful to all the members of the PhD jury: Prof. Anne-Catherine Schmit, Dr. Fredy Barneche, Dr. Célia Jager-Baroux and Dr. Franziska Turck, who have kindly accepted to evaluate my PhD work.

I thank the IBMP laboratory members Donghong Chen, Jing Feng, Qiannan Wang and Xue Zhang for their helps. I thank Nicolas Baumberger at the Platform of Protein Production and Purification in IBMP and Morgan TORCHY at the Platform of Genomics and Structural Biology in IGBMC for helping me to do the protein crystallography analysis.

I am very grateful and thankful to my parents and to my wife for their enormous support, encouragement and understanding.

GENERAL INTRODUCTION

1. Epigenetics

In eukaryotic cells, genetic information is carried by the macromolecule: deoxyribonucleic acid (DNA) (Avery et al., 1944). Indeed, many phenotypic traits are caused by the permanent alteration of the nucleotide sequence of DNA. Nevertheless, there also exist many phenomena that could not be explained by the classical genetics. The term “epigenetics” had been put forward in the early 1940s by Conrad Waddington, and originally used to explain a genetic inexplicable phenomenon that how a fertilized zygote cell developed into a complex organism with distinct cell phenotypes and functions while the DNA is essentially the same in all cells (Dupont et al., 2009; Felsenfeld, 2014).

More recently, epigenetics has been defined and broadly accepted as “the study of mitotically and/or meiotically heritable changes in gene function that cannot be explained by changes in DNA sequence” (Russo et al., 1996). In nowadays, epigenetic regulation has been extensively investigated and found to play crucial roles in many developmental phenomena such as gene imprinting, cell differentiation and reprogramming in both plants and mammals (Feng et al., 2010); in the regulation of critical processes such as position effect variegation (PEV), paramutation, X-chromosome inactivation, parent-of origin effects and therefore also diseases like cancers in animals (Poynter et al., 2016); in many aspects of plant growth and development such as floral transition, gametogenesis, seed development, root growth, stem cell maintenance as well as plant responses to environmental stresses (Pikaard et al., 2014).

At molecular level, epigenetic mechanisms primarily comprise covalent post-translational histone modifications, DNA methylation, ATP-dependent chromatin remodeling, nucleosome assembly/disassembly, histone variant incorporation and non-coding RNAs regulation (Yao et al., 2016). These mechanisms can modulate chromatin structure, define genes expression state and maintain it through multiple rounds of cell division, or even to the next generation.

Here below, I will focus my introduction on covalent histone modifications.

2. Chromatin structure and histone modifications

In eukaryotic cells, genetic information encoded by DNA is packed into chromatin, a highly complex structure consisting of DNA together with all associated proteins that contribute to its structure and function. The basic structural unit of chromatin is the nucleosome. The nucleosome is made of 146-147 base pairs of DNA wrapped in about 1.65 turns around an octamer formed by two copies of each of the core histones H2A, H2B, H3 and H4 (Luger et al., 1997; Figure 1). Individual nucleosomes are separated by linker DNA of 10–60 base pairs that is associated by histone H1 (linker histone), resulting in a ~10 nm 'beads-on-a-string chromatin fiber. The fiber can be further folded into more condensed, ~30 nm thick fibers and then 100-400 nm interphase fibers or further more highly compacted metaphase chromosome structures (during mitosis and meiosis) (Hansen, 2002; Peterson et al., 2004). The chromatin fibers can be more or less "open" or "closed" which influences fundamental DNA template processes like transcription, DNA replication, DNA-damage repair or DNA recombination.

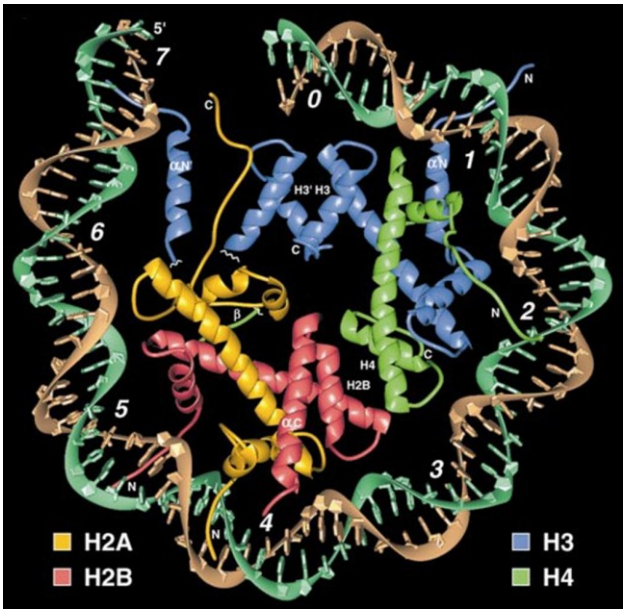

Figure 1: Nucleosome core particle, DNA is bound to an octameric complex composed of two copies of each four core histones H2A, H2B, H3 and H4 (Luger et al., 1997).

Histones are highly alkaline proteins found within eukaryotic cell nuclei. The canonical four core histones H2A, H2B, H3 and H4 are highly evolutionary conserved in eukaryotes; each of them contains a C-terminal histone fold domain and a flexible N-terminal tail domain. The N-terminal and C-terminal tails protrude from the nucleosome and are exposed on the surface of the nucleosome. They are subject to multiple types of post-translation modifications (PTMs), including methylation, acetylation, phosphorylation, ubiquitination and others (Kouzarides, 2007).

In the histone code hypothesis, the histone modifications are proposed to act in a combinatorial or sequential manner specifically regulate chromatin structure and modify the way that genes are expressed and they can be recognized by other proteins (readers and effectors) and interpreted into specific biological outcomes (Strahl et al., 2000; Turner, 2000).

3. Histone methylation

In 1964, RNA synthesis was reported to be an association of histone acetylation and methylation, opened the study of histone methylation (Allferey et al., 1964). Over the many last years, histone methylation has been one of the most extensively and best studied modifications in both animals and plants. It plays essential roles in epigenetic regulation of gene transcription and organism development as well as in response to environmental cues (Liu et al., 2010; Black et al., 2012).

Methylation can occur at different lysine (K) or arginine (R) residues of histone tails, and one residue can be methylated to different degrees depending on the number (up to three for K) of methyl groups added (Figure 2). In Arabidopsis, five lysine residues located on histone H3, i.e. (K4, K9, K23, K27 and K36) have been reported to be sites of methylation so far. In general, histone H3 di/tri-methylations on lysine 4 (H3K4me2/3) and 36 (H3K36me2/3) are associated with euchromatin and correspond to transcriptional activation; whereas methylations of H3K9 and H3K27 are associated with gene silencing (Johnson et al., 2004; Martin and Zhang, 2005). Interestingly, the more recently identified H3K23 monomethylation (H3K23me1) is linked with CG DNA

methylation but H3K23me1 enrichment along gene bodies does not correlate with transcription levels (Trejo-Arellano et al., 2017).

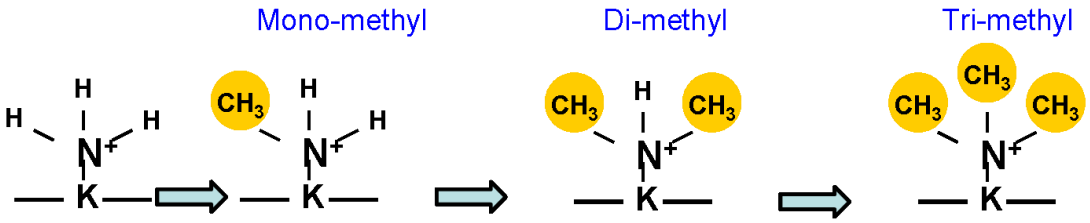

Figure 2: Schematic representation of histone lysine residue is mono, di and tri-methylated.

3.1 Genome-wide distribution of histone methylation

In Arabidopsis, H3K9me2 and H3K27me1 are heterochromatic marks, which are found essentially associated with transposons and centromeric repeat DNA sequences (Roudier et al., 2011). Within euchromatin, H3K4me3 accumulates around the TSS (Transcription Start Site) regions and is thought to be involved in transcription initiation in both animals and plants (Xiao et al., 2016; Figure 3). H3K36me2 and H3K36me3 are both enriched toward the 3' end of the gene body in animals. By contrast, in plants H3K36me2/3 are found across the transcribed regions, with H3K36me3 peaks in gene body toward the 5' end and H3K36me2 more distributed toward the 3' end of transcribed genes. Several functions of H3K36me2/3 have been described such as affecting alternative intron splicing, regulating Pol II elongation, and preventing aberrant transcription initiation within gene body (Wagner and Carpenter, 2012). H3K27me3 is at highest level in the promoter of inactive genes in animals. However, it is localized across the transcribed regions in Arabidopsis, with a remarkable bias towards the TSS mainly enriched in euchromatin regions (Figure 3). H3K27me3 is recognized as one of the primary gene silencing mechanisms and has broad functions in control of plant developmental processes (Xiao and Wagner, 2015).

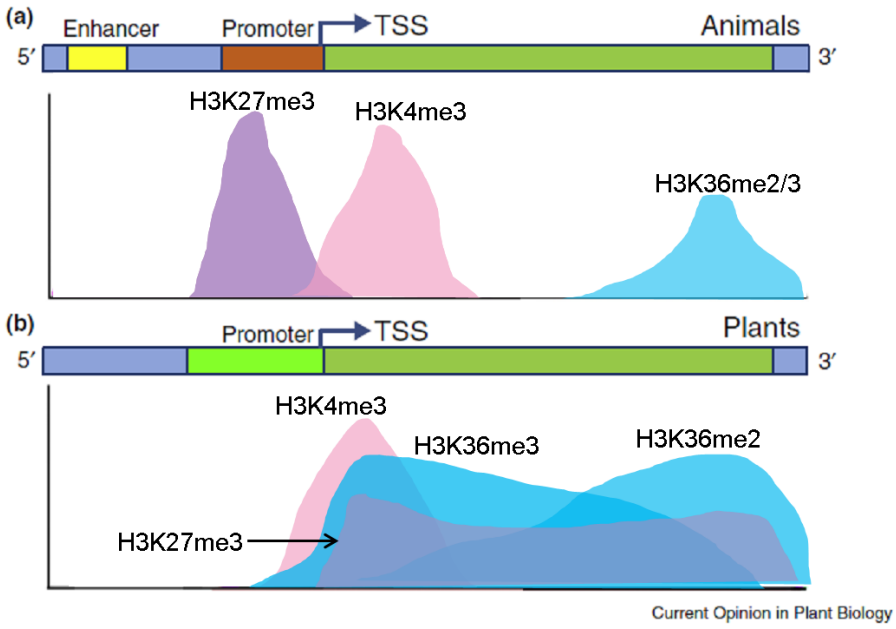

Figure 3: Histone lysine methylation distribution in animals and plants (Adapted from Xiao et al., 2016).

3.2 Writers of histone lysine methylation

Histone K methylation is catalyzed by histone lysine methyltransferases (HKMTs), 'writers' of histone code. The first discovered HKMTs are human and mouse SUV39H1 (KMT1A) and yeast CLR4 proteins (Rea et al., 2000). Later, more and more HKMTs have been identified. Excepting Dot1, a histone H3K79 methyltransferase, all the other HKMTs contain a highly conserved SET domain (Dillon et al., 2005; Ng et al., 2007). The SET domain, named after three HKMTs found in Drosophila: Suppressor variegation 3–9 (Su(var)3-9), Enhancer of Zeste (E(z)) and Trithorax (Trx), is a 130 amino acid catalytic domain (Jenuwein, 2006). It uses S-adenosylmethionine to transfer methyl groups to alkyl chain of the target lysine in a deep open hydrophobic channel, which is the key structural feature of the SET domain (Figure 4). This channel is also flexible and regulated by surrounding sequences to accommodate mono-, di- and/or tri-methyl addition.

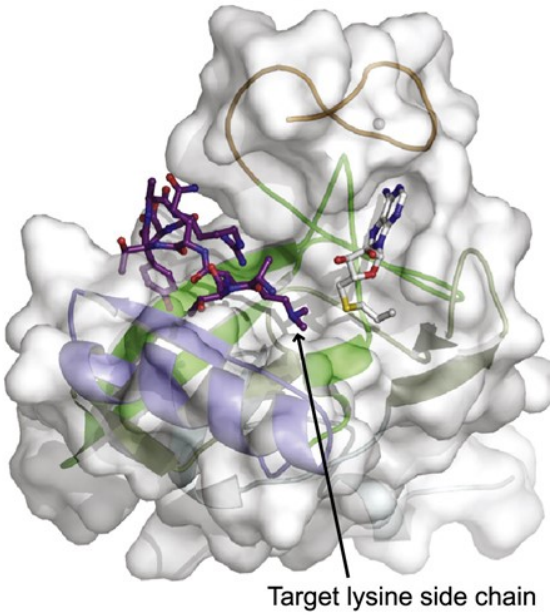

Figure 4: Representative overall structure of the SET domain of the human methyltransferase MLL1 (Southall et al., 2009).

In Arabidopsis, there are 47 SET Domain Group (SDG) proteins, which can be divided into distinct subgroups (Thorstensen et al., 2011; Ng et al., 2007). Based on sequence similarity and phylogenetic analysis, SDGs of the five Trx homologs (ATX1/SET DOMAIN GROUP27/SDG27, ATX2/SDG30, ATX3/SDG14, ATX4/SDG16, and ATX5/SDG29), seven Trx related (ATXR1/SDG35, ATXR2/SDG36, ATXR3/SDG2, ATXR4/SDG38, ATXR5/SDG15, ATXR6/SDG34, and ATXR7/SDG25), and four ASH1 homologs (ASHH1/SDG26, ASHH2/SDG8, ASHH3/SDG7, and ASHH4/SDG24) are classified into the Trithorax group (TrxG) (Berr et al., 2011). They mainly catalyze H3K4 and/or H3K36 methylation and are associated with transcriptional gene activation. The E (z) subgroup SDGs (CLF/SDG1, MEA/SDG5, and SWN/SDG10) belong to Polycomb Group (PcG) and are responsible for H3K27 methylation, which is associated with transcriptional gene silencing (Xiao et al., 2016).

3.2.1 H3K4me3 writers

Primary writers of mono-, di- and trimethylation of H3K4 include histone methyltransferase Set1 in yeast and the mixed lineage leukaemia (MLL) family proteins of MLL1-MLL4, SET1A and SET1B in mammalian. These HKMTs exert catalyzing

activity by forming complex with additional factors, called COMPASS (complex proteins associated with Set1) in yeast and COMPASS-like complexes in mammals (Shilatifard, 2012). Later, COMPASS-like complexes were also identified in plants with highly conserved subunit compositions (Jiang et al., 2011). In Arabidopsis, deletion of the core subunit *ASH2R* (*Arabidopsis Ash2 Relative*) resulted in a global decrease of H3K4me3 without affecting H3K4me1/2 at flowering genes (Jiang et al., 2014). Interestingly, two sequence-specific membrane-associated basic leucine zipper (bZIP) transcription factors bZIP28 and bZIP60 were demonstrated to physically interact with Arabidopsis COMPASS-like components both *in vitro* and *in vivo*, providing a possible mechanism for how the H3K4me2/3 writers be recruited to target loci (Song et al., 2015).

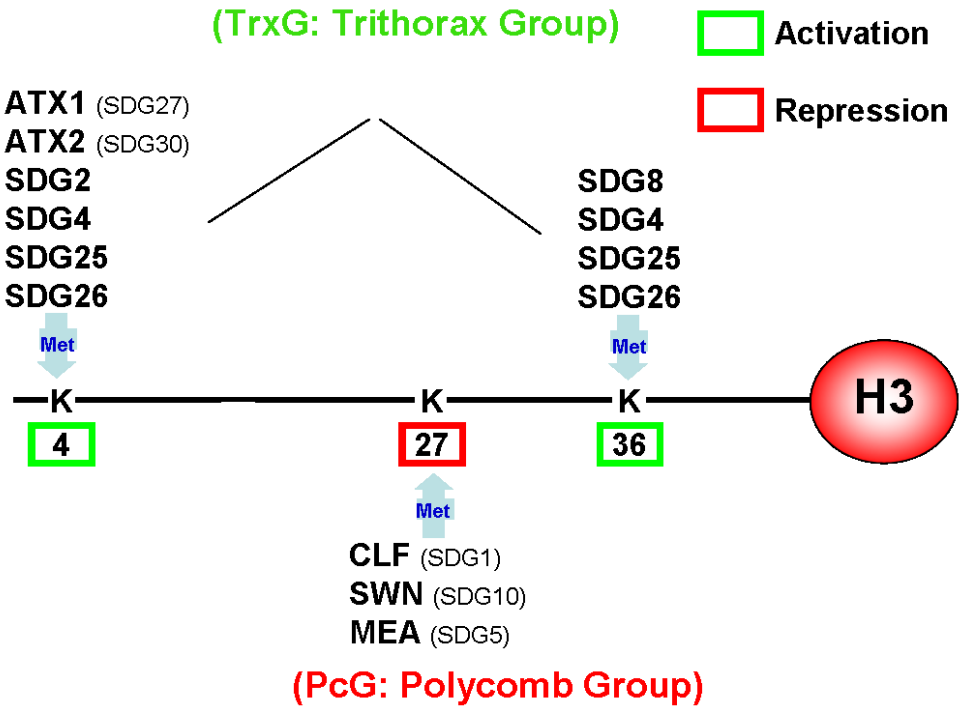

Figure 5: Writers of histone methylation in Arabidopsis, TrxG and PcG proteins.

In Arabidopsis, six SDGs in TrxG family were functionally characterized as H3K4 methyltransferase (Figure 5); they alone are able to methylate H3K4, which is in contrast to multi-protein complex requirement for enzyme activity of their homologs in animals. ARABIDOPSIS HOMOLOG of TRITHORAX1 (ATX1/SDG27), a close

homolog of yeast Set1 and human MLL1, was the first TrxG member reported in plants (Alvarez-Venegas et al., 2003). The *atx1* mutant showed slightly early-flowering phenotypes caused by a decreased expression level of *FLOWERING LOCUS C* (*FLC*) associated with reduction of H3K4me3 but not H3K4me2 at the *FLC* locus, indicating the specific tri-methylation function of ATX1 (Pien et al., 2008). In addition, mutations in *ATX1* caused slightly smaller and serrated rosette leaves, perturbed resistance to pathogens and the plant's response to drought as well as dehydration stress signaling in both abscisic acid (ABA)-dependent and ABA-independent pathways (Alvarez-Venegas et al., 2007; Ding et al., 2009; Ding et al., 2011). *ATX1* also plays roles in the regulation of flower development by activating flower homeotic genes and root development by maintaining root apical meristem activity as well as the transition to elongation (Alvarez-Venegas et al., 2003; Napsucialy-Mendivil et al., 2014).

ATX2/SDG30, a paralog of ATX1, encodes a putative H3K4me2 methyltransferase (Saleh et al., 2008). However, *atx2* single mutant did not show any obvious phenotype, while the *atx1 atx2* double mutant displayed an enhanced early-flowering phenotype compared to *atx1*, indicating some overlapping functions between *ATX1* and *ATX2* (Saleh et al., 2008; Pien et al., 2008).

SDG25/ATXR7 is a floral repressor mainly through the activation of *FLC* expression via deposition of both H3K4me2/3 and H3K36me3, possibly through a different pathway from *ATX1/ATX2* (Berr et al., 2009; Tamada et al., 2009; Shafiq et al., 2014; Berr et al., 2015). In addition to control flowering time, SDG25 is also involved in plant defense by activating some key *Resistance* (*R*) genes via deposition of H3K4me3 at those loci (Xia et al., 2013).

SDG26 was first identified as a flowering activator, but without knowing the underlying molecular mechanism (Xu et al., 2008). A more recent study demonstrated that loss of function of *SDG26* caused a decrease of both H3K4me3 and H3K36me3 at a key flowering integrator gene *SUPPRESSOR OF OVEREXPRESSION OF CONSTANS 1* (*SOC1*), leading to *SOC1* repression and late flowering (Berr et al., 2015).

SDG4/ASHR3 is potentially able to methylate H3K4me2/3 and H3K36me3, and it

was reported to function in pollen, stamen and root development (Cartagena et al., 2008; Thorstensen et al., 2008; Kumpf et al., 2014).

So far, SDG2 is the methyltransferase identified to perform genome-wide trimethylation of H3K4. Consistently, *sdg2* mutants showed decreased H3K4me3 on the global level and caused strong pleiotropic phenotypes including abnormal sporophytic and gametophytic formation, as well as root growth and development defects (Berr et al., 2010; Guo et al., 2010; Yao et al., 2013; Pinon et al., 2017).

3.2.2 H3K36me3 writers

In yeast, the SET-domain protein Set2 catalyzes mono- (me1), di- (me2) and tri-methylation (me3) at H3K36 (Venkatesh and Workman, 2013). The set2 homologue SETD2 in human specifically deposes H3K36me3 and is involved in transcriptional elongation (Carvalho et al., 2013). Moreover, some of animal proteins, like human nuclear receptor SET domain containing 1 (NSD1; also known as KMT3B), have not only H3K36 mono- and dimethylase activity but also can methylate H4K20 or even non-histones like NF-κB (nuclear factor-κB); the NSD2 (also known as WHSC1) catalyzes methylation of H3K36 as well as H3K4, H3K27 and H4K20 sites (Wagner and Carpenter, 2012).

In Arabidopsis, H3K36 methylation is primarily carried out by SDG8 (Zhao et al., 2005; Xu et al., 2008), though the previously mentioned SDG4, SDG25 and SDG26 also exhibit H3K36 methylation in addition to their H3K4 methylation activity (Cartagena et al., 2008; Shafiq et al., 2014; Berr et al., 2015). SDG8 has genome-wide catalyzing activity in H3K36me2/3 deposition (Zhao et al., 2005; Xu et al., 2008; Li et al., 2015). It plays essential roles in prevention of floral transition by increasing H3K36m2/3 at *FLC* and thus elevating its expression level (Zhao et al., 2005). In addition, *SDG8* is broadly involved in many other processes including regulation of shoot branching (Xu et al., 2008; Dong et al., 2008; Cazzonelli 2009; Bian et al., 2016), ovule and anther development (Grini et al., 2009), carotenoid biosynthesis (Cazzonelli 2009; Cazzonelli et al., 2010), plant defense responses against necrotrophic fungal pathogens (Berr et al., 2010; De-La-Peña et al., 2012), innate immunity (Palma et al.,

2010), brassinosteroid-regulated gene expression (Wang et al., 2014), seed gene repression and seed dormancy (Tang et al., 2012; Lee et al., 2014), mechanical stimulation response (Cazzonelli et al., 2014), and high-level expression of light- and/or carbon-responsive genes (Li et al., 2015). In spite of crucial functions of SDG8, how it is recruited to target loci still needs to be elucidated.

3.2.3 H3k27me3 writers

PcG proteins and TrxG proteins constitute two counteracting groups of chromatin regulators, providing an essential strategy in control of the temporal and spatial expression pattern of key developmental regulator genes in many multicellular organisms including animals and plants (Schuettengruber et al., 2011; Pu and Sung, 2015). PcG proteins, first identified in Drosophila, are nowadays known to act in multiprotein complexes for transcription repression in both plants and animals (Margueron and Reinberg, 2011). Polycomb Repressive Complex 2 (PRC2) is among the best studied and is responsible for H3K27me3 deposition.

In Drosophila, PRC2 is composed of four core subunits, namely E(z), Su(z)12 (Suppressor of zeste 12), Esc (Extra sex combs), and N55 (a 55 kDa WD40 repeat protein) (Simon and Kingston, 2013). In Arabidopsis, there are three E(z) homologs: CURLY LEAF (CLF), MEDEA (MEA) and SWINGER (SWN); three Su(z)12 homologs: EMBRYONIC FLOWER 2 (EMF2), FERTILISATION INDEPENDENT SEED2 (FIS2) and VERNALIZATION2 (VRN2); a single Esc homolog: FERTILIZATION INDEPENDENT ENDOSPERM (FIE); and five p55 homologs: MULTICOPY SUPPRESSOR OF IRA 1 (MSI1), MSI2 to MSI5 (Hennig and Derkacheva, 2009; Grossniklaus and Paro, 2014). Different PRC2 sub-complexes likely have specialized functions, e.g. the FIS2-PRC2 complex (containing MEA, FIE, FIS2 and MSI1) is involved in sporophyte to gametophyte transition and early seed development, the EMF2-PRC2 complex (containing CLF or SWN, EMF2, MSI1 and FIE) is involved in embryonic to vegetative growth transition and in flowering time regulation, while the VRN2-PRC2 (containing CLF or SWN, VRN2, FIE and MSI1) is involved in winter memory (vernalization) in flowering time control (Hennig and Derkacheva, 2009; Pu

and Sung, 2015; Mozgova and Hennig, 2015).

Within PRC2, the SDG proteins CLF/SDG1, MEA/SDG5 and SWN/SDG10 are the enzyme cores for H3K27me3 deposition. CLF was the first identified plant PcG protein, which regulates leaf and flower development by repressing the floral homeotic genes *AGAMOUS* (*AG*) and the Class I KNOX gene *SHOOTMERISTEMLESS* (*STM*) (Goodrich et al., 1997; Katz et al., 2004; Schubert et al., 2006). CLF is also implicated in flowering time regulation by represses the floral repressor genes *FLC*, *MAF4* and *MAF5* (*MADS AFFECTING FLOWERING 4/5*) as well as the activator gene *FT* (*FLOWERING LOCUS T*) via H3K27me3 deposition (Jiang et al., 2008; Shafiq et al., 2014). Lack of *SWN* function alone does not cause a clear mutant phenotype, but it can strongly enhance the *clf* phenotype. The *swn clf* double mutant plants flower after germination without a substantial vegetative growth phase, and develop embryo- or callus-like structures, in which H3K27me3 was totally lost (Chanvivattana et al., 2004; Aichinger et al., 2009; Bouyer et al., 2011; Lafos et al., 2011). *MEA* is a self-regulated imprinting gene in the endosperm with maternal allele is expressed while the paternal allele is silent (Baroux et al., 2006; Jullien et al., 2006). DEMETER (DME), a DNA glycosylase, contributes to the *MEA* imprinting by specifically removes DNA methylation at *MEA* maternal-allele and thus activates its expression, which is in turn involved in silencing the paternal allele (Gehring et al., 2006). Interestingly, it has been reported that MEA physically interact with DNA METHYLTRANSFERASE1 (MET1) and act together to regulate endosperm development in seeds, which also provides a link between histone modification and DNA methylation (Schmidt et al., 2013).

3.3 Erasers of histone methylation

Histone methylation is relatively more stable compared with other PTMs, and had been thought to be irreversible due to lacking of knowledge on histone demethylases, ‘erasers’. It has been becoming clear that histone methylation is also dynamic since the finding of the first histone lysine demethylase (KDM1): human LYSINE SPECIFIC DEMETHYLASE 1 (LSD1) (Shi et al., 2004). LSD1 is an amine oxidase that can

demethylate H3K4me1/2 in a flavine adenine dinucleotide (FAD) dependent manner or demethylate H3K9me1/2 in the presence of the androgen receptor (Shi et al., 2004; Metzger et al., 2005). Subsequently, another family of histone demethylases containing JmjC domain (JMJ) was discovered (Tsukada et al., 2005). All JMJ proteins contain a conserved JmjC domain that use a-ketoglutarate molecular oxygen and Fe(II) as cofactors to demethylate all forms of mono-/di-/trimethylated lysine residues (Tsukada et al., 2005, Klose et al., 2006a).

In plants, both types of demethylases have been identified: four homologues of LSD1 and 21 JMJs, which can be further divided into distinct subgroups based on sequence analysis (Jiang et al., 2007; Liu et al., 2008; Spedaletti et al., 2008; Chen et al., 2011). Studies over the past decade have revealed that histone demethylases play fundamental roles in the regulation of histone methylation homeostasis and diverse chromatin-based processes as well as developmental pathways in plants (Greer and Shi, 2012; Dimitrova et al., 2015; Liu et al., 2010; Chen et al., 2011; Prakash et al., 2014; Figure 6).

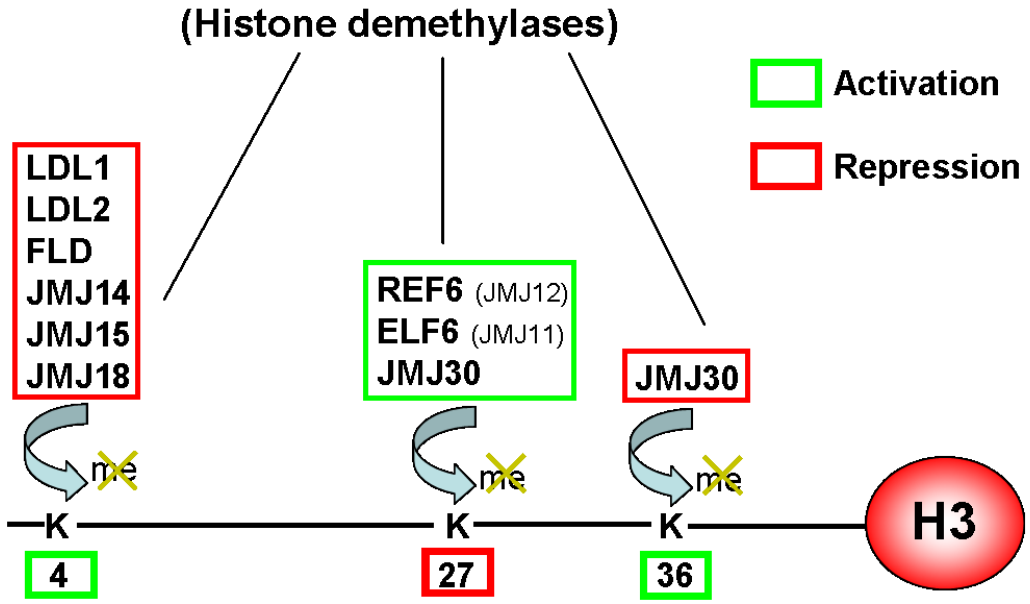

Figure 6: Erasers of histone methylation in Arabidopsis, LDL and JMJ family proteins.

3.3.1 Erasers of H3K4 methylation

In Arabidopsis, LSD1-LIKE 1 (LDL1), LDL2, LDL3 and FLOWERING LOCUS D (FLD) are homologues of human LSD1. *LDL1*, *LDL2* and *FLD* have been shown to control flowering time by repressing *FLC* expression. In both *ldl1 ldl2* and *ldl1 fld* double mutants, an increase of H3K4me2 was found at *FLC* chromatin (He et al., 2003; Jiang et al., 2007; Shafiq et al., 2014); furthermore, LDL1 showed specifically in vitro H3K4me1/2 demethylase activity (Spedaletti et al.,2008). LDL1 and LDL2 but not FLD are responsible for removal of H3K4me2 at floral repressor *FWA* chromatin and thus contribute to silencing of *FWA* during sporophytic development (Jiang et al., 2007). More recently, LDL1 and LDL2 were reported to control seed dormancy via regulation of seed dormancy-related and ABA signaling-related genes (Zhao et al., 2015).

Three of Arabidopsis JMJ proteins, JMJ14, JMJ15 and JMJ18 have been shown to act as H3K4 demethylases and involved in flowering time control by distinct mechanisms. JMJ14 is able to demethylate H3K4me1/2/3 both *in vivo* and *in vitro* and repress flowering through down-regulation of several key floral integrator genes (Lu et al., 2010). JMJ15 is implicated in regulating flowering time by removal of H3K4me3 at *FLC*, and it is also involved in regulation of plant salt tolerance and female gametophyte development (Yang et al., 2012a; Shen et al., 2014; Lu et al., 2008). JMJ18 accelerates flowering by repressing *FLC* expression via directly binding to *FLC* locus and removes H3K4me2/3 at its chromatin (Yang et al., 2012b). It is worthy to note that JMJ14 was recently found to target to flowering genes mediated by two NAC type transcription factors NAC50 and NAC52 through directly binding to their CTTGNNNNNCAAG consensus sequences (Ning et al., 2015; Zhang et al., 2014), providing a possible mechanism for how histone demethylases are recruited to specific gene target loci.

3.3.2 Erasers of H3K36 methylation

The first reported H3K36 demethylase is human KDM4A that can remove both H3K36me2/3 and H3K9me2/3 (Klose et al., 2006b). Other erasers of H3K36 methylation in animals include KDM8/JMJD5 that remove 3K36me2, KDM2A and

KDM2B that remove H3K36me1/2, as well as KDM4A, KDM4B, KDM4C, KDM4D and NO66 that remove H3K36me2/3 (Kooistra and Helin, 2012).

In plants, JMJ30 is the only H3K36 demethylase reported so far. It exhibits *in vitro* H3K36me2/3 demethylase activity and interacts with the MYB-family transcription factor EARLY FLOWERING MYB PROTEIN (EFM) to regulate H3K36me2 dynamics at *FT* to regulate flowering time (Yan et al., 2014).

3.3.3 Erasers of H3K27 methylation

In animals, KDM6A and KDM6B enzymes are involved in demethylation of H3K27me2/3. The recruitment of these two demethylases is accomplished through interaction with sequence specific DNA-binding proteins (Bosselut et al., 2016). Another histone demethylase JHDM1D, also known as KDM7A, was reported to remove H3K27me1/2 and to be involved in regulation of neural differentiation and early embryos and brain development (Tsukada et al., 2010; Kooistra and Helin, 2012).

In Arabidopsis, REF6 (JMJ12) specifically demethylates H3K27me2/3 and acts on *FLC* (Noh et al., 2004; Lu et al., 2011). ELF6 (JMJ11), a closer homolog of REF6, acts as a flowering repressor in the photoperiod pathway (Noh et al., 2004). More recently, ELF6 was shown to remove H3K27me3 for resetting *FLC* expression during reproduction to ensure a vernalization requirement in the next generation (Crevillen et al., 2014). Interestingly, REF6 was shown to be recruited to its target loci through its C-terminal C2H2 zinc-finger domain which associates with a CTCTGYTY motif on the genomic DNA (Cui et al., 2016; Li et al., 2016). JMJ30, which was shown to demethylate H3K36me2/3 *in vitro* (Yan et al., 2014), was also a potential H3K27me2/3 demethylase. At elevated temperature, stabilized JMJ30 cooperates with JMJ32 to demethylate H3K27me3 at *FLC* locus to prevent premature flowering (Gan et al., 2014).

3.4 Readers of histone methylation

The methyl group does not affect the overall charge of the modified histone molecule, but it enhances the hydrophobic force that may alter intra- or intermolecular interactions or serve as a platform to recruit specific “readers” that will recognize the methylation signals and act as effectors for further downstream events (Liu et al., 2010; Bannister and Kouzarides, 2011). Histone methylation reader proteins bind preferentially to the methylated sties through various functional domains, including PHD (Plant HomeoDomain), Chromo (Chromodomain), WD40 (Tryptophan-Aspartic dipeptide 40), MBT (Malignant Brain Tumor), PWWP (Pro-Trp-Trp-Pro), MRG (Morf Related Gene), and Tudor (Yun et al., 2011; Musselman et al., 2012; Liu and Min, 2016; Figure 7).

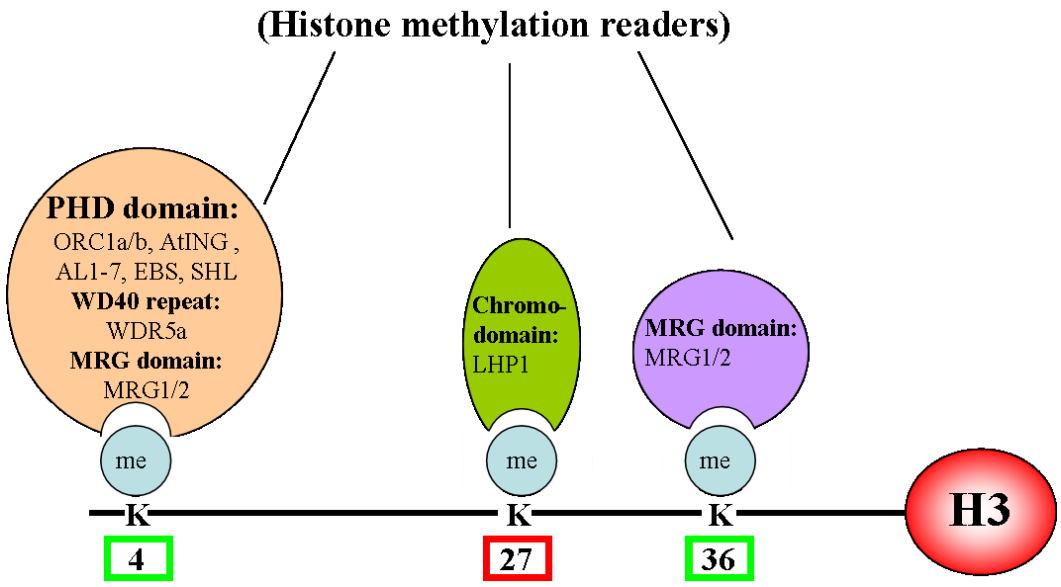

Figure 7: Readers of histone methylation in Arabidopsis, PHD domain-, WD40 repeat-, MRG domain- and Chromodomain-containing proteins.

3.4.1 Readers of H3K4 methylation

In animals, several H3K4 methylation readers have been identified and characterized, e.g. the Chromo-containing ATPase protein CHD1; the PHD-containing proteins TAF3 (component of the transcriptional machinery), ING1/2 (components of Histone acetyltransferase complex) and PHF2/8 (histone demethylation related proteins); and

the Tudor-containing histone demethylases JMJD2A/2C ((Yun et al., 2011).

In Arabidopsis, ORC1a and ORC1b contain a PHD domain that is absent in the yeast and animal ORC1 (Origin Recognition Complex subunit 1). They can interact with H3K4me3 and are involved in transcriptional activation of target genes (Sanchez and Gutierrez, 2009). AtING1/2 and Alfin1-like (AL1-7) are also PHD-containing proteins and are shown to interact with H3K4me2/3 *in vitro* (Lee et al., 2009). More recently, AL6/7 were demonstrated to interact with some PcG proteins to silence seed maturation genes during germination by promoting a switch from H3K4me3 to H3K27me3 (Moliter et al., 2014). Two other PHD-containing proteins, EBS and SHL, were found to recognize H3K4me2/3 and to play an important role in preventing early flowering. EBS and SHL interact with the histone deacetylase HDA6 to repress the expression of flowering integrator genes *FT* and *SOC1* by maintaining a low level of H3 acetylation at these loci (López-González et al., 2014). Lastly, WDR5a, a WD40 repeat containing proteins, is a conserved core component of COMPASS complex and can bind with H3K4me1/2/3 to regulate flowering time (Jiang et al., 2009).

3.4.2 Readers of H3K36 methylation

In animals, H3K36 methylation reader proteins include the Chromo-containing protein MRG15 (components of histone acetyltransferase complex), the PWWP-containing proteins DNMT3a (de novo DNA methylase), NSD1/2/3 (H3K36 histone methyltransferases) and BRPF1 (components of histone acetyltransferase complex) (Yun et al., 2011). More recently, ZMYND11 (also known as BS69) was found to specifically recognize histone H3.3 lysine 36 trimethylation (H3.3K36me3) via its PWWP domain, providing a link to regulate transcription elongation and pre-mRNA processing (Wen et al., 2014; Guo et al., 2014). Lastly, the PcG protein PHF19 binds H3K36me3 via its Tudor domain and then recruits PRC2 as well as the H3K36me3 demethylase NO66 to embryonic stem cell genes during cell differentiation (Brien et al., 2012).

In Arabidopsis, MRG1 and MRG2, two homologs of animal MRG15, were shown to recognize both the H3K36me3 and H3K4me3 marks to regulate flowering time (Bu

et al., 2014; Xu et al., 2014). MRG2 interacts with the transcription factor CONSTANS (CO) and enhances CO binding to the *FT* locus to activate its expression (Bu et al., 2014). In addition, MRG1/2 physically interacts with the histone H4 acetyltransferases HAM1/2 and jointly regulates the expression of *FLC* and *FT* through bridging H3K36me3 and H4 acetylation (Xu et al., 2014).

3.4.3 Readers of H3K27methylation

H3K27me2/3 deposited by PRC2 is read by PRC1. In animals, the PRC1 components Pc and CBX7 are Chromo-containing proteins responsible for H3K27me2/3 binding (Bannister et al., 2001; Bernstein et al., 2006). The PRC2 component EED also is able to recognize H3K27me3 via its WD40 domain (Margueron et al., 2009). In Arabidopsis, homolog of Pc/CBX7 cannot be found, but the Chromo-containing protein LHP1 (LIKE HETEROCHROMATIN PROTEIN 1) can bind H3K27me3 and may play an analogous PRC1 function (Zhang et al., 2007; Turck et al., 2007). Loss of *LHP1* causes pleiotropic defects, including early flowering, upward leaf curling, and reduced plant body and leaf size (Gaudin et al., 2003). More recently, genetic screens identified two Myb-family transcription factors TELOMEREREPEAT BINDING PROTEIN1 (TRB1) and TRB3 as the enhancer of the *lhp1* mutant. Both LHP1 and TRBs bind telobox-motif enriched and H3K27me3-marked genomic regions and are involved in silencing of target genes (Zhou et al., 2015).

4 Histone monoubiquitination

Ubiquitination is the covalent attachment of ubiquitin (Ub), a 76 amino acids and highly conserved protein in eukaryotes, to a substrate protein. It occurs via conjugation of the C-terminal residue of Ub to the side chain of a K residue of the substrate protein through three-step reactions (Hershko and Ciechanover, 1998; Weake and Workman, 2008; Voutsadakis, 2010; Figure 8).

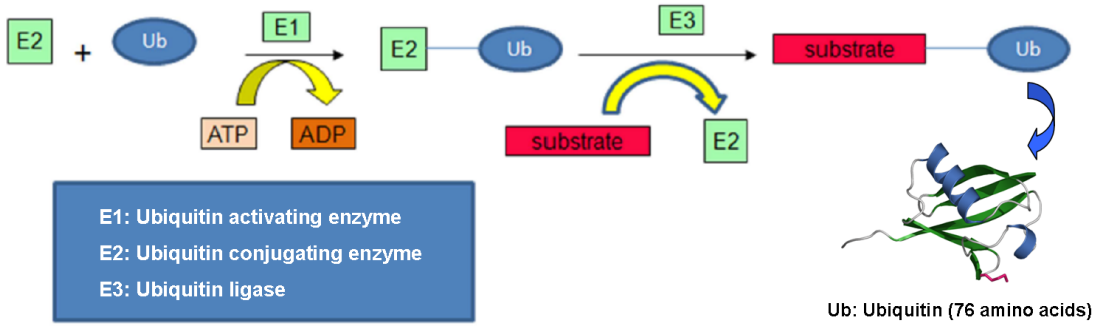

Figure 8: Enzymatic cascade of ubiquitination (Adapted from Voutsadakis, 2010).

At first step, Ub is activated by the Ub-activating (UBA) enzyme E1 in an ATP-consuming reaction. Then, the activated Ub is conjugated via a thioester bond to a cysteine residue of an Ub-conjugating (UBC) enzyme E2. Finally, the Ub from E2–Ub is transferred to the target protein by an ubiquitin-protein isopeptide ligase E3, forming a substrate–Ub via an isopeptide linkage between the C-terminus of Ub and a lysine residue of the substrate protein. A substrate may be modified by one single Ub molecule (called monoubiquitination) or by multiple Ub molecules forming a Ub chain (called polyubiquitination). Polyubiquitination via the K48 residues of the Ub molecules is recognized as a signal for targeting protein to degradation by the 26S proteasome, whereas monoubiquitination or polyubiquitination via the K63 residues of the Ub molecules is not efficiently recognized by the 26S proteasome but rather results in a modified substrate with changing activity, protein–protein interaction, subcellular localization or others (Hua and Vierstra, 2011; Braun and Madhani, 2012).

Histone ubiquitination is best studied with H2A and H2B monoubiquitination (H2Aub1 and H2Bub1), which are critical types of epigenetic marks in eukaryotes (Zhang, 2003; Feng and Shen, 2014). H2Aub1 is generally associated with transcription repression mediated by the PcG pathway, whereas H2Bub1 is involved in transcription activation (Hicke, 2001; Shilatifard, 2006; Feng and Shen, 2014).

4.1 H2B monoubiquitination

H2Bub1 is now widely accepted as an epigenetic mark involved in transcription activation. The ubiquitination site is located to a highly conserved K residue: H2BK123 in budding yeast, H2BK119 in fission yeast, H2BK120 in humans, and H2BK143 in Arabidopsis (Feng and Shen, 2014). From the genome-wide perspective, H2Bub1 is found distributed throughout the whole genome marking chromatin regions mainly in combination with H3K4me3 and/or H3K36me3 (Roudier et al., 2011).

4.1.1 Writers of H2B monoubiquitination

In yeast, the E2 enzyme Rad6 (radiation sensitivity protein 6) was firstly identified to act in conjunction with the E3 enzyme Bre1 (Brefeldin-A sensitivity protein 1) to monoubiquitinate H2B *in vivo*. Global H2Bub1 level was found decreased or undetectable in the loss-of-function mutants *rad6* and *bre1*, causing severe cell growth defects (Robzyk et al., 2000; Wood et al., 2003).

In Arabidopsis, three homologs of Rad6, namely UBC1, UBC2 and UBC3, and two homologs of Bre1, namely HISTONE MONOUBIQUITINATION1 (HUB1) and HUB2, were identified. UBC1 and UBC2 but not UBC3 have redundant functions and work together with HUB1/2 in H2Bub1 deposition (Cao et al., 2008; Gu et al., 2009; Xu et al., 2009; Fleury et al., 2007; Liu et al., 2007).

The *hub1, hub2, hub1hub2* and *ubc1ubc2* mutants display an early flowering phenotype and a reduced *FLC* expression, which is associated with reduced H2Bub1 levels at the *FLC* locus (Cao et al., 2008; Gu et al., 2009; Xu et al., 2009). In addition, the *hub* mutants showed several other defects like pale leaf coloration, modified leaf shape, reduced rosette biomass and inhibited root growth, which could be largely explained by the down-regulation of some cell cycle genes that regulate the G2-to-M transition (Fleury et al., 2007). Seed dormancy was reduced associated with altered expression levels for several dormancy-related genes in *hub* mutants (Liu et al., 2007). Several key circadian clock genes, including *CCA1 (CIR-CADIAN CLOCK ASSOCIATED1), ELF4 (EARLYF LOWERING 4) and TOC1 (TIMING OF CAB*

EXPRESSION 1), were down-regulated and exhibited reduced H2Bub1 levels in the *hub* mutants (Himanenetal et al., 2012).

H2Bub1 also plays essential roles in response to light, as evidenced by the light sensitive phenotype of the *hub1* mutant and by the finding that a large number of light responsive genes are impaired in light response during photomorphogenesis (Bourbousse et al., 2012). Moreover, *HUB1* was reported as a regulatory factor in plant defense against necrotrophic fungal pathogens. The *hub* mutants show increase susceptibility to the necrotrophic fungal pathogens *Botrytiscinerea* and *Alternaria brassicicola*, which is associated in part with modifications of cell wall and surface structures, e.g. thinner cell walls and altered surface cutin and wax compositions, together with altered induction of some defense genes (Dhawan et al., 2009; Menard et al., 2014). It was also reported that H2Bub1 modulates the dynamics of microtubules (MTs) and acts as a positive regulator of expression of genes involved in the protein tyrosine phosphatases (PTPs)-mediated signaling pathway during the plants defense response to *Verticillium dahliae* toxins (Hu et al., 2014). Lastly, *HUB1* and *HUB2* were shown to impact plant immune responses through mediating H2Bub1 at the *R* gene *SUPPRESSOR OF npr1-1 CONSTITUTIVE1 (SNC1)* locus (Zou et al., 2014).

4.1.2 Erasers of H2B monoubiquitination

H2Bub1 homeostasis is regulated additionally by deubiquitination enzymes. In yeast, H2B monoubiquitination removal is achieved by two ubiquitin-specific proteases Ubp8 and Ubp10. Ubp8 is a component of the SAGA (Spt-Ada-Gcn5-acetyltransferase) complex and it deubiquitinates H2Bub1 during transcription activation (Henry et al., 2003), whereas Ubp10 functions independently from the SAGA complex but interacts with the silencing protein Sir4 to silence telomeric and rDNA regions (Emre et al., 2005).

In Arabidopsis, there are over 50 potential deubiquitinases comprising the UBP (UBIQUITIN-SPECIFIC PROTEASE) and OTU (OVARIAN TUMOR PROTEASE) families (Yan et al., 2000; Makarova et al., 2000). Among the 27 UBPs, only UBP26 has been shown to deubiquitinate histone H2B so far. It was first reported that UBP26 deubiquitinates H2B and is involved in facilitating DNA methylation and

heterochromatin formation at transgenes and transposons (Sridhar et al., 2007). *UBP26* also played essential functions in the repression of *PHERES1* that is necessary for normal endosperm development (Luo et al., 2008). The *ubp26* mutants display an early-flowering phenotype, and molecular analysis indicates that *UBP26* is necessary for transcriptional activation of *FLC* via H2B deubiquitination (Schmitzet al., 2009). From the OTU family, OTLD1 was reported to exhibit a histone deubiquitinase activity and to interact with the histone demethylase KDM1C to repress gene repression via removal of active euchromatin marks (Krichevsky et al., 2011; Keren et al., 2016).

4.1.3 Readers of H2Bub monoubiquitination

In contrast to the small size of methyl group, Ub is about half size of histone proteins. Monoubiquitination of H2B can directly impact on nucleosome stability and chromatin function (Fierz et al., 2011). Nonetheless, studies in yeast and animals have implicated that H2Bub1 may also exert its functions by recruiting various H2Bub1-specific readers (Yun et al., 2011; Fuchs and Oren, 2014). More recently, BRG1/BAF155, a subunit of the SWI/SNF chromatin remodeling complex, was also reported to bind H2Bub1 to regulate transcription (Shema-Yaacoby et al., 2013). So far, however, specific H2Bub1 readers in Arabidopsis are still unknown.

4.2 H2A monoubiquitination

H2Aub1 was not found in yeast but was generally regarded as transcription repressive mark in both animals and plants (Weake et al., 2008; Feng et al., 2014). The human PRC1 component Ring1B (also known as Ring2 and RNF2) was the first E3 identified as involved in catalyzing H2Aub1 formation (Wang et al., 2004). In Arabidopsis, five RING-domain proteins are identified as PRC1-like components involved in catalyzing H2Aub1 formation (Molitor and Shen, 2013; Calonje, 2014).

4.2.1 Writers of H2A monoubiquitination

Based on sequence similarity, the five Arabidopsis PRC1-like RING-finger proteins can

be subdivided into two clades: RING1 (AtRING1a and AtRING1b) and BMI1 (AtBMI1a, AtBMI1b and AtBMI1c) (Sanchez-Pulido et al., 2008; Xu et al., 2008). They contain two conserved domains: an N-terminal RING-domain and a C-terminal ubiquitin-like RAWUL domain. These RING-finger proteins have been demonstrated to catalyze H2Aub1formationin *in vitro* and their loss affects H2Aub1 levels at specific genes (Bratzel et al., 2010; Li et al., 2011; Yang et al., 2013). Functional analyses have attributed crucial roles for these RING-finger proteins in plant development.

The *Atring1a* but not *Atring1b* single mutant was shown to display a late flowering phenotype, which is associated with increased expression of the *FLC*-analogous genes *MAF4* and *MAF5* (Shen et al., 2014). The double mutant *Atring1aAtring1b* displays an enlarged SAM, fascinated stem and ectopic meristem formation in cotyledons and leaves, unraveling redundant function of *AtRING1a* and *AtRING1b* in the regulation of SAM (Shoot Apical Meristem) activity (Xu et al., 2008). Accordingly, several key stem cell activity regulatory genes of the KNOX (Class IKNOTTED1-like homeobox), including *STM (SHOOT-MERISTEMLESS), BP (BRE-VIPEDICELLUS)/KNAT1, KNAT2* and *KNAT6*, were found ectopically expressed in *Atring1aAtring1b* (Xu et al., 2008). A more recent study shows that ectopic expression of *KNOX* genes also severely impacts carpel and ovule development and that *AtRING1b* but not *AtRING1a* is an imprinted gene showing exclusively maternal-preferred expression in the endosperm (Chen et al., 2016). Furthermore, the *Atring1aAtring1b* mutant exhibits perturbed cell-fate determinacy and derepression of embryonic traits during plant vegetative growth (Chen et al., 2010). Consistently, the expression level of several key embryonic regulatory genes including *ABI3* (*ABSCISIC ACIDINSENSITIVE3*), *AGL15* (*AGAMOUSLIKE 15*), *BBM* (*BABYBOOM*), *FUS3* (*FUSCA 3*), *LEC1* (*LEAFY COTYLEDON1*) and *LEC2* is drastically elevated in the mutant (Chen et al., 2010).

AtBMI1C is also a maternally endosperm imprinted gene but the single gene mutant of *Atbmi1c* does not show any obvious phenotype (Bratzel et al., 2012; Chen et al., 2016). However, overexpresion of *AtBMI1c* can cause H2Aub1 increase and can accelerate flowering time associated with reduced *FLC* expression (Li et al., 2011).

The *Atbmi1aAtbmi1b* double mutant has cell fate determinacy defects and shows ectopic expression of several seed developmental genes as observed in the *Atring1aAtring1b* mutant (Bratzel et al., 2010; Chen et al., 2010). *Atbmi1c* can enhance the *Atbmi1aAtbmi1b* mutant phenotype, unraveling thus redundant function of the three *AtBMI1* genes (Yang et al., 2013). The mutant phenotype similarity and the detection of physical interaction between AtRING1 and AtBMI1 proteins strongly indicate that these RING-finger proteins act in common complexes in transcription repression.

Interestingly, Arabidopsis PHD-domain H3K4me3-binding AL proteins were found to physically interact with both AtBMI1 and AtRING1 proteins (Moliter et al., 2014). Both *al6al7* and *Atbmi1aAtbmi1b* mutants show delayed seed germination and transcriptional derepression of seed developmental genes including *ABI3* and *DOG1*. Analyses of histone modifications indicate that the AL PHD-PRC1 complexes are involved in the H3K4me3-to-H3K27me3 chromatin state switch to repress seed developmental genes during seed germination (Moliter et al., 2014). A more recent study found that LHP1 interacts with the GAGA-motif binding factor protein BASIC PENTACYSTEINE6 (BPC6), pointing to important roles of plant GAGA binding factors in the recruitment of PRC1 components to PcG-responsive DNA element-like GAGA motifs (Hecker et al., 2015).

4.2.2 Erasers of H2A monoubiquitination

In animals, three specific H2A deubiquitinases have been identified: Ubp-M, 2A-DUB, and USP21 (Nakagawa et al., 2008). In a recently published paper, Arabidopsis UBIQUITIN SPECIFIC PROTEASES12 and 13 (UBP12 and UBP13), homologs of UBP26, were shown to have H2Aub deubiquitination activity and involved in PcG protein gene silencing; loss of *UBP12* and *UBP13* leads to defects of fertilization-independent endosperm development (Derkacheva et al., 2016).

4.2.3 Readers of H2A monoubiquitination

Human ZUOTIN-RELATED FACTOR1 (ZRF1) protein was first demonstrated to bind H2Aub1 via its UBD (ubiquitin-binding domain) domain (Richly et al., 2010). ZRF1 homologs are broadly present in the green lineage (Chen et al., 2014). The Arabidopsis genome contains two ZRF1-encoding genes, *AtZRF1a* and *AtZRF1b*. Loss of both *AtZRF1a* and *AtZRF1b* affects plant growth and development in many aspects, such as delayed seed germination, abnormal flower development and defects in both male and female transmission as well as in embryogenesis (Guzmán-López et al., 2016; Feng et al., 2016). Moreover, Arabidopsis ZRF1 proteins potentially read H2Aub1 and enhance H2Aub1 as well as H3K27me3 levels in silencing of seed developmental genes during plant vegetative growth (Feng et al., 2016).

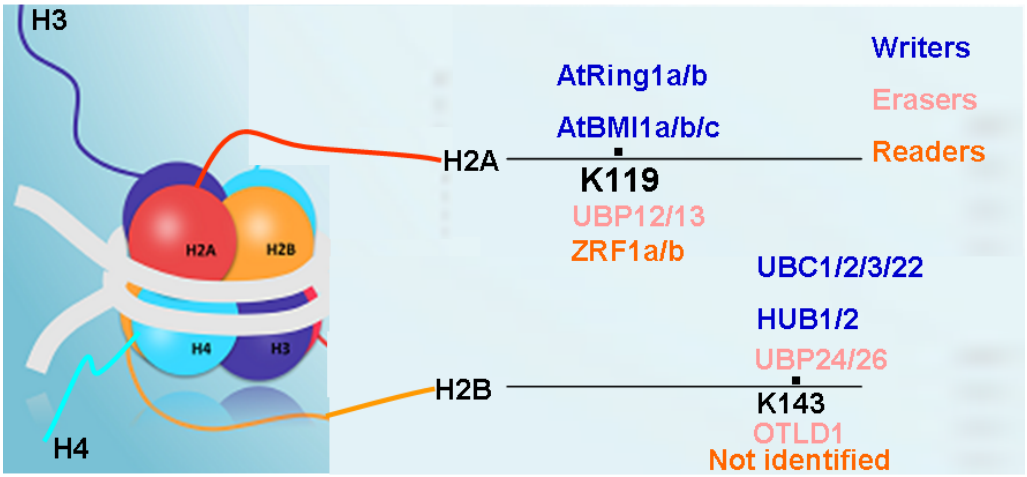

Figure 9: Writers, erasers and readers of histone H2A and H2B monoubiquitination in Arabidopsis.

5. Crosstalks between histone modifications

During the last several decades, extensive studies and significant progress have been made for the distribution, physiological and biological function of individual histone modification marks. The diversity of histone modification related proteins including writers, erasers and readers have highlighted their considerable diversity of functions. In recent years, accumulating evidence suggests that histone modifications can interplay with each other rather than only work independently, thus providing an extra

level of complexity of crosstalk regulatory network that allow the reinforcement of different effects on histone modifications in the regulation of gene transcription and organism development (Fischle et al., 2003; Berger, 2007; Fischle, 2008; Wang et al., 2015; Zhang et al., 2015).

Mechanically, crosstalk among modifications may happen at several different levels: (1) Competitive antagonism between modifications exists due to different types of modifications using the same residue, e.g. methylation and acetylation can both occur on H3K9, H3K27 and H3K36; (2) Cooperation exists between modifications, e.g. acetylated H3K9 and H3K14 help to increase H3K4me3; (3) One modification depends on another, e.g. the deposition of H3K4me3 depends on H2Bub1; (4) The protein binding ability of a particular modification can be disrupted by adjacent modification, e.g. the methylated H3K9 binding ability to HP1 is blocked by phosphorylation on adjacent H3S10; (5) An enzyme's activity can be affected by modification adjacent to its substrate e.g. the yeast Set2 is compromised by modification of isomerization happened on adjacent H3P38; (6) A second modification can cause efficient recognition of substrates by an enzyme, e.g. the GCN5 acetyltransferase recognize H3 more effectively when H3S10 is phosphorelated (Kouzarides, 2007; Suganuma and Workman 2008; Lee et al., 2010; Bannister and Kouzarides, 2011).

The crosstalks among histone modifications in plants are also widely investigated. Interestingly, Wang and her colleagues recently build a cross-talk network based on chromatin marks including histone modifications, DNA methylation, histone variants and noncoding RNAs into six classes of cross-talk interactions in Arabidopsis (Wang et al., 2015).

5. 1 Crosstalk between methylated residues

High throughput characterization of combinatorial histone marks by LC-MS/MS analysis revealed that H3K4me3 and H3K36me2/3 rarely co-occur with H3K27me3 on the same histone H3 molecule (Young et al., 2009). The *in vitro* experiments demonstrated that both H3K4me3 and H3K36me2/me3 inhibit PRC2-mediated

H3k27me3 deposition (Schmitges et al., 2011; Yuan et al., 2011).

In Arabidopsis, CLF-PRC2 is the major writer for H3K27 methylation. In *clf* mutants, H3K27me3 is decreased, which is accompanied by elevated H3K4me3 at several flowering genes including *FLC*, *MAF4*, *MAF5* and *FT* (Jiang et al., 2008). Reciprocally, reduction of H3K4me3 in the H3K4-writer mutants *atx1*, *sdg25* or *sdg26* results in an increase of H3K27me3 at *FLC* chromatin (Pien et al., 2008; Tamada et al., 2008; Berr et al., 2015). In the H3K4-eraser mutant *fld*, H3K4me3 increase is accompanied by H3K27me3 decrease (Jiang et al., 2007). Bivalent H3K4me3 and H3K27me3 have been found at many genes in Arabidopsis seedlings by epigenome profiling analysis (Roudier et al., 2011). A reciprocal antagonistic effect between H3K27me3 and H3K4me3 exists in plants as well as in animals. Remarkably, simultaneous loss of *ATX1* and *CLF* restored the leaf and flowering phenotype caused by each single mutant, thus the *atx1clf* double mutant displayed a wild-type phenotype and levels of H3K4me3 and H3K27me3 were partially restored at some genes (Saleh et al., 2007). However, such restoration had not been detected with other double mutant combinations, e.g. the *sdg25clf* double mutant displayed enhanced phenotypes compared with the *sdg25* or *clf* single mutant, and it showed an H3K27me3 reduction similar to that in *clf* and H3K4me3 reduction slightly less severe than that in *sdg25* (Shafiq et al., 2014).

An antagonistic function between H3K36me3 and H3K27me3 was observed on *FLC* expression during vernalization (Yang et al., 2014). Surprisingly, the *sdg8clf* double mutant plants showed a greater reduction in rosette size, more severely upward-curled leaves and earlier flowering time, compared with the *clf* or *sdg8* single mutant. Molecular data indicated that the increase of H3K36me3 in *clf* was attenuated in *sdg8clf*, which showed a reduction of H3K36me3 similar to that in *sdg8* but a reduction of H3K27me3 and an increase of H3K4me3 similar to those in *clf* (Shafiq et al., 2014). In addition, *sdg8clf* plants had more shoot branches with altered expression of shoot branching regulatory genes, several of which also showing reduction of H3K27me3 level as well as an elevated enrichment of H3K36me3 and H3K4me3 at those loci (Bian et al., 2016). Moreover, a drastic elevation of H3K4me3 at seed

maturation loci was observed in the *sdg8emf2* double mutant (Tang et al., 2012), but the molecular basis for this synergistic effect remains obscure. Taken together, while PcG (CLF) in transcription repression and TrxG (SDG8) in transcription activation are consistent with general knowledge, existence of a crosstalk between H3K27me3 and H3K36me3 deposition still remains elusive and needs future investigations.

In Arabidopsis H3K4me2/me3 and H3K36me3 depositions occur largely independently. It was shown that SDG8-mediated H3K36me3 overrides ATX1/ATX2-mediated H3K4me2/me3 and LDL1/LDL2-mediated H3K4 demethylation in regulating *FLC* expression (Shafiq et al., 2014). This is in contrast to the study in yeast where Set1 (H3K4 methyltransferase) is required for Set2 to perform H3K36 methylation (Biswas et al., 2006).

5. 2 Crosstalk between H3 methylation and H2A/H2B monoubiquitination

Crosstalk between different modifications can occur on the same histone (crosstalk in *cis*) or between different histones (crosstalk in *trans*). The best-studied crosstalk in *trans* is between H3K27me3 and H2Aub1 during PcG-mediated gene silencing. In general, the H3K27me3 deposited by PRC2 is read by PRC1, which in turn carries out H2Aub1 deposition (Wang et al., 2004). Another example of crosstalk in *trans* is between H3K4me3/H3K36me3 and H2Bub1 in transcription activation.

In yeast, the Rad6-mediated H2Bub1 was first found to be required for proper deposition of H3K4me3 catalyzed by Set1 within the COMPASS complex, in such H3K4me3 was almost undetected in the Rad6-depleted yeast mutant strain (Sun et al., 2002; Dover et al., 2002). Following this discovery, it was reported that Rad6-mediated H2Bub1 is also a prerequisite for the Dot1-mediated H3K79me3 deposition (Ng et al., 2002). This so-called trans-tail histone modification pathway is also conserved in human (Kim et al., 2005; Zhu et al., 2005; Kim et al., 2009).

There are several molecular mechanisms discovered for the crosstalk in yeast and human. Firstly, Cps35, an essential subunit of COMPASS complex, is required for

COMPASS' catalytic activity *in vivo*. Interestingly, Cps35 only associates with the COMPASS in activating it for catalyzing H3K4me3 when the chromatin is decorated by H2Bub1 (Lee et al., 2007). The H3K79me3 deposition by Dot1 is also dependent on Cps35 (Lee et al., 2007). Secondly, *in vitro* experiments show that chemically ubiquitinated H2B, when incorporated into nucleosomes, could directly stimulate the catalytic activity of recombinant human Dot1, suggesting an additional mechanism for crosstalk between H2Bub1 and H3K79me3 (McGinty et al., 2008). Thirdly, H2Bub1 enhances activity of the yeast Set1C methyltransferase complex *in vitro* without affecting its assembly *in vivo* (Racine et al., 2012). Fourthly, n-SET domain within yeast Set1 as well as ASH2L in the human MLL complex is essential for H2Bub1-dependent H3K4 methylation (Kim et al., 2013; Wu et al., 2013).

In addition to H2Bub1 deposition, H2B deubiquitination is also involved in regulation of *trans* crosstalk, in particular in relation with H3K36 methylation. In yeast, a mutation of the H2B deubiquitinase Ubp8 causes H2Bub1 increase together with H3K36me2 decrease, indicating that H2B deubiquitination is required for H3K36me2 deposition (Henry et al., 2003). Either substitution of the ubiquitination site in H2B (Lys123) or loss of Ubp8 can reduce specific genes expression levels, indicating that both ubiquitination and de-ubiquitination of H2B are required for gene activation, contrasting the opposite roles between histone acetylation and deacetylation in transcription regulation (Wyce et al., 2004). It was shown that deubiquitination of H2B is important for recruitment of a complex containing the kinase Ctk1, which phosphorylates the RNA polymerase II (Pol II) C-terminal domain (CTD), and for subsequent recruitment of the Set2 methyltransferase in H3K36 methylation. Thus, the H2BK123ub1 acts as a ‘‘barrier’’ to block interaction of Ctk1 with histones, thereby reducing CTDS2ph and subsequent H3K36 methylation (Wyce et al., 2007).

In summary, the studies in yeast and human indicate that H2B monoubiquitination is required for H3K4me3 deposition during transcription initiation, and its deubiquitination is necessary for H3K36me3 deposition during transcription elongation. It was proposed that similar crosstalks may also exist in Arabidopsis (Figure 10). First, the key enzymes are found in Arabidopsis: HUB1/2 and UBC1/2 were identified as the

homologue of Bre1 and Rad6, respectively, and were shown to be responsible for H2Bub1 deposition (Fleury et al., 2007; Liu et al., 2007; Cao et al., 2008; Xu et al., 2009; Gu et al., 2009); UBP26 was characterized as the H2B deubiquitination enzymes, similar to Ubp8/Ubp10 (Sridhar et al., 2007; Schmitz *et al*., 2009); SDG8 was identified as a major histone H3K36-methyltransferase, analogous to SET2 (Zhao et al., 2005; Xu et al., 2008); several H3K4-methyltransferases were also identified (Alvarez-Venegas et al., 2003; Berr et al., 2009; Berr et al., 2010; Guo et al., 2010). Second, loss of HUB1/2, UBC1/2 or UBP26 causes defects with similarity to *sdg8* mutant, e.g. early flowering, impaired resistance to pathogens (Cao et al., 2008; Schmitz *et al*., 2009; Berr et al., 2010; Zou et al., 2014). Lastly, loss of H2Bub1 reduces the H3K4me3 level and the *ubp26* mutant shows reduced H3K36me3 at *FLC* and some other genes (Cao et al., 2008; Schmitz *et al*., 2009). Nevertheless, more experimental data will be necessary to further verify/confirm/improve this model (Figure 9).

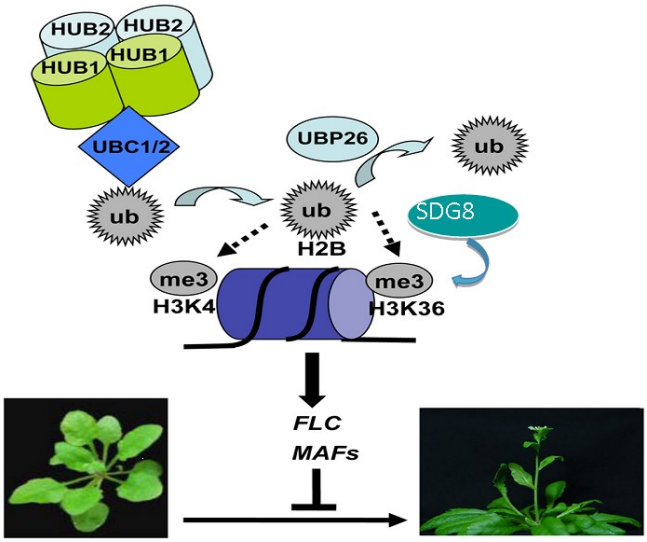

Figure 10: A proposed model for deposition and removal of histone H2B monoubiquitination in transcriptional activation of *FLC* and *MAFs* in flowering time regulation (adapted from Feng and Shen, 2014).

6. Flowering time regulation

Flowering represents the transition from the vegetative to reproductive development, commonly was referred as floral transition during plant life cycle (Figure 10). Correct timing to flowering is crucial for the reproductive success of plants, enabling completion of seed development in desirable environmental conditions. Each plant species has developed optimum systems for its flowering time regulation (Jung and Muller, 2009; Blumel et al., 2015; Bratzel and Turck, 2015). *Arabidopsis thaliana* has been the most used model plant in flowering time studies.

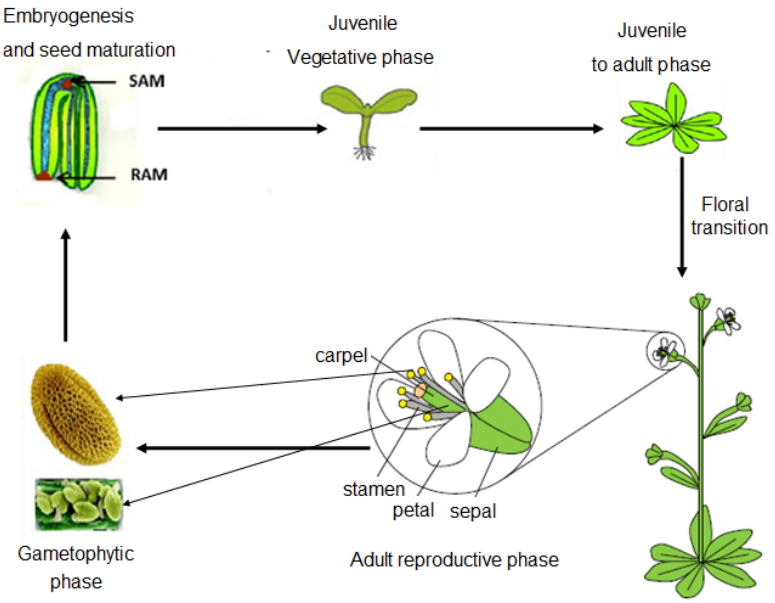

Figure 11: Phases of plant development. After fertilization, root apical meristem (RAM) and the shoot apical meristem (SAM) (red) is formed in the embryo. Upon germination, plants generally undergo two major developmental transitions, one is juvenile- to-adult phase transition (vegetative stage), followed by a vegetative to reproductive phase transition (reproductive flowering stage) and eventually seed set and senescence (Adapted from Liu et al., 2009; Huijser and Schmid, 2011; Poethig, 2013).

6.1 *Arabidopsis thaliana* as a model plant

Arabidopsis plant is small in size, thus can be easily grown in an indoor growth

chamber or greenhouse. In addition, its short life cycle (6 weeks), reproduction primarily by self-fertilization, rapid flowering and production of a large number of seeds also have helped to make it an ideal model plant (Dean, 1993; Meyerowitz and Somerville, 1994; Meinke et al., 1998). *Arabidopsis thaliana* is the first plant species to be sequenced at whole genome level (Arabidopsis Genome Initiative, 2000). It has been largely used to investigate the plant biological processes, plant physiology, molecular biology, genetics and epigenetic regulations. Genetic resources of this model organism are excellent, rich with ecotypes exhibiting different flowering times.

6.2 Genetic pathways in flowering time control

In *Arabidopsis*, the endogenous cues such as plant age and hormone (mainly giberellin acid, GA) coordinate with exogenous or environmental cues such as light (light intensity and duration of exposure) and temperature (winter vernalization) to determine when plants flower. Together, five major genetic pathways control flowering time (Figure 12).

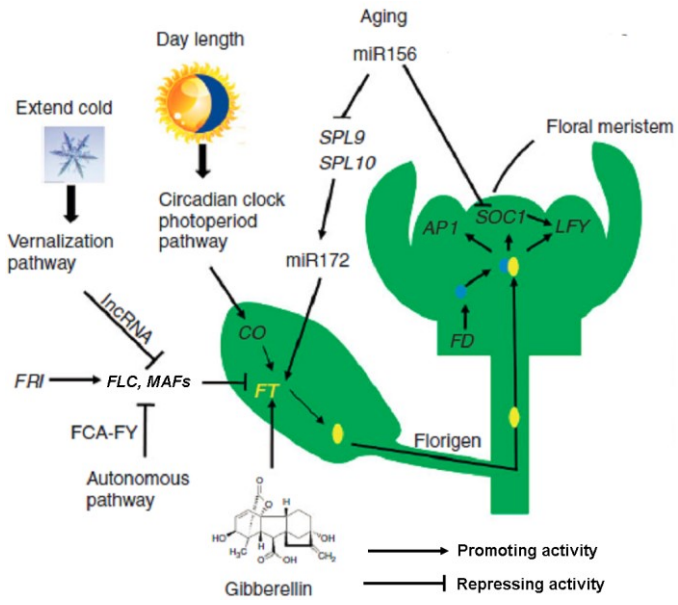

Figure 12: A simplified diagram of five independent flowering pathways in Arabidopsis: vernalization, photoperiod, autonomous, gibberellin, and aging (Adapted from Khan et al., 2013).

Different pathways converge to regulate the expression of a set of floral integrator genes, e.g. *FLOWERING LOCUS T* (*FT*), *SUPPRESSOR OF OVEREXPRESSION OF CONSTANS 1/AGAMOUS-LIKE 20* (*SOC1/AGL20*). Floral integrators in turn activate some key meristem identity genes, such as *LEAFY* (LFY), *APETALA1* (*AP1*), *SEPAL-LATA3* (*SEP3*) and *FRUITFULL* (*FUL*) that irreversibly confer the transition from a vegetative to a floral meristem (He and Amasino, 2005; Farrona et al., 2008). *FT* encodes a florigen, capable of long-distance moving from the leaves to shoot apices to promote flowering, preferentially through the photoperiod pathway (Turck et al., 2008; Andrés and Coupland, 2012; Song et al., 2015). It works as a parallel integrator as well as an upstream activator of *SOC1* (Lee and Lee, 2010).

The photoperiod pathway regulates flowering time in response to day length. Arabidopsis is a long-day facultative plant, thus its flowering is promoted at long-day photoperiod growth conditions. The genes *GIGANTEA* (*GI*), *CRYPTOCHROME2/ FHA (CRY2), FLAVIN KELCH F BOX 1* (*FKF1*) and *CONSTANS* (*CO*) have major roles in the photoperiod pathway, as evidenced by observation that mutations in these genes delay flowering in long days but not in short days (Turck et al., 2008). The *CO* gene encodes a putative zinc finger transcription factor and is essential for photoperiod perception. *GI* encodes a plant specific protein that physically interacts with ubiquitin ligase KFK1; together the blue light receptor CRY2, they act upstream of *CO* to increase its mRNA level and also stabilize CO protein (Turck et al., 2008; Andrés and Coupland, 2012).

Vernalization is a process by which exposure to prolonged cold temperatures (e.g. winter) accelerates flowering. There are two major types of Arabidopsis accessions, summer annuals (no vernalization requirement) and winter annuals (vernalization responsive). Vernalization requirement in winter annuals is conferred by dominant alleles of *FRIGIDA (FRI*) and *FLC*. *FRI* encodes a coiled-coil protein that elevates *FLC* expression to levels that inhibit flowering, resulting in the winter-annual growth habit (Johanson et al., 2000). Winter annuals only flower rapidly after exposure at a low temperature (4 °C) for 6 to 12 weeks (mimic the transition from winter to spring), during which *FLC* transcription is turn-off gradually and maintained stably later-on (Amasino,

2004; Sung 2005; Sung and Amasino, 2005; Kim et al., 2009). *FLC* encodes a MADS box transcription factor that blocks the floral transition through repression of *FT* and *SOC1*. *FLC* has five paralogs, namely *MADS AFFECTING FLOWERING 1*/*FLOWERING LOCUS M* (*MAF1*/*FLM*), and *MAF2* to *MAF5*; they have redundant functions in repressing flowering under certain conditions (Ratcliffe et al., 2001; Scortecci et al., 2003; Gu et al., 2013).

The autonomous pathway was initially defined by a group of mutants that are late flowering under all photoperiods and are highly responsive to vernalization. This pathway regulatory genes include *LUMINIDEPENDENS* (*LD*), *FCA*, *FY*, *FPA*, *FLOWERINGLOCUS D* (*FLD*), *FVE*, and *FLOWERING LOCUS K (FLK*). Arabidopsis plants containing mutations in these genes have elevated levels of *FLC* expression. Notably, their late-flowering phenotype can be overcome by vernalization treatment. Thus, the autonomous pathway constitutively activates flowering by reduce *FLC* expression (Mouradov et al., 2002; Srikanth and Schmid, 2011).

During the last decade, an endogenous pathway that adds plant age to the control of flowering time has been extensively studied. The Arabidopsis age pathway is mainly mediated by two key miRNAs, miR156 and miR172. *MiR156* is highly expressed in the juvenile stage and decreases during the following adult stage, which negatively regulate several *SQUAMOSA PROMOTER BINDING PROTEIN-LIKE* (*SPL*) genes that promotes flowering even under a non-inductive photoperiod, mainly through activating the floral meristem identity gene *LEAFY* (*LFY*). MiR172 is an activator of flowering; it has an expression pattern opposing MiR156. MiR172 directly repress its target *AP2-like* genes, including *AP2*, *SCHLAFMUTZE* (*SMZ*), *SCHNARCHZAPFEN* (*SNZ*), *TARGET OF EAT1* (*TOE1*), *TOE2*, and *TOE3* that normally repress flowering by down-regulating *SOC1*. Therefore, miR156 and miR172 form a complementary relationship in the aging pathway to fine-tune the flowering time in Arabidopsis (Khan et al., 2013; Teotia and Tang, 2015; Hyun et al., 2017).

Besides these major pathways, flowering time is also influenced by other plant hormones such as cytokinins, brassinosteroids, ethylene, salicylic acid, and abscisic acid, as well as by other environmental factors such as nutrients, ambient temperature,

drought, salinity, chemicals, and pathogenic microbes (Tang et al., 2015; Kazan and Lyons, 2015; Cho et al., 2016; Ionescu et al., 2016).

6.3 Flowering time regulation via chromatin modifications

FLC served as target has been extensively studied during the functional characterization of writers, erasers and readers of histone modifications. While other flowering genes, e.g. *FT* and *SOC1*, are also regulated by histone modifications, epigenetic regulation of *FLC* remains the best elucidated (Farrona et al., 2008; He, 2012; Hepworth and Dean, 2015; Berry and Dean, 2015). Below, I focus on both repression and activation of transcription to summarize the regulators involved in histone methylation and monoubiquitination in the regulation of *FLC* expression and flowering time.

6.3.1 Epigenetic repression of *FLC* by H3K27 methylation

H3K27me3 is a key epigenetic mark in silencing *FLC* during the process of vernalization. *VERNALIZATION INSENSITIVE3* (*VIN3*), which is quickly up-regulated upon cold exposure, functions in a cold perception system that measure the time of cold exposure. VIN3 is a plant homeodomain (PHD) protein; it has three homologs VIN3-LIKE 1(VIL1)/VERNALIZATION5 (VRN5), VIL2/VIN3-LIKE1 (VEL1) and VIL3/VEL2. During prolonged cold, VIN3, VIL1 and VIL2 act as part of VRN2-PRC2 complex by physically interact with PRC2 core subunits (Wood et al., 2006; De Lucia et al., 2008). The newly formed PHD-PRC2 complex specifically targets to the nucleation region that is located just downstream of the *FLC* transcription start site and comprises about three nucleosomes (Figure 13B).

Two long noncoding RNAs (lncRNAs), COLDAIR and COOLAIR, generated during cold exposure from *FLC*, are also involved in vernalization-mediated *FLC* repression (Swiezewski et al., 2009; Heo and Sung, 2011). COOLAIR was proposed to be required to ensure removal of activating chromatin marks at the nucleation region and to mediate *FLC* transcriptional down-regulation (Swiezewski et al., 2009; Berry

and Dean, 2015); while COLDAIR physically interact with CLF *in vivo* and was thought to recruit PHD-PRC2 complex to *FLC* (Heo and Sung, 2011).

H3K27me3 is deposited by PHD-PRC2 complex at the nucleation region of *FLC* and its level increases at this region in proportion with the length of cold experienced (Figure 13B). Upon vernalization accomplishment, PHD-PRC2 spreads to cover the whole *FLC* locus and leads to high H3K27me3 along its entire length, resulting in epigenetically silenced state of *FLC* that is stable after return to warm temperature (Figure 13C). The H3K27me3 reader LHP1 also plays an important role in maintaining epigenetic silencing of *FLC* (Mylne et al., 2006). Albeit an uncovered role of AtRING1a in flowering time regulation through repression of *MAF4/5* (Shen et al., 2014), whether PRC1-mediated H2Aub1 plays a function in repression of *MAF4/5* and/or *FLC* remains currently unclear.

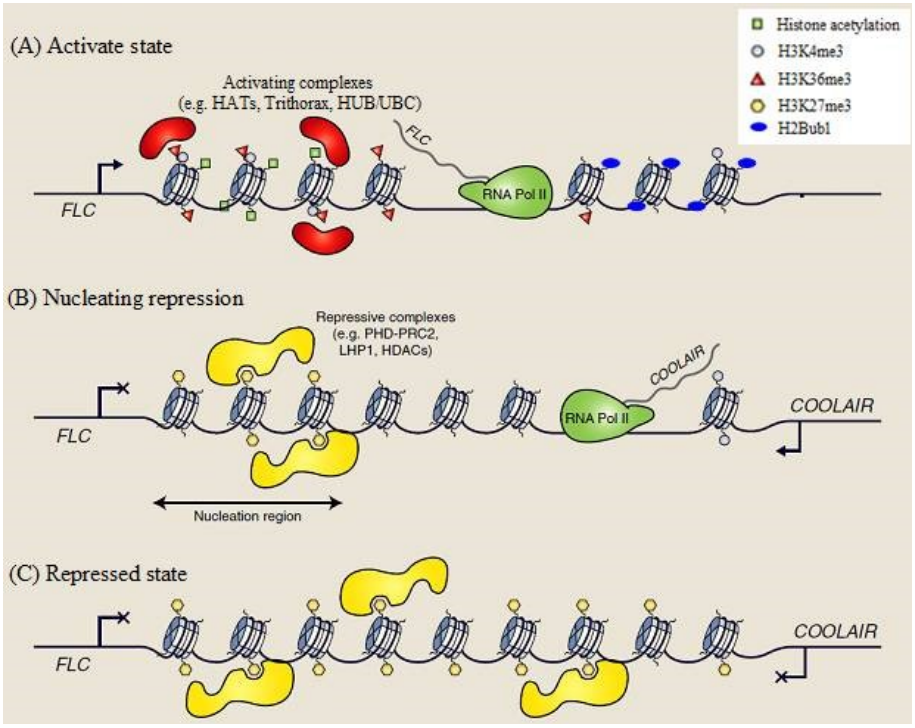

Figure 13: *FLC* chromatin state before (A), during (B) and after (C) cold in vernalization process (Adapted from Berry and Dean, 2015).

6.3.2 Epigenetic activation of *FLC* by histone modifications

FLC expression is reset to high level during embryogenesis to ensure vegetative

growth of the next generation (Sheldon et al., 2008). The H3K27me3 eraser ELF6 was found to be essential for *FLC* activation; in the next generation of *elf6* mutants, H3K27me3 levels at the *FLC* locus induced by vernalization was found not fully removed and stayed high (Crevillen et al., 2014).

In addition to H3K27me3 removal, deposition of active epigenetic marks is essential for maintaining *FLC* expression. H3K4me3, H3K36me3, H2Bub1 as well as acetylated histones are broadly found to be enriched at activated *FLC* loci, indicating these marks are involved in *FLC* activation (Berr et al., 2011; Berry and Dean, 2015)(Figure 12A). Enzymes that is responsible for deposition of active histone marks such as ATX1 and SDG25 in H3K4 methylation (Pien et al., 2008; Tamada et al., 2008; Shafiq et al., 2014), SDG8 in H3K36 methylation (Zhao et al., 2005; Shafiq et al., 2014; Berr et al., 2015), UBC1/2 and HUB1/2 in H2B monoubiquitination (Cao et al., 2008) are all involved in generating an active *FLC* chromatin state for high levels of *FLC* expression.

Objectives of Thesis

Objectives of my PhD thesis focus to identify and characterize new writers/readers of histone methylations and to dissect crosstalk between H3K36 methylation and H2B monoubiquitination for an improved understanding of function of histone modifications in the regulation of gene transcription and plant growth and development.

In collaboration with the laboratory of Dr. Richard Amasino, we functionally characterized a new TrxG member, a homologue of SDG8, named SDG7. Genetic and molecular data demonstrated its fundamental role in the proper timing of the vernalization process. The major results are published and here included as **Chapter I**.

In animal and yeast, the crosstalk between histone H3K4me3/H3K36 methylation and H2B monoubiquitination in transcription activation is well documented. In plants, considerably less is known and studies were mainly concentrated on studying the functional relationship between H2Bub1 and H3K4me3. In order to fill this shortfall, I explored the functional interaction between H2Bub1 and H3K36me3 using a genetic approach based on crosses between different histone-modifying enzyme mutants. My studies mainly focused on the interplay of these different histone marks in regulation of plant growth and gene transcription. Results from this part are presented as **Chapter II**.

Compared to modifications like acetylation and monoubiquitination, histone methylation does not per se directly trigger changes in the chromatin structure but they require specific “readers” that will recognize one or more methylation signals and interpret it. In Arabidopsis, little is currently known about histone methylation readers, and especially regarding the domains involved in this binding as well as their specificity. In the last part, I described a group of histone methylation readers with a particular attention to the binding affinity of their PWWP domain. Results from this part are presented as **Chapter III**.

CHAPTER I

Functional Characterization of SDG7

(*PNAS*, vol. 112., no. 7, page. 2269–2274)

(A)

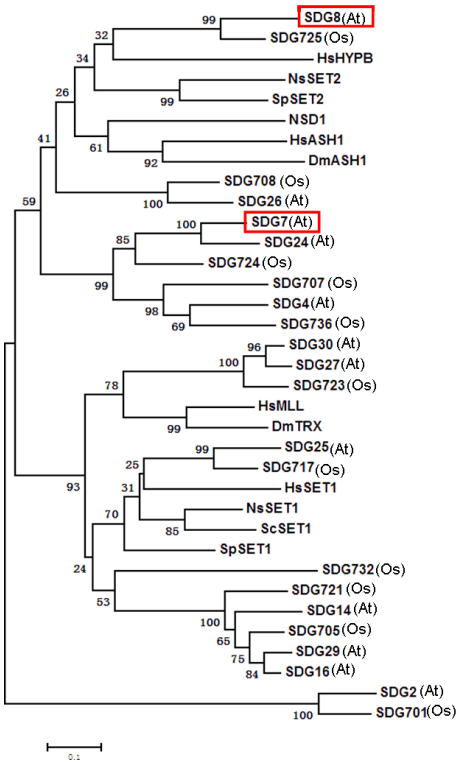

At, *Arabidopsis thaliana*;
Os, *Oryza sativa*;
Sp, *Schizosaccharomyces pombe*;
Sc, *Saccharomyces cerevisiae*;
Nc, *Neurospora crassa*;
Dm, *Drosophila melanogaster*;
Hs, *Homo sapiens*.

(B)

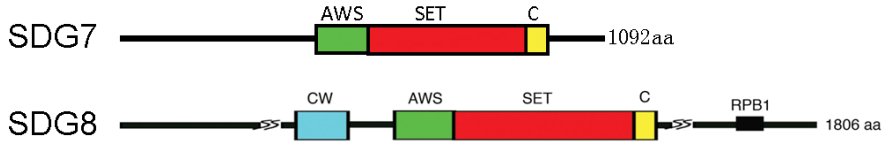

Figure (A) Phylogenetic analysis of TrxG family proteins in animals and plants. It showed that Arabidopsis proteins SDG7 and SDG8 belong to the same clade. (B) Schematic diagram of the SDG7 and SDG8 proteins. Both proteins contain the conserved domains of AWS, SET and post-SET.

A methyltransferase required for proper timing of the vernalization response in *Arabidopsis*

Joohyun Lee[a], Jae-Young Yun[a], Wei Zhao[b], Wen-Hui Shen[b], and Richard M. Amasino[a,1]

[a]Department of Biochemistry, University of Wisconsin–Madison, Madison, WI 53706; and [b]Institut de Biologie Moléculaire des Plantes du CNRS, Université de Strasbourg, Strasbourg 67084, France

Contributed by Richard M. Amasino, December 10, 2014 (sent for review October 2, 2014; reviewed by George Coupland and Ben Trevaskis)

Prolonged exposure to winter cold enables flowering in many plant species through a process called vernalization. In Arabidopsis, vernalization results from the epigenetic silencing of the floral repressor FLOWERING LOCUS C (FLC) via a Polycomb Repressive Complex 2 (PRC2)-mediated increase in the density of the epigenetic silencing mark H3K27me3 at FLC chromatin. During cold exposure, a gene encoding a unique, cold-specific PRC2 component, VERNALIZATION INSENSITIVE 3 (VIN3), which is necessary for PRC2-mediated silencing of FLC, is induced. Here we show that SET DOMAIN GROUP 7 (SDG7) is required for proper timing of VIN3 induction and of the vernalization process. Loss of SDG7 results in a vernalization-hyper-sensitive phenotype, as well as more rapid cold-mediated up-regulation of VIN3. In the absence of cold, loss of SDG7 results in elevated levels of long noncoding RNAs, which are thought to participate in epigenetic repression of FLC. Furthermore, loss of SDG7 results in increased H3K27me3 deposition on FLC chromatin in the absence of cold exposure and enhanced H3K27me3 spreading during cold treatment. Thus, SDG7 is a negative regulator of vernalization, and loss of SDG7 creates a partially vernalized state without cold exposure.

vernalization | flowering time | SET DOMAIN GROUP 7

Seasonal timing of flowering is critical for reproductive success in many plant species. The timing of flowering is often strongly influenced by seasonal variables, such as day length and temperature. Vernalization, the process by which exposure to the prolonged cold of winter enables flowering in the spring, is an example of a temperature effect on flowering (1).

Arabidopsis thaliana contains both vernalization-requiring accessions (winter annual) and accessions that do not require vernalization (summer annual). The vernalization requirement is conferred by FRIGIDA (FRI)-mediated up-regulation of the potent flowering repressor FLOWERING LOCUS C (FLC) (2, 3). The presence of active alleles of FRI and FLC ensures that flowering is repressed in the fall season. Summer annual accessions do not require vernalization to flower, because these accessions typically contain a mutant allele of FRI that is not able to up-regulate FLC (4). On perception of a sufficiently long period of cold, vernalization results in the chromatin-level suppression of FLC, which in turn provides competence to flower (3, 5). Thus, in Arabidopsis, vernalization is an environmentally induced epigenetic switch (6).

Vernalization-mediated FLC silencing is associated with an increase of two chromatin modifications involving trimethylation of histone 3 at lysine 9 (H3K9me3) and at lysine 27 (H3K27me3) (7, 8). The increase in H3K27me3 results from the action of the Polycomb Repressive Complex 2 (PRC2) on *FLC* chromatin (9). Many of the PRC2 components are conserved among plants, animals, and fungi (10, 11); however, a plant-specific PRC2-associated protein, VERNALIZATION INSENSITIVE 3 (VIN3), is required for vernalizationand is uniquely expressed during cold (6). Thus, the cold-induced expression of *VIN3* is a critical event in vernalization process (6, 12). The system by which cold perception leads to induction of *VIN3* is not well understood, however, and to date there is no evidence suggesting that it shares features with cold acclimation in *Arabidopsis* (13).

Here we report that SET DOMAIN GROUP 7 (SDG7), an extranuclear methyltransferase (14), is required for proper timing of *VIN3* induction and of the vernalization process. *SDG7* was isolated by a screening an ethyl methane sulfonate-mutagenized population for mutants in which *VIN3* is induced more rapidly during cold exposure. Loss of *SDG7* results in plants that exhibit a hypersensitive vernalization response, more rapid induction of *VIN3* during cold exposure, higher levels of the *FLC*-complementary noncoding RNAs COLDAIR (15) and COOLAIR (16) in the absence of cold, and increased H3K27me3 levels at *FLC* chromatin both with and without cold exposure.

Results and Discussion

A Mutation in *SDG7* Alters *VIN3* Expression and Flowering Behavior. To explore the system by which cold exposure leads to the induction of *VIN3* expression, we screened for mutants that exhibited altered timing of expression of a *VIN3* reporter gene construct, *VIN3p::GUS*. Because *VIN3* is induced by cold in both root and shoot apical meristems, we screened for mutants in which *VIN3* is more rapidly induced in the root apical meristem, to enable the use of a viable GUS-staining system (17) (Fig. 1*A*). We characterized in detail a mutant line that exhibits detectable expression of the *VIN3* transgene as well as the native *VIN3* gene before cold exposure and rapid induction of *VIN3* on cold exposure in both the root and shoot apices (Fig. 1 *A*–*C*). In a *FRI*-containing background, in which the presence of *FRI* creates a vernalization requirement (2–4), the mutation results in a more rapid vernalization response, as well as more rapid flowering without cold exposure (Fig. 1*D*). The mutation had no visual phenotypes other than the flowering phenotypes. It behaved recessively and segregated in a 3:1 ratio (342:110; $\chi^2 = 0.74$; $P > 0.05$) in an F2 population, indicating that the mutant phenotype is attributed to a single locus.

To identify the causative mutation, we carried out whole-genome sequencing (18–20) on DNA pooled from mutants in an

Significance

Proper timing of flowering is a key factor in reproductive success. Certain plant species require prolonged cold exposure during winter to flower in the spring; however, how plants measure the duration of cold exposure is not well understood. In this study, we describe the identification of a methyltransferase that is required for proper measurement of the duration of cold exposure.

Author contributions: J.L., J.-Y.Y., and R.M.A. designed research; J.L., W.Z., and W.-H.S. performed research; J.L. analyzed data; and J.L. and R.M.A. wrote the paper.

Reviewers: G.C., Max Planck Institute for Plant Breeding Research; and B.T., Commonwealth Science and Industry Research Organization.

The authors declare no conflict of interest.

[1]To whom correspondence should be addressed. Email: amasino@biochem.wisc.edu.

This article contains supporting information online at www.pnas.org/lookup/suppl/doi:10.1073/pnas.1423585112/-/DCSupplement

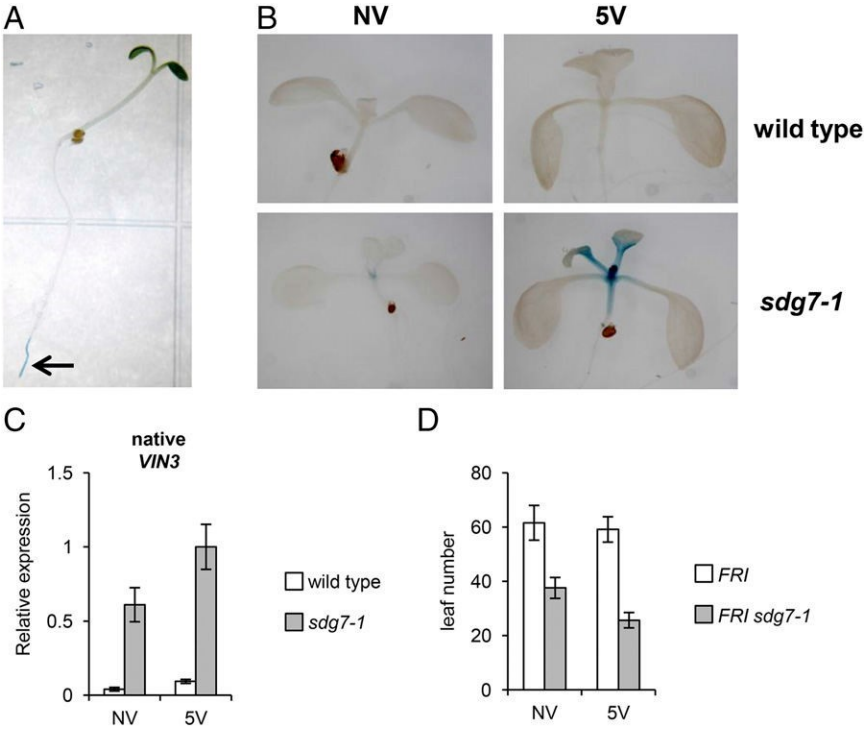

Fig. 1. Loss of *SDG7* results in increased *VIN3* expression and more rapid flowering. (*A*) *VIN3* reporter gene expression in *sdg7-1* using a viable GUS staining assay. The arrow indicates *VIN3p::GUS* expression in the root tip. (*B*) *VIN3p::GUS* expression in the shoot apex region using destructive GUS staining. (*C*) Elevated *VIN3* expression in *sdg7-1* without cold exposure (NV) and more rapid induction of *VIN3* after 5 d of cold exposure (5V). (*D*) Flowering behavior, represented as the number of rosette leaves generated on the primary shoot before the transition to flowering, of *sdg7* in the *FRIGIDA* (*FRI*) background (*FRI sdg7*) and the Col *FRI* reference line, which is *FRI* introgressed into Col (34), in long day (16 h light/8 h dark) without cold exposure (NV) and with 5 d cold exposure (5V). Expression data are presented as mean values of three biological replicates, and flowering time data are presented as mean values of 12 individual plants. Error bars indicate SD.

F2 population; as controls, Col *fri*, Col *FRI*, the *FRI*-containing mutant, and *VIN3p::GUS* lines were sequenced in parallel. Analysis of the sequence data revealed a likely causative C-to-T mutation in the *SDG7* gene on chromosome 2 (Fig. S1*A*). We refer to this mutation as *sdg7-1*. The mutation caused a missense mutation (Pro to Leu) in the SET domain, a domain conserved in certain methyltransferases in many eukaryotes (Fig. S1*B*). To evaluate whether the rapid flowering of the mutant is caused by mutation of *SDG7*, a *FRI*-containing line with the *sdg7-1* mutation was crossed to T-DNA null allele of *SDG7* (*sdg7-2*) (Fig. S1

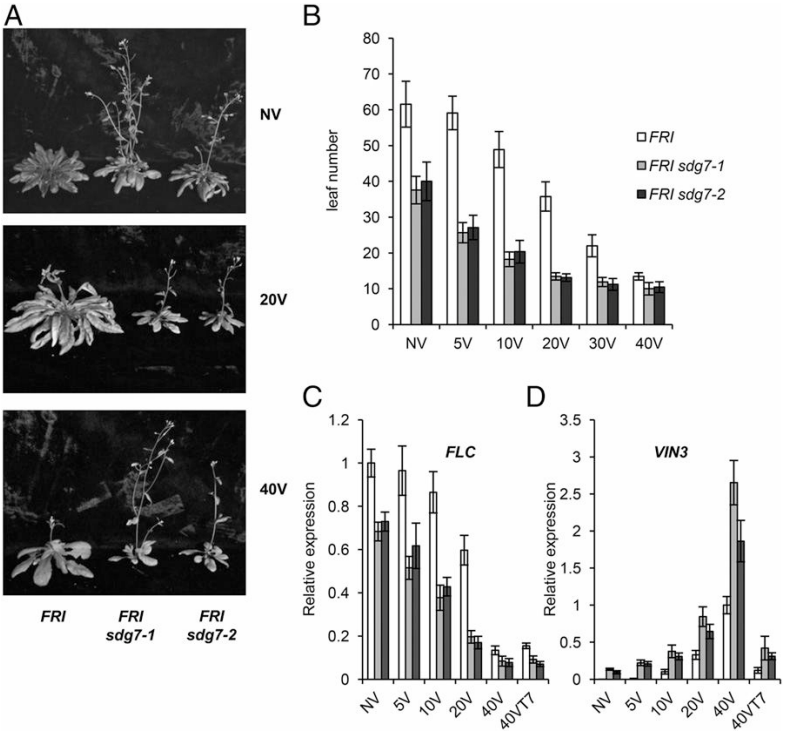

Fig. 2. Loss of *SDG7* results in a more rapid vernalization response and altered timing of *VIN3* and *FLC* expression. (*A*) Flowering phenotypes of *FRI*, *FRI sdg7-1*, and *FRI sdg7-2* without (NV) or with 20 d (20V) or 40 d (40V) of cold exposure. (*B*) Flowering behavior, measured as number of primary leaves formed, as a function of length of cold exposure. 5V, 10V, 20V, 30V, and 40V indicate the number of days of cold exposure. (*C*) *FLC* repression in *sdg7-1* and *sdg7-2* as a function of duration of cold exposure compared with Col *FRI*. 40VT7 represents 40 d of cold treatment followed by 7 d of growth at 22 °C. (*D*) *VIN3* expression as a function of duration of cold exposure in the *sdg7* mutants and WT. Flowering time data are presented as mean values of 12 individual plants, and expression data are presented as mean values of three biological replicates. Error bars indicate SD.

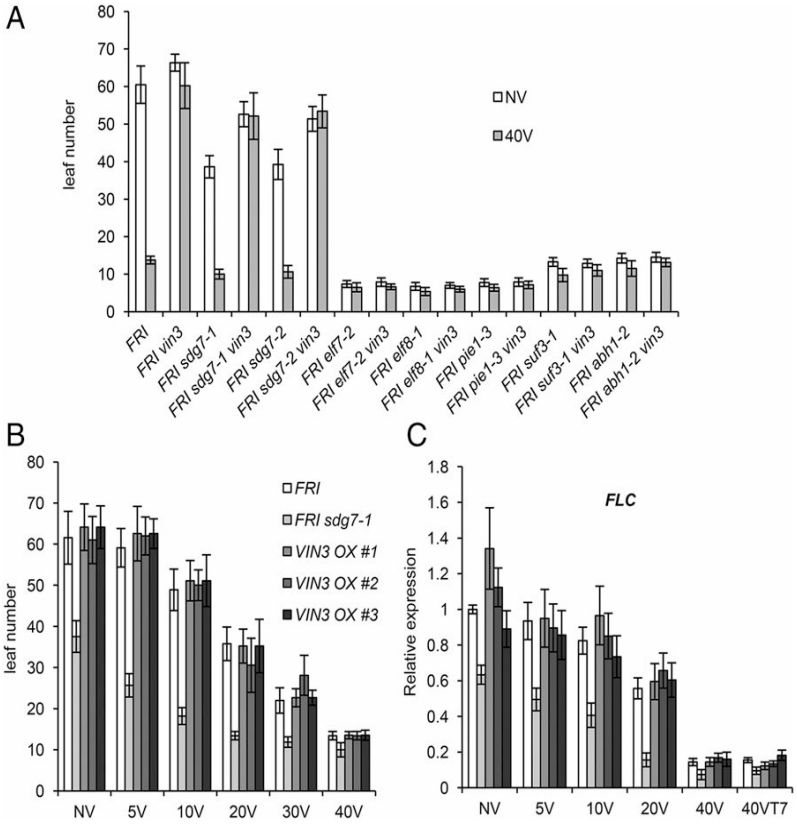

Fig. 3. *VIN3* dependence of the *sdg7* phenotype. (*A*) *VIN3*-dependent flowering in *sdg7* was evaluated by determining the primary shoot leaf number of a *FRI sdg7 vin3* mutant without vernalization (NV) and after 40 d of vernalization (40V) in long days. As a control, epistasis analysis was performed with rapid-flowering mutants in the following genes: *EARLY FLOWERING7* (*ELF7*) and *ELF8*, components of RNA polymerase II-associated factor 1 complex (Paf1c), which catalyzes H3K4 methylation; *PHOTOPERIOD INDEPENDENT EARLY1* (*PIE1*) and *SUPPRESSOR OF FRIGIDA3* (*SUF3*)/*ACTIN-RELATED PROTEIN6* (*ARP6*)/*EARLY IN SHORT DAYS1* (*ESD1*), which are components of an AtSWR1 complex involved in H2A.Z replacement; and *ABA HYPERSENSITIVE 1*(*ABH1*)/*CAP BINDING PROTEIN 80* (*CBP80*). (*B*) Flowering behavior was monitored in three individual lines of *VIN3* overexpressors with and without cold treatment. (*C*) *FLC* expression in the *VIN3* overexpressors. Flowering time data are presented as mean values of 12 individual, plants and expression data are presented as mean values of three biological replicates. Error bars indicate SD. Symbols for the duration of cold exposure are as in the legend to Fig. 2.

A and *C*). F1 plants from this cross (which had the genotype *FRI/-*; *sdg7-1/sdg7-2*) and all *FRI/-;sdg7/sdg7* plants in an F2 population derived from the F1 had the same flowering phenotype as the original *sdg7-1* mutant in the *FRI*-containing background, indicating that *SDG7* is indeed the causative gene (Fig. S1 *D* and *E*).

Vernalization Hypersensitivity of *SDG7*. To further characterize the effect of loss of *SDG7* on the vernalization process in the *FRI* background, we measured the number of leaves formed before flowering as a function of the duration of cold exposure. The *FRI sdg7-1* and *FRI sdg7-2* mutant lines flowered more rapidly than the *FRI* control line without vernalization (Fig. 2*A*). Moreover, *FRI sdg7-1* and *FRI sdg7-2* exhibited saturation of the vernali- zation response after 20 d of cold exposure, whereas saturation of the control required 40 d of cold exposure (Fig. 2*B*).

We also characterized the effect of the duration of cold on *FLC* and *VIN3* expression in the *sdg7* mutant. *sdg7* mutants had lower levels of *FLC* expression than controls before cold exposure (Fig. 2*C*), consistent with the more rapid flowering of *sdg7* without vernalization. Furthermore, in *sdg7* there was a decrease in *FLC* expression after 20 d of cold exposure, whereas in the control, a substantial decrease required 40 d of cold exposure (Fig. 2*C*). Similarly, *VIN3* mRNA levels at 20 d of cold exposure in the mutant were similar to the levels at 40 d of cold exposure in WT (Fig. 2*D*). Thus, *SDG7* is required for proper control of the timing of *VIN3* and *FLC* expression changes during cold exposure.

***VIN3* Dependence of the *sdg7* Phenotype.** As noted above (Fig. 2*D*), loss of *SDG7* results in *VIN3* expression without cold exposure and more rapid *VIN3* induction during cold exposure. To determine whether the alteration of *VIN3* expression is required for the *sdg7* mutant phenotype, we generated *sdg7-1 vin3* and *sdg7-2 vin3* double mutants in the *FRI*-containing background and characterized their flowering phenotypes. The *vin3* mutation partially suppressed the *sdg7* phenotype in plants not exposed to cold (Fig. 3*A*). This is an interesting result, because in WT, VIN3 appears to function only during cold exposure; a *vin3* single mutant has no flowering phenotype in the absence of cold exposure, and in WT, *VIN3* is expressed only during cold exposure (6). That the *vin3* mutant is epistatic to *sdg7* in plants not exposed to cold, however, reveals a conditional "noncold" *vin3* phenotype in the *sdg7* mutant, and indicates that loss of *SDG7* results in a partial vernalization in the absence of cold. As expected, *vin3* also suppressed the more rapid vernalization phenotype of *sdg7* (Fig. 3*A*). As controls, we combined the *vin3* mutation with a range of other mutations that result in early flowering in the absence of cold (21–24). Unlike for *sdg7*, there was no interaction of *vin3* with any of these mutations (Fig. 3*A*).

The *sdg7* Mutant Exhibits Elevated Levels of Noncoding RNAs Generated from *FLC* and Increased H3K27me3 of *FLC* Chromatin. As discussed above, *VIN3* is necessary for the *sdg7* phenotype; however, overexpression of *VIN3* is not sufficient to cause the *sdg7* mutant phenotype. In *VIN3*, overexpression lines that contain even higher

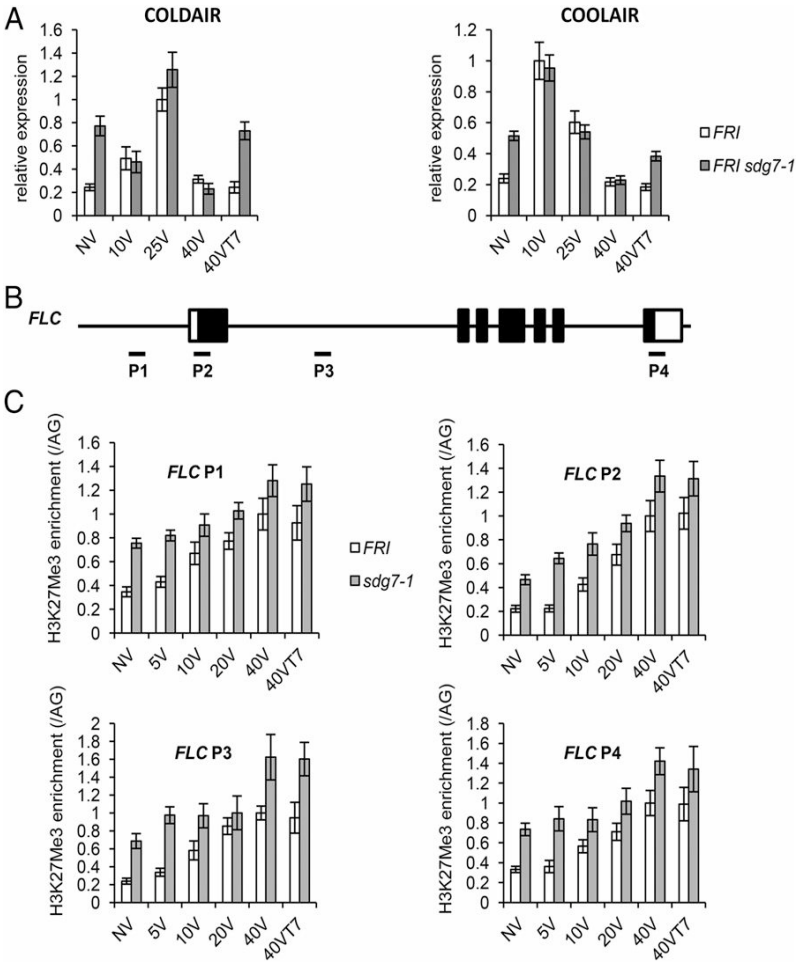

Fig. 4. Loss of *SDG7* results in increased levels of lncRNAs and increased H3K27me3 density without cold exposure. (*A*) COLDAIR and COOLAIR expression without cold exposure and after various durations of cold exposure in *sdg7* and WT. (*B*) Schematic representation of the *FLC* genomic region and probes used for ChIP analysis. (*C*) H3K27me3 density of the indicated regions of *FLC* chromatin in *sdg7* and WT after various durations of cold exposure. Expression and ChIP data are presented as mean values of three biological replicates. Error bars indicate SD. Symbols for the duration of cold exposure are as in the legend to Fig. 2.

VIN3 mRNA levels than the *sdg7* mutant (Fig. S2*A*), there was no effect on flowering or *FLC* expression in the absence of cold, nor more rapid vernalization (Fig. 3 *B* and *C*). The *VIN3* overexpression construct rescues *vin3* mutants, indicating that the construct is functional (Fig. S2*B*). The finding that *VIN3* overexpression does not affect flowering in a WT background was also noted in work using a different *VIN3* transgene (6).

Because *VIN3* overexpression is not sufficient to account for the *sdg7* phenotype, loss of *SDG7* may affect other factors involved in vernalization. Two long noncoding RNAs (lncRNAs), COLDAIR (15) and COOLAIR (16), generated from *FLC* are up-regulated during cold exposure and are thought to be involved in vernalization-mediated *FLC* repression (15, 16). Therefore, we determined expression levels of these two lncRNAs in the *sdg7* mutant. Interestingly, levels of these two lncRNAs were elevated in *sdg7* in the absence of cold (Fig. 4*A*). Thus, all of the known cold-inducible components of the vernalization response required for *FLC* repression—*VIN3*, COOLAIR, and COLDAIR—are more highly expressed without cold in *sdg7*, consistent with the mutation causing partial vernalization without cold, as well as a more rapid vernalization response.

FLC repression during vernalization results from quantitatively increased H3K27me3 deposition (25). Interestingly, in *sdg7*, all tested regions of *FLC* chromatin (Fig. 4*B*) have increased levels of H3K27me3 relative to WT in the absence of cold exposure (Fig. 4*C*). Furthermore, the *sdg7* mutant exhibits enhanced H3K27me3 spreading at *FLC* during cold exposure (Fig. 4*C*). As noted above for *VIN3*, COLDAIR, and COOLAIR expression, the *sdg7* H3K27me3 phenotype indicates that loss of *SDG7* results in a partially vernalized state of *FLC* chromatin before cold exposure, and a more rapid chromatin-based repression during cold exposure.

Loss of *SDG7* Does Not Affect Global Histone Methylations. Based on its overall structure and phylogenetic relationships, SDG7 is classified as a class II SET domain group protein. It resides in class II SET domain orthology group II-1 along with maize SDG110 and rice SDG724 (26, 27) (Fig. S3*A*). Members of this subgroup contain three conserved domains: an Associated with SET (AWS) domain, an SET domain, and a post-SET domain (26, 27). A recent study proposed that rice SDG724 is a histone methyltransferase, because loss of *SDG724* resulted in a decrease of global H3K36 methylation, and an in vitro assay revealed histone methyltransferase activity (28).

We determined whether loss of *SDG7* affects certain histone methylations on a global level using antibodies that recognize H3K36me1, H3K36me3, H3K4me2, H3K4me3, or H3K27me3. As a control, we assessed the effect of loss of the histone H3K36 methyltransferase, SDG8 (29), which results in decreased global

H3K36me3 levels; however, loss of *SDG7* had no effect on the global levels of modifications of the histones examined (Fig. 5*A*). Consistent with a role of rice SDG724 in histone methylation, SDG724 and maize SDG110 contain a predicted nuclear localization signal in the C terminus (30). However, the C-terminal regions of SDG7, SDG724, and SDG110 are quite divergent, and there are no predicted nuclear localization signals in SDG7 (Fig. S3*B*). Consistent with the lack of a predicted nuclear localization signal in SDG7, an SDG7-GFP fusion localizes to the cytosol (14). Furthermore, although SDG7 has Lys methylation activity in vitro against an aquaporin substrate (14), we could not detect any histone methyltransferase activity toward individual histones in an in vitro assay (Fig. 5*B*). Thus, the biochemical role of SDG7 in the timing of the vernalization response is not clear. The role of SDG7 in vernalization could be via Lys methylation of a cytosolic protein or proteins. Recent studies indicate that Lys methylation of extranuclear proteins is widespread in human cells (31), although the role of much of this Lys methylation is not known (32). The vernalization system of *Arabidopsis* provides a model system for exploring the role of a specific Lys-methyltransferase in the context of an environmentally induced developmental switch.

Conclusions

Because loss of *SDG7* results in a more rapid vernalization response, as well as certain features of vernalization in the absence of cold, such as higher levels of *VIN3*, lncRNAs complementary to *FLC*, and elevated basal levels of H3K27me3 at *FLC* chromatin, SDG7 is a negative regulator of the vernalization response (Fig. S4). The timing of the vernalization response is critical. If plants were to vernalize too rapidly, then in temperate climates in the fall season, short periods of cold followed by warm could result in deleterious flowering before winter. Thus, it is likely that natural selection has resulted in vernalization systems that are well adapted to particular climates (33), and *SDG7* is an example of a gene involved in the timing of upstream vernalization events.

Methods

Plant Materials and Growth Conditions. The mutant screen was done in the Columbia accession (Col) containing a *VIN3p::GUS* transgene. The *VIN3p::GUS* line does not have *FRI*; thus, to test for a vernalization phenotype, the mutants were introgressed into the Col *FRI* line (3, 34). Seeds were sown without stratification and grown in Petri dishes containing 2 mM MES at pH 5.7, 0.8% (wt/vol) Phytoblend agar (Caisson Laboratories) with 0.65 g L^{-1} Peter's Excel 15-5-15 CalMag fertilizer. Young seedlings were incubated at 4 °C under short days for vernalization treatment or transferred to soil (Metro-Mix 360; Sun Gro Horticulture) and fertilized with Peters Excel CalMag at weekly intervals under long days (16-h light/8-h dark cycle).

DNA Constructs. The *VIN3p::GUS* construct was created by amplifying a *VIN3* genomic fragment from 2 kb upstream of the start site of the *VIN3* mRNA to end of the second exon and joining this fragment to *GUS* in a translational fusion. The fragments were cloned into the D-TOPO entry vector (Life Tech- nologies) and then cloned into the pMDC164 destination vector using the Gateway cloning system (Life Technologies). For *VIN3* overexpression, a *VIN3* genomic fragment from transcription start site to transcription end site was cloned into pMDC32 (35), which drives *VIN3* from the 35S promoter.

GUS Assays. For viable GUS staining, seedlings were grown on filter paper in vertically placed Petri dishes for 7 d. The filter papers with seedlings were then incubated for 3–5 h in viable GUS staining solution [0.2 M NaPO4 pH 7.0, 50 mM K3[Fe(CN)6], 50 mM K4[Fe(CN)6], and 0.5 mM X-Gluc (5-bromo-4-chloro-3-indolyl beta-D-glucuronide cyclohexamine salt)]. Mutants were then rinsed and transferred to soil to produce seed for further studies. For de- structive GUS assays, seedlings grown on vertical agar plates were collected and vacuum-infiltrated for 15 min in GUS staining solution, and then in- cubated at 37 °C for 3–5 h (36).

Gene Expression Assays. Total RNA was isolated from seedlings grown on Petri dishes using TRIzol (Life Technologies) according to the instructions provided from the manufacturer, and treated with DNase (RQ1 RNase-Free Dnase; Promega). cDNA was generated from DNA-free RNA using qScript cDNA SuperMix (Quanta Biosciences), and quantitative RT-PCR was performed with an Applied Biosystems 7500 Fast Real-Time PCR System (Life Technologies). RNA levels were normalized using *Arabidopsis UBQ10* as an internal control. Because COLDAIR RNA is not polyadenylated, we used a COLDAIR-specific antisense primer, 5′-CTTCCATAGAAGGAAGCGACTA-3′, for cDNA synthesis reactions.

Histone Extraction and Immunoblot Analysis. Histone extraction and Western blot analyses were performed as described previously (29) using 3-wk-old plants and the following antibodies: anti-histone H3 (trimethyl K36) antibody (ab9050; Abcam; www.abcam.com), anti-histone H3 (monomethyl K36) antibody (ab9048; Abcam), anti-trimethyl-histone H3 (Lys4) antibody (07-473; Merck Millipore; www. merckmillipore.com), anti-trimethyl-histone H3 (Lys27) antibody (07-449; Merck Millipore), and anti-histone H3 antibody (05-499; Merck Millipore).

Histone Methyltransferase Assays. The full-length SDG7 recombinant protein was produced using the Gateway pDEST vector and then purified using His- tag affinity chromatography according to the manufacturer's instructions (Invitrogen; www.lifetechnologies.com). The SDG7 protein was tested for methlytransferase activity using 14C-labeled S-adenosyl-L-methionine (Per- kinElmer; www.perkinelmer.com) as a substrate in the histone methyl- transferase assay as described previously (29).

ChIP Assay. ChIP assays were performed using anti-H3K27me3 antibody (07-449; Merck Millipore) as described previously (37). Quantitative RT-PCR was performed using Applied Biosystems 7500 Fast Real-Time PCR System (Life Technologies). The data were normalized to the level of enrichment of the *AGAMOUS* gene as described previously (15).

Gene Sequences and Mutants. All sequence data used in this work are de- posited in the GenBank Nucleotide Core (At5g10140 for FLC, At4g00650 for

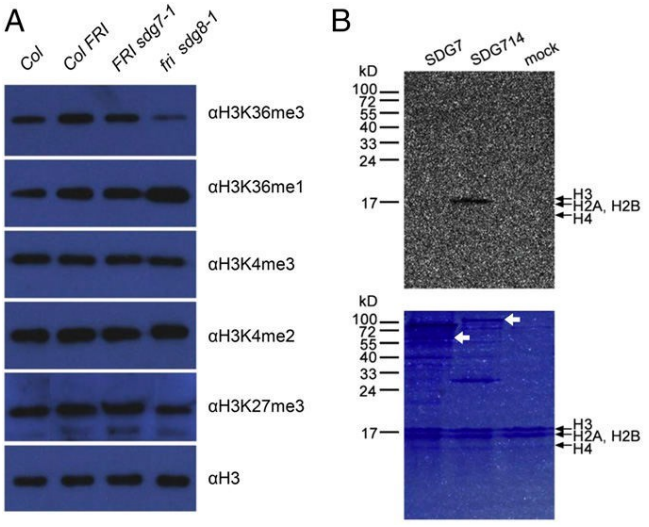

Fig. 5. SDG7 does not affect global histone modifications and lacks detectable HMTase activity. (*A*) Analysis of global histone methylation in the *FRI*-containing *sdg7* mutant (*FRI sdg7-1*). Col, Col *FRI*, and *fri sdg8-1* served as controls. The *sdg8-1* control exhibits reduced H3K36me3 and increased H3K36me1, whereas *sdg7-1* did not exhibit any changes in histone methylation. (*B*) Histone methyltransferase assay of SDG7. (*Upper*) Assay for incorporation 14C-labeled S-adenosyl-L-methionine into histones. SDG714 and mock control were used as positive and negative controls, respectively. (*Lower*) Coomassie blue staining of the same gel. Arrows indicate the bands corresponding to SDG7 and SDG714 proteins. Gel migration positions are indicated for the four nucleosomal core histones H2A, H2B, H3, and H4. Histones were assayed as oligonucleosomes, mononucleosomes, and free histones. Only results obtained on oligonucleosomes are shown; however, none of these different forms of histones were substrates for SDG7.

FRI, *At5g57380* for *VIN3*, and *At2g44150* for *SDG7*). The following mutant lines were used: *sdg7-2* (*SALK_131218*), *sdg7-3* (*SALK_072682*), *sdg8-1* (39), *elf7-2* (37), *elf8-1* (21), *pie1-3* (22), *suf3-1* (23) and *abh1-2* (40).

ACKNOWLEDGMENTS. We thank Donna Fernandez, Xuehua Zhong and members of R.M.A.'s laboratory for useful discussions, and Juan Gao for assistance with the HMTase assays. Work in R.M.A.'s laboratory was supported by the College of Agricultural and Life Sciences, Graduate School of the University of Wisconsin; the National Institutes of Health (Grant 1R01GM079525); the Great Lakes Bioenergy Research Center (US Department of Energy Office of Biological and Environmental Research Grant DE-FCO2-07ER64494) and the National Science Foundation (Grant IOS-1258126). Work in W.H.S.'s laboratory was supported in part by the French Agence Nationale de la Recherche (Grant ANR-12-BSV2-0013-02) and the European Commission (FP7-PEOPLE-2013-ITN; Grant 607880).

1. Lang A (1965) Physiology of flower initiation. *Encyclopedia of Plant Physiology*, ed Rutland W (Springer, Berlin), pp 1371–1536.
2. Lee J, Amasino RM (2013) Two FLX family members are non-redundantly required to establish the vernalization requirement in *Arabidopsis. Nat Commun* 4:2186.
3. Michaels SD, Amasino RM (1999) *FLOWERING LOCUS C* encodes a novel MADS domain protein that acts as a repressor of flowering. *Plant Cell* 11(5):949–956.
4. Johanson U, et al. (2000) Molecular analysis of *FRIGIDA*, a major determinant of natural variation in *Arabidopsis* flowering time. *Science* 290(5490):344–347.
5. Sanda SL, Amasino RM (1996) Interaction of FLC and late-flowering mutations in *Arabidopsis thaliana*. *Mol Gen Genet* 251(1):69–74.
6. Sung S, Amasino RM (2004) Vernalization in *Arabidopsis thaliana* is mediated by the PHD finger protein VIN3. *Nature* 427(6970):159–164.
7. Sung S, Schmitz RJ, Amasino RM (2006) A PHD finger protein involved in both the vernalization and photoperiod pathways in *Arabidopsis. Genes Dev* 20(23):3244–3248.
8. Sung S, et al. (2006) Epigenetic maintenance of the vernalized state in *Arabidopsis thaliana* requires LIKE HETEROCHROMATIN PROTEIN 1. *Nat Genet* 38(6):706–710.
9. De Lucia F, Crevillen P, Jones AM, Greb T, Dean C (2008) A PHD-polycomb repressive complex 2 triggers the epigenetic silencing of FLC during vernalization. *Proc Natl Acad Sci USA* 105(44):16831–16836.
10. Sawarkar R, Paro R (2010) Interpretation of developmental signaling at chromatin: The Polycomb perspective. *Dev Cell* 19(5):651–661.
11. Whitcomb SJ, Basu A, Allis CD, Bernstein E (2007) Polycomb group proteins: An evolutionary perspective. *Trends Genet* 23(10):494–502.
12. Sung S, Schmitz RJ, Amasino R (2007) The role of *VIN3-LIKE* genes in environmentally induced epigenetic regulation of flowering. *Plant Signal Behav* 2(2):127–128.
13. Bond DM, Dennis ES, Finnegan EJ (2011) The low-temperature response pathways for cold acclimation and vernalization are independent. *Plant Cell Environ* 34(10):1737–1748.
14. Sahr T, Adam T, Fizames C, Maurel C, Santoni V (2010) O-carboxyl- and N-methyltransferases active on plant aquaporins. *Plant Cell Physiol* 51(12):2092–2104.
15. Heo JB, Sung S (2011) Vernalization-mediated epigenetic silencing by a long intronic noncoding RNA. *Science* 331(6013):76–79.
16. Swiezewski S, Liu F, Magusin A, Dean C (2009) Cold-induced silencing by long antisense transcripts of an *Arabidopsis* Polycomb target. *Nature* 462(7274):799–802.
17. Martin T, Schmidt R, Altmann T, Frommer W (1992) Non-destructive assay systems for detection of â-glucuronidase activity in higher plants. *Plant Mol Biol Rep* 10:37–46.
18. Austin RS, et al. (2011) Next-generation mapping of *Arabidopsis* genes. *Plant J* 67(4): 715–725.
19. Hartwig B, James GV, Konrad K, Schneeberger K, Turck F (2012) Fast isogenic mapping-by-sequencing of ethyl methanesulfonate-induced mutant bulks. *Plant Physiol* 160(2):591–600.
20. Schneeberger K, et al. (2009) SHOREmap: Simultaneous mapping and mutation identification by deep sequencing. *Nat Methods* 6(8):550–551.
21. He Y, Doyle MR, Amasino RM (2004) PAF1 complex-mediated histone methylation of *FLOWERING LOCUS C* chromatin is required for the vernalization-responsive, winter-annual habit in *Arabidopsis. Genes Dev* 18(22):2774–2784.
22. Noh YS, Amasino RM (2003) *PIE1*, an ISWI family gene, is required for FLC activation and floral repression in *Arabidopsis. Plant Cell* 15(7):1671–1682.
23. Choi K, et al. (2005) *SUPPRESSOR OF FRIGIDA3* encodes a nuclear ACTIN-RELATED PROTEIN 6 required for floral repression in *Arabidopsis. Plant Cell* 17(10):2647–2660.
24. Bezerra IC, Michaels SD, Schomburg FM, Amasino RM (2004) Lesions in the mRNA cap-binding gene *ABA HYPERSENSITIVE 1* suppress FRIGIDA-mediated delayed flowering in *Arabidopsis. Plant J* 40(1):112–119.
25. Coustham V, et al. (2012) Quantitative modulation of polycomb silencing underlies natural variation in vernalization. *Science* 337(6094):584–587.
26. Springer NM, et al. (2003) Comparative analysis of SET domain proteins in maize and *Arabidopsis* reveals multiple duplications preceding the divergence of monocots and dicots. *Plant Physiol* 132(2):907–925.
27. Ng DW, et al. (2007) Plant SET domain-containing proteins: Structure, function and regulation. *Biochim Biophys Acta* 1769(5-6):316–329.
28. Sun C, et al. (2012) The histone methyltransferase SDG724 mediates H3K36me2/3 deposition at MADS50 and RFT1 and promotes flowering in rice. *Plant Cell* 24(8): 3235–3247.
29. Xu L, et al. (2008) Di- and tri- but not monomethylation on histone H3 lysine 36 marks active transcription of genes involved in flowering time regulation and other pro- cesses in *Arabidopsis thaliana. Mol Cell Biol* 28(4):1348–1360.
30. Brameier M, Krings A, MacCallum RM (2007) NucPred—predicting nuclear localization of proteins. *Bioinformatics* 23(9):1159–1160.
31. Cao XJ, Arnaudo AM, Garcia BA (2013) Large-scale global identification of protein lysine methylation in vivo. *Epigenetics* 8(5):477–485.
32. Clarke SG (2013) Protein methylation at the surface and buried deep: Thinking outside the histone box. *Trends Biochem Sci* 38(5):243–252.
33. Li P, et al. (2014) Multiple FLC haplotypes defined by independent cis-regulatory variation underpin life history diversity in *Arabidopsis thaliana. Genes Dev* 28(15): 1635–1640.
34. Lee I, Amasino RM (1995) Effect of vernalization, photoperiod, and light quality on the flowering phenotype of *Arabidopsis* plants containing the *FRIGIDA* gene. *Plant Physiol* 108(1):157–162.
35. Curtis MD, Grossniklaus U (2003) A gateway cloning vector set for high-throughput functional analysis of genes in planta. *Plant Physiol* 133(2):462–469.
36. Jefferson RA, Kavanagh TA, Bevan MW (1987) GUS fusions: Beta-glucuronidase as a sensitive and versatile gene fusion marker in higher plants. *EMBO J* 6(13):3901–3907.
37. Tamada Y, Yun JY, Woo SC, Amasino RM (2009) *ARABIDOPSIS TRITHORAX-RELATED 7* is required for methylation of lysine 4 of histone H3 and for transcriptional activation of *FLOWERING LOCUS C. Plant Cell* 21(10):3257–3269.
38. Tamura K, Stecher G, Peterson D, Filipski A, Kumar S (2013) MEGA6: Molecular Evolutionary Genetics Analysis version 6.0. *Mol Biol Evol* 30(12):2725–2729.
39. Berr A, et al. (2010) *Arabidopsis* histone methyltransferase SET DOMAIN GROUP8 mediates induction of the jasmonate/ethylene pathway genes in plant defense re- sponse to necrotrophic fungi. *Plant Physiol* 154(3):1403–1414.
40. Kim S, et al. (2008) Two cap-binding proteins, CBP20 and CBP80, are involved in processing primary MicroRNAs. *Plant Cell Physiol* 49(11):1634–1644.

Supporting Information

Lee et al. 10.1073/pnas.1423585112

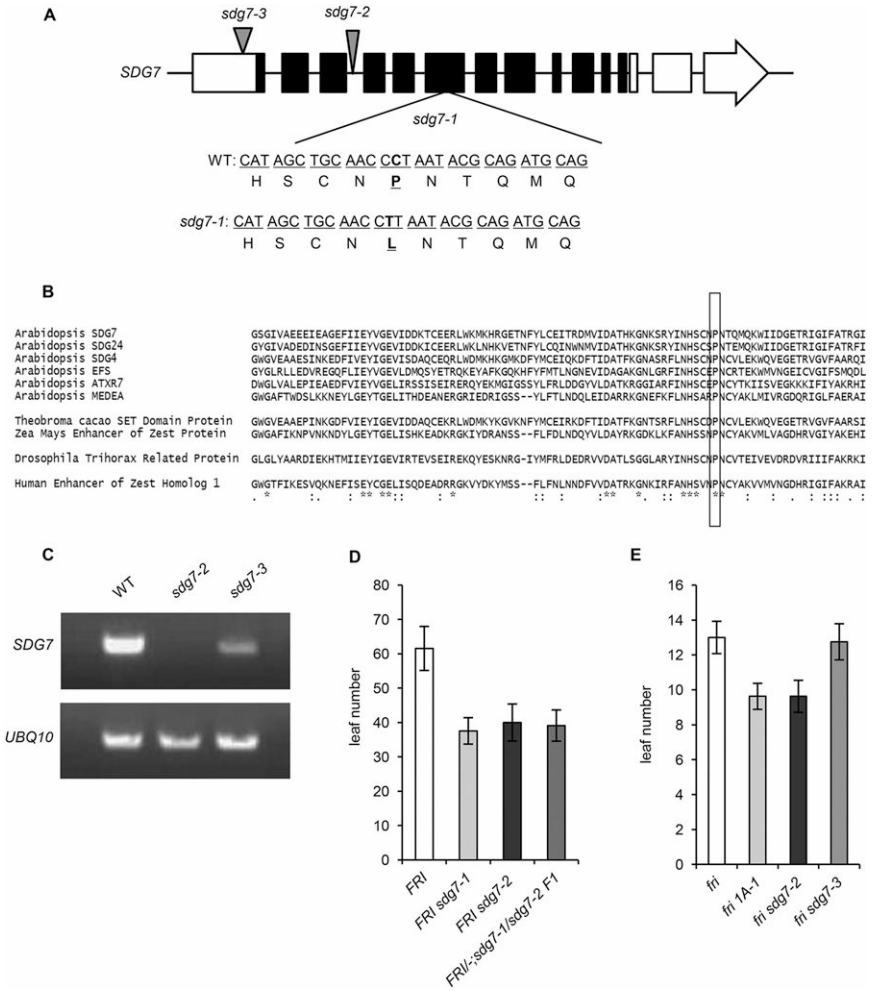

Fig. S1. *sdg7* mutant characterization. (*A*) Schematic representation of the *SDG7* genomic region and the *sdg7* mutants. (*B*) SET domain alignments per- formed using ClustalW. The highly conserved proline residue in SET domain-containing proteins of many organisms is boxed; this proline is mutated in *sdg7-1*. (*C*) Transcript levels of *SDG7* in the mutant backgrounds. (*D*) Complementation test based on evaluating flowering in *FRI*/-; *sdg7-1*/*sdg7-2* F1 plants. (*E*) Flowering behavior of *sdg7* mutants without *FRI*.

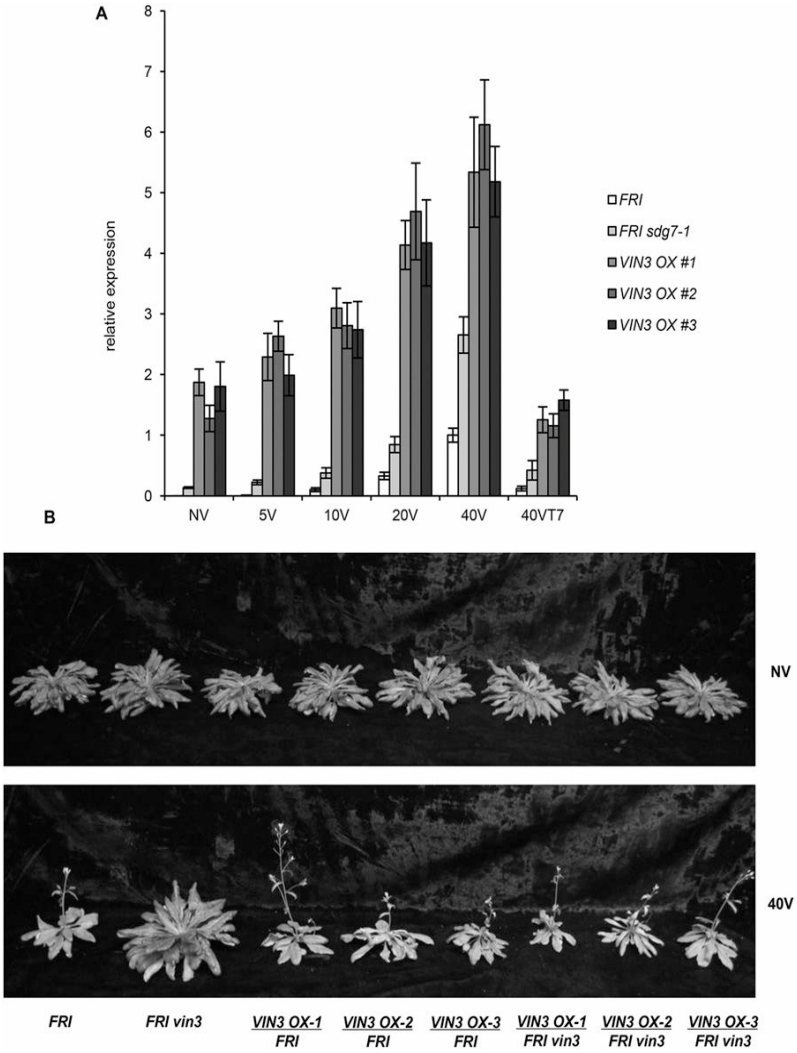

Fig. S2. *VIN3* expression and flowering phenotype in *VIN3* overexpressors. (*A*) *VIN3* expression level in *VIN3* overexpressors. (*B*) Flowering phenotype of *FRI*, *FRI vin3*, and three individual *VIN3* overexpressors in a *FRI*-containing background and in a *FRI vin3* background without (NV) or after 40 d (40V) of cold treatment.

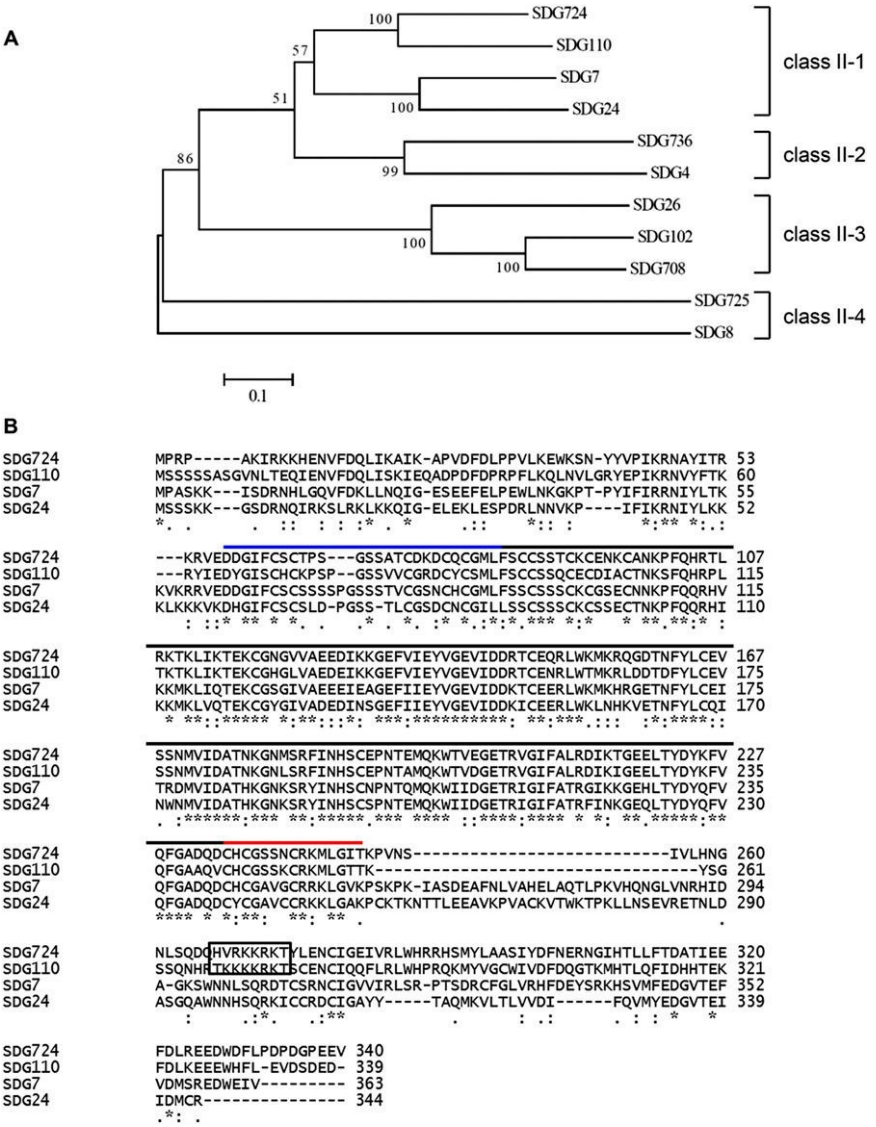

Fig. S3. Phylogenetic analysis and sequence alignments of SDG7 homologs. (*A*) Phylogenetic analysis was performed using class II-SDG7 homologs (SDG7, SDG24, SDG4, SDG26, and SDG8 in *Arabidopsis*; SDG110 and SDG102 in maize; SDG724, SDG736, SDG708, and SDG725 in rice). Orthology group 1–4 was also indicated. (*B*) Sequence alignments were represented between the orhology group 1 proteins. Blue, black, and red lines represent AWS, SET, and post-SET domains, respectively. The square box represents nuclear localization signals predicted by NucPred software (www.sbc.su.se/~maccallr/nucpred/).

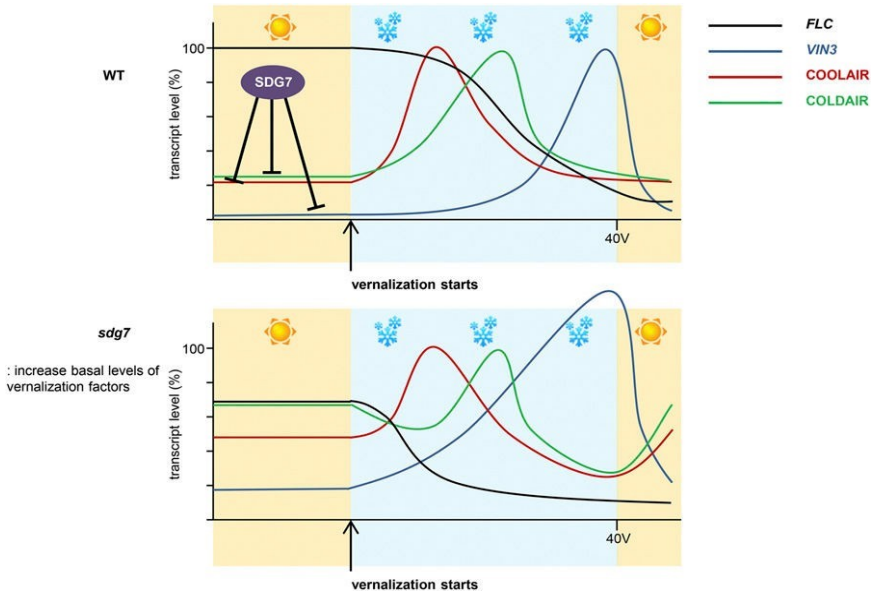

Fig. S4. Schematic representation of the role of SDG7 in the vernalization process. In WT, SDG7 is a negative regulator of *VIN3* and two lncRNAs. In the *sdg7* mutant, *VIN3* and the lncRNAs exhibit increased expression without cold, and *FLC* is more rapidly suppressed.

Table S1. Primers used in the manuscript.

Gene	Forward primers (5′ to 3′)	Reverse primers (5′ to 3′)
FLC	tccggcaagctctacagcttc	agcatgctgtttcccatatcgatc
VIN3	ctgcttcgctctcaaagatctg	ctcaatgcattcattatcttcaaacg
COLDAIR	tcacccctagttaggtccag	tattaaatcataattaagaccaggagttct
COOLAIR	accttattcgtgtgagaattgc	ttgacagaagtgaagaacacatataca
SDG7	gggagtaattgccattgtgggatg	tgtcgttgttggaacggcttattg
UBQ10	ctaccgtgatcaagatgcagatc	ttgtcgatggtgtcggagctttc
FLC P1	cgtgagtccgcccctgatagc	ggaccaaaccaaacctacaaagactttc
FLC P2	cttagtatctccggcgacttgaacc	gcgtcacagagaacagaaagctga
FLC P3	acacaacctttgtatcttgtgtcttttg	agtagacactacaccagattcaattttgac
FLC P4	gtgaatagtgattttgacctatgattatcgtacag	ggtggctaattaagtagtgggagagtcac
AG	gtgaaacaaattttcctgcagaatgtcact	agttttgaggcactaaaatctttgggtaaatc

CHAPTER II

Crosstalk of different histone modifications in the regulation of gene transcription and flowering time control in *Arabidopsis thaliana*

Wei Zhao, Pia Neyt, Mieke Van Lijsebettens, Wen-Hui Shen and Alexandre Berr

1. INTRODUCTION

Correct timing to flowering is crucial for the reproductive success of plants and thus is fine-tuned by multiple genetic and molecular pathways. Histone methylation is involved in flowering time control by regulating the expression of several flowering time genes. Among them, *FLOWERING LOCUS C* (*FLC*) encodes a MADS box transcription factor that blocks the floral transition by directly repressing the transcription of the flowering time integrators *FLOWERING LOCUS T* (*FT*) and *SUPPRESSOR OF OVEREXPRESSION OF CO 1* (*SOC1*). It is now well-known that histone methylation does not occur alone but in combination with other histone marks to define different chromatin states throughout the entire genome. This is particularly true during transcription.

In Arabidopsis, genetic interaction studies using different histone methyltransferase mutants, including *atx1, atx2, sdg8, sdg25, sdg26* and *clf* as well as the double histone demethylase mutant *ldl1ldl2*, revealed that some complex functional connections exist between H3K4me3, H3K36me3 and H3K27me3, even if they appear to act largely independently in regulating the transcription of flowering time genes (Shafiq et al., 2014; Berr et al., 2015). Further reinforcing this complexity, transcriptome analyses of various mutant combinations has strengthened the idea of their only partial functional overlapping (Berr et al., 2015; Zhao et al., 2015).

H2Bub1 is an essential epigenetic mark mainly associated with active gene transcription. Studies in yeast and animals showed that H2Bub1 regulates transcription through *trans*-crosstalks with several histone methylation marks. In a simplified way, H2Bub1 first occurs, allowing histone H3 lysine 4 and 79 trimethylation (H3K4me3 and H3K79me3) and transcription initiation and early elongation. Latter, H2Bub1 is removed promoting H3K36 trimethylation to enable transcription elongation to proceed. In yeast, H3K4 and H3K36 methylation are catalyzed by the SET domain lysine methyltransferases Set1 and Set2, respectively, while H3K79 methylation is mediated by Dot1, a non-SET domain-containing histone methyltransferase. It was proposed that similar crosstalks may also exist in Arabidopsis gene transcription regulation (Feng

and Shen, 2014). However, while homologs of Set1 and Set2 exist in Arabidopsis, the Arabidopsis genome seems to be lacking H3K79 methylation as well as a homologue of Dot1. Based on the particular distribution profile of histone methylation mark along transcribed genes in Arabidopsis, it has been suggested that H3K36me3 may play a similar role as that of H3K79me3 in animal and yeast. Indeed, the distribution of H3K36me3 in Arabidopsis is very similar to that of H3K79me3, suggesting a role for H3K36me3 in transcription elongation.

However, experimental evidence for crosstalk between H2Bub1 and H3K36me3 in Arabidopsis is largely lacking so far since studies were mainly concentrated on the functional relationship between H2Bub and H3K4me3. In order to fill this shortfall, I will explore the functional interaction between H2Bub and H3K36me3 using a genetic approach based on crosses between different histone-modifying enzyme mutants. This study particularly focused on the interplay of these different histone marks in regulation of plant growth (at organism as well as at cellular levels), in maintenance of genome transcription, and in regulation of chromatin status associated with flowering time gene expression levels to control plant flowering time.

2. RESULTS

2.1 Production of *sdg8-1 hub2-2* double mutants

In order to unravel how H3K36 methylation and H2Bub1 are functionally connected in the course of transcription, I tested the genetic interaction between the *sdg8* mutant and a mutant defective in H2Bub1, *hub1* or *hub2*.

T-DNA insertion lines *sdg8-1* (Salk_065480) and *hub2-2* (Salk_071289) or *hub1-3* (GABI_276D08) in the Col background has been characterized previously (Zhao et al., 2005; Fleury et al., 2007). Homozygous *sdg8-1* was crossed with *hub1-3* and *hub2-2*, respectively. Seeds (F1) from crosses were collected from individual silique on the parent plants and were then grown for self-pollinating to obtain the F2 generation. By phenotyping of F2 generation plants, 5 out of 96 plants were found to be the potential double *sdg8-1 hub2-2* homozygous mutants, representing 5.2 % of the total, which is in agreement with the 6.25 % predicted for Mendelian segregation. Genotypes were further validated by genomic PCR (Figure 1). A similar approach was used to isolate double *sdg8-1 hub1-3* homozygous plants (Supplemental Figure 1).

A

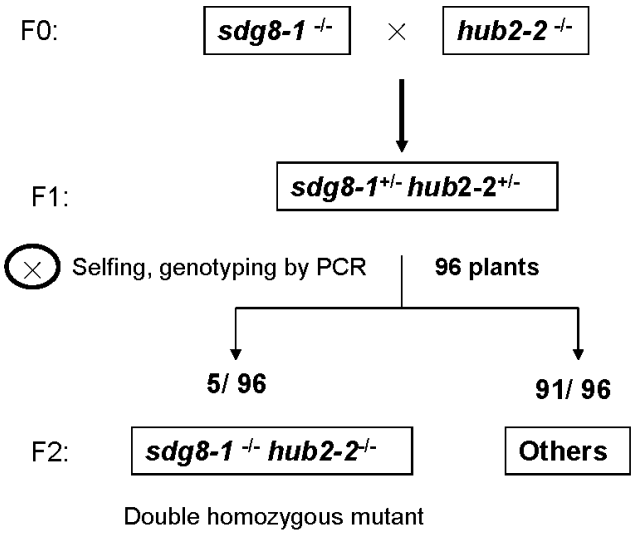

B

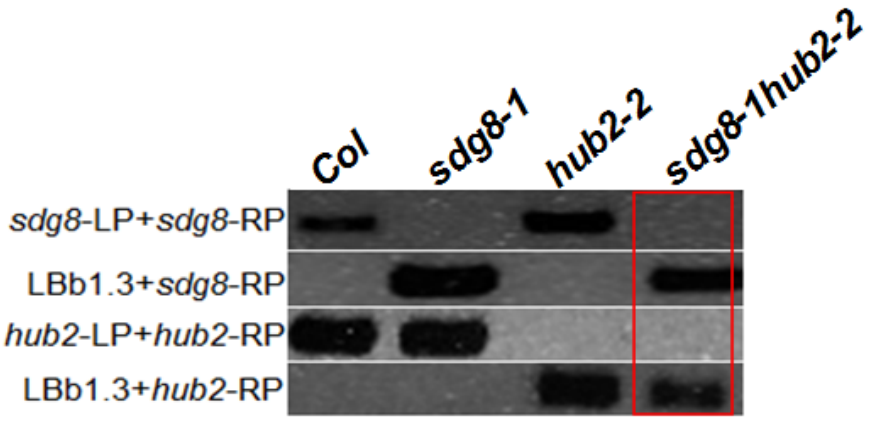

Figure 1: Identification of the double *sdg8-1 hub2-2* homozygous mutant. (A) Scheme of *sdg8-1 hub2-2* double mutant identification. (B) Genotype verification of wild-type (WT) and the *sdg8-1*, *hub2-2*, and *sdg8-1 hub2-2* mutants by PCR amplification using the specific gene/T-DNA primers as reported. PCR products separated by electrophoresis on agarose gels are shown.

2.2 Phenotypes of the *sdg8-1 hub2-2* double mutants

Under our growth conditions, *sdg8-1* mutant showed pleiotropic phenotypes including early flowering, reduced organ size and increased shoot branching, which is consistent with previously reported data (Zhao et al., 2005; Xu et al., 2008). As previously reported, the *hub2-2* mutant bolted earlier, had pale leaf coloration and modified leaf shape (Fleury et al., 2007). Compared to *sdg8-1* or *hub2-2*, the *sdg8-1 hub2-2* double mutant displays worsened phenotypes, including smaller body and rosette sizes, and earlier flowering (Figure 2). Because the *sdg8-1 hub1-3* mutant plants shows very similar phenotypes compared to *sdg8-1 hub2-2* (Supplemental Figure 2), we hereafter concentrated on *sdg8-1 hub2-2* for detailed analysis.

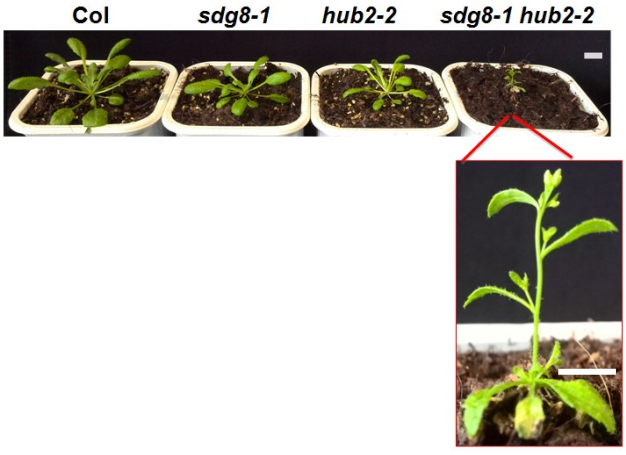

Figure 2: Representative 23-day-old seedlings of Col, *sdg8-1*, *hub2-2*, and *sdg8-1 hub2-2* grown under mid-day (MD; 12 h light and 12 h dark) photoperiod conditions. Scale bars represent 1 cm (upper) and 0.5 cm in (lower).

2.3 Global levels of histone modifications analysis in *sdg8-1 hub2-2* double mutants

To get insight into the combinatorial role of SDG8 and HUB2 in histone modifications, global level changes of histone modifications were analyzed by western blots experiment and compared between wild type and mutant plants. Antibodies specifically recognizing histone H3, monomethyl-H3K36 (H3K36me1), dimethyl-H3K36 (H3K36me2), trimethyl-H3K36 (H3K36me3), and dimethyl-H3K4 (H3K4me2), trimethyl-H3K4(H3K4me3), and trimethyl-H3K27 (H3K27me3) as well as histone H2B monoubiquitination (H2Bub1) were used on nuclear protein extracted from 3-week-old wild-type (Col) and *sdg8-1*, *hub2-2*, *sdg8-1 hub2-2* mutant plants (Figure 3).

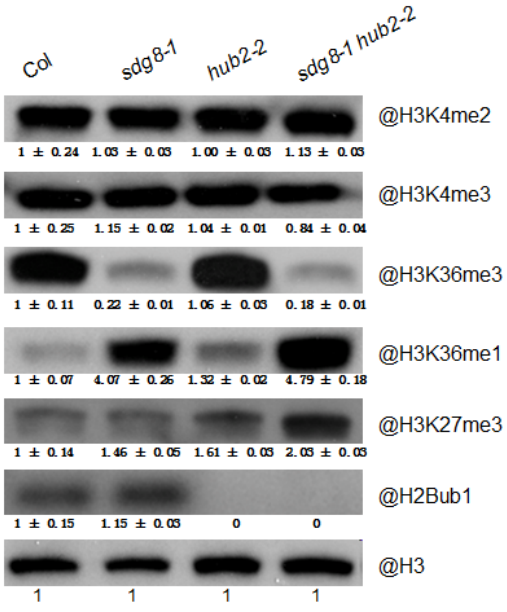

Figure 3: Western blot analysis of global levels of histone modifications in wild-type (WT) and the *sdg8-1*, *hub2-2*, and *sdg8-1 hub2-2* mutant plants. Nuclear proteins were extracted from 3-week-old plants grown under mid-day (MD; 12 h light and 12 h dark) photoperiod conditions, and were analyzed by using specific antibodies that recognize the indicated form of histones. Numbers indicate “mean (±standard error)” of densitometry values measured from at least 3 independent experiments, normalized to H3, and shown as relative to WT (set as 1).

In *sdg8-1*, while H3K4me2, H3K4me3, H2Bub1 levels appeared unchanged, the level of H3K36me3 is significantly reduced whereas H3K36me1 is increased as compared to wild-type plants. In *hub2-2*, H2Bub1 is dramatically decreased to a level below our detection limit, while levels of H3K4me2, H3K4me3, H3K36me1 and H3K36me3 are unchanged as compared to those detected in wild-type plants. The *sdg8-1 hub2-2* double mutants show a reduced level of H3K36me3 and an increased level of H3K36me1 like the single *sdg8-1* mutant, and a reduced level of H2Bub1 like the single *hub2-2* mutant. Like in single mutants, levels of H3K4me2 and H3K4me3 are unchanged in our double mutant. Interestingly, the repressive mark H3K27me3 level is only significantly increased in the *sdg8-1 hub2-2* double mutant, suggesting a combined antagonistic relationship between both H3K36me3 and H2Bub1 active marks and the repressive H3K27me3 one.

Together, our analysis of the global levels of H3K36me1/me3, H3K4me2/me3 and H2Bub1 is in agreement with the notion that SDG8 is the major H3K36me3 histone methyltransferase and HUB2 is a H2B monoubiquitinase. However, a hypothetical crosstalk between H2Bub1, H3K4me3 and H3K36me3 at the genomic scale is not detectable.

2.4 Diverse aspects of plant growth and development are dramatically affected in *sdg8-1 hub2-2* double mutants

In order to get insight into the functional relation between *SDG8* and *HUB2* in controlling plant growth and development, we conducted an exhaustive analysis of the *sdg8-1 hub2-2* double mutant phenotypes compared to those of *sdg8-1*, *hub2-2* single mutant and wild-type plants.

2.4.1 Plant body size and weight are reduced in *sdg8-1 hub2-2* mutants

Under standard laboratory growth conditions, the average plant body size of *sdg8-1 hub2-2* double mutants remained smaller along different growth stages compared to the average size of wild-type and single mutant plants (Figure 4 A-C). The plant fresh

weight was measured from at least 20 individual 5-week-old plants, grown under long-day (LD; 16 h light and 8 h dark) photoperiod conditions. Consistent with the seedling phenotype, the average plant fresh weight appears extremely reduced in *sdg8-1 hub2-2* compared to *sdg8-1*, *hub2-2* and wild-type plants (Figure 4D). Therefore, with respect to plant size, our results suggest that the two mutations have additive or even synergistic effects.

A

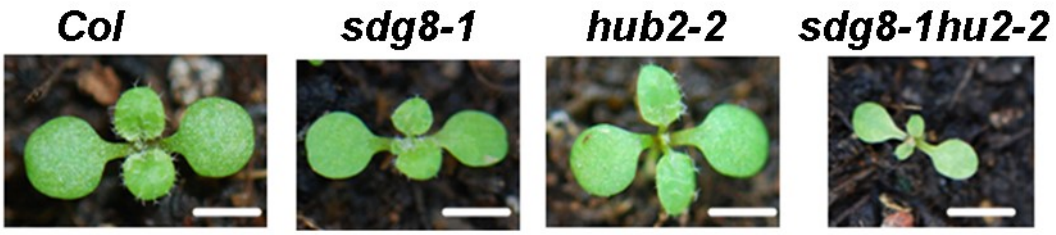

B

C

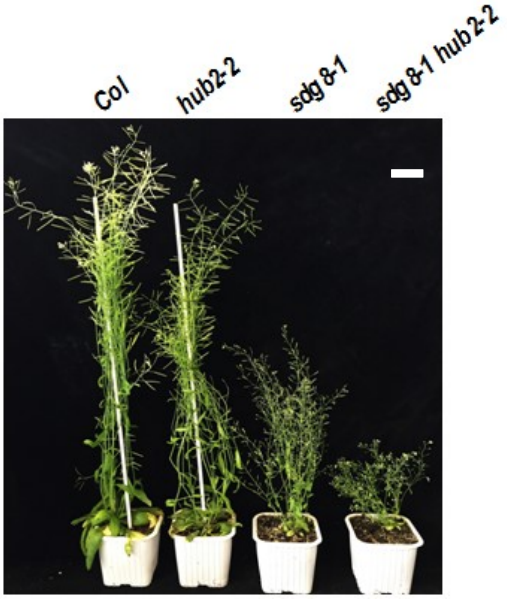

D

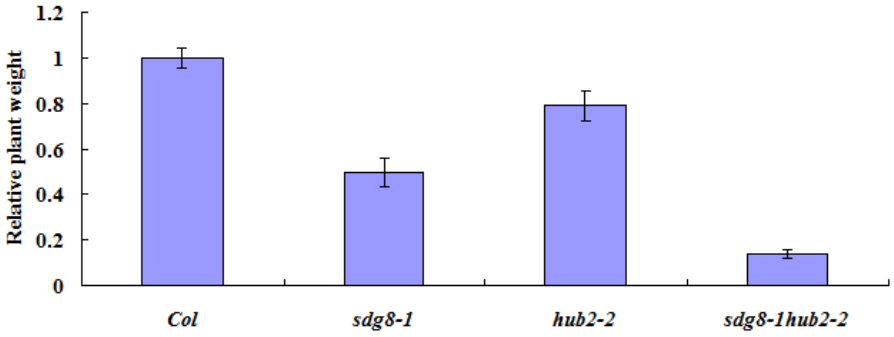

Figure 4: Representative 7-day-old (A), 18-day-old (B) and 7-week-old (C) of wild-type and mutant seedlings grown under long-day (LD; 16h light/8 h dark) photoperiod conditions, are shown. (D) Mean values ± SD of plant fresh weight are measured from over 20 individual 5-week-old plants, grown under long-day (LD; 16 h light and 8 h dark) photoperiod conditions, and are shown as relative to WT control (set as 1). SD means standard deviation. Scale bars represent 2 mm in (A) and (B), 3 cm in (C).

2.4.2 Chlorophyll content is reduced in *sdg8-1 hub2-2* mutants

Because a decrease in chlorophyll content is one of the many phenotypes characterizing the *sdg8-1* single mutant, we next address it in our double mutant. Visually, rosette leaves look slightly paler in *sdg8-1 hub2-2* mutants as compared to the *sdg8-1* single mutants (Figure 4 A-B). This observation was confirmed by measuring the chlorophyll content from over 10 individual 12-day-old plants grown under long-day (LD; 16 h light and 8 h dark) photoperiod conditions. Indeed the chlorophyll content was additively decreased in the double mutant as compared to the wild-type and single mutants (Figure 5), suggesting an additive effect of both mutations.

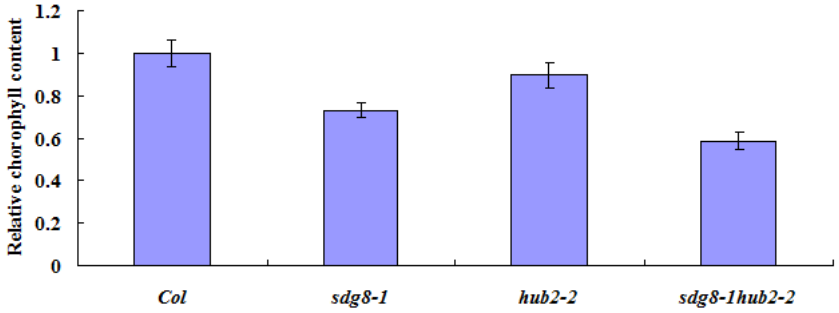

Figure 5: Mean values ± SD of the chlorophyll content measured from at least 10 individual 12-day-old plants grown under long-day (LD; 16 h light and 8 h dark) photoperiod conditions. Values are presented relative to the WT control set as 1. SD means standard deviation.

2.4.3 Siliques length is shortened in *sdg8-1 hub2-2* mutants

The *sdg8-1 hub2-2* double mutant plants are fertile, but only very few seeds can be harvested from each individual plant. Consistently, mild developmental defect of siliques was observed in *sdg8-1* and *hub2-2* single mutants, while it was much more pronounced in the double mutant (Figure 6A). The siliques length was measured from over 20 individual fully elongated siliques from plants, grown under long-day (LD; 16 h light and 8 h dark) photoperiod conditions. Consistent with our observation, the siliques length in the double mutant was additively shortened from the single mutants (Figure 6B).

A

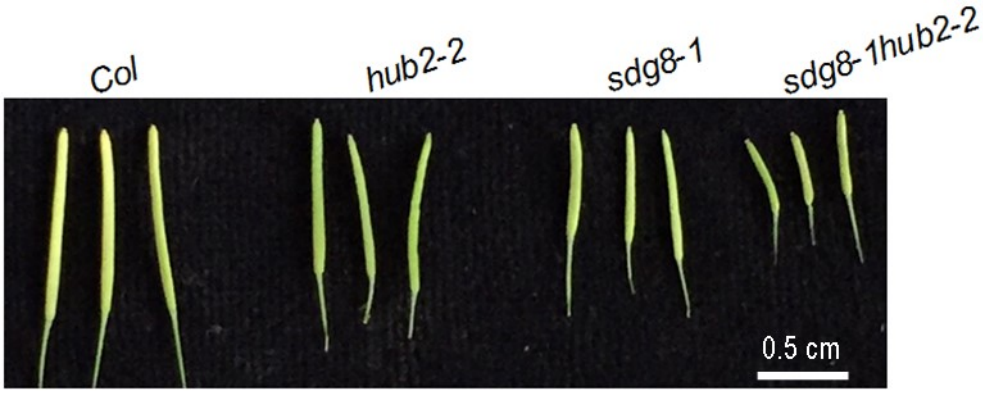

B

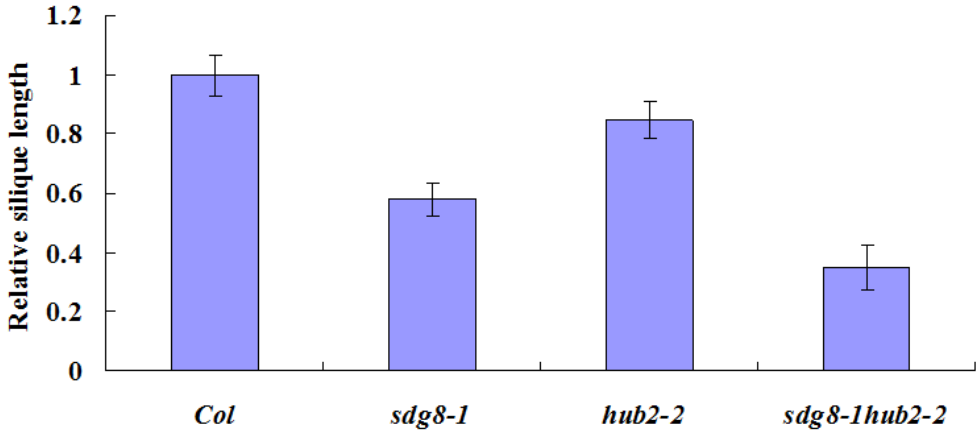

Figure 6: (A) Representative siliques from 7-week-old of wild-type and mutant plants grown under long-day (LD; 16 h light and 8 h dark) photoperiod conditions are shown. (B) Mean values ± SD of silique length measured from at least 20 individual fully elongated siliques dissected from 7-week-old plants grown under long-day (LD; 16 h light and 8 h dark) photoperiod conditions. Values are presented relative to the WT control set as 1. SD means standard deviation. Scale bar represents 0.5 cm.

2.4.4 Primary root growth and development is impaired in *sdg8-1 hub2-2* mutants

The root is a very important plant organ required for plant nutrients and water absorption from the soil. Compared to wild-type, root growth is slightly affected in *sdg8-1* and *hub2-2* but severely impaired in *sdg8-1 hub2-2* (Figure 7A).

2.4.4.1 Kinetic analysis of primary root growth

The root growth was studied by measuring root length within a window of 5 to 11 days after stratification (DAS) of seedlings grown in vertical position under continuous light. The average root length of *sdg8-1* and *hub2-2* single mutants was slightly reduced compared to that of wild type plants, while the *sdg8-1 hub*2-2 double mutant showed an enhanced phenotype (Figure 7B). Together, the shortened root length of the double mutant does not simply reflect an additive phenotype but indicate a synergistic effect of *sdg8-1* and *hub2-2*.

A

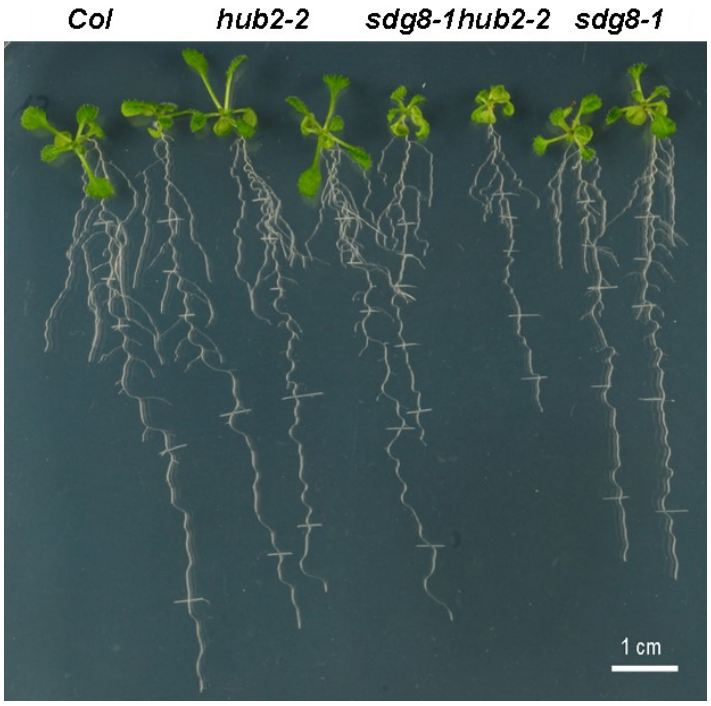

B

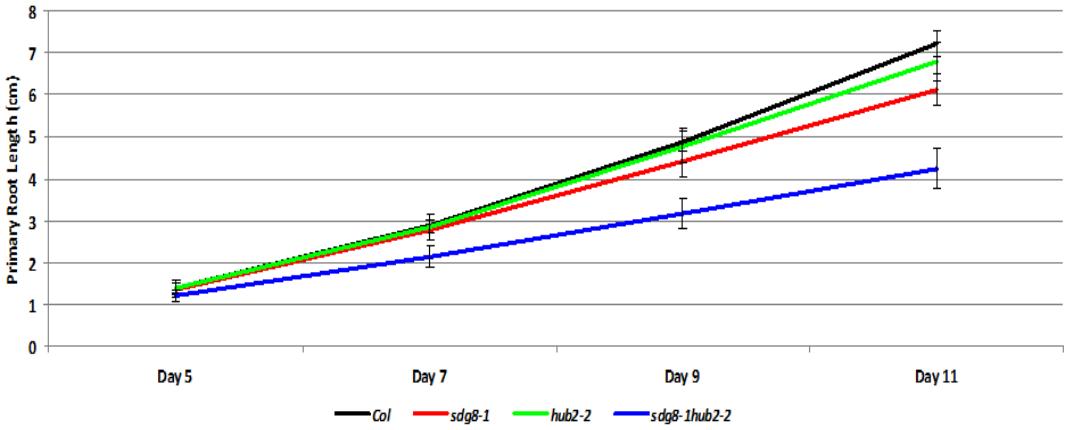

Figure 7: (A) Phenotypic appearance of 11-day-old wild-type and mutant plants grown vertically on MS under continuous-light (24h light and 0h dark). (B) Mean values ± SD of primary root length measured from at least 15 individual roots within a window of 5 to 11 days after stratification on wild-type and mutant plants grown under continuous-light (24 h light and 0 h dark). SD means standard deviation. Scale bar represents 1 cm.

2.4.4.2 Cortex cells number in primary root meristem is reduced in *sdg8-1 hub2-2* mutants

To establish whether the reduction in root length of our double mutant derived from a reduction in meristem size, we measured the size of the root meristematic zone represented as the number of cortex cells spanning from the quiescent center to the first elongated cell in the transition zone. Six-day-old primary roots of each genotype were separately stained with propodium iodide for three minutes and then imaged by laser scanning confocal microscopy (Figure 8A). The number of cortex cells was counted from at least ten roots for each genotype (Figure 8B). For both single and double mutants, shortened root phenotypes appeared to be related to the reduced meristem size. However, the meristem size in *sdg8-1 hub2-2* was not significantly smaller than in *sdg8-1* and *hub2-2* single mutants. Therefore, because the *sdg8-1 hub2-2* root length was smaller than in *sdg8-1* and *hub2-2* single mutants, other factors such as the cell elongation might also contribute to the primary root growth defects observed in our double mutants.

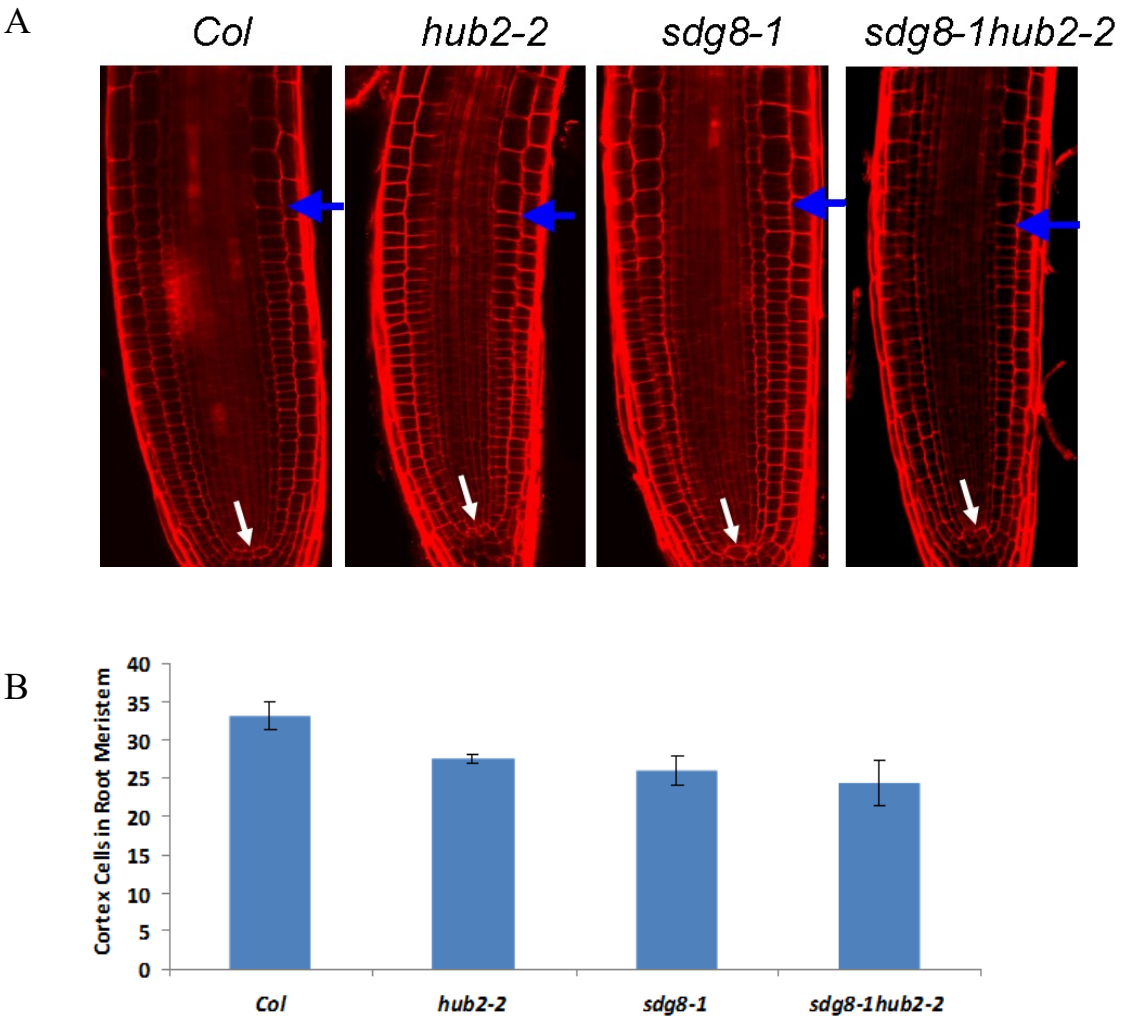

Figure 8: (A) Longitudinal view of the Arabidopsis root meristem in 6-day-old wild-type and mutant plants grown under continuous-light (24h light and 0h dark). Blue arrows indicate the transition zone, where cells leave the meristem and enter the elongation-differentiation zone. White arrows indicate the quiescent center (QC). (B) Average number of cortex cells ± SD in primary root meristem measured from at least 10 individual roots from 6-day-old plants grown under continuous-light. SD means standard deviation.

2.4.5 Rosette leaf growth and development is impaired in *sdg8-1 hub2-2* mutants

To further explore cellular parameters that may explain the drastic size decrease of our double mutant, cotyledons and rosette leaves were dissected from 23-day-old wild-type and mutant plants and analyzed in detail (Figure 9).

2.4.5.1 Quantification of leaf parameters in *sdg8-1 hub2-2* double mutants

Visually, *sdg8-1 hub2-2, sdg8-1* and *hub2-2* rosette leaves were smaller than wild type

ones, with leaves from the double mutant being the smallest ones. In addition, the *sdg8-1 hub2-2* double mutant present a lower number of rosette leaves. Moreover, the double mutant present several additional leaf defects that were not described both in both single mutants such as dentate leaf margins, irregular leaf lamina surface, asymmetric lamina or reduced venation complexity (Figure 9A).

Synchronous profiles were obtained for both single mutants, even if it was less pronounced in *sdg8-1*, thus indicating no retardation in leaf initiation (i.e. the lamina area increased from juvenile leaves 1, 2 and 3 to transition to adult leaf 4, then adult leaves 5 and 6, while it reduced for adult leaves 7, 8 and 9 and cauline leaf 10). Also, the lamina area of every leaf of the *sdg8-1* and *hub2-2* single mutant was significantly smaller than that of the wild type control, which was further exacerbated with the double *sdg8-1 hub2-2* mutant as the result of predominantly reduced lamina width and to a lesser extent reduced lamina length (Figure 9B, 9C and 9D)

A

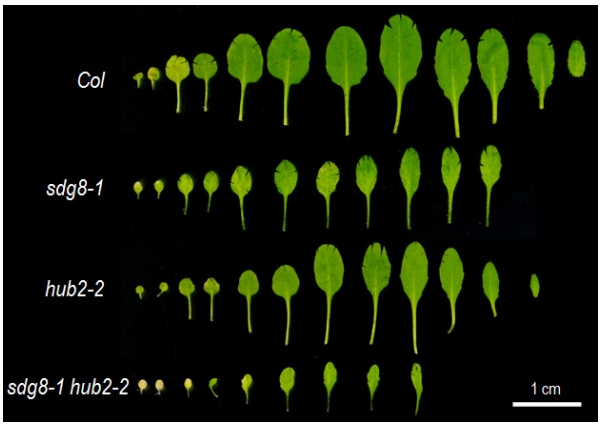

B

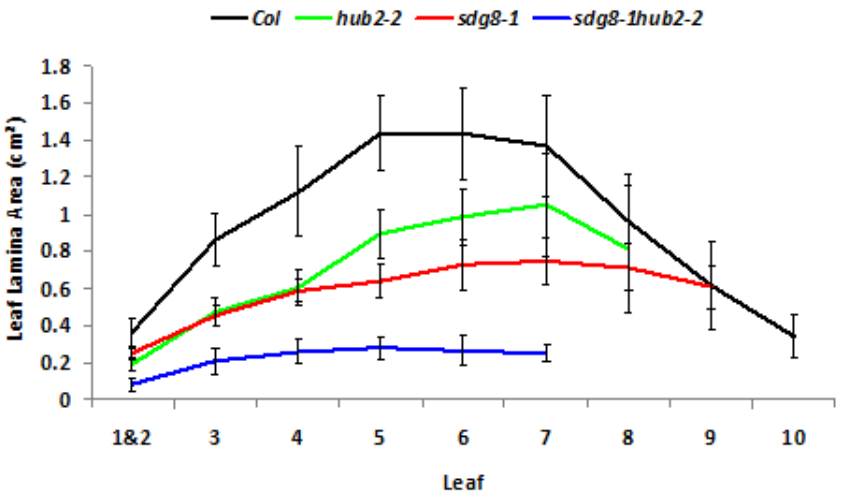

C

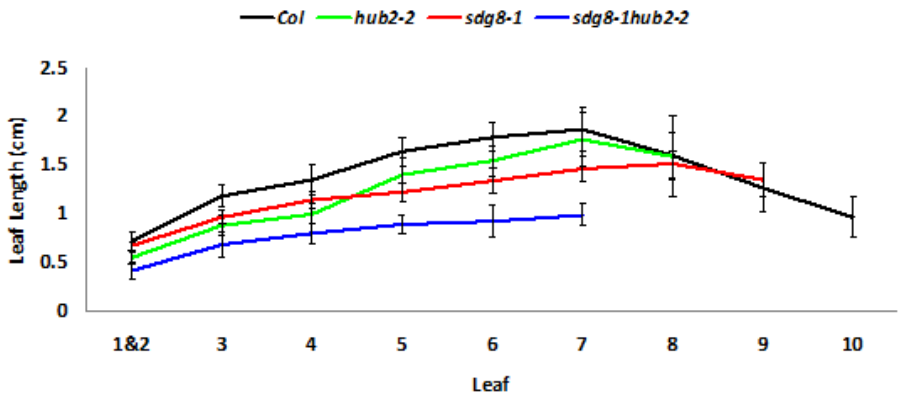

D

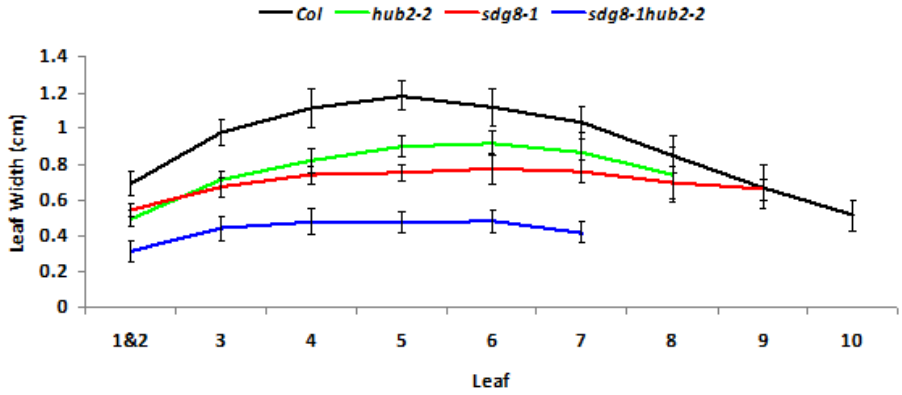

Figure 9: (A) Dissected cotyledons and leaves of 23-day-old wild-type and mutant plants; the true leaves are numbered from the base upward. Mean values ± SD of leaf area (B), leaf length (C) and leaf width (D) measured from leaves dissected from at least 5 individual 23-day-old plants grown under long-day (LD; 16 h light and 8 h dark) photoperiod conditions. SD means standard deviation. Scale bar represents 1 cm.

2.4.5.2 Quantification of leaf cellular parameters in *sdg8-1 hub2-2* mutants

To get more insight into leaf growth defects at the cellular level, leaf number 3 was taken as representative for cellular analysis because it is fully developed at 23 days with completed cell proliferation and expansion. Leaf 3 area was significantly reduced in the *sdg8-1* and *hub2-2* single mutant compared to wild type and the reduction was further enhanced in the double mutant (Figure 10A). Epidermal cell area was similar between the double mutant, *sdg8-1* and wild type, but was significantly increased in *hub2-2* (Figure 10B). Finally, the number of epidermal per leaf 3 was significantly reduced in both single mutants compared to wild type and additively reduced in our double mutant compared to *sdg8-1* and *hub2-2* (Figure 10C). Hence, it seems that the lamina area, width and length in the double mutant were reduced most likely because

of a reduction in the number of cells rather than in the cell size.

A

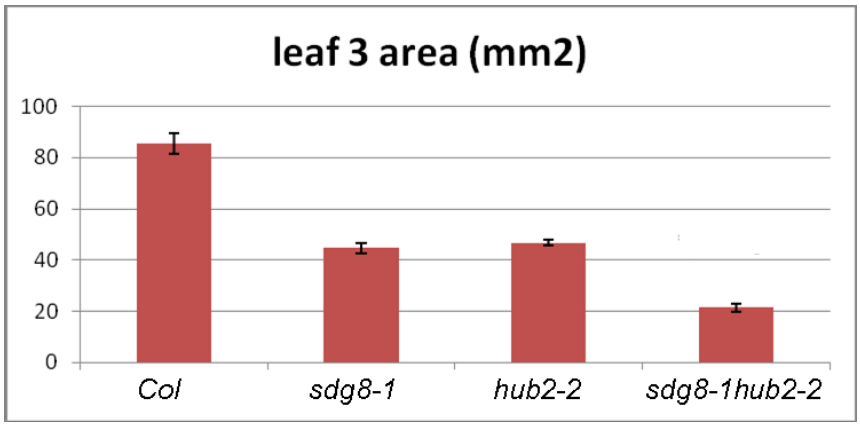

B

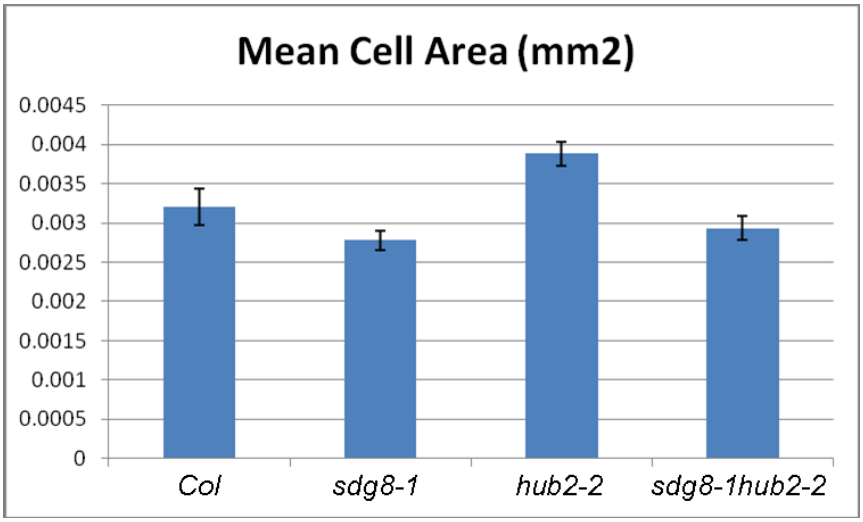

C

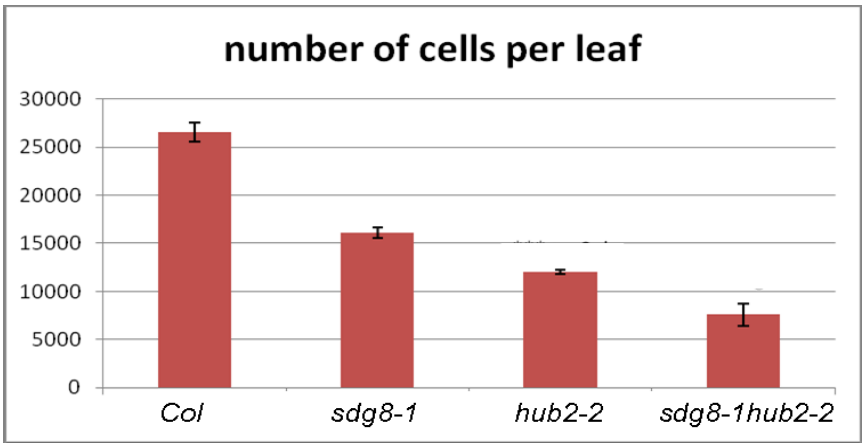

Figure 10: Mean values ± SD of leaf area (A), cell area (B) and cell number (C) measured on leaf-3 dissected from at least 5 23-day-old wild-type and mutant plants grown under long-day (LD; 16 h light and 8 h dark) photoperiod conditions. SD means standard deviation.

2.4.5.3 Analysis of ploidy levels in *sdg8-1 hub2-2* mutants

To investigate cell cycle progression and evaluate any possible effect of *SDG8* and/or *HUB2* mutations on endoreduplication, we measured by flow cytometry the ploidy levels of nuclei extracted from the first pair of true leaves of wild-type and mutant plants at 10, 11, 12, 14, 17 and 21 days after stratification (Figure 11).

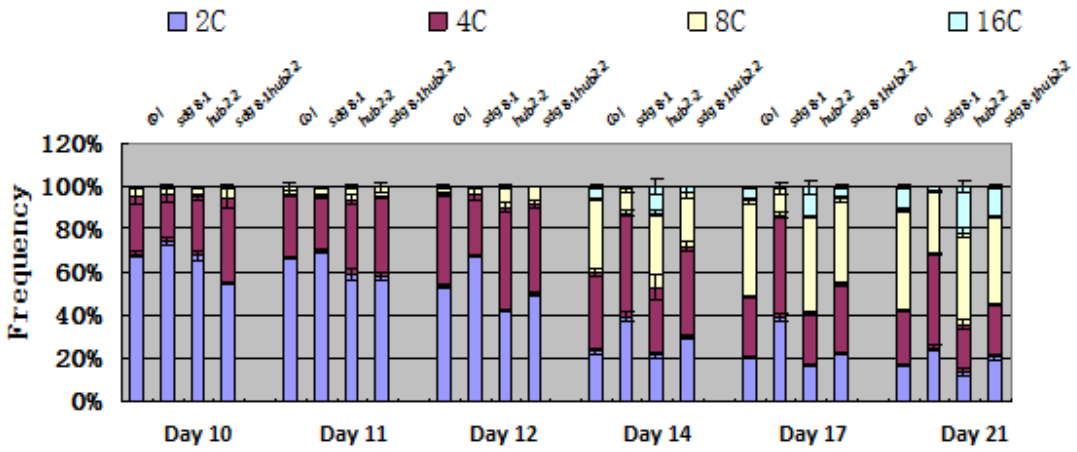

Figure 11: Mean values ± SD of the percentage of 2C, 4C, 8C and 16C nuclei extracted from the first pairs of leaves of 10, 11, 12, 14, 17, 21-day-old plants grown on ½ MS medium under long-day (LD; 16 h light and 8 h dark) photoperiod conditions. SD means standard deviation.

Already visible precociously, the proportion of nuclei in *sdg8-1* leaves with high ploidy levels (8C and 16C) was lower than in wild-type leaves, while the proportion of nuclei at the 2C and 4C levels stays abnormally high. These observations indicate that the entrance of cells in endoreduplication might be far less efficient in the mutant than in wild-type plants. Because both the cell number and the cell size were decreased in *sdg8-1* compared to wild type, this low occurrence of endoreduplication might further indicate that the mitotic cell cycle in *sdg8-1* is arrested either in the G1 phase or in the G2 phase of the diploid cell cycle.

At early stages, DNA ploidy profiles were largely similar between *hub2-2* and wild type plants, however, with aging, the proportion of 2C and 4C nuclei progressively decreased to the benefit of higher ploidy levels (8C and 16C). This change in

proportions indicate that the first endocycle occurs earlier and that subsequent endocycles succeed faster in *hub2-2* leaves than in wild-type leaves, therefore supporting the lower number of cells and their bigger size in this mutant.

Together, our results indicate that *SDG8* and *HUB2* have different direct or indirect functions regarding the control of cell cycle, with *SDG8* being involved in mitosis progression and *HUB2* in repressing the escape from a normal cell cycle to endoreduplication. Finally, in the double mutant, nuclei proportion were in between that of *sdg8-1* and *hub2-2*, thus resembling the proportion observed in wild type nuclei and further supporting the epistatic relationship that exist between this two allele regarding the control of cell cycle progression.

2.5 Flowering time analysis of *sdg8-1 hub2-2* double mutants

The most obvious phenotype of the *sdg8-1 hub2-2* (Figure 12) or *sdg8-1 hub1-3* (Supplemental Figure 3) double mutant was its precocious flowering. Therefore, we further focused our work on exploring the molecular origins of this flowering phenotype.

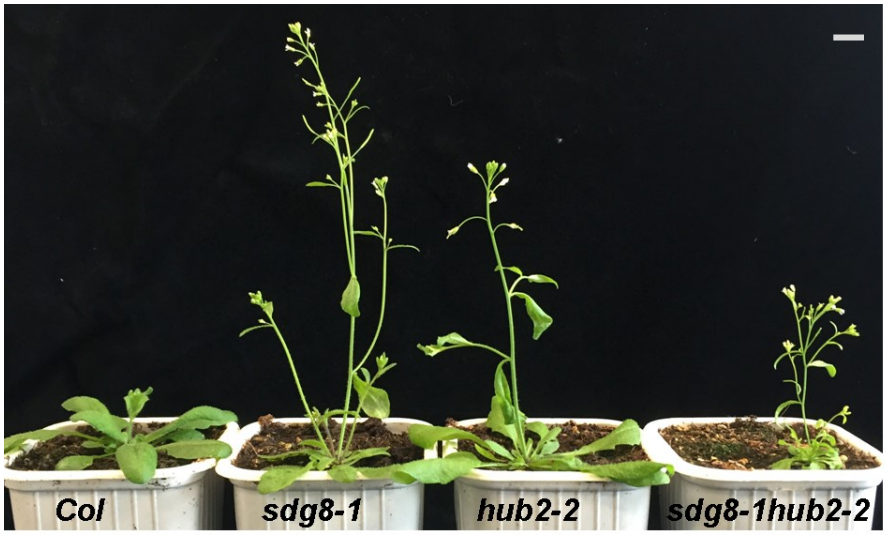

Figure 12: Representative flowering phenotype of plants grown under long-day (LD; 16 h light and 8 h dark) photoperiod conditions. Scale bar represents 1 cm.

2.5.1 Flowering time of *sdg8-1 hub2-2* mutants

Classically, flowering time can be measured as the number of days to flowering and/or as the leaf number at bolting, which represents interest of measurement from a developmental perspective (Michaels and Amasino, 1999). Both measurements were used to compare the flowering time of the wild-type and *sdg8-1*, *hub2-2*, *sdg8-1 hub2-2* mutant plants grown under long-day (LD;16 h light and 8 h dark), medium-day (MD; 12 h light and 12 h dark) or short-day (SD; 16 h light and 8 h dark) photoperiod conditions (Figure 13).

A

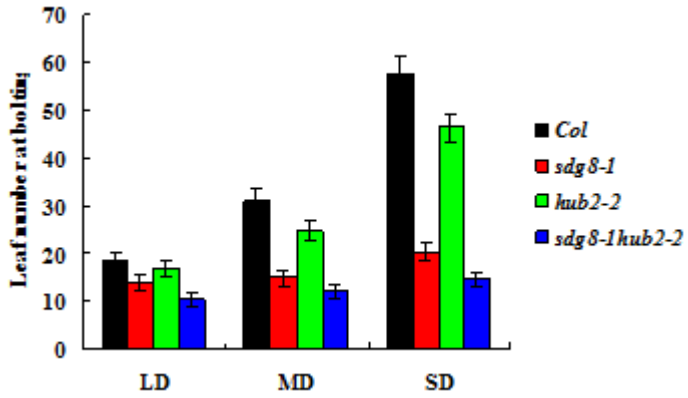

B

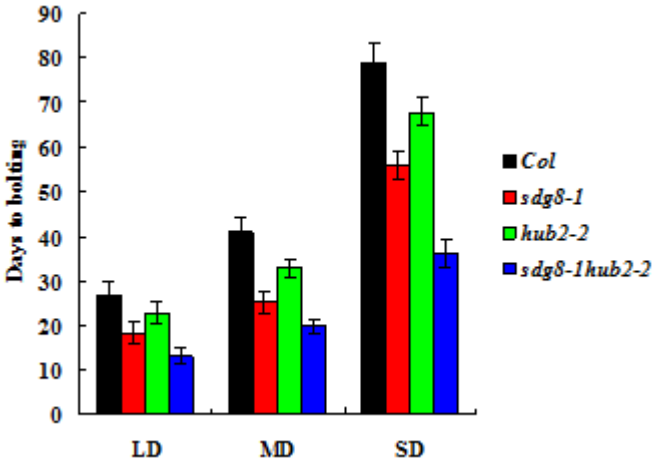

Figure 13: Flowering time measured by (A) rosette leaf number at bolting and (B) days to bolting in wild-type and mutant plants grown under long-day (LD;16 h light and 8 h dark), medium-day (MD; 12 h light and 12 h dark) or short-day (SD; 8 h light and 16 h dark) photoperiod conditions. Mean values are shown together with standard deviation bars, based on 3 independent biological replicates with each replicate comprising over 15 plants for each genotype.

2.5.2 Expression profiles of flowering time genes

Flowering represents the transition from the vegetative to reproductive development, and is mainly controlled by five flowering time pathways in Arabidopsis, including the photoperiod pathway, the vernalization pathway, the autonomous pathway, the gibberellins (GA) pathway and the age pathway (Teotia and Tang, 2015). FLC is a MADS-box transcription factor that acts as a central repressor of flowering, more specifically in the vernalization and autonomous pathways. FLC binds and represses the expression of several genes, including genes that promote flowering, the flowering time integrators *FT* and *SOC1*. The Arabidopsis genome contains five *FLC* homologs, named *MAF1* to *MAF5* that function redundantly in controlling flowering time. To investigate the molecular basis of the *sdg8-1 hub2-2* early flowering phenotype, the transcript levels of several flowering genes including major flowering repressor genes (*FLC*, *MAF1*, *MAF2*, *MAF3*, *MAF4* and *MAF5*) and flowering activator genes (*FT* and *SOC1*) were measured by quantitative RT- PCR and compared to that of *sdg8-1* and *hub2-2* single mutants (Figure 14).

In *sdg8-1* mutants, transcript levels of *MAF2* and *MAF3* were only slightly reduced, while transcript levels of other flowering repressor genes *FLC*, *MAF1*, *MAF4*, and *M*AF5 were drastically reduced. More downstream, their target genes *FT* and *SOC1* appeared increased compared to the wild-type control. In *hub2-2*, expressions of *MAF2* and *MAF3* were not significantly affected, while *FLC* and *MAF1* transcript levels were only slightly reduced. Also, *MAF4* and *MAF5* expression levels in *hub2-2* were reduced to similar levels as in *sdg8-1* and *SOC1* and *FT* expressions were increased. Interestingly, expression levels of all the examined flowering time repressor genes were down-regulated in our *sdg8-1 hub2-2* double mutants, resulting in an increase in both *SOC1* and *FT* expressions. In details, *FLC*, *MAF1* and *MAF3* were similarly decreased in our double mutant as in *sdg8-1*, without any additive effect from the *HUB2* mutation, indicating that *SDG8* dominates over *HUB2* in the regulation of the expression of these flowering time genes. *MAF2* was reproducibly more

downregulated in *sdg8-1 hub2-2* than in *sdg8-1*, indicating a possible synergistic genetic interaction between *SDG8* and *HUB2*. Interestingly, while the *FT* transcript level was synergistically increased in our double mutant compared to single ones, the *SOC1* expression was not further increased in *sdg8-1 hub2-2*. The absence of additive effect on *SOC1* expression might indicate that *SDG8* and *HUB2* act in the same pathway to activate the transcription of this locus.

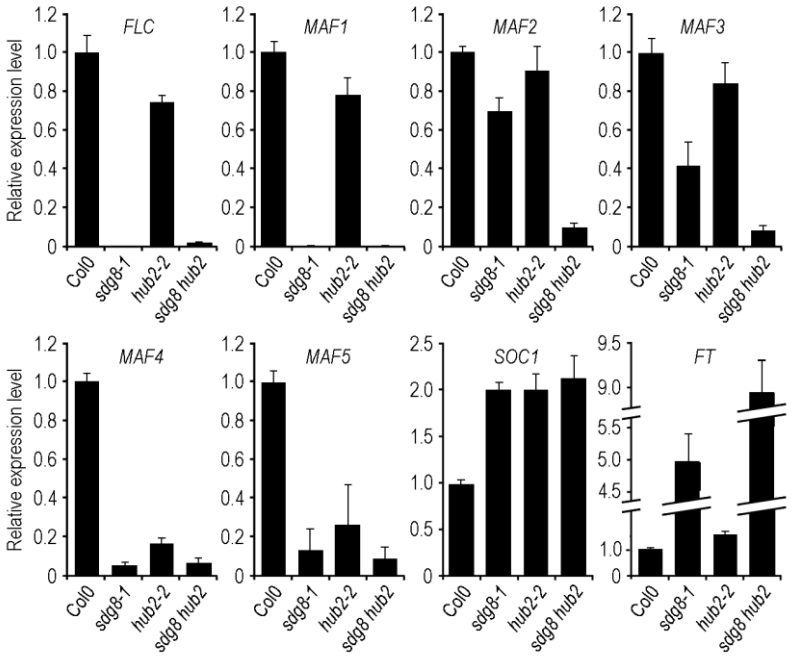

Figure 14: Quantitative RT-PCR analysis of flowering genes *FLOWERING LOCUS C* (*FLC*), *MADS AFFECTING FLOWERING 1-5* (*MAF1-5*), *SUPPRESSOR OF OVEREXPRESSION OF CO1* (*SOC1*) and *FLOWERING LOCUS T* (*FT*) in different mutants. A pool (over 10 seedlings) of 16-day-old seedlings was used for RNA extraction. Data were normalized using internal reference genes (*Tip4.1*, *Exp* and *GADPH*). Values are presented as relative to levels the wild type control (set as 1). Mean values are shown together with standard deviation bars.

2.5.3 ChIP analysis on flowering time genes

To gain insight into the molecular mechanism involved in the transcriptional mis-regulation of some flowering genes, ChIP (Chromatin ImmunoPrecipitation) assay was used to analyze and compare the level of H3K4me3, H3K36me3, H3K27me3 and H2Bub1 along the chromatin of *FLC*, *MAF3*, *MAF4*, *MAF5*, *SOC1* and *FT* between wild-type and mutant seedlings (Figure 15).

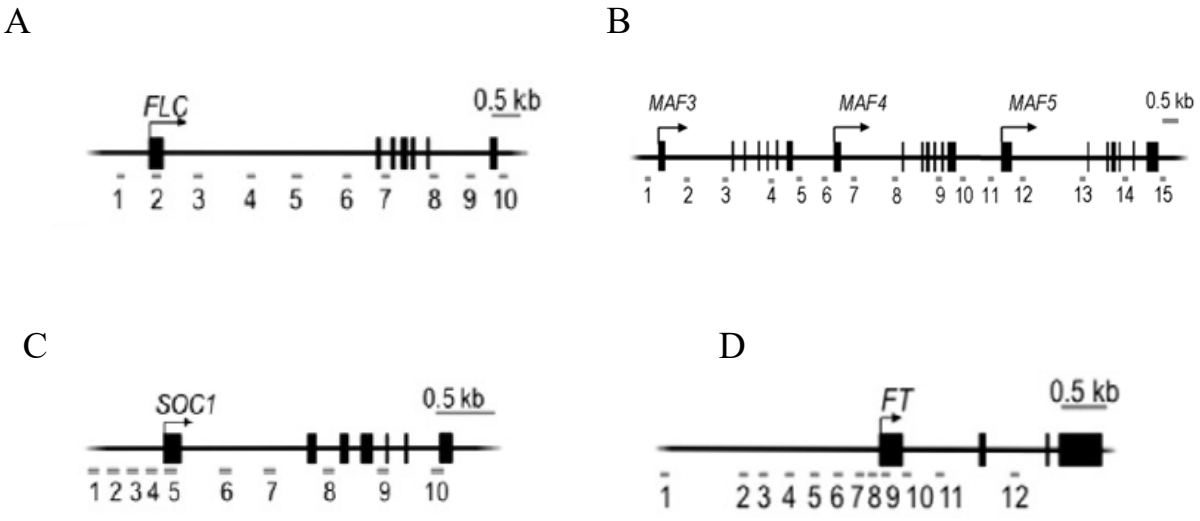

Figure 15: The different regions are numbered from the 5′-end to the 3′-end of the gene and their positions are indicated under the schematic presentation of *FLC* (A), *MAF3*, *MAF4* and *MAF5* (B), *SOC1* (C) and *FT* (D) gene structure showing black boxes for exons, black lines for promoters and introns, and arrows for transcription start sites.

2.5.3.1 ChIP analysis on *FLC* gene

Firstly, while comparing the different studied marks, it is interesting to notice that H3K4me3 formed a peak at the 5'-regions of *FLC*, around the Transcription Start Site (TSS), while H3K36me3, H2Bub1 and H3K27me3 were more spread along its chromatin. More precisely, in *sdg8-1*, the level of H3K4me3 was unchanged compared to the wild-type control, whereas levels of H3K36me3 and H2Bub1 were reduced all along *FLC* chromatin (Figure 16A, B and C). Probably benefiting from the decrease of HK36me3 and H2Bub1, the level of H3K27me3 was inversely increased all along *FLC* chromatin (Figure 16D), suggesting that H3K36me3 and/or H2Bub1 might contribute to prevent the spread of the H3K27me3 repressive mark. Overall, this set of results again confirms that SDG8 is per se an H3K36-specific methyltransferase essential for *FLC* transcription and suggest that at *FLC*, H3K36me3 is required for H2Bub1.

In *hub2-2*, the level of H2Bub1 was decreased, reinforcing the idea that HUB2 may function as an E3-ligase responsible for H2Bub1 deposition at *FLC*. Interestingly, both H3K4me3 and H3K36me3 levels were found decreased at *FLC* chromatin in *hub2-2* mutants and surprisingly the decrease in H3K36me3 was similar as the one observed in *sdg8-1* (Figure 16A, B and C). These observations indicate that at *FLC*

H2Bub1 is required for both H3K4 and H3K36 methylation. Put into perspective with our Q-PCR analyses (Figure 14), a directional dependence might therefore exist regarding the impact of histone mark variations on transcription. Indeed, the requirement of H3K4 and H3K36 methylation over H2Bub1 seems to have a lower impact on *FLC* transcription than the requirement of H2Bub1 over H3K36me3. As in *sdg8-1*, the level of H3K27me3 was globally increased in *hub2-2*, although less markedly, especially at the 3' end of *FLC* (Figure 16D).

In *sdg8-1 hub2-2*, the level of H3K4me3 was similarly reduced as in *hub2-2*, and H2Bub1 was found decreased like in *sdg8-1* or *hub2-2* (Figure 16A and C). Thus, at *FLC* chromatin, the H3K4me3 deposition is dependent from HUB2 but independent from the SDG8-mediated H3K36me3 deposition. Surprisingly, the H3K36me3 level in *sdg8-1 hub2-2* was additively reduced with respect to *sdg8-1* and *hub2-2* (Figure 16B). This result might indicate that the deposition of the H3K36me3 mark first strongly depend on SDG8 and second can be subdivided in two categories, (*i*) one that is required for H2Bub1 deposition and (*ii*) another one, in line with the hierarchical model of histone modification during transcription in animal and yeast, which dependent on H2Bub1 deposition. Finally, the H3K27me3 enrichment was similar between *sdg8-1* and *sdg8-1 hub2-2.* This last observation, together with the difference observed between *sdg8-1* and *hub2-2* regarding the enrichment of H3K27me3, indicate that the H3K36 trimethylation arising from the H2Bub1 deposition might directly or even indirectly less well restrain the spreading of H3K27me3.

A

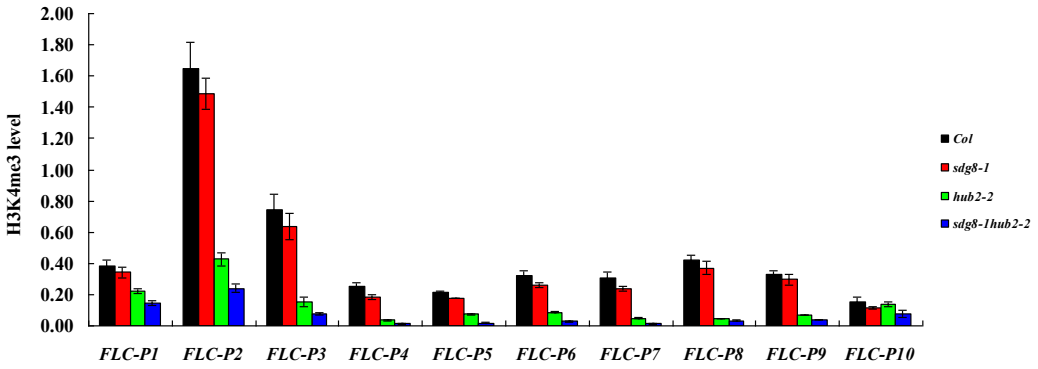

B

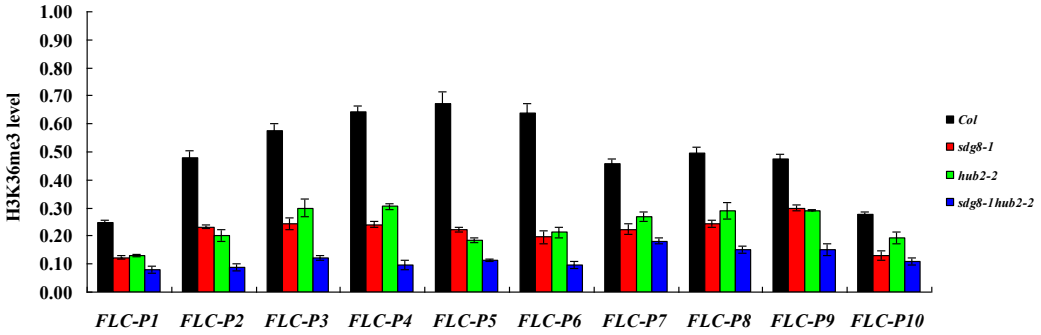

C

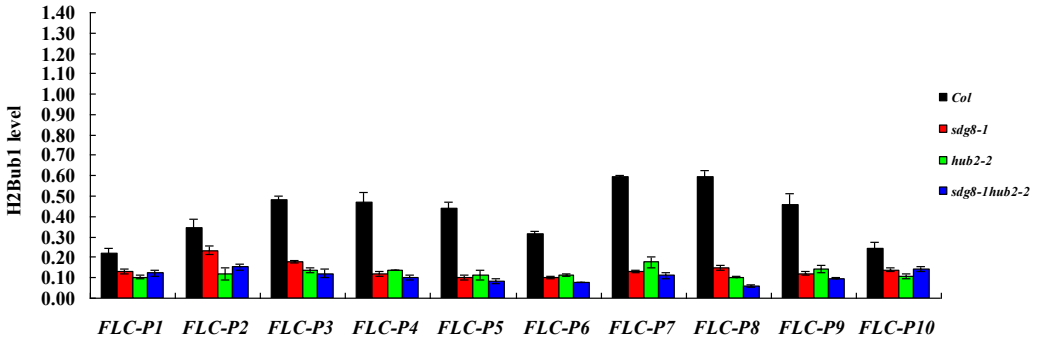

D

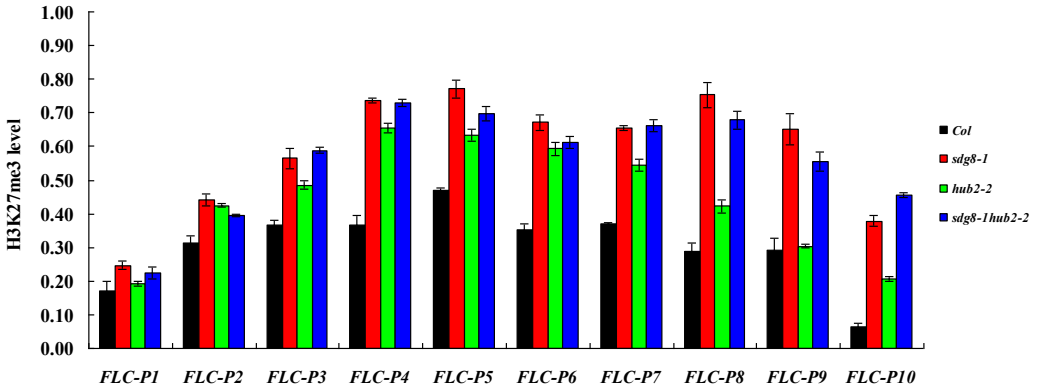

Figure 16: ChIP analyses of H3K4me3 (A), H3K36me3 (B), H2Bub1 (C) and H3K27me3 (D) levels in *sdg8-1*, *hub2-2* and *sdg8-1 hub2-2* mutant plants along the chromatin of *FLC*. Chromatin was prepared from 16-day-old plants grown under medium-day (MD; 12 h light and 12 h dark) photoperiod conditions. Data were normalized to the input and presented relative to *Tubulin 2* (*Tub2*) in the wild-type control.

2.5.3.2 ChIP analysis on *MAF3/4/5* genes

Overall, it is interesting to notice that levels of H3K4me3, H3K36me3 and H2Bub1 in wild type plants were higher on *MAF3* than on *MAF4* and *MAF5*, while it was the opposite for H3K27me3 (Figure 17). This feature will require further work, but it might indicate that in this gene cluster *MAF3* is regulated differently than *MAF4* and *MAF5*. Supporting this hypothesis, CT values obtained during our Q-PCR analysis were systematically lower for *MAF3* (around 25.3) than for *MAF4* and *MAF5* (from 26.4 to 28.3), therefore reflecting a stronger level of transcript and probably a stronger expression. Moreover, one should also notice that unlike what we previously described for *FLC* chromatin, H3K4me3, H3K36me3 and H2Bub1 profiles were mostly overlapped.

When comparing mutants to wild type profiles, the H3K4me3 behavior along the chromatin of *MAF3*, *4* and *5* in *sdg8-1*, *hub2-2* and *sdg8-1 hub2-2* appeared very similar as what we described for *FLC* (Figure 17A). However, while an additive effect was observed at *FLC* in our double mutant, the level of H3K36me3 was decreased similarly in *sdg8-1*, *hub2-2* and *sdg8-1 hub2-2* (Figure 17B). Another difference between *FLC* and this gene cluster was observable for the level of H2Bub1. Indeed, while the H2Bub1 decrease along *FLC* was very similar between *sdg8-1*, *hub2-2* and *sdg8-1 hub2-2*, the level of H2Bub1 in *sdg8-1* was intermediate between the wild type level and the *hub2-2* and *sdg8-1 hub2-2* ones (Figure 17C). Regarding H3K27me3, its level was increased in both single and double mutants, but the increase was lower in *hub2-2* than in *sdg8-1* and *sdg8-1 hub2-2* and was limited to *MAF4* and *MAF5* chromatins (Figure 17D). As a result of the comparison between histone marks profiles and transcript levels, we propose that the decrease in *MAF3* mRNA observed for *sdg8-1* and the double mutants cannot be only explained by the decrease in the loading of the studied active marks or the increase in the H3K27me3 repressive one that we address in this work. Indeed, other marks, such as H3K36me2 that is known to be affected in *sdg8-1* (Xu et al., 2008), might explain with despite very similar histone profiles, *MAF3* is downregulated in *sdg8-1* and unchanged in *hub2-2*. Because

changes in active marks were weaker in *MAF4* compared to *MAF3* and to a lower extent to *MAF5*, while the level of H3K27me3 was the highest, we further propose that the decrease in *MAF4* mRNA observed for all mutant combinations might be essentially due to the increase in the loading of the studied repressive mark. Finally, because *MAF5* can be roughly defined as being half-way between *MAF3* and *MAF4* in terms of histone profiles, we propose that the decrease in *MAF5* mRNA observed for all mutant combinations might be due to the combined effect of the increase and the decrease in the loading of the studied repressive and active marks, respectively. Together, the here reported differences between *MAF3*, *MAF4* and *MAF5* strengthen the above-mentioned hypothesis that while being on a gene cluster, *MAF3*, *MAF*4 and *MAF5* might be transcriptionally regulated differently by histone modifications.

A

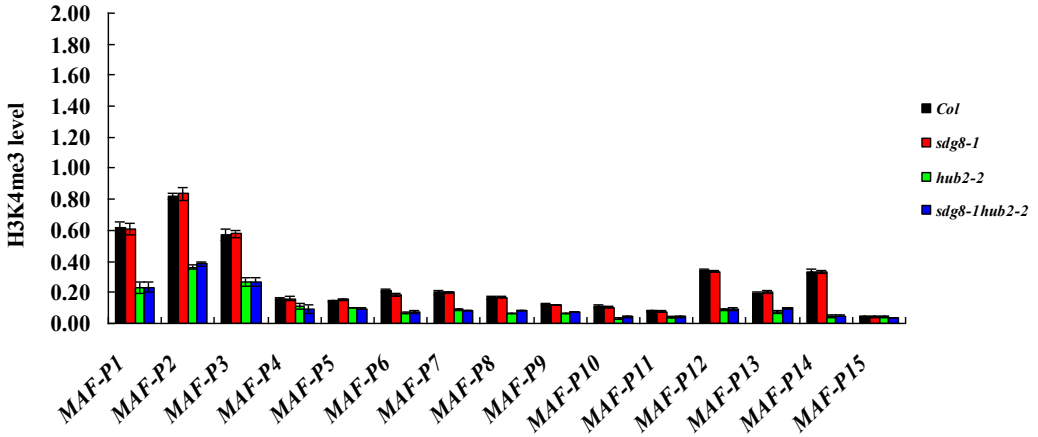

B

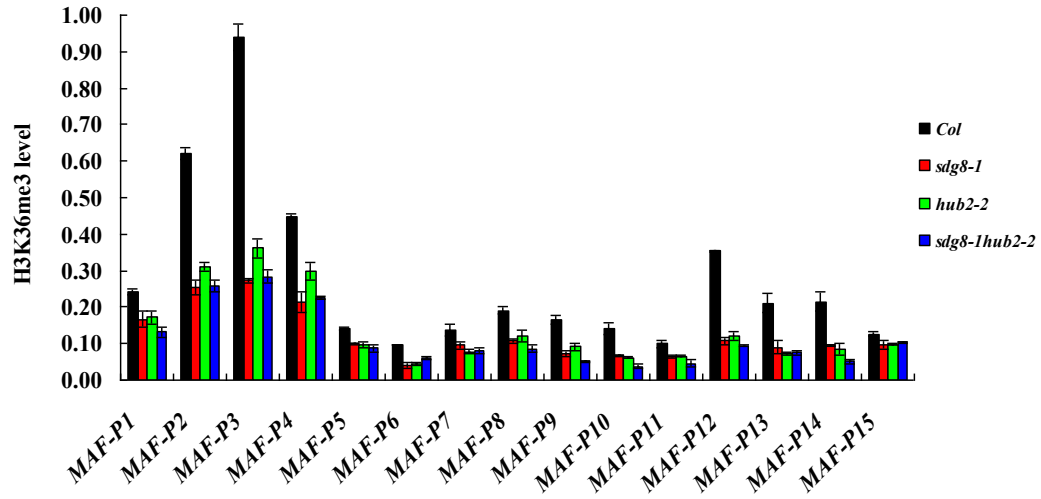

C

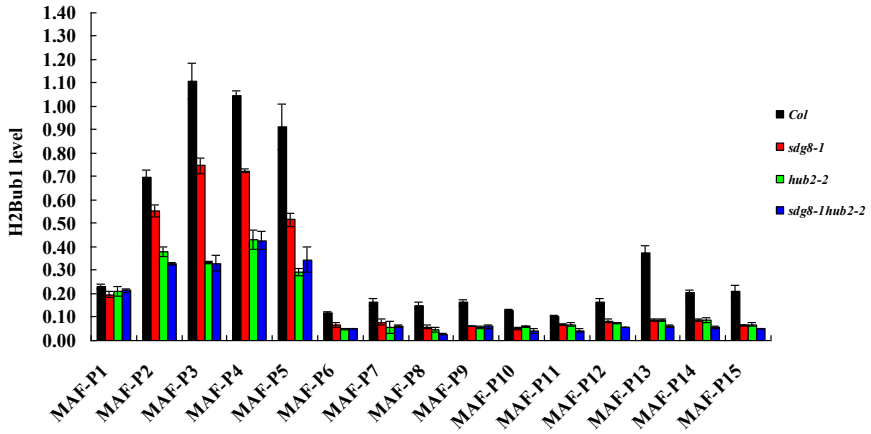

D

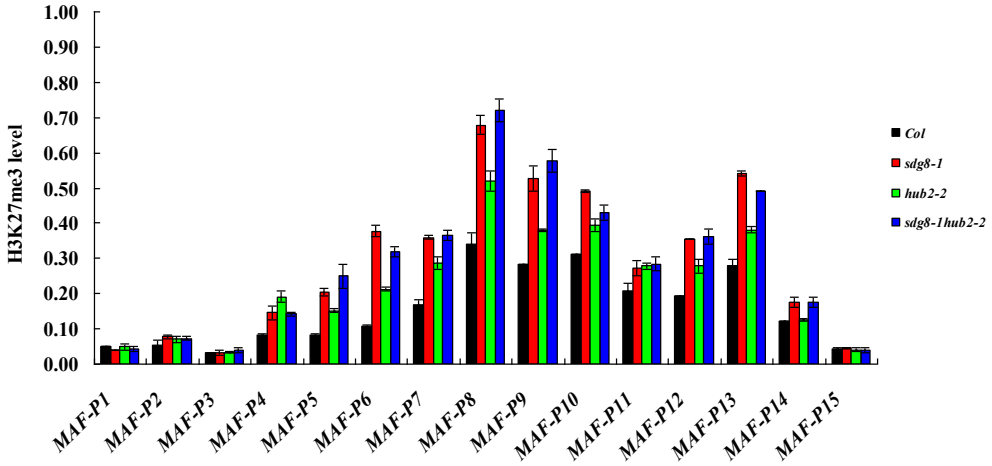

Figure 17: ChIP analyses of H3K4me3 (A), H3K36me3 (B) and H2Bub1 (C) and H3K27me3 (D) levels in *sdg8-1*, *hub2-2* and *sdg8-1 hub2-2* mutant plants along the chromatins of *MAF3/4/5*. Chromatin was prepared from 16-day-old plants grown under medium-day (MD; 12 h light and 12 h dark) photoperiod conditions. Data were normalized to the input and presented relative to *Tubulin 2* (*Tub2*) in the wild type control.

2.5.3.3 ChIP analysis on *SOC1* gene

Like *FLC*, a H3K4me3 peak was visible around the *SOC1* TSS and the H2Bub1 mark was more dispersed along its chromatin (Figure 18). However, unlike *FLC* but similarly to *MAF3*, the H3K36me3 peak was almost overlapping with H3K4me3 one.

In general, the chromatin behavior of the three studied active marks along *SOC1* was very similar to that of *FLC* in our different mutant combinations (Figure 18A, B and C). In details, H3K4me3 was unchanged in *sdg8-1*, while its level was decreased similarly in *hub2-2* and *sdg8-1 hub2-2* (Figure 18A). Next, the level of H3K36me3 along *SOC1* chromatin was equally decreased in *sdg8-1* and *hub2-2* (Figure 18B). In *sdg8-1 hub2-2,* a subtle and less-than-additive effect was detectable, especially around the Transcription Start Site (TSS), where the H3K36me3 peaks. This observation might indicate that, like for *FLC* chromatin but less pronounced, part of the H3K36me3 deposition is dependent on the presence of H2Bub1, while the other part seems inversely required for H2B monoubiquitination. Another feature that distinguishes *SOC1* from *FLC* or the *MAF* gene cluster is regarding the H3K27me3 enrichment observed in *hub2-2* which reach a similar level as the ones observed with either *sdg8-1* or *sdg8-1 hub2-2*. We believe that this might be due to the less pronounced additive effect observed between *sdg8-1* and *hub2-2* for the level of H3K36me3 in our double mutant. Together, the mutations of *SDG8* and/or *HUB2* contribute to roughly similar effect on the level of H3K4me3, H3K36me3, H2Bub1 and H3K27me3, while the impacts of these mutations on transcription were opposite, with *FLC*, *MAF3*, *MAF4* and *MAF5* being downregulated and *SOC1* being upregulated. As a possible explanation, we proposed that the expected inhibitory effect on *SOC1* expression that would have resulted from the decrease in H3K4me3, H3K36me3 and H2Bub1 and the increase in H3K27me3 observed in our mutants might have been over-compensated by the low expression levels of its repressors *FLC*, *MAF3*, *MAF4* and *MAF5*.

A

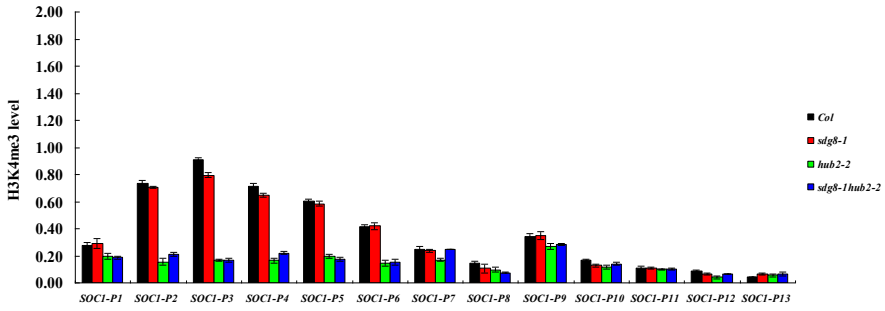

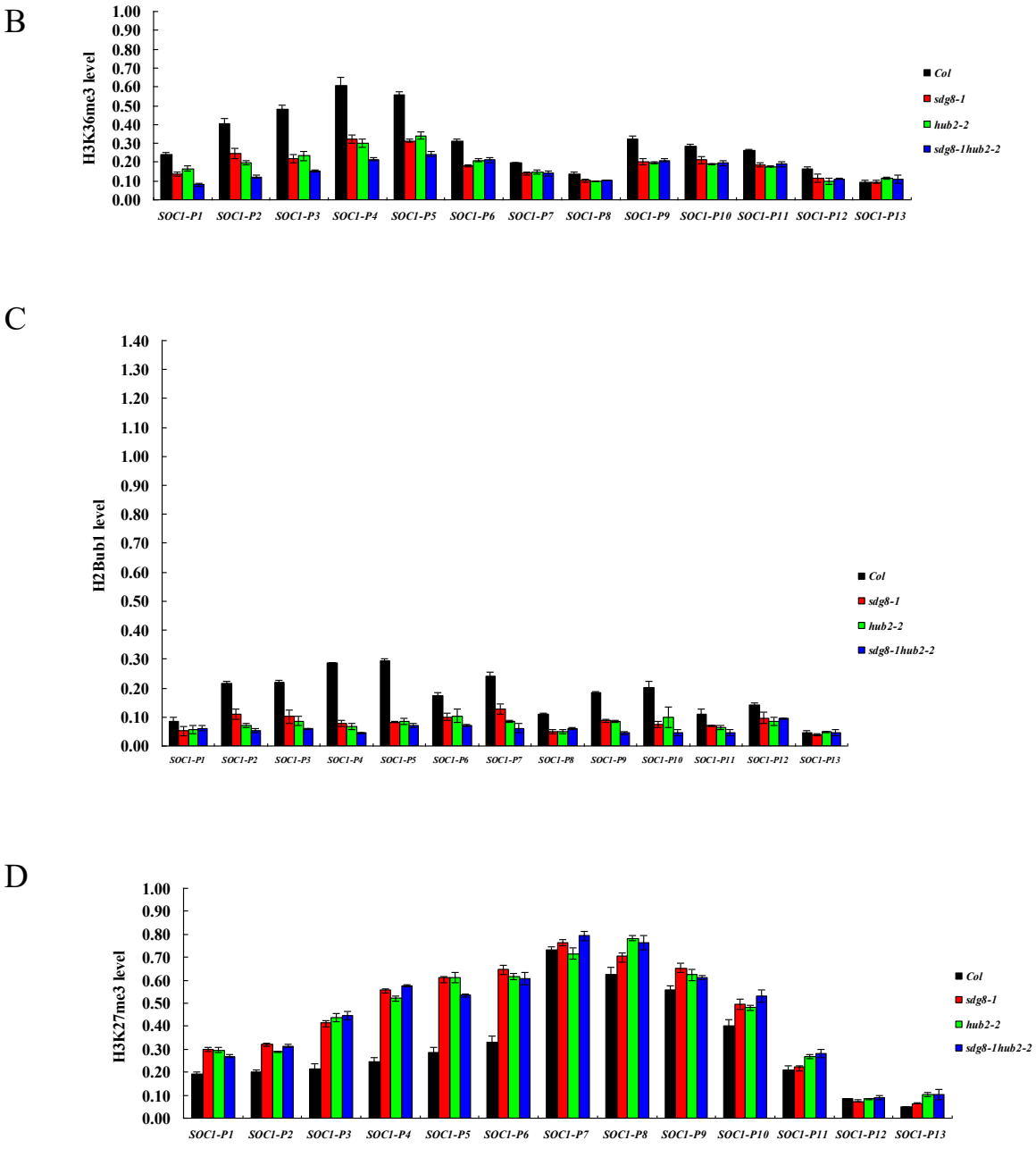

Figure 18: ChIP analyses of H3K4me3 (A), H3K36me3 (B) and H2Bub1 (C) and H3K27me3 (D) levels in *sdg8-1*, *hub2-2* and *sdg8-1 hub2-2* mutant plants along the chromatins of *SOC1*. Chromatin was prepared from 16-day-old plants grown under medium-day (MD; 12 h light and 12 h dark) photoperiod conditions. Data were normalized to the input and presented relative to *Tubulin 2* (*Tub2*) in the wild type control.

2.5.3.4 ChIP analysis on *FT* gene

Another floral integrator gene, *FT*, was also analyzed by ChIP. Our choice to present ChIP results as relative to our reference gene in the wild type control and not relative to wild type at each primer pair enabled us to explore variations of histone mark profiles along each gene, and made it also possible to compare profiles between the studied genes. Thus, when comparing the chromatin of *FT* with the one of other flowering genes, it becomes evident that levels of H3K4me3, H3K36me3, H2Bub1 and H3K27me3 were dramatically lower (Figure 16, 17, 18 and 19). Unfortunately, our ChIP procedure does not enable us to address specifically chromatin profiles in cells were the gene of interest is expressed. Therefore, chromatin profiles of cells where a gene is active get “diluted” in chromatin profiles from cells where the gene is silenced or inactive. This technical limit might therefore explain, at least partially, the distinctive observation we made for the *FT* chromatin profile, especially when considering that prior flowering *FT* is far less widely expressed than *FLC* and *SOC1* (Searle et al.,2006; Farrona et al., 2012).

Of course, a supplementary explanation would simply be that FT transcription is weakly influenced by the variability of histone modification levels, but is more under the direct control of its repressors (i.e. *FLC*, *MAF3*, *MAF4* and *MAF5*). Supporting this last hypothesis, it is interesting to notice that despite the low levels of active marks along *FT* chromatin and their slight variations in our mutants, the *FT* expression was found upregulated as the result of the low expression levels of its repressors (Figure 14).

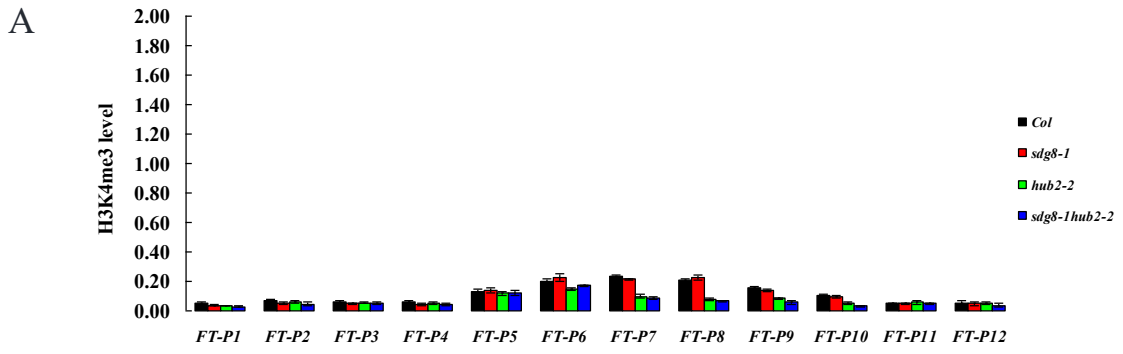

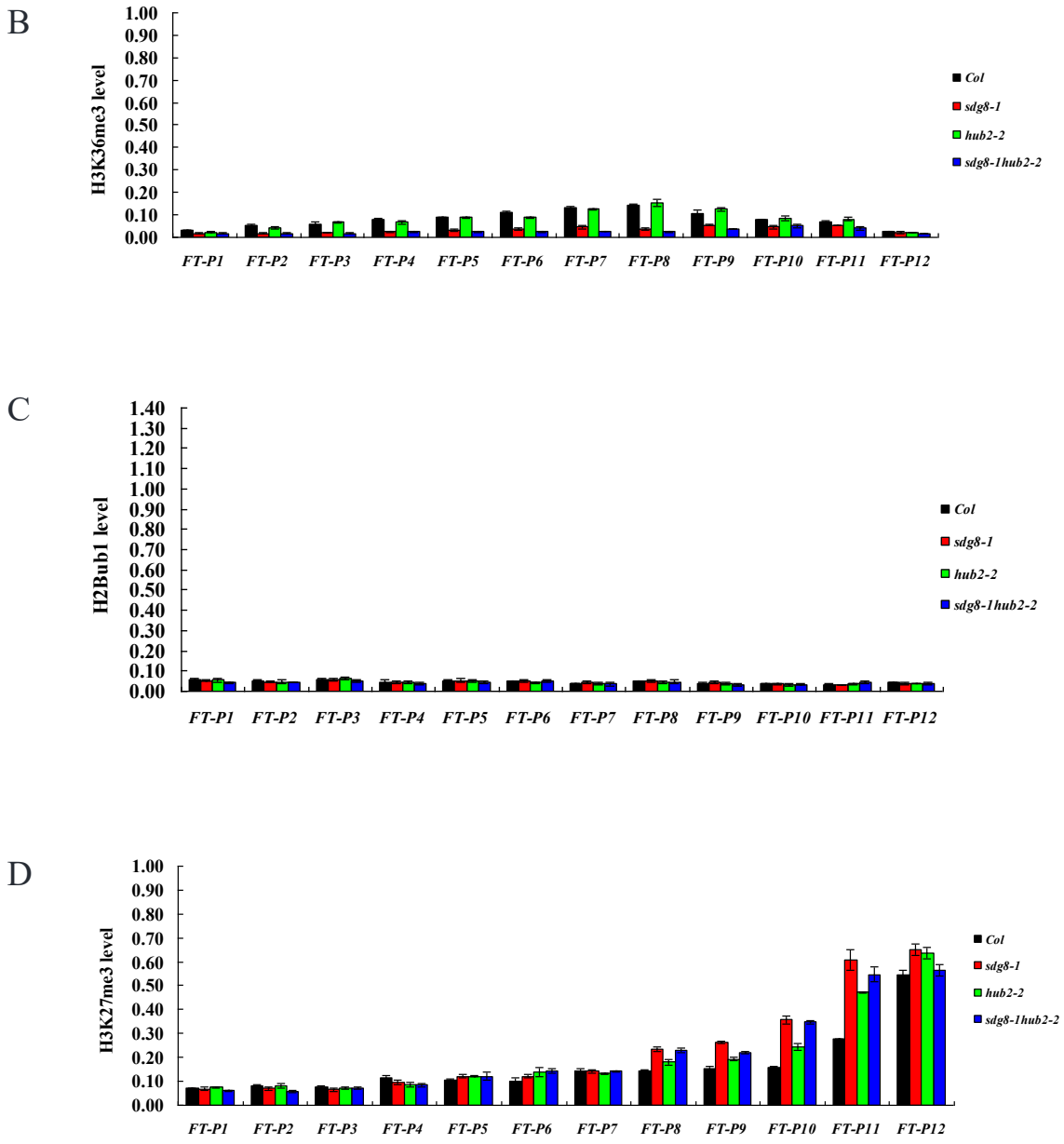

Figure 19: ChIP analyses of H3K4me3 (A), H3K36me3 (B) and H2Bub1 (C) and H3K27me3 (D) levels in *sdg8-1*, *hub2-2* and *sdg8-1 hub2-2* mutant plants along the chromatins of *FT*. Chromatin was prepared from 16-day-old plants grown under medium-day (MD; 12 h light and 12 h dark) photoperiod conditions. Data were normalized to the input and presented relative to *Tubulin 2* (*Tub2*) in the wild type control.

2.6 Transcriptome analysis of *sdg8-1 hub2-2* double mutants

In order to investigate the role of *SDG8* and *HUB2* in genome expression pattern, transcriptome analysis was performed for the *sdg8-1*, *hub2-2*, and *sdg8-1 hub2-2* mutants. Genes showing greater than 1.5-fold changes and with a *P* values less than 0.05 ($P \leq 0.05$) were considered as differentially expressed genes as compared to our wild-type control.

In *sdg8-1*, 1094 genes were found as differentially expressed (Supplemental Figure 4), with 721 (65.9%) and 373 (34.1%) genes being down-regulated and up-regulated, respectively (Figure 20). In *hub2-2*, 300 genes were differentially expressed (Supplemental Figure 4), with 156 (52%) and 144 (48%) genes being down-regulated and up-regulated, respectively (Figure 20). Remarkably, *SDG8* and *HUB2* have both common and different target genes in the genome. Comparison of differentially expressed genes between the *sdg8-1* and *hub2-2* mutants revealed an overlap of 108 genes, a number relatively small but significantly above the random value expected for two independent regulators (Representation Factor (RF) = 5.8, P<2.46E54; RF and statistical significance was measured with a hyper-geometric test using the web-based calculator http://nemates.org/MA/progs/overlap_stats.html. An RF>1 indicates more overlap than expected between two groups at random). Also, it is interesting to notice that the large majority (87%) of the 108 overlapping genes were mis-regulated in the same direction, with 66 genes being up-regulated and 28 genes being down-regulated in both *sdg8-1* and *hub2-2* (Figure 20).

In the *sdg8-1 hub2-2* double mutant, 1472 genes in total were found as differentially expressed (Supplementary Table 5), with 909 (61.7) and 563 (38.3%) genes being down-regulated and up-regulated, respectively (Figure 20). Among down-regulated genes, about 30%, 4.9% and 3.1% are overlapping with *sdg8-1*, *hub2-2*, or both, respectively (Figure 20A). Among up-regulated genes, about 22%, 3.0% and 4.1% are overlapping with *sdg8-1*, *hub2-2*, or both, respectively (Figure 20B). The remaining differentially expressed genes (about 62% and 71% for down-regulated and up-regulated genes, respectively) are specifically found in the *sdg8-1 hub2-2* double

mutant but not in the *sdg8-1* and *hub2-2* single mutants, suggesting the synergistic/redundant co-regulation of these genes by *SDG8* and *HUB2* (Figure 20).

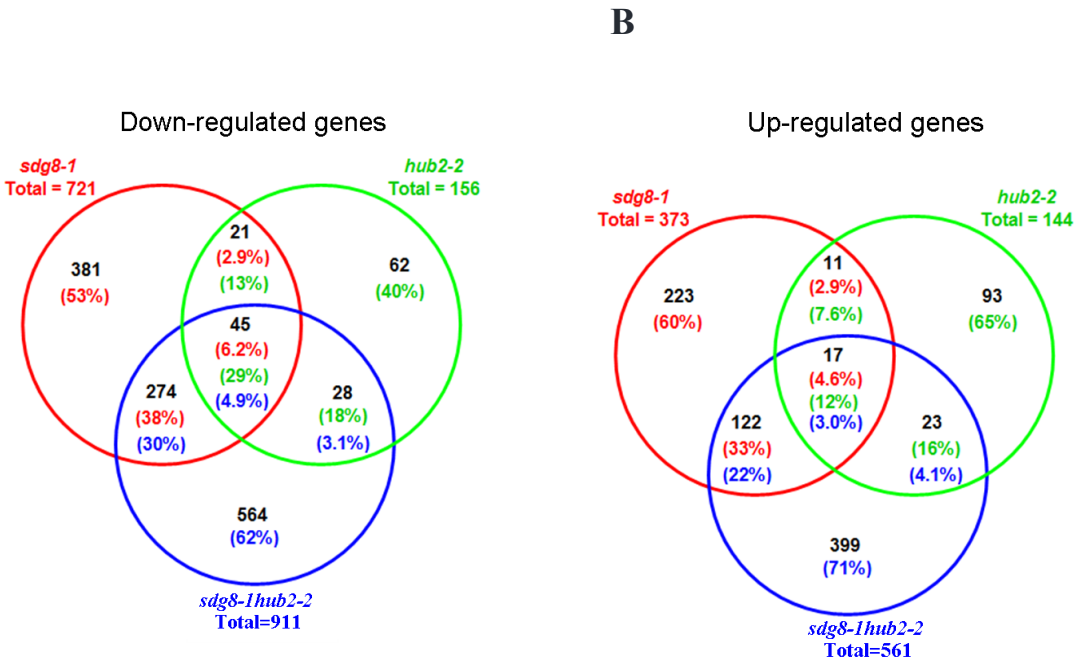

Figure 20: Venn diagrams display numbers of down-regulated genes (A) and up-regulated genes (B) identified by microarray analysis of wild-type and the mutant plants. Numbers in parentheses represent the percentage of overlap in the different mutants as indicated by the corresponding different colors.

3. Discussion and conclusions

SDG8 encodes a major H3K36me2/3 methyltransferase as in *sdg8* mutants, H3K36me2/3 level was globally decreased (Zhao et al., 2005; Xu et al., 2008; Liu et al., 2016; this study). H2B monoubiquitination is catalyzed by the E2 ubiquitin-conjugating enzymes UBC1 and UBC2 together with the E3 ubiquitin-ligation enzymes HUB1 and HUB2. H2Bub1 levels are globally lost in *hub1* and *hub2* single mutants as well as in the *hub1 hub2* and *ubc1 ubc2* double mutants, but are unaffected in the *ubc1*, *ubc2* single mutants (Cao et al., 2008; Gu et al., 2009; Xu et al., 2009). To investigate the possible crosstalk between H2Bub1 and H3K36me3 in Arabidopsis we generated the *sdg8-1 hub2-2* double mutant by classical genetic cross between *sdg8-1* and *hub2-2*.

3.1 Crosstalks among H3K4me3, H3K36me3 and H2Bub1 are not present on the genome-wide in Arabidopsis.

H3K4me3, H3K36me3 and H2Bub1 are major active histone marks in yeast, animals and plants. Studies in yeast and animals have uncovered intriguing crosstalks among these marks in concert to control organism development and particularly focused on gene transcription. In yeast, loss-of-function of Bre1, the homologue of HUB2, causes a total loss of H3K4me3 (Hwang et al., 2003; Zhu et al., 2005) and loss-of-function of Ubp8, the H2B deubiquitinase, causes a decreased in H3K36me2 at specific loci. A model of active transcription was built with histone modifications occurring in a sequential manner. In this model, H2Bub1 is required for H3K4me3 deposition during transcription initiation, the removal of H2Bub1 is latter necessary for H3K36me3 deposition during transcription elongation. It is thus of great interest to investigate the conservation of such a crosstalk in Arabidopsis.

By western blots, we did not observe any changes of H3K4me3 in *hub2-2* as well as in *sdg8-1 hub2-2*. Moreover, global level of H3K36 methylation and H2Bub1 in the double mutant was similar as in *sdg8-1* and *hub2-2* single ones, respectively. These

data strongly indicate that a clear crosstalk between H2Bub1, H3K4me3 and H3K36me3 is not evident in Arabidopsis as in animal or yeast at a global genomic-scale. However, a significant increase of the global level of the repressive mark H3K27me3 was observed in our double mutant, indicating that *SDG8* and *HUB2* might together contribute to limit the spread of this repressive mark. Because CLF is one of the H3K27me3 methyltransferase in Arabidopsis of which the mutation is causing a global decrease of H3K27me3 (Jiang et al., 2008), it will be very interesting to investigate the H3K27me3 level in *sdg8-1 hub2-2 clf* triple mutants.

3.2 *SDG8* and *HUB2* act synergistically to regulate Arabidopsis plant growth.

Since the depletion of either *SDG8* or *HUB2* leads to smaller plant size, H3K36me2/3 and H2Bub1 might be positively linked to plant growth. It is thus of great interest to uncover possible functional relationships between histone methylation and monoubiquitination during plant growth. To this end, we have thoroughly analyzed phenotypes of *sdg8-1 hub2-2* mutants and found that double mutant plants display an enhanced reduction of silique length, chlorophyll content, root length, plant body size and rosette leave size compared to the *sdg8-1* and *hub2-2* single mutants.

The plant size is intrinsically determined by cell division and cell expansion. Because no retardation in leaf initiation was observed, we measured the cell size and number parameters in rosette leaf to uncover the mechanisms underlying the growth defect of our mutants. Interestingly, we observed that the decrease of the cell number per leaf was enhanced in the double mutants, suggesting that *SDG8* and *HUB2* synergistically regulate cell proliferation. The cell area was decreased in *sdg8-1* and *sdg8-1 hub2-2*, while it was increased in *hub2-2*, indicating that *SDG8* and *HUB2* may act in opposite manner along the same regulatory pathway, with *SDG8* acting upstream of *HUB2*. However, our flow cytometry data demonstrates that cell cycle progression and endoreduplication are differently affected in our mutants, suggesting that the number of cells is indeed decreased in both *sdg8-1* and *hub2-2*, but for different reasons (i.e. a delay in mitosis for *sdg8-1* and a precocious entry in endoreduplication

for *hub2-2*).

Altogether, these results reveal that while plant growth is synergistically affected by the two mutations, *SDG8* and *HUB2* act separately, with *SDG8* being more involved in the mitosis progression and *HUB2* the mitosis-to-endoreplication transition.

3.3 *SDG8* and *HUB2* synergistically regulate Arabidopsis flowering time.

Since the most obvious phenotype of *sdg8-1* and *hub2-2* mutants is their early flowering, it is evident that H3K36me2/3 and H2Bub1 play together or not an important role in preventing precocious flowering. It is therefore of great interest to unveil if a crosstalk exist between these marks to control flowering time. Previously, some genetic interactions were tested regarding the control of flowering time in which the *SDG8* mutation was combined with different mutants encoding different histone methylation enzymes (i.e. comprising the histone methyltransferase ATX1/2, SDG25, SDG26, CLF) and the histone demethylase LDL1/2 (Shafiq et al., 2014; Berr et al., 2015; Liu et al., 2016). These combined mutants showed different flowering behavior with *sdg8 atx1*, s*dg8 atx2*, *sdg8 sdg25* or *sdg8 sdg26, sdg8 ldl1ldl2* displaying a *sdg8*-like early-flowering phenotype, while *sdg8 clf* was flowering even earlier than either *sdg8* or *clf* single mutant.

In this vein, we here addressed the question of the flowering control in our *sdg8-1 hub2-2* double mutant. We observed that *sdg8-1 hub2-2* was flowering earlier than each single mutant, at a similar level as what was previously published for *sdg8 clf*, suggesting that an additive or even synergistic interaction occurred between *SDG8* and *HUB2* to control flowering.

3.4 Crosstalk between histone methylation and monoubiquitination during transcription.

To address the molecular mechanism underlying the additive or synergistic interaction

that exist between *SDG8* and *HUB2* to control flowering, we explored transcriptional and chromatin changes at different flowering time genes. Previously, SDG8, SDG25, SDG26, ATX1/2, CLF and LDL1/2 were reported to regulate largely independently flowering genes (Shafiq et al., 2014; Berr et al., 2015; Liu et al., 2016).

In this study, we found that *SDG8* and *HUB2* play related roles in the transcriptional regulation of flowering time genes. Indeed, *FLC, MAF1, MAF3, MAF4,* and *MAF5* transcript levels were decreased in *sdg8-1* and *FLC*, *MAF1*, *MAF4* and *MAF5* transcript levels were decreased in *hub2-2*, which is broadly in line with previous reports. Interestingly, all these flowering repressor genes were downregulated in the *sdg8-1 hub2-2* double mutant to levels at or below the *sdg8-1* level. These data indicate that both *SDG8* and *HUB2* are involved in the transcriptional regulation of *FLC, MAF1*, *MAF2*, *MAF3*, *MAF4* and *MAF5*, with *SDG8* playing a stronger role than *HUB2*. Correspondingly, transcript levels of the downstream gene targets *FT* and *SOC1* were increased in *sdg8-1*, *hub2-2* and *sdg8-1 hub2-2*. Interestingly, the transcript level of *FT* was further increased in *sdg8-1 hub2-2* double mutant compared to single ones, which can largely explain the flowering behavior of our double mutant. Interestingly, the *SOC1* expression is not only being repressed by *FLC*, but is also activated by *FT* (Yoo et al., 2005). Because *SOC1* is up-regulated to a similar level in both our single and double mutants, we proposed that a decrease in the transcription of one of its repressor might be enough to provoke an increase in the expression of *SOC1* to a maximum that cannot be overcome.

3.5 H3K36me2/3 and H2Bub1 in regulation of flowering time gene chromatin status.

Previous studies have demonstrated that SDG8 and HUB2 are respectively required for H3K36me2/3 and H2Bub1 deposition at *FLC* chromatin and thus promoted its gene transcription. This is consistent with the notion that H3K36me2/3 and H2Bub1 are important in establishing an active chromatin state. During transcription, H2Bub1 was proposed to be coupled to H3K4me3 and H3K36me2 in yeast and humans. In

Arabidopsis, H3K4me3 and H3K36me2 were found to be decreased on *FLC* in *hub2-2* mutant (Cao et al., 2008).

In this study, we found the H3K4me3 level on *FLC*, *MAF3/4/5* and *SOC1* was unchanged in *sdg8-1,* but decreased to a similar level in *sdg8-1 hub2-2* as in *hub2-2*. These results strongly indicate that the H3K4me3 deposition is dependent from H2Bub1 but independent from the SDG8-mediated H3K36me3 deposition.

The level of H3K36me3 was decreased in *sdg8-1* along *FLC*, *MAF3/4/5* and *SOC1* chromatin. In *hub2-2*, H3K36me3 was reduced to a similar level as in *sdg8-1* at these genes loci. Interestingly, *at MAF3/4/5*, the H3K36me3 decrease in *sdg8-1 hub2-2* double mutant was similar as in *sdg8-1*, *hub2-2* single ones, while an additive effect at *FLC* and to a less extent at *SOC1* was observed in our double mutant. This result might indicate that the deposition of the H3K36me3 mark first strongly depend on SDG8 and second can be subdivided in two categories, (*i*) one that is required for H2Bub1 deposition and (*ii*) another one, in line with the hierarchical model of histone modification during transcription in animal and yeast, which dependent on H2Bub1 deposition. In this context, it is noteworthy that the H3K36me3 in Arabidopsis has been proposed to play an equal role as H3K79me3 in yeast during transcription elongation due to their similar genome-wide distribution (Roudier et al., 2011). Given that the deposition of H3K36me3 on some specific genes loci is rely on H2Bub1, similar to that of H3K79me3 in yeast, thus provides additional evidence to support this hypothesis.

Intriguingly, H2Bub1 was reduced in *sdg8-1* and to a similar extent in *hub2-2* and *sdg8-1 hub2-2* along the chromatin of *FLC* and *SOC*1. While at *MAF3/4/5*, the level of H2Bub1 in *sdg8-1* was intermediate between the *hub2-2* and *sdg8-1 hub2-2* ones. These data uncovered that H3K36 me3 is inversely required for H2Bub1.

FT transcription seems to be less affected by the variability of histone modification levels, because the levels of H3K4me3, H3K36me3, H2Bub1 and H3K27me3 on *FT* were dramatically lower compared to those other flowering genes and only slight change can be observed among different genotypes. It is reasonable to conclude that the increase of *FT* expression is caused by reduced expression level of its repressors (i.e. *FLC*, *MAF3*, *MAF4* and *MAF5*), possibly regardless of the deposition and changes

of these transcriptional histone marks.

Collectively, on the basis of these results, we propose a model for the interplay of H3K4me3, H3K36me3 and H2Bub1 in the regulation of plant flowering genes transcription (Figure 21B). In this model, H3K4me3 is fully dependent on the loading of H2Bub1 as in animals (Figure 21). However, and in contrast with animal and yeast models (Figure 21A), there is not a fully exclusive correlation between H3K36me3 and H2Bub1 as it was not possible to clearly establish a hierarchical dependency. Therefore, SDG8 and HUB2 might mutually favor each other in establishing an active chromatin state on flowering genes (Figure 21B).

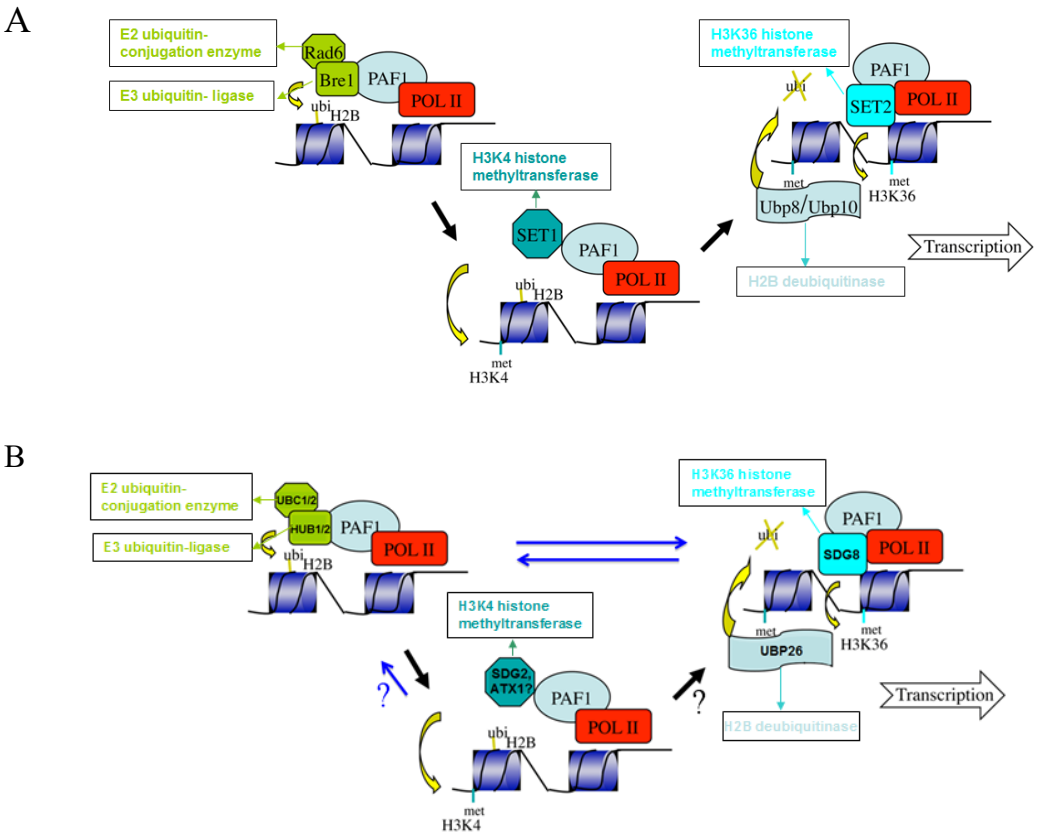

Figure 21: Model of interplay among H2Bub1, H3K4me3 and H3K36me3 on flowering genes transcription in yeast and animals (A) and Arabidopsis (B). In yeast animals and plants, H2Bub1 is necessary for the deposition of H3K4me3 during transcriptional initiation; H2Bub1 and H3K36me3 are mutually favor each other during transcriptional elongation in plants, while H2Bub1 is required for H3K36me3 in animals and yeast. It is yet not known the relationship between H2B deubiquitination and H3K36me3 deposition in plants.

Considering a weak but significant overlap of mis-regulated genes in *sdg8-1*,

hub2-2 and *sdg8-1 hub2-2* mutants revealed by our transcriptome analysis and the additive and/or even synergistic other plant growth defects in the double mutant, it is reasonable to speculate this model likely act beyond flowering genes transcription, but also involved in genes that control many other aspects of plant growth and development.

4. Supplementary data

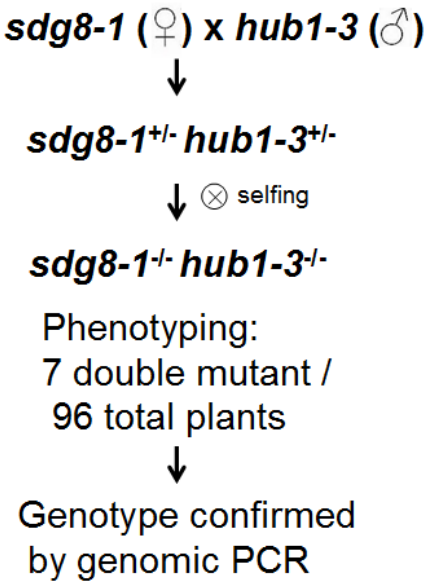

Supplemental Figure 1: Scheme of *sdg8-1 hub1-3* double mutant identification.

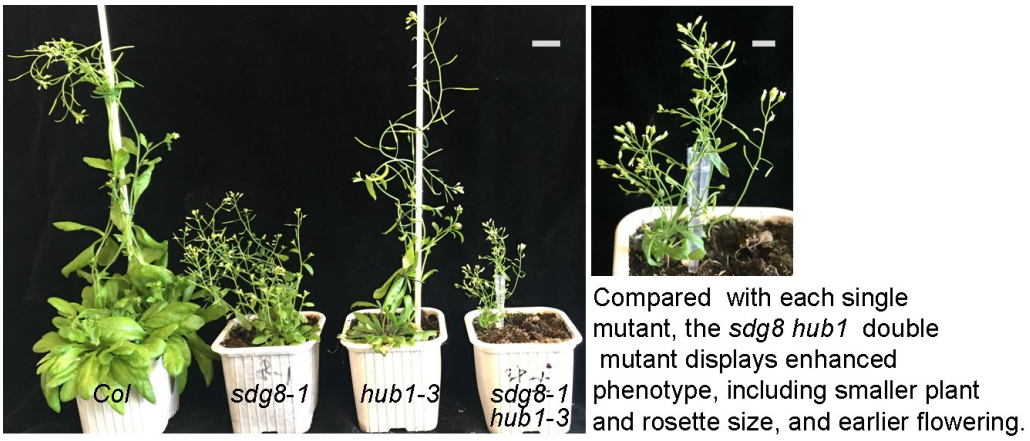

Supplemental Figure 2: Representative 40-day-old seedlings of Col, *sdg8-1*, *hub1-3*, and *sdg8-1 hub1-3* grown under long-day (LD; 16 h light and 8 h dark) photoperiod conditions. Scale bars represent 2 cm (left) and 1 cm (right).

A

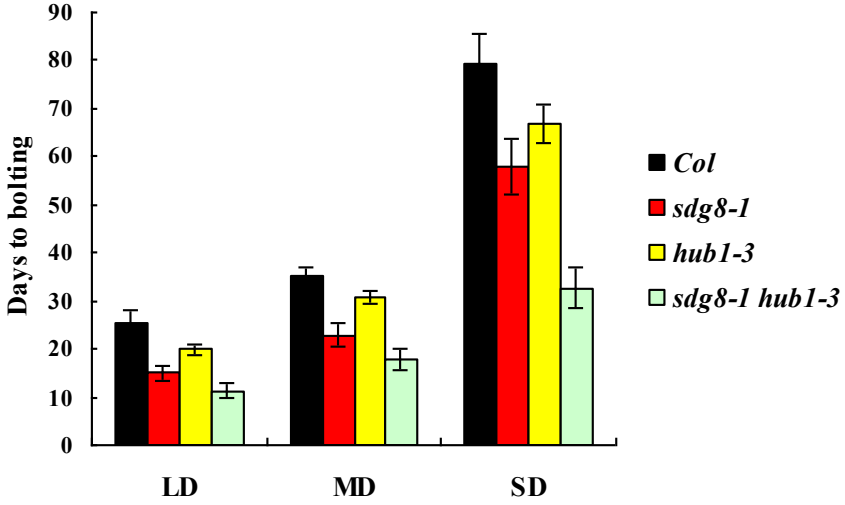

B

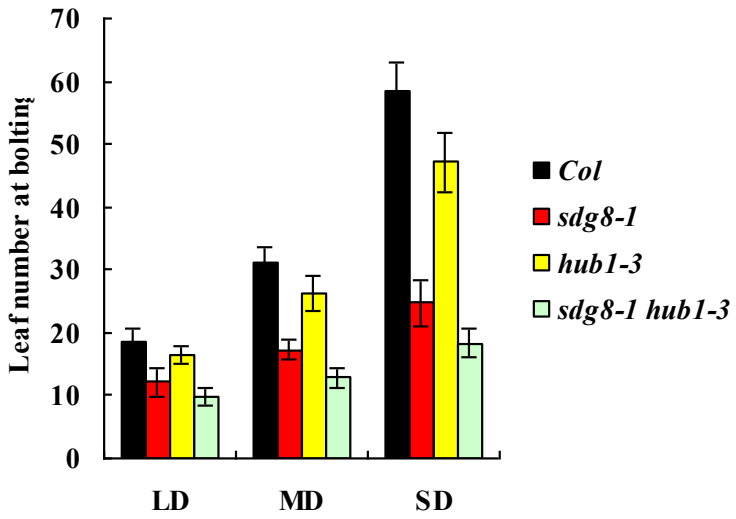

Supplemental Figure 3: Flowering time measured by (a) rosette leaf number at bolting and (b) days to bolting in wild-type and mutant plants grown under long-day (LD;16 h light and 8 h dark), medium-day (MD; 12 h light and 12 h dark) or short-day (SD; 8 h light and 16 h dark) photoperiod conditions.

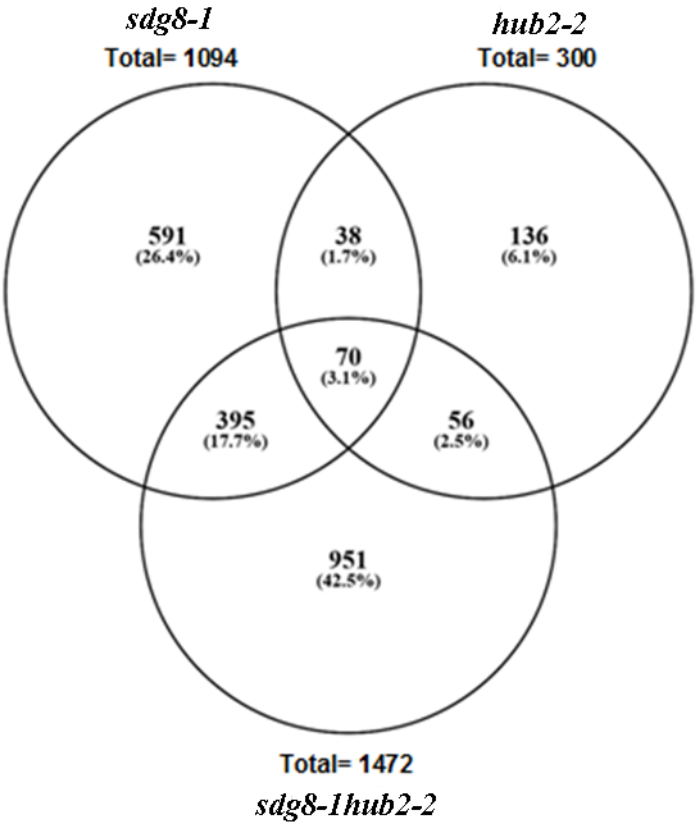

Supplemental Figure 4: Venn diagrams display numbers of differentially expressed genes identified by microarray analysis of wild-type and the mutant plants. Numbers in parentheses represent the percentage of overlap in the different mutants.

CHAPTER III

Structural and functional study of PWWP domain of HUA2/ HULK2, reader proteins of H3K36me2/3 in *Arabidopsis thaliana*

Wei Zhao, Nicolas Baumberger, Morgan Torchy, Alexandre Berr and Wen-Hui Shen

1. INTRODUCTION

SET DOMAIN GROUP 8 (SDG8)-mediated H3K36me2/3 is required for multiple developmental processes in Arabidopsis. Consistently, the *sdg8* mutant plants show globally reduced H3K36me2/3 level and thus has pleiotropic phenotypes (Zhao et al., 2005; Xu et al., 2008). However, the mechanism of H3K36me2/3 function is largely not known in plants. Compared to acetylation that changes the charge and thus reduces the interaction between histone and DNA, histone methylation does not per se directly trigger changes in the chromatin structure but it requires specific “readers” that will recognize the methylation signal and interpret it (Yun et al., 2011). In Arabidopsis, little is currently known about histone methylation readers, and especially regarding the domains involved in this binding as well as their specificity. Previously in the team, yeast two-hybrid screen was carried out using the SDG8 as bait by a colleague in our lab to investigate how SDG8 be recruited to target loci. One of the potential SDG8 partner identified in the screen was the HULK2 protein (HUA2-LIKE 2), a homolog of HUA2 (ENHANCER OF AG-4 2) (Jali et al., 2014). The most prominent feature of the HUA2 family proteins is the amino-terminal PWWP (named after the central core motif Pro-Trp-Trp-Pro) domain, which is implicated in epigenetic regulation through differentially bind methylated and/or unmethylated histones in both animals and yeast (Qin and Min, 2014). Both HUA2 and HULK2 have been reported to regulate flowering time, however, their PWWP domain was not explored (Doyle et al., 2005; Jali et al., 2014). Firstly, despite that it was failed to detect the interaction between SDG8 and HULK2 observed in yeast using other method such as pull-down assay. Nonetheless, we demonstrated that the PWWP domain of HUA2/HULK2 is able to bind H3K36 methylation by in vitro binding assay. To further explore this binding, we determined the crystal structure of the plant HUA2 PWWP domain. Finally, to better understand the role of PWWP domain in vivo, genetic interaction between *HUA2* and *SDG8* was analyzed.

2. RESULTS

2.1 Test HULK2 and SDG8 interaction by pull-down assay

To identify new partners of SDG8, my colleague performed yeast two-hybrid screen and found that a PWWP-domain protein, HULK2, could be a potential partner of SDG8. To verify this by pull-down experiment, the potential interaction domain proteins of His tagged SDG8-N terminal (1-816aa) and GST tagged HULK2-C terminal (1068-1366aa) were expressed and purified. However, we failed to detect the protein-protein interaction between SDG8 and HULK2 in pull-down assays (Figure 1).

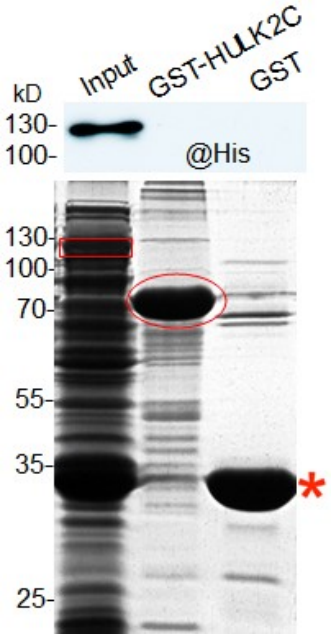

Figure 1: Pull down assay. Agarose beads coated with GST or GST-HULK2C (1068-1366aa) were incubated with an equal aliquot of His-SDG8N (1-816aa) protein. The pull down fractions and inputs were analyzed by Western blot using antibodies against the His tag.

2.2 Sequence alignment of the HUA2/HULK2 PWWP-domain

By sequence similarity, multiple alignment, and tree reconstruction approaches, the existence of three additional genes with high sequence similarity to HUA2 was identified. These genes were named HULK (HUA2 LIKE) genes and together with

HUA2, the family is referred to as the HULK gene family (Jali et al., 2014). All these four genes encode proteins containing a conserved PWWP domain; potentially has the ability to bind methylated histones. A sequence alignment of the HULK family PWWP domain with those of the mammalian PSIP1, MUM1, MSH6, DNMT3A, HDGF, NSD3_C, PWWP2B, and RBBP1 is shown in Figure 2. The overall sequence of the four HULK family proteins with human and yeast proteins showed low similarity. However, the four core residues PAWP (in black rectangle box) showed highly conservation across all the species, especially the fourth residue Pro is absolutely conserved. Thus, these residues were chosen for site directed mutagenesis to functionally analyze the HUA2 and HULK2 PWWP domain in *in vitro* histone binding assays and for complementation studies in this study.

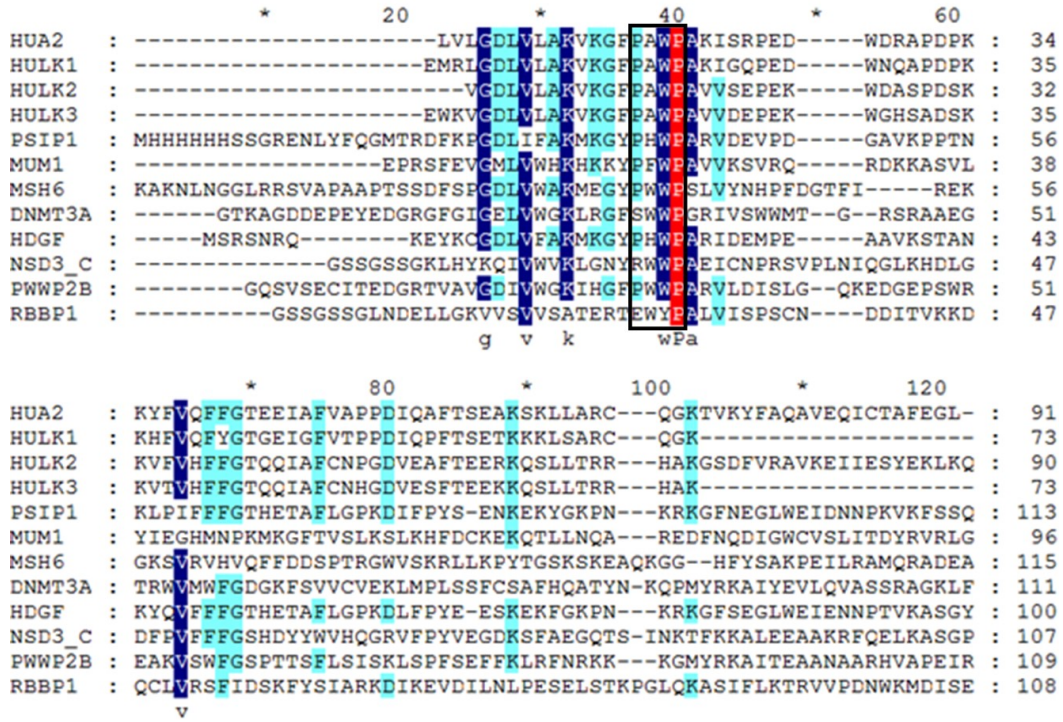

Figure 2: Alignment of HULK family PWWP domain with analyzed domains from mammalian and *S. pombe* proteins. Alignment of PWWP domains from following proteins: HUA2, HULK1, HULK2, HULK3, PSIP1, MUM1, MSH6, DNMT3A, HDGF, NSD3_C, PWWP2B, and RBBP1. Most conserved amino acids shaded in red, secondly conserved amino acids were shaded in blue and the less conserved amino acids were shaded in green. The four feature residues of PWWP domain was in black rectangle.

2.3 The HUA2/ HULK2 PWWP-domain exhibits in vitro histone peptide binding capacity

To analyze the potential histone binding capacity of the HUA2 and HULK2 PWWP-domain *in vitro*, they were fused to 6×His tag. His-HUA2-PWWP and His-HULK2-PWWP proteins were expressed in *E.coli* and were purified to incubate with synthetic biotinylated histone peptides H3K4me1, H3K4me2, H3K4me3 and H3K36me1, H3K36me2, H3K36me3, respectively. Proteins bound to the histone peptides were precipitated by Ni-NTA Agarose beads. Following western blots analysis with a alpha-biotin antibody revealed both the His-HUA2-PWWP and His-HULK2-PWWP proteins specifically bind to mono-, di- and tri-methylated H3K36 (K36me1/me2/me3) peptides, but not the H3K4me1/2/3 (Figure 3).

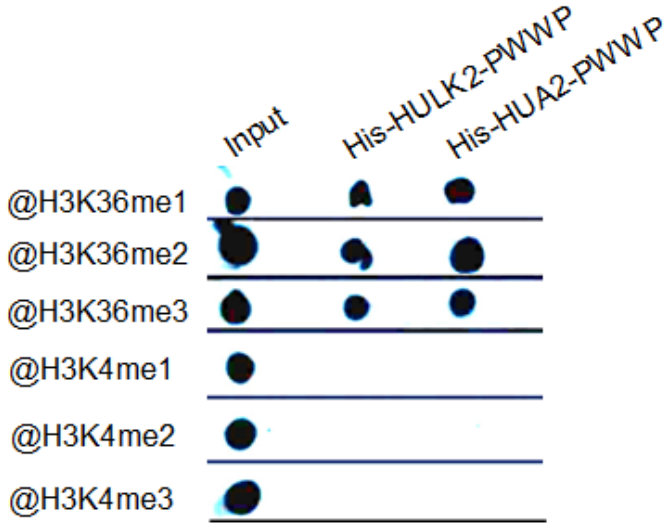

Figure 3: *In vitro* binding assays of N terminal His-tagged PWWP domains of HUA2 (His-HUA2-PWWP) and HULK2 (His-HULK2-PWWP) with H3 peptides containing mono-, di- or trimethylation on K4 or K36.

A point mutation of the conserved proline 16 to alanine HUA2-PWWP (P16A) did not alter the binding properties towards H3K36 methylation; whereas point mutated proteins HUA2-PWWP (W18A) and HUA2-PWWP (P19A) fully abolished the binding ability, suggesting that the mutation of the W18 and P19 residue alone is sufficient to alter the binding specificity of the HUA2 PWWP-domain. It is worthy to note that none of these proteins bind to H3K27me3 and thus reinforced the binding specificity.

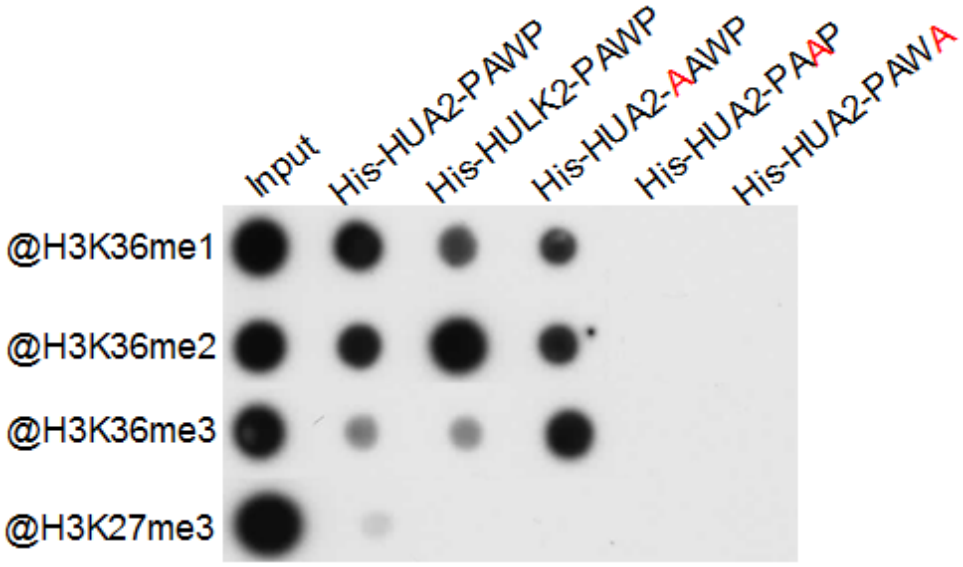

Figure 4: *In vitro* binding assay of His-HUA2-PWWP, His-HULK2PWWP and point mutated HUA2-PWWP-P16A, HUA2-PWWP-W18A, and HUA2-PWWP-W18A with H3 peptides containing mono-, di- or trimethylation on K36 and trimethylation on K27.

2.4 Protein crystallography analysis of HUA2 PWWP-domain

To obtain the first crystal structure of functionally important PWWP domains of HUA2 family proteins in plants, His-HUA2-PWWP and His-HULK2-PWWP fusion proteins were further purified by removal of the His tag and followed by chromatography IMAC. Highly pure proteins were set up for crystal screening. Crystals for HUA2 were got in two conditions but none of crystals for HULK2 (Figure 5A).

The crystals were diffracted to 1.85 Å by X-ray, and showed a primitive tetragonal space group with unit cell dimensions a=b=39.81 Å, c=116.63 Å. The structure was solved by molecular replacement with the structure of the PWWP domain of human PSIP1 (PDB ID: 4FU6) used as a search model. The HUA2 PWWP-domain contains a β-barrel-like fold formed by four anti-parallel β-strands (β1–β4), in which a short alpha helix is inserted between β2 and β3. It is slight different with reported human PWWP domains structure, which contains a complete β-barrel that has five anti-parallel β-strands (β1–β5) and a short alpha helix is inserted between β4 and β5 (Qin and Min,

2014). Nevertheless, the β-sheet core in HUA2 PWWP-domain is conserved and superimposed well with the structure of the human PSIP1 PWWP-domain (RSMD=1.5003 over 57 residues, 1-57 amino acid in HUA2 and 4-61 amino acid in PSIP1). A unique structural feature of the PWWP domain is the presence of a helix bundle of one to six a-helices following the b-barrel, which is also shared in HUA2 PWWP-domain structure (Figure 5B). However, whereas in PSIP1 the two C-terminal helices fold over the core domain, in HUA2 PWWP they maintain an extended structure. This extended helix makes contact with a symmetry related molecule and the protein appears to form a dimer (Figure 5C).

From structural perspective, we found that the P16 in the P-W-W-P motif located on a flexible loop outside the β-barrel-like fold, while W18 and P19 resides in the second β-sheet of the barrel fold (Figure 5D), which could be a reason for these residues have different effect on PWWP domain binding activity.

To provide mechanistic insight about HUA2 PWWP domain binding with H3K36me1/2/3, we aimed at to get HUA2 PWWP bound to methylated H3K36 peptides complex structure. To this end, we screened the co-crystallization of HUA2 PWWP with H3K36me2 and H3K36me3, respectively. Crystals of HUA2 with H3K36me2, H3K36me3 have been screened and got crystals in several conditions (Figure 5E).

A

B

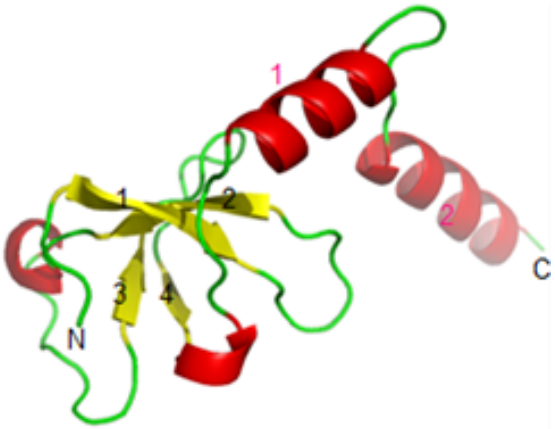

C

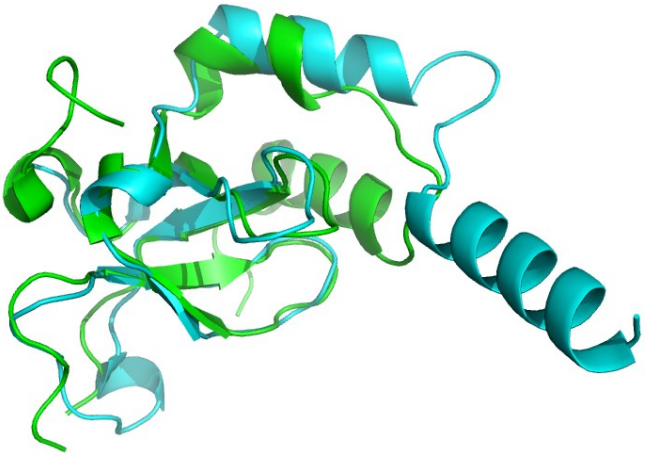

D

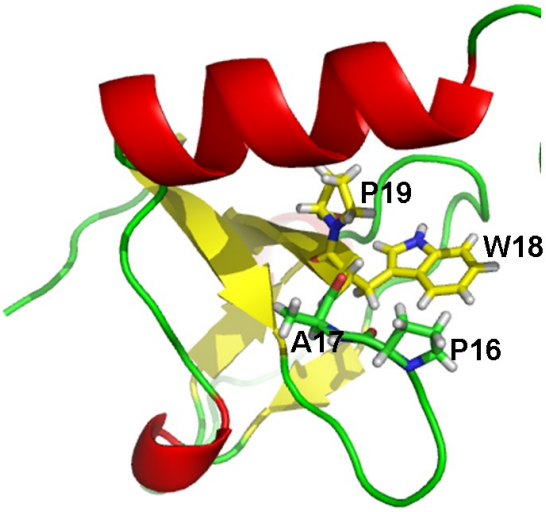

E

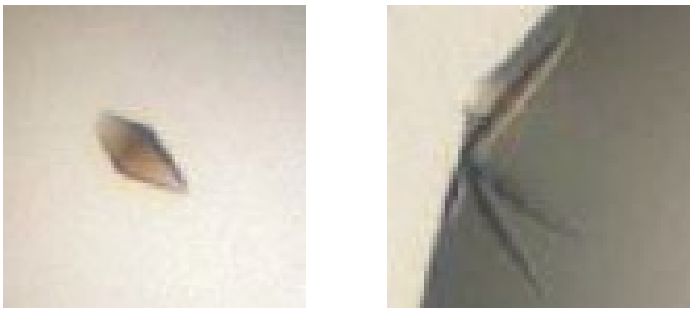

Figure 5: (A) Crystals of HUA2 PWWP-domain grown in solutions of 3.2 M AmSO4 ;100 mM Tris-HCl pH 8.0 (Left) and 2.4 M AmSO4; 100 mM Citric acid pH 5.0 (Right). (B) Crystal structure of HUA2 PWWP-domain. (C) Comparison of HUA2 PWWP-domain and human PSIP1 PWWP-domain structures. (D) Structural analysis of residues in P-W-W-P motif. (E) Crystals of HUA2 PWWP-domain bound with H3K36me2/3 peptides grown in solutions of 2.2 M Ammonium sulfate; 0.2 M NaH2PO4 (Left) and 12.5% MPD/ 12.5% PEG 1000/ 12.5% PEG3350, 20 mM L-Na-Glutamate; 20 mM Alanine; 20 mM Glycine; 20 mM Lysine HCl; 20 mM Serine; 0.1 M Sodium HEPES; MOPS pH 7.5 (Right).

2.5 Genetic interaction between *SDG8* and *HUA2*

We have identified the HUA2 PWWP-domain has the ability to bind methylated H3K36. Because SDG8 is the major H3K36 methyltransferase in Arabidopsis (Zhao et al., 2005; Xu et al., 2008) and because its corresponding mutant is early flowering like the *hua2* mutant, thus the genetic interaction analysis between *sdg8-1* and *hua2-7* was carried out.

2.5.1 Production of *sdg8-1 hua2-7* mutants

T-DNA insertion lines *sdg8-1* (Salk_065480) and *hua2-7* (reference number: 314_A08.b.1a.Lb3Fa) have been characterized previously (Zhao et al., 2005; Wang et al., 2007). Seeds (F1) from crosses were collected from individual siliques on the parent plants and were then grown and self-pollinated to obtain the F2 generation (Figure 6A). These F2 plants were genotyped by PCR. A total of 192 F2 plants were genotyped to identify double *sdg8-1 hua2-7* homozygous mutants (Figure 6B).

A

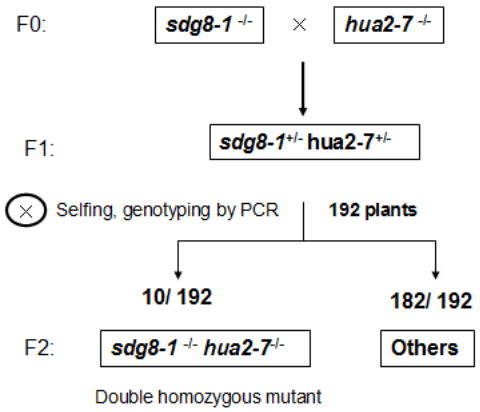

B

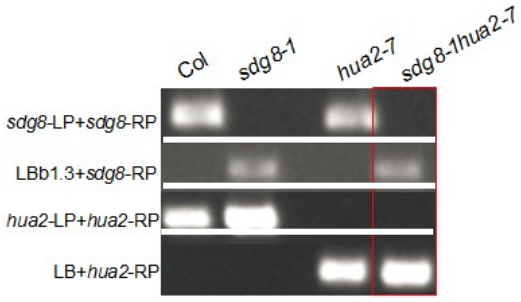

Figure 6: (A) Scheme of *sdg8-1 hua2-7* double mutants' identification. (B) Example of genotyping results from 4 plants of *wild-type*, *sdg8-1*, *hua2-7* and *sdg8-1 hua2-7*.

2.5.2 Phenotypes of the *sdg8-1 hua2-7* mutants

Under our growth conditions, *hua2-7* mutant bolted earlier that wild type and did not show other obvious phenotypes, as previously reported (Wang et al., 2007); *sdg8-1* mutant had pleiotropic phenotypes including early flowering, reduced organ size, and increased shoot branching. Interestingly, *sdg8-1 hua2-7* double mutant showed a reduced size as compared to single mutant, flowering time was early as compared to wild-type.

Figure 7: Representative 18-day-old seedlings of Col, *sdg8-1*, *hua2-7*, and *sdg8-1 hua2-7* grown under long-day (LD; 16 h light and 8 h dark) photoperiod conditions.

2.5.3 Flowering time analysis of *sdg8-1 hua2-7* mutants

To explore the functional interaction between *SDG8* and *HUA2* in the flowering time regulation, flowering time was measurement by total number of rosette leaves at the time of bolting and days to bolting under long-day (LD: 16 h light: 8 h dark), medium-day (MD; 12 h light: 12 h dark) and short-day (SD; 8 h light: 16 h dark) photoperiod conditions (Figure 8). The *sdg8-1 hua2-7* double mutants showed an early flowering time compared to wild-type and was in between *sdg8-1* and *hua2-7*.

A

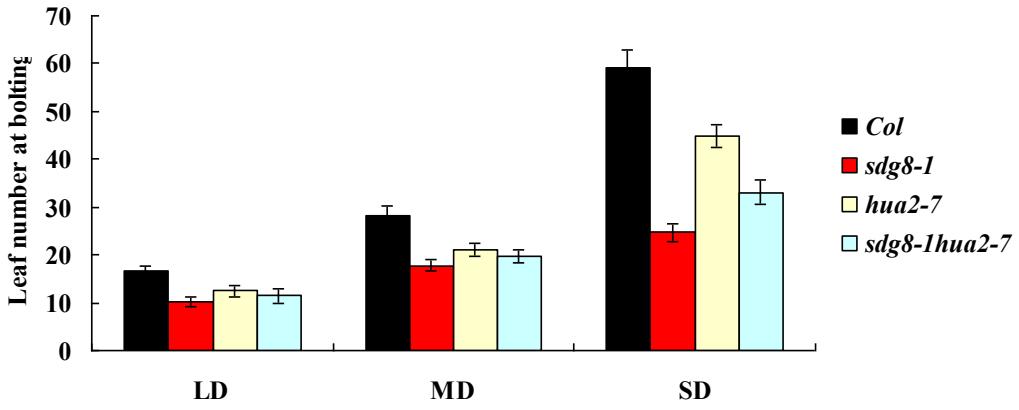

B

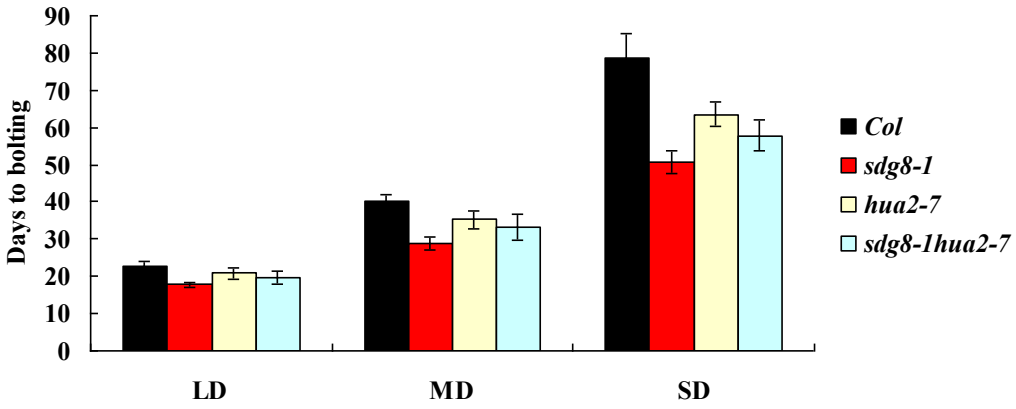

Figure 8: Flowering time measured by (A) rosette leaf number at bolting and (B) days to bolting in wild-type and mutant plants grown under long-day (LD;16 h light : 8 h dark), medium-day (MD; 12 h light : 12 h dark) or short-day (SD; 16 h light : 8 h dark) photoperiod conditions.

2.5.4 Expression profiles of flowering time genes

To investigate the molecular mechanism underlying the flowering behavior of *sdg8-1 hua2-7* mutant plants, the expression level of major flowering repressor genes *FLC*, *MAF1*-5 and flowering activator genes *FT* and *SOC1* was compared in the *sdg8-1 hua2-7* double mutants and *sdg8-1* and *hua2-7* single ones by quantitative RT-PCR analysis. Interestingly, the *FLC* mRNA level was similar between both single and double mutants indicating a redundancy between *SDG8* and *HUA2*. More downstream along the flowering genetic pathway, the *FT* transcript level in the double mutant was

in between the one observed in *sdg8-1* and *hua2-7* single mutants indicating that at this level *SDG8* and *HUA2* regulate *FT* independently. Together, our work indicates that, at least for *FLC*, *SDG8* and *HUA2* may functionally interact to regulate gene transcription.

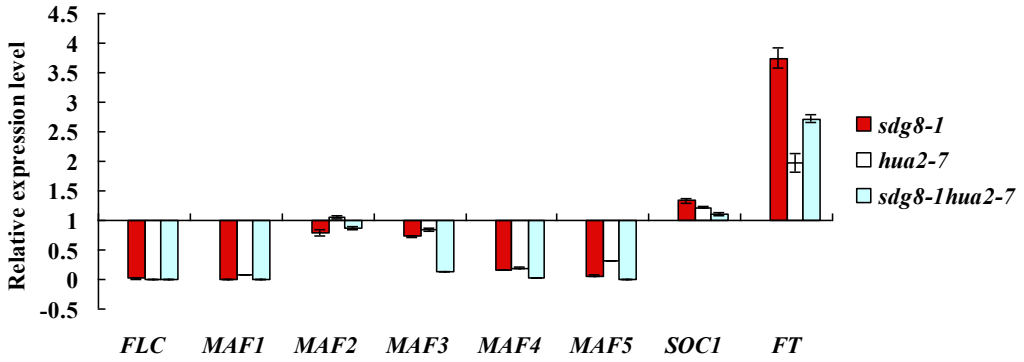

Figure 9: Quantitative RT-PCR analysis of flowering genes expression in different mutants. A pool of 16 days old seedlings was used for RNA extraction and each experiment was normalized to internal reference genes (*Tip4.1*, *Exp* and *GADPH*) expression. Values are presented as relative to levels in Col-0 (set as 1), error bar indicates standard deviation (SD).

3. Discussion and conclusions

H3K36 di- and tri- methylation (H3K36me2/3) play critical roles in epigenetic activation of gene expression in both animals and plants. Although Arabidopsis MRG has been reported as H3K36me2/3 reader protein, however, it binds to H3K4me2/3 as well (Bu et al., 2014; Xu et al., 2014). It is thus of great interest to identify H3K36 methylation specific readers to elucidate the mechanism of roles of H3K36me2/3 in Arabidopsis.

3.1. Functional and structural analysis of the HUA2/HULK2 PWWP domain

We performed *in vitro* binding assay and found that HUA2/HULK2 PWWP domain specifically binds to H3K36me1/2/3 but not H3K4me1/2/3 or H3K27me3. This result demonstrates that HUA2 and HULK2 as novel H3K36 methylation specific binding proteins via their PWWP domain. However, we have failed to verify the specificity of the binding by isothermal titration calorimetry (ITC) so far, suggesting that the interaction between PWWP domain and H3K36me1/2/3 peptide is likely weak. Indeed, many histone reader proteins show very weak affinity to histone peptide in ITC and sometimes even make it undetectable by ITC (Bu et al., 2014).

To further explore this binding, we determined the crystal structure of the HUA2 PWWP domain by protein crystallography method. It contains a classical β-barrel-like fold formed by four anti-parallel β-strands (β1–β4) that also present in animal and yeast PWWP domain. Thus, this domain appeared highly conserved among plant, animal and yeast, albeit their amino acid sequence have less similarities. However, animals and yeast PWWP domain was shown to be able to bind diverse methylated histone peptides. For example, human BRPF1-PWWP binds H3K36me3, HDGF2-PWWP binds both H4K20me3 and H3K79me3, and yeast Pdp1-PWWP could specifically recognize H4K20me (Qin and Min, 2014). Interestingly, we found that HUA2-PWWP structure superimposed best with the structure of human PISP-PWWP, which also bounds with H3K36me3. Structural analysis

of the PWWP bounds with histone peptide complex structures identified a conserved hydrophobic pocket for methyl-lysine binding, which is composed of mainly aromatic residues. Consistently, in this work, we found that the interaction between HUA2-PWWP domain and H3K36me1/me2/me3 is fully abolished by mutation of the third W (W18) and the fourth P (P19), but not the first P (P16) in the P-W-W-P motif (PAWP in HUA2 and other HULK2 family members). This bias can be very nicely explained from the structural point of view, the P16 located on a flexible loop outside the β-barrel-like fold, indicating it is not functionally important; on the contrary, W18 and P19 resides in the second β-sheet of the barrel fold, with high possibility to constitute the aromatic cage that makes it indispensable to fulfill its binding ability. Indeed, several human proteins such as RBBP1 and NSD1, the PWWP domain contains an incomplete aromatic cage that does not show any binding to methylated histone peptides.

Because the dimension of these cages decides their selectivity toward mono-, di- or tri-methylated lysines, and given the fact that the HUA2-PWWP present as a dimer, it is very unlikely that the HUA2-PWWP domain uses a unique or flexible mechanism to accommodate the different size of H3K36me1/2/3. It will be very important to solve the HUA2-PWWP domain bounds with H3K36 peptide complex structure that we are currently working on and reasonable to expect that will offer evidence to support these ideas.

Furthermore, we aimed to test if the P19 residue is important for *in vivo* HUA2 function, we constructed P19A substitution in the HUA2 genomic DNA fragment introduced them into the *hua2* mutant. We will test if the transgenetic line be able to rescue the *hua2* mutant early flowering phenotype.

3.2. *SDG8* and *HUA2* function related in regulation of flowering time

HUA2 has been reported to regulate flowering time (Jali et al., 2014), however, little is known about the underlying mechanisms. The *hua2* mutant is early flowering like *sdg8* mutant, which is defective in H3K36 di- and tri-methylation (Zhao et al., 2005).

By flowering time measurement, we found that *sdg8-1 hua2-7* double mutant flowered in between *sdg8-1* and *hua2-7* single mutant, suggesting *SDG8* and *HUA2* are genetically

related in flowering time regulation. Consistent with the flowering phenotype, our molecular data showed that *FT* transcription level is intermediary between that in *sdg8-1* and *hua2-7*. Interestingly, *FLC* mRNA level was decreased to the similar level in both single and double mutants, indicating *SDG8* and *HUA2* act in a same pathway to regulate *FLC* transcription. In this context, we would like to investigate if the disruption of the PWWP domain abolishes or reduces H3K36me3 levels at *FLC* chromatin and further lead to its depression. Therefore, transgenic lines expressing tagged HUA2 protein has been generating and will be used for ChIP-Seq analysis to test histone methylation level changes *in vivo*.

All together, this work is important for mechanistic understanding of SDG8 catalyzed H3K36 methylation function in flowering time control.

GENERAL CONCLUSIONS

AND

PERSPECTIVE

In this work, we present results from diverse aspects of studying Arabidopsis TrxG family proteins.

Firstly, in collaboration with the laboratory of Dr. Richard Amasino, a novel role for TrxG proteins was identified. By providing genetic and molecular data, we demonstrated that SDG7, a close homolog of the H3K36 methyltransferase SDG8, plays crucial role in repression of vernalization process. And this novel function seemed to be independent its methyltransferase activity, as evidenced by our western blot analysis, in which we were not able to detect any significant changes in the level of different histone methylation marks in *sdg7* mutant plants, and recombinant SDG7 protein could not methylate histones. Thus, the biochemical role of SDG7 in the timing of the vernalization response still needs to be investigated. A possibility is SDG7 fulfills its role in vernalization by methylating a cytosolic protein or proteins, supported by the fact that SDG7 lacks a nuclear localization signal and was demonstrated to methylate aquaporins *in vitro* (Sahr et al., 2010). To verify this, other potential substrates of SDG7 should be further explored. Furthermore, the Arabidopsis genome encoding around 12 TrxG members, and some of them already have been shown to play distinct biological roles. Thus, molecular and functional characterization of other TrxG genes are desperately necessary to broad our knowledge on their diverse functions in regulation of plant growth and development.

Secondly, by the phenotype and molecular analysis of the combined Arabidopsis mutants defective in histone H3K36me3 methyltransferase SDG8 and H2B monoubiquitinase HUB2, we found that an ordered dependency between H2Bub1 and H3K36me3 depositions cannot be clearly established; rather SDG8 and HUB2 mutually favor each other in establishing active chromatin state. This contrasts the yeast model where H3K36me3 deposition occurs at downstream and in a dependent manner of H2Bub1. Because H3K36 methylation and H2B deubiquitination are also functionally connected in the course of transcription in yeast, it is thus of great interest to test the conservation of this crosstalk in Arabidopsis. Based on previously reported largely independent role between histone methyltransferases and demethylases and the results present here, it is reasonable to conclude that connections between histone marks in Arabidopsis are numerous, varied and extremely sophisticated, rendering difficult, if not

impossible, to establish a simple functional network with clear hierarchical interconnections. Such complexity might reflect a certain degree of flexibility, which is in line with the modular concept of plant developmental plasticity.

Finally, we found Arabidopsis HUA2/HULK2 proteins act as histone methylation reader proteins via their PWWP domain. Our *in vitro* binding data revealed that the PWWP domain of HUA2 preferably interacts with H3K36 methylation (H3K36me1/me2/m3). In Arabidopsis, there are at least 16 PWWP-domain containing proteins, the binding ability and/or specificity of other PWWP domains towards modified histone peptides still needs to be investigated. Because the PWWP domain in human and yeast showed binding activity to differently methylated histones despite of their overall structure of this domain is conserved across many spices, we speculate the role of Arabidopsis PWWP domain played both redundant and divergent roles in reading methylation. The further work is necessary to gain insight into the mechanisms their binding specificity. Because *HUA2* and *SDG8* were genetically linked to control flowering time by redundantly repress *FLC* transcription. It is also interestingly to detect the H3K36 methylation changes on *FLC* chromatin, which will provide us mechanistic sight to understand the role of H3K36me2/3 in Arabidopsis flowering time regulation.

Collectively, results from my thesis work contribute to significant progresses of our understanding on molecular mechanisms about deposition and reading of histone methylation marks in transcription and regulation of plant development.

MATERIALS

AND

METHODS

1. Materials

1.1 Plant Materials

Arabidopsis thaliana is a flowering plant used as a model species for basic research in genetic and molecular biology. The Columbia (Col-0) ecotype was used as genetic background for wild-type and all the mutants listed below are in the Col-0 background. Arabidopsis thaliana mutants carrying a T-DNA insertion in this study are listed in Table 1-1. Seeds were ordered from the European Arabidopsis Stock Center (NASC).

Table 1-1 List of mutants and transgenic lines.

Name	Locus	Insertion/Description	Seed Source
sdg8-1	AT5G23150	SALK_065480	Zhao et al., 2005
hub2-2	AT1G55250	SALK_071289	Liu et al., 2007
hub1-3	AT2G44950	GABI_276D08	Liu et al., 2007
ubp26-4	AT3G49600	SALK_024392	NASC
hua2-7	AT5G23150	SAIL_314_A08	Wang et al., 2007

1.2 Bacterial strains

All bacterial strains are listed in **Table 1-2.**

Table 1-2 List of bacteria strains used in this study

Bacteria Strains	Application
E. coli strain DH5α	Plasmids amplification
E. coli strain TOP10	Transformation
BL21 (DE3)	Protein expression

1.3 Constructs and Vectors

All vectors were created using the GATEWAY® cloning system (Invitrogen™) or by using restriction endonucleases and ligation.

Table 1-3-1 List of empty vectors.

Name	Selection in bacteria	Application
Entry vectors		
pDONR_207	Gentamycin	Gateway cloning
pDONR_221	Kanamycin	Gateway cloning
Destination vectors		
pGWB	Spectinomycin	Gateway cloning
pGWB604	Spectinomycin	Gateway cloning
pGWB616	Spectinomycin	Gateway cloning
PET28a-SUMO	Kanamycin	Protein expression
pGEX-4T-1	Ampicillin	Protein expression

Table 1-3-2 List of created entry clones in this study

Name
HUA2-promoter and genomic DNA in pDONR_207
HUA2- promoter and genomic DNAΔPAWP in pDONR_207
HUA2- promoter and genomic DNAΔPAWP in pDONR_207
HUA2-promoter and genomic DNA without stop codon in pDONR_221

Table 1-3-3 List of created destination clones.

Name	Vector backbone	Experiment
pGWB-HUA2	pGWB	Complementation of Mutant Plants
pGWB-HUA2- ΔPAWP (P to A)	pGWB	Complementation of Mutant Plants
pGWB-HUA2- ΔPAWP (W to A)	pGWB	Complementation of Mutant Plants
HUA2-GFP	pGWB604	Plant transformation
HUA2-MYC	pGWB616	Plant transformation
His-HUA2-PWWP-domain	PET28a-SUMO	in vitro binding assay and crystallization
His-HUA2-PWWP-domain (P16A)	PET28a-SUMO	in vitro binding assay
His-HUA2-PWWP-domain (W18A)	PET28a-SUMO	in vitro binding assay
His-HUA2-PWWP-domain (P19A)	PET28a-SUMO	in vitro binding assay
His-SDG8-N terminal domain	PET28a-SUMO	puLl-down assay
GST-HULK2-C terminal-domain	pGEX-4T-1	puLl-down assay

1.4 Transgenic plants created in this study

All HUA2 related destination vectors were introduced into *Agrobacterium tumefaciens*, followed by transforming to the *hua2-7* mutant plants by the floral-dip method (Clough and

Bent, 1998). All the transgenic *Arabidopsis thaliana* lines generated are listed in Table 1-4.

Table 1-4 List of created transgenetic lines.

Name	Selection in medium/soil	description
hua2-7::HUA2-GFP	BASTA	transgentic lines with GFP tag
hua2-7::HUA2-MYC	BASTA	transgentic lines with MYC tag
hua2-7::HUA2	Kanamycin	transgentic lines for complementation
hua2-7::HUA2△PAWP	Kanamycin	mutated (P to A) transgentic lines for complementation
hua2-7::HUA2△PAWP	Kanamycin	mutated (W to A) transgentic lines for complementation

1.5 Antibodies and peptides

Table 1-5 Antibodies and peptides

Name	Company (Cat. #)	Dilution	Host	Purpose
Primary antibodies				
anti-H3	Merck Millipore (05-499)	1:5000	rabbit	western blot, ChIP
anti-H3K36me3	Abcam (ab9050)	1:5000	rabbit	western blot, ChIP
anti-H3K36me1	Abcam (ab9048)	1:5000	rabbit	western blot
anti-H3K4me3	Merck Millipore (07-473)	1:5000	rabbit	western blot, ChIP
anti-H3K4me2	Merck Millipore (04-790)	1:5000	rabbit	western blot
anti-H2Bub1	Merck Millipore (05-1312)	1:5000	rabbit	western blot, ChIP
anti-H3K27me3	Merck Millipore (07-449)	1:5000	rabbit	western blot, ChIP
anti-6x-His Tag	Thermofisher (MA1-21315)	1:5000	rabbit	western blot
Secondary antibodies				
anti-rabbit-HRP conjugated	Sigma-Aldrich (A9169)	1:10000	goat	western blot
anti-mouse-HRP conjugated	Thermofisher (62-6520)	1:10000	goat	western blot
Biotinylated peptides				
H3K4me1 (residues 1–21)	synthesized by Scilight Biotechnology	2μg		*in-vitro* IP
H3K4me2 (residues 1–21)	synthesized by Scilight Biotechnology	2μg		*in-vitro* IP
H3K4me3 (residues 1–21)	synthesized by Scilight Biotechnology	2μg		*in-vitro* IP
H3K36me1 (residues 21–44)	synthesized by Scilight Biotechnology	2μg		*in-vitro* IP
H3K36me2 (residues 21–44)	synthesized by Scilight Biotechnology	2μg		*in-vitro* IP
H3K36me3 (residues 21–44)	synthesized by Scilight Biotechnology	2μg		*in-vitro* IP
H3K27me3 (residues 21–44)	synthesized by Scilight Biotechnology	2μg		*in-vitro* IP
Ni-NTA Agarose	QIAGEN (No.1000632)	6×His-tagged protein expression		
Glutathione Sepharose 4B	GE Healthcare (No. 17075601)	GST tagged protein expression		
PureProteom™ Protein G	Millipore (CA 925590)	ChIP		

1.6 Primers

Sequences of primers used for genotyping are listed in Table 1-6 (below).

Primer	AGI ID	Gene name	Sequence (5'⟶3')
SDG8.1-LP	AT5G23150	*SDG8*	CCTTCATCGCAATCGTAAATC
SDG8.1-RP	AT5G23150	*SDG8*	TTTTGCGCTAAACTAGTTGGG
HUB1.3-LP	AT2G44950	*HUB1*	GGATTTTTTAATTGGCATTG
HUB1.3-RP	AT2G44950	*HUB1*	GCCGTTATCAACCCAAAACT
HUB2.2-LP	AT1G55250	*HUB2*	CATGGTACCACATCCAAGGTC
HUB2.2-RP	AT1G55250	*HUB2*	CCTCTTTAGGCCGATCAAAAC
HUA2.7-LP	AT5G23150	*HUA2*	TCGTCGAATTGAGCTCTAGTGT
HUA2.7-RP	AT5G23150	*HUA2*	GAAACACCTGATAACCGAGGTC
UBP26.4-LP	AT3G49600	*UBP26*	TTGTGGAAACACCCCACAAAA
UBP26.4-RP	AT3G49600	*UBP26*	TTGGCTTCGTCTATGGGCTGA
GABI LB			ATATTGACCATCATACTCATTGC
SAIL LB			TAGCATCTGAATTTCATAACC AATCTCGATACAC
LBb1.3			ATTTTGCCGATTTCGGAAC

Sequences of primers used for quantitative RT-PCR analyses are listed in Table 1-7

(below).

Primer	AGI ID	Gene name	Sequence (5’ ⟶ 3’)
FLC-F	At5g10140	*FLC*	CCTAATTTGATCCTCAGGTTTGGG
FLC-R	At5g10140	*FLC*	CCGACGAAGAAAAAGTAGATAGGCAC
MAF1-F	At1g77080	*MAF1*	GGAAAGAATACGTTGCTGGCAACA
MAF1-R	At1g77080	*MAF1*	CCGTTGATGATGGTGGCTAATTGA
MAF2-F	At5g65050	*MAF2*	GGCTCCGGAAAACTCTACAA
MAF2-R	At5g65050	*MAF2*	TTCTGCAAGATCTAAGGCTTCA
MAF3-F	At5g65060	*MAF3*	ACAGAACTAATGATGGAGGATATGAA
MAF3-R	At5g65060	*MAF3*	CTTCTTCCCCACCTGGCTA
MAF4-F	At5g65070	*MAF4*	GAGCAATGTCACCGGAAAGTAG
MAF4-R	At5g65070	*MAF4*	CAGTCGTTGGTGATGGTGGTTA
MAF5-F	At5g65080	*MAF5*	AAGAGCAGTAATGTCACCGGAA
MAF5-R	At5g65080	*MAF5*	ACTTGAGAAGCGGGAGAGTC
SOC1-F	At2g45660	*SOC1*	GCTCTCAGTGCTTTGTGATGC
SOC1-R	At2g45660	*SOC1*	A AGAACGTACTTGGAGCTGGC
FT-F	At1g65480	*FT*	GAGACCCTCTTATAGTAAGCAGAGTTG
FT-R	At1g65480	*FT*	GGGAGTTCAAGTGAAAGAACCAAAGT
Tip 4.1-F	At2g25810	*Tip 4.1*	GTGAAAACTGTTGGAGAGAAGCAA
Tip4.1-R	At2g25810	*Tip 4.1*	TCAACTGGATACCCTTTCGCA
EXP-F		*EXP*	GAGCTGAAGTGGCTTCCATGA
EXP-R		*EXP*	GGATCATGGGTATGTCGGACC
GADPH-F	At1g13440	*GADPH*	TTGGTGACAACAGGTCAAGCA
GADPH-R	At1g13440	*GADPH*	AAACTTGTCGCTCAATGCAATC

Sequences of primers used for Chromatin ImmunoPrecipitation (ChIP) analyses are listed in Table 1-8 (below).

Primer	AGI ID	Gene name	Sequence (5’ ⟶ 3’)
FLC1-F	At5g10140	*FLC*	ATTTAGCAACGAAAGTGAAAACTAAGG
FLC1-R	At5g10140	*FLC*	GCCACGTGTACCGCATGAC
FLC2-F	At5g10140	*FLC*	AGAAATCAAGCGAATTGAGAACAA

FLC2-R	At5g10140	*FLC*	CGTTGCGACGTTTGGAGAA
FLC3-F	At5g10140	*FLC*	AATTGCATGTCATTCACGATTTG
FLC3-R	At5g10140	*FLC*	TGAAACTTCACTCAACAACATCGA
FLC4-F	At5g10140	*FLC*	TTATCGCCCTTAATCTTATCATCGT
FLC4-R	At5g10140	*FLC*	AAGATTGAGGTTGTGGATTGTCAA
FLC5-F	At5g10140	*FLC*	CCGCCACATCATCATTATCATC
FLC5-R	At5g10140	*FLC*	ACAAGGTTTTTTCCAGCGATAGA
FLC6-F	At5g10140	*FLC*	AAGCCAGCGCTATCACTAAACTTT
FLC6-R	At5g10140	*FLC*	TCGGCAGATTGAAAATGACATT
FLC7-F	At5g10140	*FLC*	CATCTCTCCAGCCTGGTCAAG
FLC7-R	At5g10140	*FLC*	GGCTTTAAGATCATCAGCATGCT
FLC8-F	At5g10140	*FLC*	AGCCAGGTAACGAAAGCTACATTT
FLC8-R	At5g10140	*FLC*	ACATGGACATTGGACACACAACA
FLC9-F	At5g10140	*FLC*	CATCATGTGGGAGCAGAAGCT
FLC9-R	At5g10140	*FLC*	CGGAAGATTGTCGGAGATTTG
FLC10-F	At5g10140	*FLC*	TTTTTGGGCCTATGTCGGTCA
FLC10-R	At5g10140	*FLC*	GGTCGGTCACGTTAACAGCA
MAF4-F1	At5g65070	*MAF4*	CTTCCTCGCTTCAAAACGGC
MAF4-R1	At5g65070	*MAF4*	TGATCCTAACCACCGGGGAC
MAF4-F2	At5g65070	*MAF4*	TCCACATTGATGCATCCCCA
MAF4-R2	At5g65070	*MAF4*	ATGGTACACACCGAAAAGGGT
MAF4-F3	At5g65070	*MAF4*	ATGTAGGCGCATGCTTCAGT
MAF4-R3	At5g65070	*MAF4*	TCGGTTGGAGGAATTTATAGAGTGA
MAF4-F4	At5g65070	*MAF4*	AGTCACTTCAAGAAAGGGTACG
MAF4-R4	At5g65070	*MAF4*	TCAGCATTACCCTACAATATGGCT
MAF4-F5	At5g65070	*MAF4*	AAAAGTACGGATTGGATTCAAAAGA
MAF4-R5	At5g65070	*MAF4*	GGAAAACCAAAGGAATTAAGAAGCT
MAF4-F6	At5g65070	*MAF4*	GACCAACGCGCCACAAG
MAF4-R6	At5g65070	*MAF4*	CGGTGCGTTTTTAATAGGAGTTTAG

MAF5-F1	At5g65080	*MAF5*	TGGTGTCCAAAGTCCAGAGATG
MAF5-R1	At5g65080	*MAF5*	CCTTGCAACAAATGAAAACAATAGA
MAF5-F2	At5g65080	*MAF5*	CCGAATTGAGACCTTGTAGAAGTAGA
MAF5-R2	At5g65080	*MAF5*	ATCAAGCATTTGTGGTGTTAAGTATGA
MAF5-F3	At5g65080	*MAF5*	GTTGTTTTCCTTTTCTGTTGTTTATCTATG
MAF5-R3	At5g65080	*MAF5*	ATACTTACATTATCGCTTTTCGCTTCT
MAF5-F4	At5g65080	*MAF5*	GCGGAAAGCCGGTAAAAGAC
MAF5-R4	At5g65080	*MAF5*	CGAATCTGGGCTTAACAGTAACAGT
SOC1-1-F	At2g45660	*SOC1*	GGGCATATAGGTACGAGAGAGTG
SOC1-1-R	At2g45660	*SOC1*	CTAGTTGGATGGAAATGCCTGT
SOC1-2-F	At2g45660	*SOC1*	AGCAGAGAGAGAAGAGACG
SOC1-2-R	At2g45660	*SOC1*	GAAGTAGCTTTCCTCGTTTCAT
SOC1-3-F	At2g45660	*SOC1*	CTTTCTTTCTTCTTCTCCCTCCAGT
SOC1-3-R	At2g45660	*SOC1*	CCTAACCAGGAGGAAGCTTTCG
SOC1-4-F	At2g45660	*SOC1*	GCATCCTTCAATTAAACCGATAAC
SOC1-4-R	At2g45660	*SOC1*	AAGTCAACGAAAGATTAAGTACCC
SOC1-5-F	At2g45660	*SOC1*	TCTGTGTGCAAGGGAAATTAAC
SOC1-5-R	At2g45660	*SOC1*	GAGAAAGTCACTTGTCTGCT
SOC1-6-F	At2g45660	*SOC1*	TGGATTTGATTGGCCTTTTGTGGAA
SOC1-6-R	At2g45660	*SOC1*	AGCCCTAATTTTGCAGAAACCAAG
SOC1-7-F	At2g45660	*SOC1*	CCCTCATGCTTCATTTCATGCTC
SOC1-7-R	At2g45660	*SOC1*	GGTTTGGCTAGCTAGCTTTGAGT
SOC1-8-F	At2g45660	*SOC1*	ATCTCAAGGTCACAGGATCAAGTC
SOC1-8-R	At2g45660	*SOC1*	TGCTGCTTCATATTTCAAATGCTGT
SOC1-9-F	At2g45660	*SOC1*	GCAGCTCAAGCAAAAGGTAAAGTAG
SOC1-9-R	At2g45660	*SOC1*	GCACAAGAGGCTTACTTACTTGGAA
SOC1-10F	At2g45660	*SOC1*	CATGAAAGCGAAGTTTGGTC
SOC1-10R	At2g45660	*SOC1*	GTAACCCAATGAACAATTGCG
FT-1-F	At1g65480	*FT*	GCATGCGAAAATCTAGTGGAAGA

FT-1-R	At1g65480	*FT*	GTCGCATAATGTTCGCAACCT
FT-2-F	At1g65480	*FT*	GCGACTGCGACCTATTTTTTTC
FT-2-R	At1g65480	*FT*	GCTATATGCACTTTTTAACGACTAGC
FT-3-F	At1g65480	*FT*	GCTAGTCGTTAAAAAGTGCATATAG
FT-3-R	At1g65480	*FT*	CCACTGTTCTACACGTCCATAG
FT-4-F	At1g65480	*FT*	TCCTTTATTTTCCAGTTTGGACAG
FT-4-R	At1g65480	*FT*	ACCATAGCCTAACAACTGTAGGAA
FT-5-F	At1g65480	*FT*	CCTACAGTTGTTAGGCTATGGT
FT-5-R	At1g65480	*FT*	CTAACCATCCATTTGCACGAC
FT-6-F	At1g65480	*FT*	TCTAACCTGAAGGATCCCTTG
FT-6-R	At1g65480	*FT*	AATTCGAAAGCGAAAACGTTC
FT-7-F	At1g65480	*FT*	GAACGTTTTCGCTTTCGAATT
FT-7-R	At1g65480	*FT*	GAAAAAAGTAGGGTACCGCC
FT-8-F	At1g65480	*FT*	AGTGTGGTGGGTTTGGAATAC
FT-8-R	At1g65480	*FT*	GCATTAACTCGGGTCGGTGA
FT-9-F	At1g65480	*FT*	AGAGGGTTCATGCCTATGATAC
FT-9-R	At1g65480	*FT*	CTTTGATCTTGAACAAACAGGTG
FT-10-F	At1g65480	*FT*	GAGACCCTCTTATAGTAAGCAGA
FT-10-R	At1g65480	*FT*	GTATAGAAGTTCCTGAGGTCTTC
FT-11-F	At1g65480	*FT*	GACAATGTGTGATGTACGTAGAATCAGT
FT-11-R	At1g65480	*FT*	CGGTGAAATCATAACCACAATCTT
FT-12-F	At1g65480	*FT*	GCCAGCCTTTAAGATACTCTCTGCTA
FT-12-R	At1g65480	*FT*	TGAGATAACACAAGAAAGAAGAAGAAAACT

Sequences of primers used for GATEWAY® cloning system (Invitrogen™) or restriction endonucleases and ligation system are listed in Table 1-9 (below).

Primer	Sequence (5’ ⟶ 3’)	Description
HUA2-PWWP-F	GCTC**GGATCC**TTGGTTCTCGGTGATCTGGTTCTC	BamHI site
HUA2-PWWP-R	ATGC**GTCGAC**TCACAACCCTTCAAATGCAGTGCAGAT	SalI site
HULK2-PWWP-F	GCTC**GGATCC**AAGGTGGGCGACCTTGTGCTT	BamHI site
HULK2-PWWP-R	ATGC**GTCGAC**TCAAGCTCGTTCTTGCTGCTTGAGCTT	SalI site
HULK2-C terminal-F	GCTC**GGATCC**GTCTCGTCATCCACGGCTGAAA	BamHI site
HULK2-C terminal-R	ATGC**GTCGAC**TCACTAGTCACTTCTCTGATGCCACATTCC	SalI site
SDG8-N terminal-F	AGGC**GAATTC**ATGGACTGTAAGGAAAACGGTGTTG	EcoRI site

SDG8-N terminal-R	ACGC**GTCGAC**TTCATTTTTTCTCCCGTCTTTGG	SalI site
HUA2-PWWP (P16A)-F	GTCAAAGGCTTCGCTGCTTGGCCTG	Mutated domain protein
HUA2-PWWP (P16A)-R	CAGGCCAAGCAGCGAAGCCTTTGAC	
HUA2-PWWP (W18A)-F	GTCAAAGGCTTCCCTGCTGCGCCTGCCAAGATCAG	Mutated domain protein
HUA2-PWWP (W18A)-R	CTGATCTTGGCAGGCGCAGCAGGGAAGCCTTTGAC	
HUA2-PWWP (P19A)-F	CTTCCCTGCTTGGGCTGCCAAGATCAG	Mutated domain protein
HUA2-PWWP (P19A)-R	CTTCCCTGCTTGGGCTGCCAAGATCAG	
HUA2-F	**GGGGACAAGTTTGTACAAAAAAGCAGGCTCT**TGACGTGGTTGCGAATAACATGGA	*HUA2* full length genomic fragment. Promoter, genomic DNA and 3'UTR.
HUA2-R	**GGGGACCACTTTGTACAAGAAAGCTGGGTC**GAAAAAAAAAACTATGTTTGA	
HUA2-PWWP (P to A)-F	GTCAAAGGCTTCGCTGCTTGGCCTG	Point mutation in *HUA2* full length genomic fragment
HUA2-PWWP (P to A)-R	CAGGCCAAGCAGCGAAGCCTTTGAC	Point mutation in *HUA2* full length genomic fragment
HUA2-PWWP (W to A)-F	GTCAAAGGCTTCCCTGCTGCGCCTGCCAAGGTGCGTTATC	Point mutation in *HUA2* full length genomic fragment
HUA2-PWWP (W to A)-R	GATAACGCACCTTGGCAGGCGCAGCAGGGAAGCCTTTGAC	

2 Methods

2.1 Plant Methods

2.1.1 Seeds sterilization

Seeds were sterilized by using chlorine gas. Few hundreds of Arabidopsis seeds were disposed in an opened 1.5 ml eppendorf tube in a desiccator in a fume hood. A beaker containing 100ml of bleach (FLOREAL Haagen) was placed in the desiccator next to the seeds. Then, 5 ml of 37% HCl was added to the bleach and the lid of the desiccator was immediately closed tightly to keep the seeds dry.

Seeds of *Arabidopsis thaliana* were either surface sterilized by treatment with 70% ethanol for 10 min followed by 5 min with 96% ethanol, and then dried in a clean bench.

2.1.2 Plant growth conditions

Arabidopsis thaliana plants were grown on soil under long day (LD; in 16 h light: 8 h dark), medium day (MD; 12 h light: 12 h dark) or short day (SD; 8 h light: 16 h dark) photoperiod conditions in greenhouse. Seeds were either sowed on 1/2 MS medium; after stratification for 48 hours at 4°C to synchronize the germination time, the seeds were transferred into a 21°C, 16/8 h light-dark cycle growth chamber.

2.1.3 Crossing *Arabidopsis* plants

In inflorescences of a recipient" / "female" plant (4 to 6 weeks old), mature opened flowers as well as buds that have already a white tip or buds that are too small were removed; the flower buds have the right size and contain short immature stamens with anthers should remain. The anthers in the selected buds were then removed using fine forceps. Two days after emasculation, stigmas were manually pollinated with pollens from a "donor" / "male" plant. Following a successful pollination, the pistils will elongate as the seeds in siliques developed. After dried, seeds (F1) in separate silique were harvested.

2.1.4 *Arabidopsis* transformation by floral dip method

Arabidopsis plants were grown under long day (16 h light/ 8 h dark) conditions until flowering. The first bolts were clipped to induce proliferation of more secondary bolts. Plants generated a lot of immature flower clusters and less fertilized siliques after about 1 week of clipping, and will be ready for *Agrobacterium tumefaciens* mediated transformation. *Agrobacterium tumefaciens* strain carrying gene of interest on a binary vector will be prepared. A single colony was inoculated in 3 ml LB with antibiotics and incubated at 28 °C overnight. The overnight culture was then diluted in 300 ml LB supplements with the same antibiotics followed by incubated at 28 °C for 16-24 hours. The bacteria cells were harvested by centrifugation at 5000 rpm for 10 min, and resuspended to OD_{600} value close to 0.8 in 5% sucrose solution. Silwet L-77 was added to the solution to a final concentration of 0.05% (500 L /L) and mixed well. Above-ground parts of plant were dipped into 100-200 ml Agrobacterium solution for less than1 min with gentle agitation. Dipped plants were placed either under a dome or cover to maintain high humidity for 16 to 24 hours. Plants were grown in greenhouse under normal growth conditions until seeds were harvested.

2.1.5 Genotyping

Seeds (F1) from crosses were grown and self-pollinated to obtain the F2 generation. The F2 plants were genotyped by PCR. Genomic DNA was extracted from F2 plants by the DNA extraction buffer and then used as PCR template for genotyping. The primers for PCR genotyping were used as listed. For wild type alleles, PCR was carried out using a pair of gene specific primers, named Left and Right genomic primer (LP and RP) flanking the T-DNA insertion site on the genomic sequence. For the detection of mutant alleles, PCR was carried out using the gene specific right primer RP and the Left Border primer of the T-DNA insertion (i.e. primer LBb1.3 for SALK T-DNA insertion lines).
DNA extraction buffer: 50 mM Tris-HCl pH 7.2; 300 mM NaCl; 300 mM sucrose.

2.1.6 *Arabidopsis* total RNA isolation

100-200 mg of 16-day-old young seedlings grown at 22 °C under long day (16 h light/ 8 h dark) photoperiod conditions were harvested into an eppendorf tube containing glass

beads (diameter 1 mm) and frozen in liquid nitrogen. Samples were grinded using the Silama S5 apparatus (Ivoclar, Vivadent). Total RNA was extracted by using the Nucleospin RNA kit (Macherey-Nagel) according to the manufacturer's instructions. RNA concentration was evaluated using nanodrop 2000 by measuring the absorbance at 260 nm (1 unit of OD_{260} = 40µg /ml of RNA).

2.1.7 Reverse transcription

10 µL RNA (≤5 µg), 5 µL of reverse transcription 10X buffer (Promega) and 5 µL of 25 mM $MgCl_2$ were mixed in a 200 µL PCR tube and treated with 1 µL of RQ1 Dnase (Promega) at 37 °C for 10 min to eliminate genomic DNA from RNA samples, and followed by at 65°C for 10 min to inactivate the Dnase activity. 1 µL of 100 mM oligo dT was added to the reaction and incubate it at 70 °C for 5 min, then put it on ice immediately for 5 min. 2.5 µL of 10 mM dNTPs and 1 µL of Impro II Reverse Transcriptase (Promega) were added into the mixture and incubated at 42 °C for 70 min, followed inactivation by heating at 70 °C for 15 min. The synthesized cDNA was used as template for quantitative PCR.

2.1.8 Quantitative PCR

Quantitative PCR was used to detect relative or absolute gene expression level. It was performed in 384 wells optical plate on a light cycler 480 II (Roche) apparatus, according to the manufacturer's instructions. PCR total volume was scaled to 10 µl for each reaction, including 2 µL of mixed primers (containing 2.5 mM forward and reverse gene specific primers), 5 µL of 480 SYBER Green fluorescent reporter, 2 µL water and 1 µL cDNA template. For each sample, PCR was performed in triplicate using fixed amounts of cDNA template. *GADPH*, *EXP* and *Tip4.1* were used as internal reference genes. PCR was carried out by following procedures: pre-heating at 95 °C for 10 min, followed by 40 cycles of 15 sec at 95 °C, 30 sec at 60 °C and 15 sec at 72 °C. Melting curves of PCR reactions were checked to ensure the quality of PCR reaction and to avoid any DNA contamination. The threshold cycle value (CT) was set so that the fluorescent signal was above the baseline noise but as low as possible in the exponential amplification phase.

2.1.9 Microarray analysis

The microarray analysis was performed in Shanghai Biotechnology Corporation (China). Total RNA was isolated from a pool of about 100 individual 6-day-old wild-type and *sdg8-1*, *hub2-2* and *sdg8-1 hub2-2* homozygous mutant seedlings grown at 22 °C under long-day (LD, 16 h light and 8 h dark) photoperiod conditions. The RNA integrity was inspected by an Agilent Bioanalyzer 2100 (Agilent technologies, Santa Clara, CA, US) and qualified total RNA was further purified by RNeasy mini kit (Cat#74106, QIAGEN, GmBH, Germany) and RNase-Free DNase Set (Cat#79254, QIAGEN, GmBH, Germany). Array hybridization and wash was performed using GeneChip® Hybridization, Wash and Stain Kit (Cat#900720, Affymetrix, Santa Clara, CA, US) in Hybridization Oven 645 (Cat#00-0331-220V, Affymetrix, Santa Clara, CA, US)and Fluidics Station 450 (Cat#00-0079, Affymetrix, Santa Clara, CA, US) followed the manufacturer's instructions. Microarray slides were scanned by GeneChip® Scanner 3000 (Cat#00-00212, Santa Clara, CA, US) and Command Console Software 4.0 (Affymetrix, Santa Clara, CA, US) with default settings. Raw data were normalized by MAS 5.0 algorithm, Affy packages in R. Gene expression analysis was performed using two independent experiments obtained each with three independently derived sets of RNA for each plant genotype. Genes with at least a 1.5-fold expression change and the P-values inferior to 0.05 in the three independent biological replicates were considered as significantly perturbed in the mutant compared to the wild-type control.

2.1.10 Nuclear protein extraction

3-week-old of Arabidopsis seedlings grown under medium day (MD; 16 h light and 8 h dark) were harvested in liquid nitrogen to a quantity of 3-5 grams. Then nuclear protein extraction steps are as listed below.

1. Grind the tissues to a fine powder in liquid nitrogen (3-5 ml materials) using cold mortar and pestle. The powder was then put into a 50 mL Falcon tube.
2. Add 30 mL cold Lysis buffer into the powder, vortex and place on a rotation wheel for 30 min at 4 °C.

3. Filter the solution through a 100 um nylon mesh.

4. Centrifuge the filtered homogenate at 4000 rpm at 4 °C for 20 min to pellet the nuclei and discard the supernatant.

5. Resuspend the pellet in 1ml to 1.5 ml Lysis Buffer and transfer it to a 2 ml tube.

6. Centrifuge the solution at 4000 rpm at 4 °C for 20 min and remove the supernatant.

7. Resuspend the pellet in 200 µL (150 µL to 400 µL) 1 x SDS loading buffer (depending on the starting powder quantity).

8. Incubate at 95 °C, 10 min.

9. Centrifuge the sample at 12000 rpm at 25 °C for 5 min.

10. Remove the supernatant to a new tube. Use 10 µL to load for western blot. Material can be store at -20 °C for no more than 2-3 weeks.

11. Test with antibody specifically against H3 to adjust quantities between samples.

Low salt wash buffer (200 ml): 20 ml 0.5 M HEPES pH 7.5 + 6 ml 5 M NaCl + 400 µL 500 mM EDTA (keep at 4 °C)

Lysis Buffer (50 ml): 45 ml low salt wash buffer + 500 µl Triton X-100 + 5 ml glycerol + 50 µL 100 mM PMSF + 20 µL β-mercaptoethanol (on ice)

Note: Lysis Buffer should be prepared at least 30min in advance for correct homogenization; PMSF should be kept at 25 °C for 5-10 min and added at last.

TE buffer: 10 mM Tris HCl pH 8.0 1mM EDTA pH 8.0

2.1.11 SDS (sodium dodecyl suLfate)-polyacrylamide gel electrophoresis (PAGE)

1. Protein samples (in 1×SDS loading buffer) were heated at 95 °C for 10 minutes and then centrifuged at 13200 rpm for 5 minutes.

2. Load protein samples and pre-stained standard protein to a PAGE gel.

3. Run the gel in 1x SDS electrophoresis buffer at 100 volt (V) to separate proteins with different size. Incubate the gel in a Coomassie solution with shaking for 20 minutes at 25 °C. Remove Coomassie solution and incubate the gel with shaking in destaining solution until the proteins on the gel can be visualized.

A PAGE gel includes two parts, resolving gel and stacking gel.

Resolving gel: 10-15% Acrylamide/ Bis-acrylamide (29:1); 375 mM Tris-HCl pH 8.8; 0.1% SDS; 0.1% Ammonium persulfate (AP); 0.4 µl/ ml TEMED

Stacking gel: 5% Acrylamide/ Bis-acrylamide (29:1); 125 mM Tris-HCl pH 6.8; 0.1% SDS; 0.1% AP; 1 µL / ml TEMED

1X SDS running buffer: 25 mM Tris pH 8.0; 250 mM glycine; 0.1% SDS

1X SDS loading buffer: 50 mM Tris-HCl pH 6.8; 100 mM DTT; 2% SDS; 0.1% bromophenol blue; 10% glycerol

Coomassie blue solution: 40% methanol; 10% acetic acid; 50% water; 0.1% (w/v) Coomassie brilliant blue R250

Coomassie destaining solution (1L): 400 mL Ethanol 100%; 100 mL Acetic Acid; 500 mL H_2O

2.1.12 Western blots

1. Nuclear protein samples were separated on 15% percentage gel by SDS-PAGE, and then the gel is equilibrated in transfer buffer for at least 10 min before transference.
2. Proteins on the gel were transferred into the immobilon-P PVDF transfer membrane in transfer buffer at 300 milliampere (mA) for 2 hours at 4 °C. Membrane should be washed by 100% methanol for 1 minute, and then by transfer buffer for 10 minutes before use.
3. Washed the membrane in 1×TTBS (1×TBS buffer with 0.1% Triton-X100) buffer for 5 minutes.
4. Blocked the membrane in milk-TTBS (5% non-fat milk in 1×TTBS) buffer for 1 hour
5. Incubated the membrane in diluted primary antibody (1:5000) at 4 °C overnight.
6. Rinsed the membrane briefly in 1×TTBS buffer for 10 minutes.
7. Incubated the membrane in the diluted secondary antibody (1:10000) for 1 hour at 25 °C.
8. Rinsed the membrane 3 times with 1×TTBS buffer, and each time for 10 min.
9. Put the membrane in ECL western blot detection reagents for 3 minutes at 25 °C
10. Capture WB image on the film.

Transfer buffer: 25 mM Tris pH 8.0; 192 mM glycine; 15% methanol

TBS buffer: 20 mM Tris-HCl pH7.4; 150 mM NaCl

2.1.13 Chromatin ImmunoPrecipitation (ChIP)

Day 1: Arabidopsis 16 days old seedlings were harvested in 100 ml fixation buffer followed cross-linking by vacuum infiltration for 10 minutes. Cross-linking was quenched by adding 5 ml of 2.5 M glycine and continued to infiltrate in vacuum for 5 minutes. Seedlings were rinsed with water 5 times and dried as much as possible. The dried seedlings were subsequently grinded in liquid nitrogen to a fine powder and kept at -80 °C.

Day 2: 30 ml of ChIP lysis buffer was added to 5 ml powder of each sample, and incubated on a rotation wheel for 40 min at 4°C. The mixture was filtered through 100 µm nylon meshes and centrifuged at 4000 rpm at 4°C for 20 min. After removing supernatant, the pellet may appear grey; otherwise the pellet was resuspended again in ChIP lysis buffer and centrifuged again. The pellet was resuspended in 570 µL of ChIP lysis buffer and transferred to a new 1.5 ml tube. Centrifuged solution at 4000 rpm at 4 °C for 20 min. Removed supernatant as much as possible and resuspended pellet in 570 µL lysis buffer plus 30 µL of 10% SDS. Chromatin was sonicated four times with a Bioruptor (Diagenode) in ice water, 30 seconds ON and 30 seconds OFF at high power during 5 minutes for each time. The sonicated chromatin sample was centrifuged at 13000 rpm at 4 °C for 10 min. Supernatant was transferred to a new tube and added up 2 ml with ChIP lysis buffer. To check the sonication efficiency, 40 µL of solution was taken and 360 µl ChIP elution buffer and 16 µl of 5 M NaCl were added and incubated at 65 °C least 6 hour or overnight. DNA was recovered by NucleoSpin® Gel and PCR Clean-up kit (MACHEREY-NAGEL, Germany) and eluted in 30µl H2O. Then 5µl DNA was treated with 1µl RNase and used for agarose gel electrophoresis to visualize the quality of the sonication (DNA fragment should be 100-500 bp). The residue DNA was used later as input for qPCR analysis. After confirming the sonication was well done, 300 µL of chromatin was added up to 2 ml by antibody binding buffer and used for ImmunoPrecipitation by incubating with 1 to 3 µL desired antibodies overnight at 4 °C under rotation. Parallel, chromatin without any antibody was used as a mock control.

Day 3: Chromatin with antibody complex was collected by adding 20 µl of slurry magnetic Protein A beads (Millipore) for each reaction and incubated at 4 °C for 1-3 hours under

rotation. The beads were pelleted using a Magana GrIP racks (Millipore) and washed successively with 500 µL of low salt wash buffer, high salt wash buffer, LiCl wash buffer under rotation at 4 °C for 10 min and finally 500 µL TE buffer under rotation 25 °C for 10 minutes, then removed TE buffer as much as possible. The beads-antibody chromatin complex was eluted in 100 µl elution buffer with 1 µL of protease K and incubated at 65 °C overnight under agitation.

Day 4: The beads were pelleted by the Magna GrIP rack and the supernatant was transferred to a new 1.5 ml tube. DNA was recovered by NucleoSpin® Gel and PCR Clean-up kit (MACHEREY-NAGEL, Germany) and was then used for quantitative real-time PCR analysis.

Fixation buffer: 0.4 M sucrose; 10 mM Tris-HCl pH 8.0; 1 mM EDTA pH 8.0; 1.0% Formaldehyde; 1mM PMSF/AEBSF

ChIP lysis buffer: 50 mM HEPES pH 7.5; 1 mM EDTA pH 8.0; 150 mM NaCl; 1% Triton X-100; 5 mM β-mercaptoethanol; 10% glycerol; Proteinase inhibitors

Antibody binding buffer: 50 mM Tris-HCl pH 8.0; 1 mM EDTA pH 8.0; 150 mM NaCl; 0.1% Triton X-100; 5 mM β-mercaptoethanol; Proteinase inhibitors

Low salt wash buffer: 50 mM HEPES pH 7.5; 150 mM NaCl; 1 mM EDTA pH 8.0

High salt wash buffer: 50 mM HEPES pH 7.5; 500 mM NaCl; 1 mM EDTA pH 8.0

LiCl wash buffer: 10 mM Tris-HCl pH 8.0; 1 mM EDTA pH 8.0; 0.5% NP-40; 0.25 M LiCl

TE buffer: 10 mM Tris-HCl pH 8.0; 1 mM EDTA pH 8.0

Elution buffer: 1% SDS; 0.1 M NaHCO3

2.1.14 Flow cytometry

Several the first pair of rosette leaves collected from seedlings grown on 1/2 MS medium under long-day (LD; 16 h light and 8 h dark) photoperiod conditions were roughly chopped (1-2 mm side pieces or strips) with a razor blade in nuclear extraction buffer (CyStain UV precise P kit, Partec) and stained by nuclear staining buffer (CyStain UV-precise P) containing 4, 6-diamidino-2-phenylindole (DAPI). The mixed solution was subsequently filtered through 50µm (pore diameter) nylon mesh. Flow cytometry was performed on a

Ploidy Analysis PA-1 (Partec) and a total of 20000 nuclei per sample were counted. Ploidy levels data was analyzed by Flowjo (TreeStar).

2.2 Bacterial techniques

2.2.1 Preparation of competent cells for heat shock using $CaCl_2$

A single bacterial colony was inoculated in 5 ml LB medium and incubated with shaking at 37 °C overnight. The culture was used to inoculate 500 ml LB (1: 100) and incubated by shaking at 37 °C until OD_{600} value reaches 0.4-0.6. Cells were harvested by centrifugation at 3000 rpm for 10 minutes at 4 °C and resuspended in 50 ml of ice-cold 0.1 M $CaCl_2$ solution on ice. After centrifugation at 4000 rpm for 10 minutes at 4 °C, supernatant was poured off and cells were resuspended gently in 3 ml of ice-cold 50 mM CaCl2/ 15% glycerol on ice. The competent cells were then dispensed into 100 µL aliquots, frozen in liquid nitrogen and stored in -80 °C.
LB medium: 10 g/ L Tryptone; 5 g/ L Yeast extract; 10 g/ L NaCl

2.2.2 Transformation by heat shock

1µL plasmids, 1-5 µL of DNA ligation or BP/ LR recombination reaction products were added into 100 µL competent cells in a sterile tube and mixed well by swirling gently. After keeping on ice for 30 minutes, the tube was put on a rack and transferred to preheated 42 °C circulating water bath for 45 seconds to 60 seconds. The tube was then chilled in ice for 3-5 minutes and added into 400 µL LB medium. The culture was incubated t at 37 °C 1 hour with gentle shaking to recover the bacteria. Proper volume of transformed competent cells was transferred onto LB agar medium plate with appropriate antibiotic. The plate was incubated at 37 °C and colonies should appear in 12-16 hours.

2.2.3 Agrobacterium Transformation by electroporation

2 µL LR recombination reaction plasmids mixed with 50µL Agrobacterium competent cells in a sterile tube was transferred into a cold electroporation cuvette. The cuvette outside

was dried and was put in a white plastic holder of Biorad apparatus that delivering an electrical pulse of 25 uF capacitance, 2.5 kV and 200Ω to carry out the transformation. The transformation was finished after hearing a high constant tone, and then immediately added 1ml of LB medium to the cuvette. Cells were transferred from the cuvette into a 1.5ml eppendorf tube and incubated at 28 °C for 1-3 hours to recover the bacteria. Proper volume of transformed culture was transferred onto LB agar medium plate with appropriate antibiotic. The plate was incubated at 37 °C and colonies should appear in 48 hours.

2.2.4 Gateway cloning

The Gateway® Cloning Technology (Invitrogen Corporation) is an excellent cloning system and provides a rapid and highly efficient way to clone or sub-clone DNA segments and thus facilitates gene functional analysis, protein expression. It is achieved by two recombination reactions (BP and LR reactions) for transferring DNA segments between different cloning vectors. The BP reaction involves the transfer of PCR product of interest flanked by attB1 and attB2 sites into a donor (pDONR™) vector which has attP1 and attP sites flanking the cloning site to create an entry clone. The LR reaction is able to transfer the PCR product in the Entry Clone to one or more destination vectors with attR1 and attR2 sites and yields expression clone(s).

BP reaction: The gene or DNA fragment was amplified with flanking sequence of attB sites by PCR. Purified attB-PCR products (≈150 ng), donor vector (pDONR207 or pDONR) and TE buffer were added to a final volume of 8 µl in 1.5 ml tubes at 25 °C. The BP clonase TM II enzyme was kept in ice for 2 minutes to saw, and then 2 µl of enzyme was put into the reaction. After mixing well by brief vortex twice, the reaction was incubated at 25 °C for 2 hours or overnight. Finally, 1 µL of proteinase K was added and incubated at 37 °C for 10 min to stop the reaction.

LR reaction: Entry clone (≈150 ng), destination vector (pGWB604 and pGWB616 ≈150 ng) and TE buffer was added to a final volume of 8 µL in 1.5 ml tubes at 25 °C. After thawed in ice for 2 minutes, 2 µL of the LR clonase TM II enzyme was added to the reaction and mixed well by vortex briefly. The reaction was incubated at 25 °C for 2 hours or overnight

followed by adding 1 µL of proteinase K to stop the reaction by incubating at 37 °C for 10 minutes.

2.2.5 Extraction of plasmid DNA

1.5 ml bacterial culture was incubated at 37 °C overnight and cells were harvested by centrifugation 30 seconds at 11000 rpm. Plasmid DNA was extracted using the NucleoSpin® Plasmid QuickPure kit (MACHEREY -NAGEL, Germany) according to manufacturers' instructions.

2.2.6 Protein expression and purification in *E. coli*

Constructs of pGEX4T1-HULK2-C terminal, pET28a-SUMO-SDG8-N terminal, pET28a-SUMO-HULK2-PWWP, pET28a -SUMO-HUA2- PWWP, pET28a-SUMO-HUA2-PWWP (P16A), pET28a-SUMO-HUA2- PWWP (W18A) and pET28a-SUMO-HUA2-PWWP (P19A) were transformed into BL21 (DE3) competent cells. The transformed cells were grown at 37 °C overnight in 5 ml of liquid LB medium supplemented with antibiotics (100 mg/ ml ampicilin for pGEX4T1 fusion construct and 50 mg/ ml kanamycin for pET28a fusion construct). 1 ml of the bacterial cell suspension from each culture was used inoculated for 100 ml of LB medium supplemented with antibiotics. The bacteria cultures were grown at 37 °C with shaken until the value of OD_{600} reaches 0.6, then 1 mM IPTG was added, and the cultures were vigorously shaken for an additional 5 hours at room temperature. The cultures were harvested by centrifugation at 5000 × g for 20 min at 4 °C. The supernatants were decanted, and the pellets were frozen and stored at -80 °C, until further analysis.

2.2.7 Purification of 6x His-tagged proteins for crystallization

His-tagged proteins expressed cells were resuspended in 40 ml loading buffer and disrupted by sonication. After centrifugation at 15000 rpm for 1 hour, the supernatant was

loaded onto a His Trap column (GE) for affinity chromatography. Proteins were eluted by AKTA system using elution buffer. The 6x His SUMO tag was cleavage by 50 µL of 5 mg/ ml ULP1 enzyme at 16 °C for 5 hours. Then Ni NTA Qiagen resin was added and after several times wash by wash buffer the 6x His SUMO tag was removed. Protein was further purified by molecular sieve chromatography using Superdex G 75 16/60 column. Pure protein was concentrated by ultra filtration with Amicon ULTRA cutoff 3 kDa at 4 °C and frozen in liquid nitrogen and stored at 80 °C for crystallization use.

Loading buffer: 50 mM Tris-HCl pH 8.8; NaCl 300 mM; 5%Glycerol

Elution buffer: 50 mM Tris-HCl pH 8.8; 500 mM Imidazole; 300 mM NaCl; 5% glycerol

Wash buffer: 50 mM Tris-HCl pH 8.8; 10 mM Imidazole; 300 mM NaCl; 5% glycerol

Gel filtration buffer: 25 mM Tris-HCl pH 8.8; 100 mM NaCl

2.2.8 GST fusion protein purification

GST-tagged proteins expressed cells were resuspended in 20 ml of ice-cold GST lysis buffer with 100 µg/ ml lysozyme and protease inhibitor cocktail (Roche). After disrupting the cells by sonication, the cell lysate was centrifuged at 13200 rpm for 20 min at 4 °C. Then the supernatant was mixed with settled glutathion-Sepharose-4B beads (Amersham Bioscences), which was pre-washed 3 times with water and 3 times with 1X PBS buffer. The suspension was incubated on a rotation wheel for 2 hours or overnight at 4 °C. Beads were spun down and washed once in 1X PBS with 0.1% Triton X-100 buffer followed by 3 times in 1X PBS with 10% glycerol buffer. Finally, 1X PBS with10% glycerol buffer was added to make 10% slurry. GST-tagged proteins were fixed to the beads and determined by SDS-PAGE for further use.

GST lysis buffer: 1X PBS buffer; 0.1% Triton X-100; 1 mM DTT; 10% glycerol

1X PBS buffer: 140 mM NaCl; 2.7 mM KCl; 10 mM Na_2HPO_4; 1.8 mM KH_2PO_4; pH 7.4

2.3 Protein crystallization

For crystallization, purified HUA2 PWWP-domain protein was concentrated to round 130 µL at 5 mg/ mL (in total of 650 µg) in 50 mM Tris-HCl pH 8.0, 300 mM NaCl, 5% glycerol,

1 mM DDT; HULK2 PWWP domain-protein was concentrated to around 150 µL at 40 mg/ mL (in total of 6 mg) in 50 mM Tris-HCl pH 8.8, 300 mM NaCl, 5% glycerol, 1 mM DDT. A sparse and general screening was performed with five commercial screens including AmSO4, Index, JCGS, PACT and PEGs. Drops of 200 nL protein with 200 nL of each screening solution were set up in MRC2 plates (50 µL of reservoir) and stored in Rock Imager at 20 °C with regular imaging.

2.4 GST pull-down assays

Purified His-tagged protein (without cleavage of the 6x His SUMO tag) was mixed with GST or GST fusion protein (fixed on beads), respectively. After rotating for 2 hours or overnight at 4°C on a wheel, the beads were washed four times with pull-down buffer. After washing, specifically bound proteins are eluted from the beads by pull-down buffer containing 1 M NaCl and then precipitated by 10% TCA. A quarter of each pull-down fraction was analyzed by SDS-PAGE and western blots using His antibody.
Pull-down buffer: 20 mM Tris-HCl (pH 8.0); 200 mM NaCl; 1 mM EDTA (pH 8.0); 0.5% Nonidet P-40; 25 µg/ mL PMSF

2.5 In vitro binding assay (using peptide) and dot western

1. Purify 6x His-tagged proteins with Ni-NTA beads.
2. Wash with 1*PBS buffer twice.
3. Add the following reagents in one reaction (no DTT):
    a. 20-25 µg protein (normally 20-25 µg means only 2-3 µL beads)
    b. 25 µL Ni-NTA beads (pre-washed by 1*PBS)
    c. 100 µg BSA (optional, used to block unspecific binding)
    d. X µg peptide (make the molar ratio of protein and peptide to be about 1:3)
    e. Up to 1 ml by 1*PBS
4. Incubate at least 2 hours at 4 °C.
5. Wash with 1*PBS 4 times. For every wash, rotate 10 min at 4 °C.

6. After the 4th washing, remove the supernatant as much as possible.
7. Add 30 μl elution buffer (20mM Tris 8.0, 0.2M NaCl, 0.3M imidazole and 10% glycerol) and incubate 45 min at 4 °C.
8. Centrifuge 4000 rpm for 5min at 4 °C.
9. Take 5 μL supernatant for dot western, and take 0.1 μg peptide for input.

The following procedure is for dot western:

10. Cut the PVDF membrane to 0.6 cm wide and X cm long (X depends on the number of dots on each membrane).
11. Use a pencil to draw the dots on PVDF membrane. There should be 1 cm space between every two dots.
12. Rinse in methanol once.
13. Put the membrane on one piece of filter and air dry.
14. Dot the proteins prepared in Step 9 on the PVDF membrane.
15. Air dries COMPLETELY.
16. Rinse in methanol once.
17. Rinse in TTBS once.
18. Equivalence in Milk-TTBS at 1 hour at 37 °C.
19. The following procedure is same as western blot.

REFERENCE

Aichinger E, Villar CB, Farrona S, Reyes JC, Hennig L, Kohler C (2009) CHD3 proteins and polycomb group proteins antagonistically determine cell identity in Arabidopsis. PLoS Genet **5:** e1000605

Allfrey V, Faulkner R, Mirsky A (1964) Acetylation and methylation of histones and their possible role in the regulation of RNA synthesis. Proceedings of the National Academy of Sciences **51:** 786-794

Alvarez-Venegas R, Abdallat AA, Guo M, Alfano JR, Avramova Z (2007) Epigenetic Control of a Transcription Factor at the Cross Section of Two Antagonistic Pathways. Epigenetics **2:** 106-113

Alvarez-Venegas R, Pien S, Sadder M, Witmer X, Grossniklaus U, Avramova Z (2003) ATX-1, an Arabidopsis Homolog of Trithorax, Activates Flower Homeotic Genes. Current Biology **13:** 627-637

Amasino R (2004) Take a cold flower. Nature genetics **36:** 111-113

Andres F, Coupland G (2012) The genetic basis of flowering responses to seasonal cues. Nat Rev Genet **13:** 627-639

Arabidopsis Genome Initiative (2000) Analysis of the genome sequence of the flowering plant Arabidopsis thaliana. Nature **408:** 796

Avery OT, MacLeod CM, McCarty M (1944) Studies on the chemical nature of the substance inducing transformation of pneumococcal types: induction of transformation by a desoxyribonucleic acid fraction isolated from pneumococcus type III. The Journal of experimental medicine **79:** 137

Bannister AJ, Kouzarides T (2011) Regulation of chromatin by histone modifications. Cell Res **21:** 381-395

Bannister AJ, Zegerman P, Partridge JF, Miska EA, Thomas JO, Allshire RC, Kouzarides T (2001) Selective recognition of methylated lysine 9 on histone H3 by the HP1 chromo domain. Nature **410:** 120-124

Baroux C, Gagliardini V, Page DR, Grossniklaus U (2006) Dynamic regulatory interactions of Polycomb group genes: MEDEA autoregulation is required for

imprinted gene expression in Arabidopsis. Genes & development **20:** 1081-1086.

Berger SL (2007) The complex language of chromatin regulation during transcription. Nature **447:** 407-412

Bernstein E, Duncan EM, Masui O, Gil J, Heard E, Allis CD (2006) Mouse polycomb proteins bind differentially to methylated histone H3 and RNA and are enriched in facultative heterochromatin. Mol Cell Biol **26:** 2560-2569

Berr A, McCallum EJ, Alioua A, Heintz D, Heitz T, Shen WH (2010) Arabidopsis histone methyltransferase SET DOMAIN GROUP8 mediates induction of the jasmonate/ethylene pathway genes in plant defense response to necrotrophic fungi. Plant Physiol **154:** 1403-1414

Berr A, McCallum EJ, Menard R, Meyer D, Fuchs J, Dong A, Shen WH (2010) Arabidopsis SET DOMAIN GROUP2 is required for H3K4 trimethylation and is crucial for both sporophyte and gametophyte development. Plant Cell **22:** 3232-3248

Berr A, Shafiq S, Pinon V, Dong A, Shen WH (2015) The trxG family histone methyltransferase SET DOMAIN GROUP 26 promotes flowering via a distinctive genetic pathway. Plant J **81:** 316-328

Berr A, Shafiq S, Shen WH (2011) Histone modifications in transcriptional activation during plant development. Biochim Biophys Acta **1809:** 567-576

Berr A, Xu L, Gao J, Cognat V, Steinmetz A, Dong A, Shen WH (2009) SET DOMAIN GROUP25 encodes a histone methyltransferase and is involved in FLOWERING LOCUS C activation and repression of flowering. Plant Physiol **151:** 1476-1485

Berry S, Dean C (2015) Environmental perception and epigenetic memory: mechanistic insight through FLC. Plant J **83:** 133-148

Bian S, Li J, Tian G, Cui Y, Hou Y, Qiu W (2016) Combinatorial regulation of CLF and SDG8 during Arabidopsis shoot branching. Acta Physiologiae Plantarum **38**

Biswas D, Dutta-Biswas R, Mitra D, Shibata Y, Strahl BD, Formosa T, Stillman DJ (2006) Opposing roles for Set2 and yFACT in regulating TBP binding at promoters. The EMBO journal **25:** 4479-4489

Black JC, Van Rechem C, Whetstine JR (2012) Histone lysine methylation dynamics: establishment, regulation, and biological impact. Mol Cell **48:** 491-507

Blumel M, Dally N, Jung C (2015) Flowering time regulation in crops-what did we learn from Arabidopsis? Curr Opin Biotechnol **32:** 121-129

Bond DM, Wilson IW, Dennis ES, Pogson BJ, Jean Finnegan E (2009) VERNALIZATION INSENSITIVE 3 (VIN3) is required for the response of Arabidopsis thaliana seedlings exposed to low oxygen conditions. Plant J **59:** 576-587

Bourbousse C, Ahmed I, Roudier F, Zabulon G, Blondet E, Balzergue S, Colot V, Bowler C, Barneche F (2012) Histone H2B monoubiquitination facilitates the rapid modulation of gene expression during Arabidopsis photomorphogenesis. PLoS Genet **8:** e1002825

Bouyer D, Roudier F, Heese M, Andersen ED, Gey D, Nowack MK, Goodrich J, Renou JP, Grini PE, Colot V, Schnittger A (2011) Polycomb repressive complex 2 controls the embryo-to-seedling phase transition. PLoS Genet **7:** e1002014

Bratzel F, Lopez-Torrejon G, Koch M, Del Pozo JC, Calonje M (2010) Keeping cell identity in Arabidopsis requires PRC1 RING-finger homologs that catalyze H2A monoubiquitination. Curr Biol **20:** 1853-1859

Bratzel F, Turck F (2015) Molecular memories in the regulation of seasonal flowering: from competence to cessation. Genome biology **16:** 192

Bratzel F, Yang C, Angelova A, Lopez-Torrejon G, Koch M, del Pozo JC, Calonje M (2012) Regulation of the new Arabidopsis imprinted gene AtBMI1C requires the interplay of different epigenetic mechanisms. Mol Plant **5:** 260-269

Braun S, Madhani HD (2012) Shaping the landscape: mechanistic consequences of ubiquitin modification of chromatin. EMBO Rep **13:** 619-630

Brien GL, Gambero G, O'Connell DJ, Jerman E, Turner SA, Egan CM, Dunne EJ, Jurgens MC, Wynne K, Piao L, Lohan AJ, Ferguson N, Shi X, Sinha KM, Loftus BJ, Cagney G, Bracken AP (2012) Polycomb PHF19 binds H3K36me3 and recruits PRC2 and demethylase NO66 to embryonic stem cell genes during differentiation. Nat Struct Mol Biol **19:** 1273-1281

Bu Z, Yu Y, Li Z, Liu Y, Jiang W, Huang Y, Dong A-W (2014) Regulation of Arabidopsis flowering by the histone mark readers MRG1/2 via interaction with CONSTANS to modulate FT expression. PLoS Genet **10:** e1004617

Calonje M (2014) PRC1 marks the difference in plant PcG repression. Mol Plant **7:** 459-471

Carvalho S, Raposo AC, Martins FB, Grosso AR, Sridhara SC, Rino J, Carmo-Fonseca M, Almeida SF (2013) Histone methyltransferase SETD2 coordinates FACT recruitment with nucleosome dynamics during transcription. Nucleic acids research **41:** 2881-2893

Cao Y, Dai Y, Cui S, Ma L (2008) Histone H2B monoubiquitination in the chromatin of FLOWERING LOCUS C regulates flowering time in Arabidopsis. Plant Cell **20:** 2586-2602

Cartagena JA, Matsunaga S, Seki M, Kurihara D, Yokoyama M, Shinozaki K, Fujimoto S, Azumi Y, Uchiyama S, Fukui K (2008) The Arabidopsis SDG4 contributes to the regulation of pollen tube growth by methylation of histone H3 lysines 4 and 36 in mature pollen. Dev Biol **315:** 355-368

Cazzonelli CI, Cuttriss AJ, Cossetto SB, Pye W, Crisp P, Whelan J, Finnegan EJ, Turnbull C, Pogson BJ (2009) Regulation of carotenoid composition and shoot branching in Arabidopsis by a chromatin modifying histone methyltransferase, SDG8. Plant Cell **21:** 39-53

Cazzonelli CI, Nisar N, Roberts AC, Murray KD, Borevitz JO, Pogson BJ (2014) A chromatin modifying enzyme, SDG8, is involved in morphological, gene expression, and epigenetic responses to mechanical stimulation. Front Plant Sci **5:** 533

Cazzonelli CI, Roberts AC, Carmody ME, Pogson BJ (2010) Transcriptional control of SET DOMAIN GROUP 8 and CAROTENOID ISOMERASE during Arabidopsis development. Mol Plant **3:** 174-191

Chanvivattana Y, Bishopp A, Schubert D, Stock C, Moon YH, Sung ZR, Goodrich J (2004) Interaction of Polycomb-group proteins controlling flowering in Arabidopsis. Development **131:** 5263-5276

Chen D, Molitor A, Liu C, Shen WH (2010) The Arabidopsis PRC1-like ring-finger proteins

are necessary for repression of embryonic traits during vegetative growth. Cell Res **20:** 1332-1344

Chen DH, Huang Y, Liu C, Ruan Y, Shen WH (2014) Functional conservation and divergence of J-domain-containing ZUO1/ZRF orthologs throughout evolution. Planta **239:** 1159-1173

Chen D, Molitor AM, Xu L, Shen WH (2016) Arabidopsis PRC1 core component AtRING1 regulates stem cell-determining carpel development mainly through repression of class I KNOX genes. BMC Biol **14:** 112

Chen X, Hu Y, Zhou DX (2011) Epigenetic gene regulation by plant Jumonji group of histone demethylase. Biochim Biophys Acta **1809:** 421-426

Cho LH, Yoon J, An G (2016) The control of flowering time by environmental factors. Plant J

Clough SJ, Bent AF (1998) Floral dip: a simplified method for Agrobacterium-mediated transformation ofArabidopsis thaliana. The plant journal **16:** 735-743

Crevillen P, Dean C (2011) Regulation of the floral repressor gene FLC: the complexity of transcription in a chromatin context. Curr Opin Plant Biol **14:** 38-44

Crevillen P, Yang H, Cui X, Greeff C, Trick M, Qiu Q, Cao X, Dean C (2014) Epigenetic reprogramming that prevents transgenerational inheritance of the vernalized state. Nature **515:** 587-590

Cui X, Lu F, Qiu Q, Zhou B, Gu L, Zhang S, Kang Y, Cui X, Ma X, Yao Q, Ma J, Zhang X, Cao X (2016) REF6 recognizes a specific DNA sequence to demethylate H3K27me3 and regulate organ boundary formation in Arabidopsis. Nature genetics **48:** 694-9

Sanchez M, Gutierrez C (2009) Arabidopsis ORC1 is a PHD-containing H3K4me3 effector that regulates transcription. Proc Natl Acad Sci U S A **106:** 2065-2070

Lucia F, Crevillen P, Jones AM, Greb T, Dean C (2008) A PHD-polycomb repressive complex 2 triggers the epigenetic silencing of FLC during vernalization. Proc Natl Acad Sci U S A **105:** 16831-16836

Dean C (1993) Advantages of Arabidopsis for Cloning Plant Genes. Philosophical

Transactions of the Royal Society B: Biological Sciences **342:** 189-195

De-La-Pena C, Rangel-Cano A, Alvarez-Venegas R (2012) Regulation of disease-responsive genes mediated by epigenetic factors: interaction of Arabidopsis-Pseudomonas. Mol Plant Pathol **13:** 388-398

Derkacheva M, Liu S, Figueiredo DD, Gentry M, Mozgova I, Nanni P, Tang M, Mannervik M, Kohler C, Hennig L (2016) H2A deubiquitinases UBP12/13 are part of the Arabidopsis polycomb group protein system. Nat Plants **2:** 16126

Dhawan R, Luo H, Foerster AM, Abuqamar S, Du HN, Briggs SD, Mittelsten Scheid O, Mengiste T (2009) HISTONE MONOUBIQUITINATION1 interacts with a subunit of the mediator complex and regulates defense against necrotrophic fungal pathogens in Arabidopsis. Plant Cell **21:** 1000-1019

Dillon SC, Zhang X, Trievel RC, Cheng X (2005) The SET-domain protein superfamily: protein lysine methyltransferases. Genome Biol **6:** 227

Ding Y, Avramova Z, Fromm M (2011) The Arabidopsis trithorax-like factor ATX1 functions in dehydration stress responses via ABA-dependent and ABA-independent pathways. Plant J **66:** 735-744

Ding Y, Lapko H, Ndamukong I, Xia Y, Al-Abdallat A, Lalithambika S, Sadder M, Saleh A, Fromm M, Riethoven J-J (2009) TheArabidopsis Chromatin Modifier ATX1, the Myotubularin-like AtMTM, and the response to Drought; a view from the other end of the pathway. Plant signaling & behavior **4:** 1049-1058

Dong G, Ma DP, Li J (2008) The histone methyltransferase SDG8 regulates shoot branching in Arabidopsis. Biochem Biophys Res Commun **373:** 659-664

Dover J, Schneider J, Tawiah-Boateng MA, Wood A, Dean K, Johnston M, Shilatifard A (2002) Methylation of histone H3 by COMPASS requires ubiquitination of histone H2B by Rad6. J Biol Chem **277:** 28368-28371

Doyle MR, Bizzell CM, Keller MR, Michaels SD, Song J, Noh YS, Amasino RM (2005) HUA2 is required for the expression of floral repressors in Arabidopsis thaliana. Plant J **41:** 376-85

Dupont C, Armant DR, Brenner CA (2009) Epigenetics: definition, mechanisms and clinical perspective. Semin Reprod Med **27:** 351-357

Emre NC, Ingvarsdottir K, Wyce A, Wood A, Krogan NJ, Henry KW, Li K, Marmorstein R, Greenblatt JF, Shilatifard A, Berger SL (2005) Maintenance of low histone ubiquitylation by Ubp10 correlates with telomere-proximal Sir2 association and gene silencing. Mol Cell **17:** 585-594

Farrona S, Coupland G, Turck F (2008) The impact of chromatin regulation on the floral transition. Seminars in cell & developmental biology **19:** 560-573

Farrona S, Thorpe FL, Engelhorn J, Adrian J, Dong X, Sarid-Krebs L, Goodrich J, Turck F (2011) Tissue-specific expression of FLOWERING LOCUS T in Arabidopsis is maintained independently of polycomb group protein repression. Plant Cell **23:** 3204-14

Felsenfeld G (2014) A brief history of epigenetics. Cold Spring Harb Perspect Biol **6**

Feng J, Chen D, Berr A, Shen WH (2016) ZRF1 Chromatin Regulators Have Polycomb Silencing and Independent Roles in Development. Plant Physiol **172:** 1746-1759

Feng J, Shen WH (2014) Dynamic regulation and function of histone monoubiquitination in plants. Front Plant Sci **5:** 83

Feng S, Jacobsen SE, Reik W (2010) Epigenetic reprogramming in plant and animal development. Science **330:** 622-627

Fierz B, Chatterjee C, McGinty RK, Bar-Dagan M, Raleigh DP, Muir TW (2011) Histone H2B ubiquitylation disrupts local and higher-order chromatin compaction. Nature chemical biology **7:** 113-119

Finnegan EJ, Dennis ES (2007) Vernalization-induced trimethylation of histone H3 lysine 27 at FLC is not maintained in mitotically quiescent cells. Curr Biol **17:** 1978-83

Fischle W (2008) Talk is cheap--cross-talk in establishment, maintenance, and readout of chromatin modifications. Genes Dev **22:** 3375-3382

Fischle W, Wang Y, Allis CD (2003) Histone and chromatin cross-talk. Current Opinion in Cell Biology **15:** 172-183

Fleury D, Himanen K, Cnops G, Nelissen H, Boccardi TM, Maere S, Beemster GT, Neyt P, Anami S, Robles P, Micol JL, Inze D, Van Lijsebettens M (2007) The Arabidopsis thaliana homolog of yeast BRE1 has a function in cell cycle regulation during early leaf and root growth. Plant Cell **19:** 417-432

Fuchs G, Oren M (2014) Writing and reading H2B monoubiquitylation. Biochim Biophys Acta **1839:** 694-701

Gan ES, Xu Y, Wong JY, Goh JG, Sun B, Wee WY, Huang J, Ito T (2014) Jumonji demethylases moderate precocious flowering at elevated temperature via regulation of FLC in Arabidopsis. Nat Commun **5:** 5098

Gehring M, Huh JH, Hsieh TF, Penterman J, Choi Y, Harada JJ, Goldberg RB, Fischer RL (2006) DEMETER DNA glycosylase establishes MEDEA polycomb gene self-imprinting by allele-specific demethylation. Cell **124:** 495-506

Goodrich J, Puangsomlee P, Martin M, Long D, Meyerowitz EM, Coupland G (1997) A Polycomb-group gene regulates homeotic gene expression in Arabidopsis. Nature **386:** 44

Greer EL, Shi Y (2012) Histone methylation: a dynamic mark in health, disease and inheritance. Nat Rev Genet **13:** 343-357

Grini PE, Thorstensen T, Alm V, Vizcay-Barrena G, Windju SS, Jørstad TS, Wilson ZA, Aalen RB (2009) The ASH1 HOMOLOG 2 (ASHH2) histone H3 methyltransferase is required for ovule and anther development in Arabidopsis. PloS one **4:** e7817

Grossniklaus U, Paro R (2014) Transcriptional silencing by polycomb-group proteins. Cold Spring Harb Perspect Biol **6:** a019331

Gu X, Jiang D, Wang Y, Bachmair A, He Y (2009) Repression of the floral transition via histone H2B monoubiquitination. Plant J **57:** 522-533

Gu X, Le C, Wang Y, Li Z, Jiang D, Wang Y, He Y (2013) Arabidopsis FLC clade members form flowering-repressor complexes coordinating responses to endogenous and environmental cues. Nat Commun **4:** 1947

Guo L, Yu Y, Law JA, Zhang X (2010) SET DOMAIN GROUP2 is the major histone H3 lysine [corrected] 4 trimethyltransferase in Arabidopsis. Proc Natl Acad Sci U S A **107:** 18557-18562

Guo R, Zheng L, Park JW, Lv R, Chen H, Jiao F, Xu W, Mu S, Wen H, Qiu J, Wang Z, Yang P, Wu F, Hui J, Fu X, Shi X, Shi YG, Xing Y, Lan F, Shi Y (2014) BS69/ZMYND11 reads and connects histone H3.3 lysine 36 trimethylation-

decorated chromatin to regulated pre-mRNA processing. Mol Cell **56:** 298-310

Guzman-Lopez JA, Abraham-Juarez MJ, Lozano-Sotomayor P, de Folter S, Simpson J (2016) Arabidopsis thaliana gonidialess A/Zuotin related factors (GlsA/ZRF) are essential for maintenance of meristem integrity. Plant Mol Biol **91:** 37-51

Hansen JC (2002) Conformational dynamics of the chromatin fiber in solution: determinants, mechanisms, and functions. Annu Rev Biophys Biomol Struct **31:** 361-392

He Y (2012) Chromatin regulation of flowering. Trends in plant science **17:** 556-562

He Y, Amasino RM (2005) Role of chromatin modification in flowering-time control. Trends Plant Sci **10:** 30-35

He Y, Michaels SD, Amasino RM (2003) Regulation of flowering time by histone acetylation in Arabidopsis. Science **302:** 1751-1754

Hecker A, Brand LH, Peter S, Simoncello N, Kilian J, Harter K, Gaudin V, Wanke D (2015) The Arabidopsis GAGA-Binding Factor BASIC PENTACYSTEINE6 Recruits the POLYCOMB-REPRESSIVE COMPLEX1 Component LIKE HETEROCHROMATIN PROTEIN1 to GAGA DNA Motifs. Plant Physiol **168:** 1013-1024

Hennig L, Derkacheva M (2009) Diversity of Polycomb group complexes in plants: same rules, different players? Trends Genet **25:** 414-423

Henry KW, Wyce A, Lo WS, Duggan LJ, Emre NC, Kao CF, Pillus L, Shilatifard A, Osley MA, Berger SL (2003) Transcriptional activation via sequential histone H2B ubiquitylation and deubiquitylation, mediated by SAGA-associated Ubp8. Genes Dev **17:** 2648-2663

Heo JB, Sung S (2011) Vernalization-mediated epigenetic silencing by a long intronic noncoding RNA. Science **331:** 76-79

Hepworth J, Dean C (2015) Flowering Locus C's Lessons: Conserved Chromatin Switches Underpinning Developmental Timing and Adaptation. Plant Physiol **168:** 1237-1245

Hershko A, Ciechanover A (1998) The ubiquitin system. Annual review of biochemistry **67:** 425-479

Hicke L (2001) Protein regulation by monoubiquitin. Nature reviews Molecular cell biology **2:** 195-201

Himanen K, Woloszynska M, Boccardi TM, De Groeve S, Nelissen H, Bruno L, Vuylsteke M, Van Lijsebettens M (2012) Histone H2B monoubiquitination is required to reach maximal transcript levels of circadian clock genes in Arabidopsis. Plant J **72:** 249-260

Hu M, Pei BL, Zhang LF, Li YZ (2014) Histone H2B monoubiquitination is involved in regulating the dynamics of microtubules during the defense response to Verticillium dahliae toxins in Arabidopsis. Plant Physiol **164:** 1857-1865

Hua Z, Vierstra RD (2011) The cullin-RING ubiquitin-protein ligases. Annu Rev Plant Biol **62:** 299-334

Huijser P, Schmid M (2011) The control of developmental phase transitions in plants. Development **138:** 4117-4129

Hyun Y, Richter R, Coupland G (2017) Competence to Flower: Age-Controlled Sensitivity to Environmental Cues. Plant Physiol **173:** 36-46

Ionescu IA, Møller BL, Sánchez-Pérez R (2016) Chemical control of flowering time. Journal of Experimental Botany**:** erw427

Jali SS, Rosloski SM, Janakirama P, Steffen JG, Zhurov V, Berleth T, Clark RM, Grbic V (2014) A plant-specific HUA2-LIKE (HULK) gene family in Arabidopsis thaliana is essential for development. Plant J **80:** 242-54

Jenuwein T (2006) The epigenetic magic of histone lysine methylation. FEBS J **273:** 3121-3135

Jiang D, Gu X, He Y (2009) Establishment of the winter-annual growth habit via FRIGIDA-mediated histone methylation at FLOWERING LOCUS C in Arabidopsis. Plant Cell **21:** 1733-1746

Jiang D, Kong NC, Gu X, Li Z, He Y (2011) Arabidopsis COMPASS-like complexes mediate histone H3 lysine-4 trimethylation to control floral transition and plant development. PLoS Genet **7:** e1001330

Jiang D, Wang Y, Wang Y, He Y (2008) Repression of FLOWERING LOCUS C and FLOWERING LOCUS T by the Arabidopsis Polycomb repressive complex 2

components. PLoS One **3:** e3404

Jiang D, Yang W, He Y, Amasino RM (2007) Arabidopsis relatives of the human lysine-specific Demethylase1 repress the expression of FWA and FLOWERING LOCUS C and thus promote the floral transition. Plant Cell **19:** 2975-2987

Johanson U, West J, Lister C, Michaels S, Amasino R, Dean C (2000) Molecular analysis of FRIGIDA, a major determinant of natural variation in Arabidopsis flowering time. Science **290:** 344-347

Johnson L, Mollah S, Garcia BA, Muratore TL, Shabanowitz J, Hunt DF, Jacobsen SE (2004) Mass spectrometry analysis of Arabidopsis histone H3 reveals distinct combinations of post-translational modifications. Nucleic Acids Res **32:** 6511-6518

Jones AL, Sung S (2014) Mechanisms underlying epigenetic regulation in Arabidopsis thaliana. Integr Comp Biol **54:** 61-7

Jullien PE, Katz A, Oliva M, Ohad N, Berger F (2006) Polycomb group complexes self-regulate imprinting of the Polycomb group gene MEDEA in Arabidopsis. Curr Biol **16:** 486-492

Jung C, Muller AE (2009) Flowering time control and applications in plant breeding. Trends Plant Sci **14:** 563-573

Katz A, Oliva M, Mosquna A, Hakim O, Ohad N (2004) FIE and CURLY LEAF polycomb proteins interact in the regulation of homeobox gene expression during sporophyte development. The Plant Journal **37:** 707-719

Kazan K, Lyons R (2015) The link between flowering time and stress tolerance. J Exp Bot **67:** 47-60

Keren I, Citovsky V (2016) The histone deubiquitinase OTLD1 targets euchromatin to regulate plant growth. Sci. Signal. **9:** ra125-ra125

Khan MR, Ai XY, Zhang JZ (2013) Genetic regulation of flowering time in annual and perennial plants. Wiley Interdiscip Rev RNA **5:** 347-359

Kim DH, Doyle MR, Sung S, Amasino RM (2009) Vernalization: winter and the timing of flowering in plants. Annu Rev Cell Dev Biol **25:** 277-299

Kim DH, Sung S (2013) Coordination of the vernalization response through a VIN3 and FLC gene family regulatory network in Arabidopsis. Plant Cell **25:** 454-469

Kim J, Guermah M, McGinty RK, Lee JS, Tang Z, Milne TA, Shilatifard A, Muir TW, Roeder RG (2009) RAD6-Mediated transcription-coupled H2B ubiquitylation directly stimulates H3K4 methylation in human cells. Cell **137:** 459-471

Kim J, Hake SB, Roeder RG (2005) The human homolog of yeast BRE1 functions as a transcriptional coactivator through direct activator interactions. Mol Cell **20:** 759-770

Kim J, Kim JA, McGinty RK, Nguyen UT, Muir TW, Allis CD, Roeder RG (2013) The n-SET domain of Set1 regulates H2B ubiquitylation-dependent H3K4 methylation. Mol Cell **49:** 1121-1133

Klose RJ, Kallin EM, Zhang Y (2006a) JmjC-domain-containing proteins and histone demethylation. Nat Rev Genet **7:** 715-727

Klose RJ, Yamane K, Bae Y, Zhang D, Erdjument-Bromage H, Tempst P, Wong J, Zhang Y (2006b) The transcriptional repressor JHDM3A demethylates trimethyl histone H3 lysine 9 and lysine 36. Nature **442:** 312-316

Kohler C, Makarevich G (2006) Epigenetic mechanisms governing seed development in plants. EMBO Rep **7:** 1223-1227

Kooistra SM, Helin K (2012) Molecular mechanisms and potential functions of histone demethylases. Nat Rev Mol Cell Biol **13:** 297-311

Kouzarides T (2007) Chromatin modifications and their function. Cell **128:** 693-705

Krichevsky A, Zaltsman A, Lacroix B, Citovsky V (2011) Involvement of KDM1C histone demethylase-OTLD1 otubain-like histone deubiquitinase complexes in plant gene repression. Proc Natl Acad Sci U S A **108:** 11157-11162

Kumpf R, Thorstensen T, Rahman MA, Heyman J, Nenseth HZ, Lammens T, Herrmann U, Swarup R, Veiseth SV, Emberland G, Bennett MJ, De Veylder L, Aalen RB (2014) The ASH1-RELATED3 SET-domain protein controls cell division competence of the meristem and the quiescent center of the Arabidopsis primary root. Plant Physiol **166:** 632-643

Lafos M, Kroll P, Hohenstatt ML, Thorpe FL, Clarenz O, Schubert D (2011) Dynamic regulation of H3K27 trimethylation during Arabidopsis differentiation. PLoS Genet **7:** e1002040

Lee J, Lee I (2010) Regulation and function of SOC1, a flowering pathway integrator. J

Exp Bot **61:** 2247-2254

Lee JS, Shukla A, Schneider J, Swanson SK, Washburn MP, Florens L, Bhaumik SR, Shilatifard A (2007) Histone crosstalk between H2B monoubiquitination and H3 methylation mediated by COMPASS. Cell **131:** 1084-1096

Lee JS, Smith E, Shilatifard A (2010) The language of histone crosstalk. Cell **142:** 682-685

Lee N, Kang H, Lee D, Choi G (2014) A histone methyltransferase inhibits seed germination by increasing PIF1 mRNA expression in imbibed seeds. Plant J **78:** 282-293

Lee WY, Lee D, Chung WI, Kwon CS (2009) Arabidopsis ING and Alfin1-like protein families localize to the nucleus and bind to H3K4me3/2 via plant homeodomain fingers. Plant J **58:** 511-524

Li C, Gu L, Gao L, Chen C, Wei CQ, Qiu Q, ... & Chen XM, Cui YH (2016) Concerted genomic targeting of H3K27 demethylase REF6 and chromatin-remodeling ATPase BRM in Arabidopsis. Nature genetics **48:** 687-93

Li W, Wang Z, Li J, Yang H, Cui S, Wang X, Ma L (2011) Overexpression of AtBMI1C, a polycomb group protein gene, accelerates flowering in Arabidopsis. PLoS One **6:** e21364

Li Y, Mukherjee I, Thum KE, Tanurdzic M, Katari MS, Obertello M, Edwards MB, McCombie WR, Martienssen RA, Coruzzi GM (2015) The histone methyltransferase SDG8 mediates the epigenetic modification of light and carbon responsive genes in plants. Genome Biol **16:** 79

Liu C, Lu F, Cui X, Cao X (2010) Histone methylation in higher plants. Annu Rev Plant Biol **61:** 395-420

Liu C, Thong Z, Yu H (2009) Coming into bloom: the specification of floral meristems. Development **136:** 3379-3391

Liu Y, Koornneef M, Soppe WJ (2007) The absence of histone H2B monoubiquitination in the Arabidopsis hub1 (rdo4) mutant reveals a role for chromatin remodeling in seed dormancy. Plant Cell **19:** 433-444

Liu Y, Min J (2016) Structure and function of histone methylation-binding proteins in plants.

Biochemical Journal **473:** 1663-1680

Lopez-Gonzalez L, Mouriz A, Narro-Diego L, Bustos R, Martinez-Zapater JM, Jarillo JA, Pineiro M (2014) Chromatin-dependent repression of the Arabidopsis floral integrator genes involves plant specific PHD-containing proteins. Plant Cell **26:** 3922-3938

Lu F, Cui X, Zhang S, Jenuwein T, Cao X (2011) Arabidopsis REF6 is a histone H3 lysine 27 demethylase. Nat Genet **43:** 715-719

Lu F, Cui X, Zhang S, Liu C, Cao X (2010) JMJ14 is an H3K4 demethylase regulating flowering time in Arabidopsis. Cell Res **20:** 387-390

Lu F, Li G, Cui X, Liu C, Wang XJ, Cao X (2008) Comparative analysis of JmjC domain-containing proteins reveals the potential histone demethylases in Arabidopsis and rice. J Integr Plant Biol **50:** 886-896

Luger K, Mäder AW, Richmond RK, Sargent DF, Richmond TJ (1997) Crystal structure of the nucleosome core particle at 2.8 Å resolution. Nature **389:** 251-260

Luo M, Luo MZ, Buzas D, Finnegan J, Helliwell C, Dennis ES, Peacock WJ, Chaudhury A (2008) UBIQUITIN-SPECIFIC PROTEASE 26 is required for seed development and the repression of PHERES1 in Arabidopsis. Genetics **180:** 229-236

Makarova KS, Aravind L, Koonin EV (2000) A novel superfamily of predicted cysteine proteases from eukaryotes, viruses and Chlamydia pneumoniae. Trends Biochem Sci **25:** 50-2

Margueron R, Justin N, Ohno K, Sharpe ML, Son J, Drury WJ, 3rd, Voigt P, Martin SR, Taylor WR, De Marco V, Pirrotta V, Reinberg D, Gamblin SJ (2009) Role of the polycomb protein EED in the propagation of repressive histone marks. Nature **461:** 762-767

Margueron R, Reinberg D (2011) The Polycomb complex PRC2 and its mark in life. Nature **469:** 343-349

Martin C, Zhang Y (2005) The diverse functions of histone lysine methylation. Nat Rev Mol Cell Biol **6:** 838-849

McGinty RK, Kim J, Chatterjee C, Roeder RG, Muir TW (2008) Chemically ubiquitylated

histone H2B stimulates hDot1L-mediated intranucleosomal methylation. Nature **453:** 812-816

Meinke DW (1998) Arabidopsis thaliana: A Model Plant for Genome Analysis. Science **282:** 662-682

Ménard R, Verdier G, Ors M, Erhardt M, Beisson F, Shen W-H (2014) Histone H2B monoubiquitination is involved in the regulation of cutin and wax composition in Arabidopsis thaliana. Plant and Cell Physiology **55:** 455-466

Metzger E, Wissmann M, Yin N, Muller JM, Schneider R, Peters AH, Gunther T, Buettner R, Schule R (2005) LSD1 demethylates repressive histone marks to promote androgen-receptor-dependent transcription. Nature **437:** 436-439

Meyerowitz, E.M. and Somerville, C (1994). Arabidopsis (New York: Cold Spring Harbor Laboratory Press).

Michaels SD, Amasino RM (1999) FLOWERING LOCUS C encodes a novel MADS domain protein that acts as a repressor of flowering. Plant Cell **11:** 949-56

Molitor A, Shen WH (2013) The polycomb complex PRC1: composition and function in plants. J Genet Genomics **40:** 231-238

Molitor AM, Bu Z, Yu Y, Shen W-H (2014) Arabidopsis AL PHD-PRC1 complexes promote seed germination through H3K4me3-to-H3K27me3 chromatin state switch in repression of seed developmental genes. PLoS Genet **10:** e1004091

Mouradov A, Cremer F, Coupland G (2002) Control of flowering time interacting pathways as a basis for diversity. The Plant Cell **14:** S111-S130

Mozgova I, Hennig L (2015) The polycomb group protein regulatory network. Annu Rev Plant Biol **66:** 269-296

Musselman CA, Lalonde ME, Côté J, Kutateladze TG (2012) Perceiving the epigenetic landscape through histone readers. Nature structural & molecular biology **19:** 1218-1227

Mylne JS, Barrett L, Tessadori F, Mesnage S, Johnson L, Bernatavichute YV, Jacobsen SE, Fransz P, Dean C (2006) LHP1, the Arabidopsis homologue of HETEROCHROMATIN PROTEIN1, is required for epigenetic silencing of FLC. Proc Natl Acad Sci U S A **103:** 5012-5017

Nakagawa T, Kajitani T, Togo S, Masuko N, Ohdan H, Hishikawa Y, Koji T, Matsuyama T, Ikura T, Muramatsu M, Ito T (2008) Deubiquitylation of histone H2A activates transcriptional initiation via trans-histone cross-talk with H3K4 di- and trimethylation. Genes Dev **22:** 37-49

Napsucialy-Mendivil S, Alvarez-Venegas R, Shishkova S, Dubrovsky JG (2014) Arabidopsis homolog of trithorax1 (ATX1) is required for cell production, patterning, and morphogenesis in root development. J Exp Bot **65:** 6373-6384

Ng DW, Wang T, Chandrasekharan MB, Aramayo R, Kertbundit S, Hall TC (2007) Plant SET domain-containing proteins: structure, function and regulation. Biochim Biophys Acta **1769:** 316-329

Ng HH, Xu RM, Zhang Y, Struhl K (2002) Ubiquitination of histone H2B by Rad6 is required for efficient Dot1-mediated methylation of histone H3 lysine 79. J Biol Chem **277:** 34655-34657

Ning YQ, Ma ZY, Huang HW, Mo H, Zhao TT, Li L, Cai T, Chen S, Ma L, He XJ (2015) Two novel NAC transcription factors regulate gene expression and flowering time by associating with the histone demethylase JMJ14. Nucleic Acids Res **43:** 1469-1484

Noh B, Lee SH, Kim HJ, Yi G, Shin EA, Lee M, Jung KJ, Doyle MR, Amasino RM, Noh YS (2004) Divergent roles of a pair of homologous jumonji/zinc-finger-class transcription factor proteins in the regulation of Arabidopsis flowering time. Plant Cell **16:** 2601-2613

Palma K, Thorgrimsen S, Malinovsky FG, Fiil BK, Nielsen HB, Brodersen P, Hofius D, Petersen M, Mundy J (2010) Autoimmunity in Arabidopsis acd11 is mediated by epigenetic regulation of an immune receptor. PLoS Pathog **6:** e1001137

Park HJ, Kim WY, Pardo JM, Yun DJ (2016) Molecular Interactions Between Flowering Time and Abiotic Stress Pathways. Int Rev Cell Mol Biol **327:** 371-412

Peterson CL, Laniel MA (2004) Histones and histone modifications. Curr Biol **14:** R546-551

Pien S, Fleury D, Mylne JS, Crevillen P, Inze D, Avramova Z, Dean C, Grossniklaus U (2008) ARABIDOPSIS TRITHORAX1 dynamically regulates FLOWERING LOCUS

C activation via histone 3 lysine 4 trimethylation. Plant Cell **20:** 580-588

Pikaard CS, Mittelsten SO (2014) Epigenetic regulation in plants. Cold Spring Harb Perspect Biol **6:** a019315

Pinon V, Yao X, Dong A, Shen WH (2017) H3K4me3 is crucial for chromatin condensation and mitotic division during male gametogenesis. Plant physiology

Poethig RS (2013) Vegetative phase change and shoot maturation in plants. Current topics in developmental biology 105: 125.

Poynter ST, Kadoch C (2016) Polycomb and trithorax opposition in development and disease. Wiley Interdiscip Rev Dev Biol **5:** 659-688

Prakash S, Singh R, Lodhi N (2014) Histone demethylases and control of gene expression in plants. Cell. Mol. Biol **60:** 97-105

Pu L, Sung ZR (2015) PcG and trxG in plants - friends or foes. Trends Genet **31:** 252-262

Qin S, Min J (2014) Structure and function of the nucleosome-binding PWWP domain. Trends Biochem Sci **39:** 536-47

Racine A, Page V, Nagy S, Grabowski D, Tanny JC (2012) Histone H2B ubiquitylation promotes activity of the intact Set1 histone methyltransferase complex in fission yeast. J Biol Chem **287:** 19040-19047

Ratcliffe OJ, Nadzan GC, Reuber TL, Riechmann JL (2001) Regulation of Flowering in Arabidopsis by an FLC Homologue. Plant Physiology **126:** 122-132

Rea S, Eisenhaber F, O'carroll D, Strahl BD, Sun Z-W, Schmid M, Opravil S, Mechtler K, Ponting CP, Allis CD (2000) Regulation of chromatin structure by site-specific histone H3 methyltransferases. Nature **406:** 593-599

Richly H, Rocha-Viegas L, Ribeiro JD, Demajo S, Gundem G, Lopez-Bigas N, Nakagawa T, Rospert S, Ito T, Di Croce L (2010) Transcriptional activation of polycomb-repressed genes by ZRF1. Nature **468:** 1124-1128

Robzyk K, Recht J, Osley MA (2000) Rad6-dependent ubiquitination of histone H2B in yeast. Science **287:** 501-504

Roudier F, Ahmed I, Berard C, Sarazin A, Mary-Huard T, Cortijo S, Bouyer D, Caillieux E, Duvernois-Berthet E, Al-Shikhley L, Giraut L, Despres B, Drevensek S, Barneche F, Derozier S, Brunaud V, Aubourg S, Schnittger A, Bowler C,

Martin-Magniette ML, Robin S, Caboche M, Colot V (2011) Integrative epigenomic mapping defines four main chromatin states in Arabidopsis. EMBO J **30:** 1928-1938

Russo VEA, Martienssen, RA, and Riggs, AD (1996) Epigenetic Mechanisms of Gene Regulation. Cold Spring Harbor Laboratory Press, Cold Spring Harbor, NY.

Sahr T, Adam T, Fizames C, Maurel C, Santoni V (2010) O-carboxyl- and N-methyltransferases active on plant aquaporins. Plant Cell Physiol **51:** 2092-104

Saleh A, Al-Abdallat A, Ndamukong I, Alvarez-Venegas R, Avramova Z (2007) The Arabidopsis homologs of trithorax (ATX1) and enhancer of zeste (CLF) establish 'bivalent chromatin marks' at the silent AGAMOUS locus. Nucleic Acids Res **35:** 6290-6296

Saleh A, Alvarez-Venegas R, Yilmaz M, Le O, Hou G, Sadder M, Al-Abdallat A, Xia Y, Lu G, Ladunga I, Avramova Z (2008) The highly similar Arabidopsis homologs of trithorax ATX1 and ATX2 encode proteins with divergent biochemical functions. Plant Cell **20:** 568-579

Sanchez-Pulido L, Devos D, Sung ZR, Calonje M (2008) RAWUL: a new ubiquitin-like domain in PRC1 ring finger proteins that unveils putative plant and worm PRC1 orthologs. BMC Genomics **9:** 308

Schmidt A, Wohrmann HJ, Raissig MT, Arand J, Gheyselinck J, Gagliardini V, Heichinger C, Walter J, Grossniklaus U (2013) The Polycomb group protein MEDEA and the DNA methyltransferase MET1 interact to repress autonomous endosperm development in Arabidopsis. Plant J **73:** 776-787

Schmitges FW, Prusty AB, Faty M, Stutzer A, Lingaraju GM, Aiwazian J, Sack R, Hess D, Li L, Zhou S, Bunker RD, Wirth U, Bouwmeester T, Bauer A, Ly-Hartig N, Zhao K, Chan H, Gu J, Gut H, Fischle W, Muller J, Thoma NH (2011) Histone methylation by PRC2 is inhibited by active chromatin marks. Mol Cell **42:** 330-341

Schmitz RJ, Tamada Y, Doyle MR, Zhang X, Amasino RM (2009) Histone H2B deubiquitination is required for transcriptional activation of FLOWERING LOCUS C and for proper control of flowering in Arabidopsis. Plant Physiol **149:** 1196-1204

Schubert D, Primavesi L, Bishopp A, Roberts G, Doonan J, Jenuwein T, Goodrich J

(2006) Silencing by plant Polycomb-group genes requires dispersed trimethylation of histone H3 at lysine 27. The EMBO journal **25:** 4638-4649

Schuettengruber B, Chourrout D, Vervoort M, Leblanc B, Cavalli G (2007) Genome regulation by polycomb and trithorax proteins. Cell **128:** 735-45

Schuettengruber B, Martinez AM, Iovino N, Martinez AM, Iovino N, Cavalli G (2011) Trithorax group proteins: switching genes on and keeping them active. Nature reviews Molecular cell biology **12:** 799-814.

Scortecci K, Michaels SD, Amasino RM (2003) Genetic interactions between FLM and other flowering-time genes in Arabidopsis thaliana. Plant molecular biology **52:** 915-922

Shafiq S, Berr A, Shen WH (2014) Combinatorial functions of diverse histone methylations in Arabidopsis thaliana flowering time regulation. New Phytol **201:** 312-322

Sheldon CC, Hills MJ, Lister C, Dean C, Dennis ES, Peacock WJ (2008) Resetting of FLOWERING LOCUS C expression after epigenetic repression by vernalization. Proc Natl Acad Sci U S A **105:** 2214-2219

Shema-Yaacoby E, Nikolov M, Haj-Yahya M, Siman P, Allemand E, Yamaguchi Y, Muchardt C, Urlaub H, Brik A, Oren M, Fischle W (2013) Systematic identification of proteins binding to chromatin-embedded ubiquitylated H2B reveals recruitment of SWI/SNF to regulate transcription. Cell Rep **4:** 601-608

Shen L, Thong Z, Gong X, Shen Q, Gan Y, Yu H (2014) The putative PRC1 RING-finger protein AtRING1A regulates flowering through repressing MADS AFFECTING FLOWERING genes in Arabidopsis. Development **141:** 1303-1312

Shen WH, Xu L (2009) Chromatin remodeling in stem cell maintenance in Arabidopsis thaliana. Mol Plant **2:** 600-609

Shen W-H, Meyer D (2004) Ectopic expression of the NtSET1 histone methyltransferase inhibits cell expansion, and affects cell division and differentiation in tobacco plants. Plant and cell physiology **45:** 1715-1719

Shen Y, Conde ESN, Audonnet L, Servet C, Wei W, Zhou DX (2014) Over-expression

of histone H3K4 demethylase gene JMJ15 enhances salt tolerance in Arabidopsis. Front Plant Sci **5:** 290

Shi Y, Lan F, Matson C, Mulligan P, Whetstine JR, Cole PA, Casero RA, Shi Y (2004) Histone demethylation mediated by the nuclear amine oxidase homolog LSD1. Cell **119:** 941-953

Shilatifard A (2006) Chromatin modifications by methylation and ubiquitination: implications in the regulation of gene expression. Annu. Rev. Biochem. **75:** 243-269

Shilatifard A (2012) The COMPASS family of histone H3K4 methylases: mechanisms of regulation in development and disease pathogenesis. Annu Rev Biochem **81:** 65-95

Simon JA, Kingston RE (2013) Occupying chromatin: Polycomb mechanisms for getting to genomic targets, stopping transcriptional traffic, and staying put. Mol Cell **49:** 808-824

Song YH, Shim JS, Kinmonth-Schultz HA, Imaizumi T (2015) Photoperiodic flowering: time measurement mechanisms in leaves. Annu Rev Plant Biol **66:** 441-464

Song Z-T, Sun L, Lu S-J, Tian Y, Ding Y, Liu J-X (2015) Transcription factor interaction with COMPASS-like complex regulates histone H3K4 trimethylation for specific gene expression in plants. Proceedings of the National Academy of Sciences **112:** 2900-2905

Southall SM, Wong PS, Odho Z, Roe SM, Wilson JR (2009) Structural basis for the requirement of additional factors for MLL1 SET domain activity and recognition of epigenetic marks. Mol Cell **33:**181-91.

Spedaletti V, Polticelli F, Capodaglio V, Schininà ME, Stano P, Federico R, Tavladoraki P (2008) Characterization of a lysine-specific histone demethylase from Arabidopsis thaliana. Biochemistry **47:** 4936-4947

Sridhar VV, Kapoor A, Zhang K, Zhu J, Zhou T, Hasegawa PM, Bressan RA, Zhu JK (2007) Control of DNA methylation and heterochromatic silencing by histone H2B deubiquitination. Nature **447:** 735-738

Srikanth A, Schmid M (2011) Regulation of flowering time: all roads lead to Rome. Cell Mol Life Sci **68:** 2013-2037

Strahl BD, Allis CD (2000) The language of covalent histone modifications. Nature **403:** 41-45

Suganuma T, Workman JL (2008) Crosstalk among Histone Modifications. Cell **135:** 604-607

Sun Z-W, Allis CD (2002) Ubiquitination of histone H2B regulates H3 methylation and gene silencing in yeast. Nature **418:** 104-108

Sung S, Amasino RM (2004) Vernalization in Arabidopsis thaliana is mediated by the PHD finger protein VIN3. Nature **427:** 159-64

Sung S, Amasino RM (2005) Remembering winter: toward a molecular understanding of vernalization. Annu. Rev. Plant Biol. **56:** 491-508

Swiezewski S, Liu F, Magusin A, Dean C (2009) Cold-induced silencing by long antisense transcripts of an Arabidopsis Polycomb target. Nature **462:** 799-802

Tamada Y, Yun JY, Woo SC, Amasino RM (2009) ARABIDOPSIS TRITHORAX-RELATED7 is required for methylation of lysine 4 of histone H3 and for transcriptional activation of FLOWERING LOCUS C. Plant Cell **21:** 3257-3269

Tang X, Lim MH, Pelletier J, Tang M, Nguyen V, Keller WA, Tsang EW, Wang A, Rothstein SJ, Harada JJ, Cui Y (2012) Synergistic repression of the embryonic programme by SET DOMAIN GROUP 8 and EMBRYONIC FLOWER 2 in Arabidopsis seedlings. J Exp Bot **63:** 1391-1404

Teotia S, Tang G (2015) To bloom or not to bloom: role of microRNAs in plant flowering. Mol Plant **8:** 359-377

Thorstensen T, Grini PE, Mercy IS, Alm V, Erdal S, Aasland R, Aalen RB (2008) The Arabidopsis SET-domain protein ASHR3 is involved in stamen development and interacts with the bHLH transcription factor ABORTED MICROSPORES (AMS). Plant Mol Biol **66:** 47-59

Thorstensen T, Grini PE, Aalen RB (2011) SET domain proteins in plant development. Biochim Biophys Acta **1809:** 407-20

Trejo-Arellano MS, Mahrez W, Nakamura M, Moreno-Romero J, Nanni P, Kohler C, Hennig L (2017) H3K23me1 is an evolutionarily conserved histone modification associated with CG DNA methylation in Arabidopsis. Plant J **90:** 293-303

Tsukada YI, Fang J, Erdjument-Bromage H, Warren M E, Borchers CH, Tempst P, Zhang Y (2006) Histone demethylation by a family of JmjC domain-containing proteins. Nature **439:** 811-816

Tsukada Y, Ishitani T, Nakayama KI (2010) KDM7 is a dual demethylase for histone H3 Lys 9 and Lys 27 and functions in brain development. Genes Dev **24:** 432-437

Turck F, Fornara F, Coupland G. (2008) Regulation and identity of florigen: FLOWERING LOCUS T moves center stage. Annual review of plant biology **59:** 573-594

Turck F, Roudier F, Farrona S, Martin-Magniette M-L, Guillaume E, Buisine N, Gagnot S, Martienssen RA, Coupland G, Colot V (2007) Arabidopsis TFL2/LHP1 Specifically Associates with Genes Marked by Trimethylation of Histone H3 Lysine 27. PLoS Genetics **preprint:** e86

Turner BM (2000) Histone acetylation and an epigenetic code. Bioessays **22:** 836-845

Venkatesh S, Workman JL. (2013) Set2 mediated H3 lysine 36 methylation: regulation of transcription elongation and implications in organismal development. Developmental biology **2:** 685-700

Voutsadakis IA (2010) Ubiquitin, ubiquitination and the ubiquitin-proteasome system in cancer. Atlas of Genetics and Cytogenetics in Oncology and Haematology

Wagner EJ, Carpenter PB (2012) Understanding the language of Lys36 methylation at histone H3. Nat Rev Mol Cell Biol **13:** 115-126

Wang J, Meng X, Yuan C, Harrison AP, Chen M (2015) The roles of cross-talk epigenetic patterns in Arabidopsis thaliana. Brief Funct Genomics **15:** 278-287

Wang L, Brown JL, Cao R, Zhang Y, Kassis JA, Jones RS (2004) Hierarchical recruitment of polycomb group silencing complexes. Mol Cell **14:** 637-646

Wang Q, Sajja U, Rosloski S, Humphrey T, Kim MC, Bomblies K, Weigel D, Grbic V (2007) HUA2 caused natural variation in shoot morphology of A. thaliana. Curr Biol **17:**1513-9

Wang S, Cao L, Wang H (2016) Arabidopsis ubiquitin-conjugating enzyme UBC22 is required for female gametophyte development and likely involved in Lys11-linked ubiquitination. J Exp Bot **67:** 3277-3288

Wang X, Chen J, Xie Z, Liu S, Nolan T, Ye H, Zhang M, Guo H, Schnable PS, Li Z, Yin

Y (2014) Histone lysine methyltransferase SDG8 is involved in brassinosteroid-regulated gene expression in Arabidopsis thaliana. Mol Plant **7:** 1303-1315

Weake VM, Workman JL (2008) Histone ubiquitination: triggering gene activity. Mol Cell **29:** 653-663

Wen H, Li Y, Xi Y, Jiang S, Stratton S, Peng D, Tanaka K, Ren Y, Xia Z, Wu J, Li B, Barton MC, Li W, Li H, Shi X (2014) ZMYND11 links histone H3.3K36me3 to transcription elongation and tumour suppression. Nature **508:** 263-268

Wood A, Krogan NJ, Dover J, Schneider J, Heidt J, Boateng MA, Dean K, Golshani A, Zhang Y, Greenblatt JF (2003) Bre1, an E3 ubiquitin ligase required for recruitment and substrate selection of Rad6 at a promoter. Molecular cell **11:** 267-274

Wood CC, Robertson M, Tanner G, Peacock WJ, Dennis ES, Helliwell CA (2006) The Arabidopsis thaliana vernalization response requires a polycomb-like protein complex that also includes VERNALIZATION INSENSITIVE 3. Proc Natl Acad Sci U S A **103:** 14631-14636

Wu L, Lee SY, Zhou B, Nguyen UT, Muir TW, Tan S, Dou Y (2013) ASH2L regulates ubiquitylation signaling to MLL: trans-regulation of H3 K4 methylation in higher eukaryotes. Mol Cell **49:** 1108-1120

Wyce A, Henry KW, Berger SL (2004) H2B ubiquitylation and de-ubiquitylation in gene activation. *In* Novartis Foundation symposium. Chichester; New York; John Wiley; 1999, pp 63-77

Wyce A, Xiao T, Whelan KA, Kosman C, Walter W, Eick D, Hughes TR, Krogan NJ, Strahl BD, Berger SL (2007) H2B ubiquitylation acts as a barrier to Ctk1 nucleosomal recruitment prior to removal by Ubp8 within a SAGA-related complex. Mol Cell **27:** 275-288

Xia S, Cheng YT, Huang S, Win J, Soards A, Jinn TL, Jones JD, Kamoun S, Chen S, Zhang Y, Li X (2013) Regulation of transcription of nucleotide-binding leucine-rich repeat-encoding genes SNC1 and RPP4 via H3K4 trimethylation. Plant Physiol **162:** 1694-1705

Xiao J, Lee US, Wagner D (2016) Tug of war: adding and removing histone lysine

methylation in Arabidopsis. Curr Opin Plant Biol **34:** 41-53

Xiao J, Wagner D (2015) Polycomb repression in the regulation of growth and development in Arabidopsis. Current opinion in plant biology **23:** 15-24

Xu L, Menard R, Berr A, Fuchs J, Cognat V, Meyer D, Shen WH (2009) The E2 ubiquitin-conjugating enzymes, AtUBC1 and AtUBC2, play redundant roles and are involved in activation of FLC expression and repression of flowering in Arabidopsis thaliana. Plant J **57:** 279-288

Xu L, Shen WH (2008) Polycomb silencing of KNOX genes confines shoot stem cell niches in Arabidopsis. Curr Biol **18:** 1966-1971

Xu L, Zhao Z, Dong A, Soubigou-Taconnat L, Renou JP, Steinmetz A, Shen WH (2008) Di- and tri- but not monomethylation on histone H3 lysine 36 marks active transcription of genes involved in flowering time regulation and other processes in Arabidopsis thaliana. Mol Cell Biol **28:** 1348-1360

Xu Y, Gan ES, Zhou J, Wee WY, Zhang X, Ito T (2014) Arabidopsis MRG domain proteins bridge two histone modifications to elevate expression of flowering genes. Nucleic Acids Res **42:** 10960-10974

Yan N, Doelling JH, Falbel TG, Durski AM, Vierstra RD (2000) The ubiquitin-specific protease family from Arabidopsis. AtUBP1 and 2 are required for the resistance to the amino acid analog canavanine. Plant physiology **124:** 1828-1843

Yan Y, Shen L, Chen Y, Bao S, Thong Z, Yu H (2014) A MYB-domain protein EFM mediates flowering responses to environmental cues in Arabidopsis. Dev Cell **30:** 437-448

Yang C, Bratzel F, Hohmann N, Koch M, Turck F, Calonje M (2013) VAL- and AtBMI1-mediated H2Aub initiate the switch from embryonic to postgerminative growth in Arabidopsis. Curr Biol **23:** 1324-1329

Yang H, Mo H, Fan D, Cao Y, Cui S, Ma L (2012a) Overexpression of a histone H3K4 demethylase, JMJ15, accelerates flowering time in Arabidopsis. Plant cell reports **31:** 1297-1308

Yang H, Han Z, Cao Y, Fan D, Li H, Mo H, Feng Y, Liu L, Wang Z, Yue Y, Cui S, Chen S, Chai J, Ma L (2012b) A companion cell-dominant and developmentally regulated

H3K4 demethylase controls flowering time in Arabidopsis via the repression of FLC expression. PLoS Genet **8:** e1002664

Yang H, Howard M, Dean C (2014) Antagonistic roles for H3K36me3 and H3K27me3 in the cold-induced epigenetic switch at Arabidopsis FLC. Curr Biol **24:** 1793-1797

Yao B, Christian KM, He C, Jin P, Ming GL, Song H (2016) Epigenetic mechanisms in neurogenesis. Nat Rev Neurosci **17:** 537-549

Yao X, Feng H, Yu Y, Dong A, Shen WH (2013) SDG2-mediated H3K4 methylation is required for proper Arabidopsis root growth and development. PLoS One **8:** e56537

Yao X, Shen W (2011) Crucial function of histone lysine methylation in plant reproduction. Chinese Science Bulletin **56:** 3493-3499

Yoo SK, Chung KS, Kim J, Lee JH, Hong SM, Yoo SJ, Yoo SY, Lee JS, Ahn JH (2005) CONSTANS activates SUPPRESSOR OF OVEREXPRESSION OF CONSTANS 1 through FLOWERING LOCUS T to promote flowering in Arabidopsis. Plant physiology **139:** 770-778

Young NL, DiMaggio PA, Plazas-Mayorca MD, Baliban RC, Floudas CA, Garcia BA (2009) High throughput characterization of combinatorial histone codes. Molecular & Cellular Proteomics **8:** 2266-2284

Yuan W, Xu M, Huang C, Liu N, Chen S, Zhu B (2011) H3K36 methylation antagonizes PRC2-mediated H3K27 methylation. J Biol Chem **286:** 7983-7989

Yun M, Wu J, Workman JL, Li B (2011) Readers of histone modifications. Cell Res **21:** 564-578

Zhang S, Zhou B, Kang Y, Cui X, Liu A, Deleris A, Greenberg MV, Cui X, Qiu Q, Lu F, Wohlschlegel JA, Jacobsen SE, Cao X (2015) C-terminal domains of a histone demethylase interact with a pair of transcription factors and mediate specific chromatin association. Cell Discov **1**

Zhang T, Cooper S, Brockdorff N (2015) The interplay of histone modifications - writers that read. EMBO Rep **16:** 1467-1481

Zhang X, Clarenz O, Cokus S, Bernatavichute YV, Pellegrini M, Goodrich J, Jacobsen SE (2007) Whole-genome analysis of histone H3 lysine 27 trimethylation in Arabidopsis. PLoS Biol **5:** e129

Zhang Y (2003) Transcriptional regulation by histone ubiquitination and deubiquitination. Genes Dev **17:** 2733-2740

Zhao M, Yang S, Liu X, Wu K (2015) Arabidopsis histone demethylases LDL1 and LDL2 control primary seed dormancy by regulating DELAY OF GERMINATION 1 and ABA signaling-related genes. Front Plant Sci **6:** 159

Zhao W, Shafiq S, Berr A, Shen W-H (2015) Genome-wide gene expression profiling to investigate molecular phenotypes of Arabidopsis mutants deprived in distinct histone methyltransferases and demethylases. Genomics Data **4:** 143-145

Zhao Z, Yu Y, Meyer D, Wu C, Shen W-H (2005) Prevention of early flowering by expression of FLOWERING LOCUS C requires methylation of histone H3 K36. Nature cell biology **7:** 1256-1260.

Zhou Y, Hartwig B, James GV, Schneeberger K, Turck F (2015) Complementary Activities of TELOMERE REPEAT BINDING Proteins and Polycomb Group Complexes in Transcriptional Regulation of Target Genes. Plant Cell **28:** 87-101

Zhu B, Zheng Y, Pham AD, Mandal SS, Erdjument-Bromage H, Tempst P, Reinberg D (2005) Monoubiquitination of human histone H2B: the factors involved and their roles in HOX gene regulation. Mol Cell **20:** 601-611

Zou B, Yang DL, Shi Z, Dong H, Hua J (2014) Monoubiquitination of histone 2B at the disease resistance gene locus regulates its expression and impacts immune responses in Arabidopsis. Plant Physiol **165:** 309-318

ABBREVIATIONS

AP	Ammonium persulfate
ATP	Adenosine Triphosphate
Amp	Ampicillin
bp	base pair
cm	centimeter
Col	Columbia
ChIP	Chromatin Immunoprecipitation
Da	Dalton
DAPI	4, 6-diamidino-2-phenylindole
DAS	Days After Stratification
DNA	DeoxyriboNucleic Acid
DTT	dithiothreitol
EDTA	Ethylene Diamine Tetraacetic Acid
GST	Glutathione-S-Transferase
g	gram
h	hour
His	histidine
Kana	Kanamycin
kb	kilo base pairs
LD	Long Day
µ	micro
M	Molar (mole/ liter)
MD	Medium Day
min	minutes
MS	Murashige and Skoog
MW	molecular weight
nm	nanometer
OD_{600}	Optical Density, measured at 600 nm
PAGE	PolyAcrylamide Gel Electrophoresis

PBS	Phosphate Buffer Saline
PCR	Polymerase Chain Reaction
PI	Propidium Iodide
PMSF	Phenyl Methyl Sulphony Fluoride
PVDF	PolyVinylidene DiFluoride
qPCR	quantitative Polymerase Chain Reaction
RNA	RiboNucleic Acid
rpm	rotations per minute
RT	room temperature
RT PCR	Reverse Transcription Polymerase Chain Reaction
SD	Short Day
SDS	Sodium Dodecyl Sulphate
T-DNA	Transfer-DNA
TE	Tris-EDTA buffer
TEMED	N, N, N', N'-tetramethyl-ethylenediamine. 1,2-diamine
Tris	Tris(hydroxymethyl) aminomethane
TTBS	Triton-Tris Buffer Saline
Ub	ubiquitin

Caractérisation moléculaire et fonctionnelle des gènes impliqués dans la mise en place et la lecture de la méthylation d'histones chez l'*Arabidopsis thaliana*

Chez les eucaryotes, l'ADN nucléaire contenant l'information génétique s'assemble avec des protéines de type histones pour former la chromatine. D'une part, le compactage de la chromatine protège l'ADN des dommages, mais d'autre part cette structure empêche également l'accès des enzymes impliquées dans la transcription des gènes. Par conséquent, plusieurs mécanismes ont évolué pour moduler dynamiquement la structure de la chromatine afin de réguler correctement l'expression génique, constituant ainsi un niveau supplémentaire de contrôle. Parmi divers processus, le remodelage de la chromatine est possible au travers d'une pléthore de modifications covalentes post-traductionnelles des histones, comprenant l'acétylation, la méthylation, la phosphorylation, l'ubiquitinylation, et d'autres encore. Comparé à l'acétylation qui modifie la charge et donc l'interaction entre les histones et l'ADN, la méthylation des histones ne provoque pas en soi de changement direct de la structure chromatinienne, mais nécessite des « lecteurs » spécifiques qui reconnaîtront le signal de méthylation et l'interpréteront. Chez Arabidopsis, peu de choses sont actuellement connues sur ces lecteurs de méthylation des histones, et en particulier sur les domaines protéiques impliqués dans cette liaison ainsi que sur leur spécificité. Dans la première partie de ma thèse, je vais décrire mes résultats sur un groupe récemment identifié de lecteurs de méthylation d'histone avec une attention particulière pour l'affinité de liaison de leur domaine PWWP. De plus, la méthylation des histones n'agit pas seule mais en association avec d'autres marques d'histones pour définir différents états chromatiniens tout au long du génome. Ceci est particulièrement vrai lors de la transcription. En effet, le modèle actuel de transcription active est construit autour d'une chronologie précise de modifications d'histones. De manière simplifiée, la monoubiquitination de l'histone H2B (H2Bub1) se produit en premier, permettant ensuite la triméthylation de l'histone H3 sur la lysine 4 (H3K4me3) et l'initiation de la transcription. Enfin, H2Bub1 est éliminé permettant à la triméthylation de H3K36 (H3K36me3) de se produire en début d'élongation. Bien que chez les animaux et la levure le modèle décrit ci-dessus soit bien documenté, chez les plantes, beaucoup moins d'informations sont disponibles et les quelques études ont été principalement concentrées sur la relation fonctionnelle entre H2Bub1 et

H3K4me3. Afin de combler cette lacune, j'explorerais, dans une deuxième partie, l'interaction fonctionnelle entre H2Bub1 et H3K36me3 en utilisant une approche génétique basée sur des croisements entre différents mutants d'enzymes de modification les histones. Parmi les enzymes modifiant les histones, la superfamille de protéines du groupe à domaine SET (SDG) comprend des protéines connues pour méthyler les histones sur différents résidus de lysine. Au sein de cette grande famille, nous savons que les protéines du groupe Trithorax (TrxG), conservées chez la plupart des eukaryotes, sont à l'origine de la méthylation de H3K4 et / ou H3K36 permettant de favoriser la transcription en réponse à divers signaux développementaux et environnementaux. Chez Arabidopsis, le groupe TrxG a été impliqué dans le contrôle de plusieurs processus fondamentaux et comprend environ 12 membres, dont moins de la moitié a été fonctionnellement caractérisée. La méthyltransférase SDG27 / ATX1 et la H3K4 méthyltransférase SDG8 sont les plus étudiées. Dans la dernière partie de ma thèse, je décrirais un homologue d'ATX1 et SDG8 nommé SDG7 et je démontrerais son rôle fondamental dans le contrôle du processus de vernalisation.

HUA2 et HULK2, des lecteurs de H3K36 methylée

Précédemment, HULK2 (HUA2-LIKE 2) a été identifié dans l'équipe comme un partenaire protéique potentiel de SDG8 par la technique de double hybride chez la levure. HULK2 contient un domaine PWWP conservé connu pour lier indifféremment des histones méthylées ou non méthylées chez l'animal. Chez Arabidopsis, les protéines de domaine PWWP HUA2 (AGENT DE AG-4 2) et HULK2 ont été récemment impliquées dans la régulation de la floraison, cependant, le(s) rôle(s) de leur domaine PWWP n'a pas été exploré(s) (Jali et al., 2014). Malgré l'impossibilité de démontrer l'interaction observée chez la levure à l'aide d'autres méthodes, mon travail s'est focalisé dans un premier temps à tester l'affinité de liaison du domaine PWWP à différentes histones modifiées. Les protéines de fusion marquées HUA2-PWWP et HULK2-PWWP ont été purifiées et incubées séparément avec les peptides histones modifiés synthétiques H3K4me1, H3K4me2, H3K4me3 ainsi que H3K36me1, H3K36me2 et H3K36me3. Ensuite, par western blot, j'ai pu démontrer la liaison des protéines de fusion His-HUA2-PWWP et His-HULK2-PWWP spécifiquement aux peptides H3K36me1/me2/me3, et non aux peptides H3K4me1/2/3. Afin d'explorer davantage cette liaison, j'ai déterminé la structure

cristalline du domaine HUA2 PWWP d'Arabidopsis. Ce domaine contient un pli de type tonneau ß (ß-barrel) formé par quatre brins anti-parallèles (β1-β4) très conservé chez les plantes, les animaux et la levure. Parce que SDG8 est la principale méthyltransférase d'H3K36 chez Arabidopsis (Zhao et al., 2005) et parce que son mutant présente un phénotype de floraison précoce tout comme le mutant *hua2*, j'ai ensuite généré le double mutant *sdg8 hua2* et caractérisé son phénotype. Alors que le double mutant *sdg8 hua2* présente une taille réduite par rapport aux mutants simples, sa floraison est comprise entre celles de *sdg8* et de *hua2*. Afin d'explorer davantage ce phénotype de floraison, les niveaux de transcription de plusieurs gènes de floraison ont ensuite été analysés par PCR quantitative. De manière intéressante, le niveau d'ARNm de *FLC* apparait similaire entre les mutants simples et doubles indiquant une redondance fonctionnelle entre *SDG8* et *HUA2*. Plus en aval le long de la voie génétique de régulation de la floraison, le niveau de transcription de *FT* dans le double mutant est lui exactement entre celui observé chez *sdg8* et *hua2*, indiquant qu'à ce niveau, *SDG8* et *HUA2* régulent *FT* indépendamment. Dans son ensemble, cette partie de ma thèse indique que, au moins pour *FLC*, *SDG8* et *HUA2* peuvent interagir génétiquement pour réguler la transcription génique.

Collaboration entre histone méthylation et monoubiquitination lors de la transcription

Afin de déterminer si la méthylation de H3K36 et la monoubiquitination d'H2B interagissent fonctionnellement lors de la transcription, j'ai testé une éventuelle interaction génétique entre le mutant *sdg8* et un mutant défectueux dans l'H2Bub1, *hub1-3* et *hub2-2* (Fleury et al., 2007). Après avoir été généré par croisements, les phénotypes du double mutant ont été soigneusement analysés. En général, par rapport à chaque mutant simple, le double mutant présente un phénotype accentué, les plantes étant plus petites et la floraison se produisant plus tôt dans toutes les conditions de photopériode testées. Par western blot, j'ai également observé que les niveaux globaux de méthylation d'H3K36 et d'H2Bub1 dans le double mutant étaient similaires à ceux observés chez *sdg8* et chez *hub2*, respectivement. Cependant, une augmentation significative du niveau global de la marque répressive H3K27me3 n'a été détectée que chez le double mutant, suggérant que SDG8 et HUB2 pourraient ensemble limiter la propagation de cette marque répressive. L'analyse de la croissance du double mutant indique de plus que SDG8 et HUB2 agissent en grande

partie de manière synergique dans la régulation de la taille des organes de la plante. La floraison précoce étant le phénotype le plus évident de mon double mutant, j'ai ensuite concentré mes analyses moléculaires sur plusieurs gènes de floraison, tels que les répresseurs de floraison *FLC*, *MAF1*/*FLM*, *MAF2*, *MAF3*, *MAF4* et *MAF5* ainsi que les activateurs de floraison *FT* et *SOC1*. Par rapport au control sauvage, mes analyses de RT-PCR quantitative indiquent que chez *sdg8*, et comme précédemment publié (Zhao et al., 2005), les niveaux de transcription de *MAF2* et *MAF3* demeurent inchangés, tandis que ceux de *FLC*, *MAF1*, *MAF4* et *MAF5* sont drastiquement diminués et de *FT* et *SOC1* sont augmentés. Chez *hub2*, le niveau de transcription de *MAF4* et *MAF5* est lui considérablement réduit, alors qu'il est augmenté pour *FT*. Fait intéressant, le niveau de transcription de *FT* est également augmenté chez le double mutant *sdg8 hub2* à un niveau compris entre celui de *sdg8* et celui de *hub2*. Ensuite, j'ai utilisé la technique d'immunoprécipitation de la chromatine (ChIP) pour adresser la question de l'état chromatinien des gènes *FLC*, *MAF4*, *MAF5*, *FT* et *SOC1* à l'aide d'anticorps anti-H3, -H3K4me3, -H3K36me3 et -H3K27me3 et d'amorces couvrant la majeure partie de leurs unités de transcription. En général, les profils observés chez le double mutant apparaissent similaires à ceux observés pour H3K4me3 chez *hub2* et H2Bub1 chez *sdg8* et *hub2*. Spécifiquement pour *FLC*, le niveau d'H3K36me3 chez *sdg8 hub2* est diminué de manière additive par rapport aux diminutions observées chez *sdg8* et *hub2*, ce qui indique que pour ce gène, la méthylation d'H3K36 pourrait être mise en place à la fois de manière dépendante et indépendante d'H2Bub1. De plus, alors que le niveau d'H3K4me3 est diminué chez *hub2* et inchangé chez *sdg8*, H3K36me3 et H2Bub1 sont diminués de manière identique chez *sdg8*, *hub2* et *sdg8 hub2* chez tous les autres gènes étudiés à l'exception de *FT*. En effet, *FT* semble être moins sous le control de variations au niveau de sa chromatine que les autres gènes de floraison analysés, les niveaux de H3K4me3 et H3K36me3 étant beaucoup plus faibles et de H2Bub presque absents. L'ensemble de mes données de ChIP indiquent que, comme chez l'animal, H3K4me3 dépend entièrement de H2Bub1. Cependant, contrairement au modèle animal et à la levure, il n'y a pas de corrélation exclusive entre H3K36me3 et H2Bub1, rendant impossible d'établir une dépendance hiérarchique claire. Par conséquent, il semble que SDG8 et HUB2 soient capable de se promouvoir mutuellement dans l'établissement d'un état chromatinien actif.

SDG7, une méthyltransferase atypique chez Arabidopsis

La vernisation est un processus par lequel l'exposition prolongées à des températures froides accélère la floraison dans de nombreuses espèces végétales. Chez Arabidopsis, la vernalisation est initiée par l'induction de VERNALISATION INSENSITIVE3 (VIN3) lors de l'exposition au froid. VIN3 forme un complexe avec le Complexe Répressif Polycomb 2 (PRC2) et est nécessaire pour que le PRC2 puisse induire l'extinction épigénétique de *FLC* suite au dépôt de la marque d'histone répressive H3K27me3 sur la chromatine de *FLC*. Cependant, la façon dont l'exposition au froid conduit à l'induction du *VIN3* est encore largement inconnue. En collaboration avec le laboratoire du Dr Richard Amasino, nous avons montré que SET DOMAIN GROUP 7 (SDG7) est nécessaire au bon déroulement de l'induction de *VIN3* et du processus de vernalisation. Des données génétiques et moléculaires nous ont permis de démontrer que la mutation de SDG7 entraîne une réaction de vernalisation plus rapide que chez le contrôle sauvage, voir même un état partiellement vernalisé sans exposition au froid, impliquant SDG7 comme régulateur négatif de la vernalisation. Par western blot, j'ai ainsi observé que les niveaux de différentes marques de méthylation des histones étaient inchangés chez le mutant *sdg7*. De plus, la mesure de l'activité méthyltransférase in vitro nous a permis de démontrer que la protéine SDG7 recombinante est incapable de méthyler les histones. Dans leur ensemble, nos résultats indiquent que SDG7 pourrait méthyler une protéine non histone encore inconnue dans la régulation de la transcription et le contrôle de la durée de l'exposition au froid nécessaire au processus de vernalisation (Lee et al., 2015).

Dans leur ensemble, les résultats de mon travail de thèse ont permis de réaliser des progrès significatifs de notre compréhension des mécanismes moléculaires de dépôt et de lecture des marques de méthylation d'histone lors de la transcription et de la régulation du développement des plantes. En mettant l'accent sur la famille TrxG, mon travail a également permis de démontrer que les connexions entre les marques d'histones chez Arabidopsis sont nombreuses, variées et extrêmement sophistiquées, rendant difficile, sinon impossible, d'établir un réseau fonctionnel simple avec des interconnexions hiérarchiques claires. Une telle complexité peut parfaitement refléter un certain degré de flexibilité, ce qui est conforme au concept de modularité et de plasticité du développement des plantes.

In eukaryotes, nuclear DNA containing the genetic information assembles with histone proteins to form chromatin. On the one hand, the chromatin compaction protects DNA from damage, but on the other hand this structure also impedes the access of enzymes involved in gene transcription. Therefore, several mechanisms have evolved to dynamically modulate the chromatin structure in order to properly regulate gene expression, thus providing an extra layer of control. Among other processes, chromatin remodeling is exercised through a plethora of covalent post-translational modifications of histone proteins, including acetylation, methylation, phosphorylation, ubiquitinylation, and others. Compare to acetylation that modifies the charge and thus the interaction between histone and DNA, histone methylation does not *per se* directly trigger changes in the chromatin structure but it requires specific "readers" that will recognize the methylation signal and interpret it. In *Arabidopsis*, little is currently known about histone methylation readers, and especially regarding the domains involved in this binding as well as their specificity. In the first part of my thesis, I will describe my results on a recently identified group of histone methylation readers with a particular attention to the binding affinity of their PWWP domain. Also, histone methylation does not act alone but in combination with other histone marks to define different chromatin states throughout the entire genome. This is particularly true during transcription. Indeed, the actual model of active transcription is built around a precise chronology of histone modifications. In a simplified way, histone H2B monoubiquitination (H2Bub1) first occurs, allowing histone H3 lysine 4 trimethylation (H3K4me3) and transcription initiation. Latter, H2Bub is removed enabling H3K36me3 to occur at the onset of elongation. While in animal and yeast, the above described model is well documented, in plants, considerably less is known and studies were mainly concentrated on studying the functional relationship between H2Bub and H3K4me3. In order to fill this shortfall, I will explore, in the second part of my thesis, the functional interaction between H2Bub and H3K36me3 using a genetic approach based on crosses between different histone-modifying enzyme mutants. Among histone-modifying enzymes, the SET-domain group (SDG) protein superfamily includes proteins known to methylate histones on lysine residues. Within this large family, the evolutionarily conserved Trithorax group (TrxG) proteins are known to mediate methylation on H3K4 and/or H3K36 in order to promote transcription in response to diverse developmental and environmental cues. In *Arabidopsis*, the TrxG group was involved in the control of multiple fundamental processes and comprises

around 12 members, with less than half being functionally characterized. The H3K4 methyltransferase SDG27/ATX1 and the H3K36 methyltransferase SDG8 are the most studied. In the last part of my thesis, I will describe a homologue of ATX1 and SDG8 named SDG7 and demonstrate its fundamental role in the proper timing of the vernalization process.

HUA2 and HULK2 function as H3K36 methylation readers

Previously in the team, HULK2 (HUA2-LIKE 2) was identified as a prey using a yeast two-hybrid system screen with SDG8 as the bait protein. HULK2 contain a conserved PWWP domain known to indifferently bind methylated/unmethylated histones in animal. In Arabidopsis, the PWWP domain proteins *HUA2 (ENHANCER OF AG-4 2)* and *HULK2* have been reported to regulate flowering time, however, their PWWP domain was not explored (Jali et al., 2014). Firstly, despite that it was not possible to demonstrate the interaction observed in yeast using other methods, my work aims at testing the binding affinity of the PWWP domain to modified histones. The His tagged HUA2-PWWP and HULK2-PWWP fusion proteins were purified and separately incubated with synthetic modified histone peptides H3K4me1, H3K4me2, H3K4me3 as well as H3K36me1, H3K36me2 and H3K36me3. Using western blots analysis, I demonstrated the binding of the His-HUA2-PWWP and His-HULK2-PWWP fusion proteins specifically to H3K36me1/me2/me3 peptides, and not H3K4me1/2/3 ones. To further explore this binding, we determined the crystal structure of the plant HUA2 PWWP domain. This domain contains aβ-barrel-like fold formed by four anti-parallelβ-strands (β1–β4) and appeared highly conserved among plant, animal and yeast. Because SDG8 is the major H3K36 methyltransferase in *Arabidopsis* (Zhao et al., 2005) and because its corresponding mutant is early flowering like the *hua2* mutant, I next generated the *sdg8 hua2* double mutant and characterized its phenotype. While the *sdg8 hua2* double mutant showed a reduced size as compared to single mutants, flowering time was in between *sdg8* and *hua2*. To further explore this flowering phenotype, the transcript level of several flowering genes was analyzed using quantitative PCR. Interestingly, the *FLC* mRNA level was similar between both single and double mutants indicating a redundancy between SDG8 and HUA2. More downstream along the flowering genetic pathway, the *FT* transcript level in the double mutant was in between the one observed in sdg8 and hua2 single mutants indicating that at this level SDG8 and HUA2 regulate *FT* independently. Together my work

indicates that, at least for *FLC*, SDG8 and HUA2 may functionally interact to regulate gene transcription.

Crosstalk between histone methylation and monoubiquitination during transcription

In order to unravel how H3K36 methylation and H2Bub1 are functionally connected in the course of transcription, I tested the genetic interaction between the *sdg8* mutant and a mutant defective in H2Bub1, *hub1-3* and *hub2-2* (Fleury et al., 2007). After being generated by crosses, the phenotype of the double mutant was thoroughly analyzed. In general, compared to each single mutant, the double mutant displayed an enhanced phenotype, with plants being smaller and flowering occurring earlier under all tested photoperiod conditions. Using western blot, I further observed that the global level of H3K36 methylation and H2Bub1 in the double mutant were similar as in *sdg8* and *hub2* single ones, respectively. However, a significant increase in the global level of the H3K27me3 repressive mark was only detected in the double mutant, thus suggesting that *SDG8* and *HUB2* might together limit the spread of this repressive mark. Analyses of the plant growth phenotype indicate that *SDG8* and *HUB2* act largely in a synergistic manner in the regulation of plant body and organ size. Because early flowering was the most obvious phenotype of my different mutant I next focus my molecular analyses on several flowering genes including the flowering repressor *FLC, MAF1/FLM, MAF2, MAF3, MAF4* and *MAF5* as well as the flowering activator *FT* and *SOC1.* My quantitative RT-PCR analysis indicate that in *sdg8* and as previously published, the transcript level of *MAF2* and *MAF3* remained unchanged, while the *FLC, MAF1, MAF4,* and *MAF5* transcript levels were drastically decreased, and *FT* and *SOC1* transcript levels were increased as compared to the wild-type. In *hub2*, the transcript level of *MAF4* and *MAF5* was significantly reduced, while it was increased for *FT*. Interestingly, the transcript level of *FT* was increased in *sdg8 hub2* double mutant compared to single ones to a level in between the ones observed in *sdg8* and *hub2* single mutants. Next, I used Chromatin Immuno Precipitation (ChIP) to address the question of the chromatin state of these genes using antibodies for H3, H3K4me3, H3K36me3 and H3K27me3 and primers covering *FLC*, *MAF4*, *MAF5*, *FT* and *SOC1* genes. In general, profiles observed in the double mutant were similar to the ones observed for H3K4me3 in *hub2* and H2Bub1 in *sdg8* and *hub2*. Specifically for *FLC*, the level of H3K36me3 in *sdg8 hub2* was additively decreased from *sdg8* and

hub2, indicating that for this gene, H3K36 methylation might present both a dependent and independent loading from H2Bub1. Also, while H3K4me3 was decreased in *hub2* and unchanged in *sdg8*, H3K36me3 and H2Bub1 were similarly decreased between *sdg8*, *hub2* and *sdg8 hub2* at all other genes except *FT*. Indeed, *FT* seems to be regulated slightly differently from the other analyzed flowering genes as levels of H3K4me3 and H3K36me3 were lower and H2Bub was almost absent. Together, my ChIP data indicate that like in animal H3K4me3 is fully dependent on the loading of H2Bub1. However, and in contrast with animal and yeast models, there is not a fully exclusive correlation between H3K36me3 and H2Bub1 as it was not possible to clearly establish a hierarchical dependency. Therefore, *SDG8* and *HUB2* might mutually favor each other in establishing an active chromatin state.

SDG7, an atypical methyltransferase in Arabidopsis

Vernalization is a process by which exposure to prolonged cold temperatures accelerates of flowering in many plant species. In Arabidopsis, vernalization is initiated by the induction of VERNALIZATION INSENSITIVE3 (VIN3) upon cold exposure. VIN3 forms a complex with Polycomb Repressive Complex 2 (PRC2) and is necessary for PRC2 to mediate the epigenetic silencing of *FLC* through the deposition of the repressive histone mark H3K27me3 at *FLC* chromatin. However, how cold exposure leads to the induction of *VIN3* is largely unknown. In collaboration with the laboratory of Dr. Richard Amasino, we showed that *SET DOMAIN GROUP 7* (*SDG7*) is required for proper timing of *VIN3* induction and duration of the vernalization process. Genetic and molecular data demonstrated that the *SDG7* loss-of-function mutant results in a more rapid vernalization response or even creates a partially vernalized state without cold exposure, implying SDG7 as a negative regulator of vernalization. Using western blot analyses, I showed that levels of different histone methylation marks remain unchanged in *sdg7* mutant plants. Furthermore, recombinant SDG7 protein could not methylate histones in in vitro histone methyltransferase assays. Taken together, our results indicate that SDG7 might methylate a yet unknown non-histone protein in regulation of transcription and proper measurement of the duration of cold exposure in the vernalization process (Lee et al., 2015).

As a whole, results from my thesis work contribute to significant progresses of our understanding on molecular mechanisms about deposition and reading of histone

methylation marks in transcription and regulation of plant development. By focusing on the TrxG family, my work also has demonstrated that connections between histone marks in Arabidopsis are numerous, varied and extremely sophisticated, rendering difficult, if not impossible, to establish a simple functional network with clear hierarchical interconnections. Such complexity might reflect a certain degree of flexibility, which is in line with the modular concept of plant developmental plasticity.

Wei ZHAO

Caractérisation moléculaire et fonctionnelle des gènes impliqués dans la mise en place et la lecture de la méthylation d'histones chez l'*Arabidopsis thaliana*

Résumé

La méthylation des histones constitue un niveau important de contrôle épigénétique chez les eucaryotes. Mes études portent sur la caractérisation des facteurs potentiellement intervenant dans la mise en place et la lecture de la méthylation pour mieux apprécier son rôle et des mécanismes sous-jacents dans la régulation de la transcription et du développement des plantes chez l'*Arabidopsis thaliana*. Ainsi, la première partie de mes travaux de thèse a contribué à l'étude d'une protéine à domaine SET (SET DOMAIN GROUP7, SDG7) et à montrer que SDG7 est nécessaire au bon déroulement de l'induction de *VIN3* et du processus de vernalisation pour la floraison. Nos résultats suggèrent que SDG7 pourrait méthyler une protéine non-histone encore inconnue dans la régulation de la transcription et le contrôle de la durée de vernalisation. La deuxième partie de ma thèse porte sur l'étude de SDG8 et les H2B-UBIQUITIN-ligases HUB1/HUB2 pour examiner un cross-talk éventuel entre la triméthylation de H3K36 (H3K36me3) et la monoubiquitination d'H2B (H2Bub1). Nous avons montré que H3K36me3 et H2Bub1 sont déposés largement indépendamment, qui diffère d'une dépendance hiérarchique de déposition préalablement observée chez la levure. La dernière partie de ma thèse a permis l'identification des protéines HUA2/HULK2 à domaine PWWP comme lecteurs éventuels de H3K36me3 dans la régulation de la floraison et du développement des plantes.

Mots clés: Epigénétique, Chromatine, Modification d'histones, Transcription, Floraison, Arabidopsis.

Résumé en anglais

Histone methylation is one of the keys epigenetic marks evolutionarily conserved in eukaryotes. My study focuses on the characterization of factors potentially involved in the deposition and reading of lysine (K) methylation to appreciate its role and underlying mechanisms in the regulation of transcription and plant development, using *Arabidopsis thaliana* as a model organism. In the first part of my thesis, I report on our study of SET DOMAIN GROUP7 (SDG7), a protein containing the evolutionarily conserved SET domain, which is generally recognized as a signature of K-methyltransferases. We found that SDG7 plays an important role in the regulation of *VIN3* induction associated with cold duration measure during vernalization treatment. Intriguingly, levels of several different histone methylations were found unchanged in the *sdg7* mutant plants and the recombinant SDG7 protein failed to show a histone-methyltransferase activity in vitro. We thus conclude that SDG7 might methylate a yet unknown non-histone protein to regulate transcription and proper measurement of the duration of cold exposure in the vernalization process. In the second part, I studied interaction between SDG8 and HISTONE MONOUBIQUITINATION1 (HUB1) and HUB2. My results unravel that H3K36me3 and H2Bub1 are deposited largely independently in Arabidopsis, which is in contrast to the dependent crosstalk of these two different epigenetic marks previously reported in yeast. In the last part of my thesis, I report on the identification of the PWWP-domain proteins HUA2/HULK2 as readers of H3K36me3 and demonstrate that *sdg8* and *hua2* genetically interacts in the regulation of flowering time.

Keys words: Epigenetics, Chromatin, Histone Modification, Transcription, Flowering, Arabidopsis.